ICARDA
Science for Better Livelihoods in Dry Areas

Working Paper 27

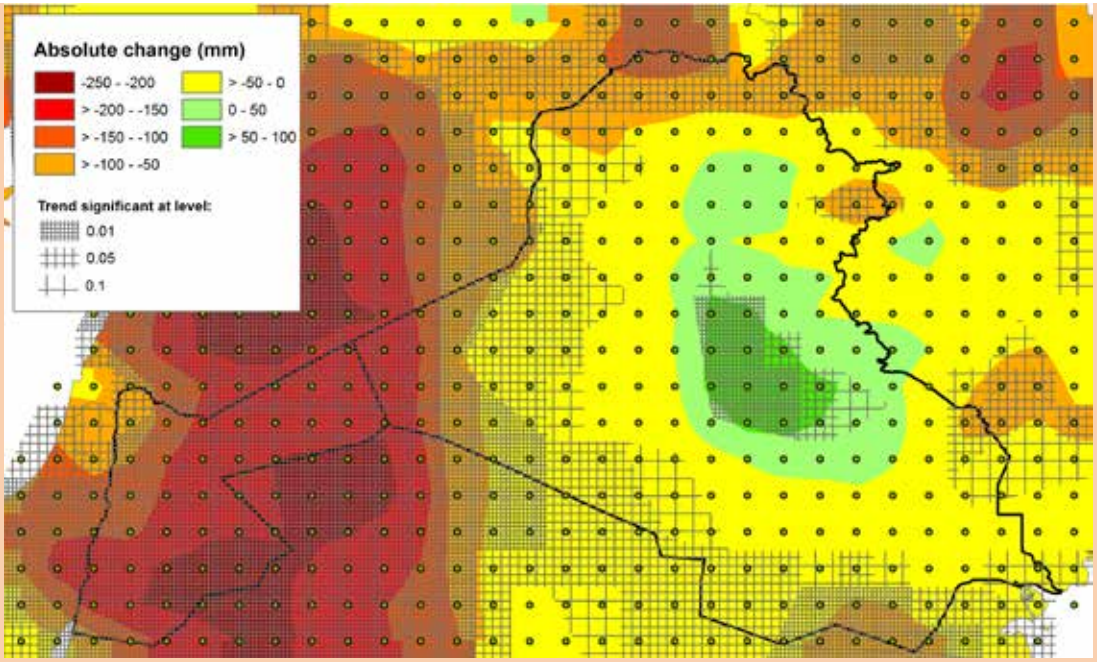

Mapping climate change in Iraq and Jordan

Eddy De Pauw, Muna Saba, and Sabah H. Ali

IFAD
INTERNATIONAL
FUND FOR
AGRICULTURAL
DEVELOPMENT

Acknowledgements

Authors: Eddy De Pauw, Muna Saba, and Sabah H. Ali

The authors would like to express their gratitude to those who contributed to this paper: Ministries of Agriculture in Iraq and Jordan, and to the collaborating institutions and universities in both the countries. Thanks are also extended to ICARDA management, programs and units for their support. Thanks and appreciation are due to the International Fund for Agriculture Development (IFAD) for their financial contribution and for their keen interest in achieving better understanding and finding solutions to the climate change phenomenon. Special thanks are extended to all farmers and their communities for their support and friendliness.

This working paper is an output of the the project on "Improving food security and climate change adaptability of livestock producers using the rainfed barley-based system in Iraq and Jordan" (IFAD Grant 1240-ICARDA)

ICARDA Working Papers document the progress of the ICARDA research program and its support to country partners in more than 40 drylands countries. Working Papers are one of ICARDA's global public goods; they capture and share knowledge and learning from projects and research partnerships. Each paper is internally reviewed as part of the center's publishing process.

ISBN: 92-91274739

Key words: Aridity index, climate change, food security, Iraq, Jordan, map downscaling, projected climate change, rainfed systems.

Feedback: ICARDA welcomes comment and feedback on this publication.

icarda@cgiar.org

www.icarda.org

International Center for Agricultural Research in the Dry Areas (ICARDA)

PO Box 114/5055, Beirut, Lebanon

FOREWORD

This is an introduction to the Working Paper on the IFAD-funded project "Improving food security and climate change adaptability of livestock producers using the rainfed barley-based system in Iraq and Jordan". The longer-term goal of this project is improved food security, livelihoods, and climate change adaptability for poor rural households in rainfed areas dependent on barley and livestock production. Its immediate objective is to improve the awareness of the seriousness of climate change for policy makers, development organizations and communities and emphasize the importance of the promising agricultural technologies relevant for adaptation to climate change. In order to achieve this objective, the project builds on previous ICARDA research initiatives to improve awareness of climate change at the policy and community levels, deliver technologies to resource-poor communities, and encourage farmers to adopt sustainable agricultural practices. Thus the IFAD-funded project is a multi-disciplinary project, with components on farming systems, crop improvement, water conservation through conservation agriculture and livestock improvement. The novel approach adopted in the project is to link these technologies and practices to a solid foundation of climate change assessment in a Geographic Information Systems (GIS) framework. This project has been contributing to the CGIAR Research Programs Dryland Systems and Climate Change, Agriculture and Food Security.

Climate change assessments are based on predictions, or - more accurately - projections of future conditions of temperature and precipitation in a given area. These projections are generated by very complex models, Global Circulation Models (or GCMs). There are three major hurdles in interpreting correctly the results from these models: (i) there are several GCMs that do not yield similar results for the same locations; (ii) their resolution is very coarse, hence they can provide unique projections only for very large areas, thus ignoring local specificity, and (iii) GCMs operate on assumptions of future greenhouse gas emissions (a.k.a. 'scenarios'), therefore their outputs refer to divergent futures.

The GIS studies, summarized in this Working Paper, offer an approach for dealing with the above challenges: they provide a downscaling method for making the GCM projections location-specific, incorporate different GCM models, and include different scenarios for the future.

It is important to emphasize that the GIS component of this project has also invested heavily in capacity-building in all aspects of the methods used, which has yielded national Climate Change Atlases for Iraq and Jordan, entirely produced by the national partner institutions. This emphasis on sharing methodologies is reflected in this Working Paper. It is, therefore, expect that the level of methodological detail provided in this publication will facilitate the application or adaptation of the methods developed by the IFAD project in other projects and countries.

It is important to express ICARDA's great appreciation to Their Excellencies the Ministers of Agriculture in Jordan and Iraq, for their support to this project and to the climate change component in particular. Sincere thanks are also extended to the Directors General of research in both these countries and to their climate change teams, and ICARDA colleagues for their dedication and hard work to achieve this important publication. Great appreciation is also due to the International Fund for Agriculture Development (IFAD) for their financial support and for their keen interest in achieving better understanding and finding solutions to the climate change phenomenon and its impact on poverty.

Mahmoud El Solh

Director General

ICARDA

Table of Contents

ANNEXES

LIST OF TABLES

LIST OF FIGURES

1. INTRODUCTION

This working paper provides a synthesis of the climate change assessment studies undertaken in Iraq and Jordan in the context of the IFAD-funded and ICARDA-implemented Project 'Improving food security and climate change adaptability of livestock producers using the rainfed barley-based system in Iraq and Jordan', leading to the production of Climate Change Atlases for both countries.

The immediate objective of this project was to improve awareness of climate change for policy makers and communities and of the promising agricultural technologies that are relevant for adapting to climate change. This awareness can certainly not be taken for granted; although global climatological studies predict drier and hotter climate for the region, with more frequent climatic extreme events (drought and floods), an understanding of how these macro-level trends can be interpreted at the local level is rather limited. Therefore, the specific challenges posed by climate change for Iraq and Jordan, in particular for their rural communities, need to be understood. A better awareness of the expected climate change effects – decrease in rainfall, increase in temperature and evapotranspiration, and shorter growing seasons – are essential for planning suitable adaptation measures.

A useful way to address these concerns is by producing downscaled (i.e. with higher resolution) spatial representations of future climates, based on Global Circulation Model (GCM) outputs under different greenhouse gas (GHG) emission scenarios. The interpretation of these maps can help in proposing suitable adaptation strategies to climate change for the barley and livestock farmers of Iraq and Jordan, by assisting adjustments in policies, farming practices, and technologies.

Whereas the project builds on the extensive drylands experience of ICARDA and its national partners, the innovation in this project is to underpin the use of appropriate dryland technologies and practices adapted to climate change by a solid foundation of climate change assessment to be provided through a Geographic Information Systems (GIS) framework. Up to now we have said "it will get hotter and drier, prepare yourselves". Through the added value of a spatial framework we can now provide concrete answers to specific questions: "where will it get hotter and drier, by how much and when, and what other effects can be expected?"

The climate change assessments for Iraq and Jordan were compiled in the form of Climate Change Atlases. The Climate Change Atlas for Iraq was produced by staff of the University of Mosul and the Department of Agriculture of Nineveh Province. The Climate Change Atlas for Jordan was produced by staff of the National Center for Agricultural Research and Extension (NCARE). In both countries, national staff produced virtually all the maps contained in their respective country atlases, under the technical supervision of ICARDA staff, provided through ICARDA's Geo-informatics Unit.

Both atlas products provide comprehensive characterizations of past and expected climatic change in the respective countries in terms of changes of temperature and precipitation patterns, changes in atmospheric water demand, climatic zones and growing periods, historical drought and wetness periods, and long-term precipitation and temperature trends. As such they are important baseline documents that will allow provision of guidance to the agricultural sector in both countries in their endeavor to cope with the effects of climate change.

It is to be noted that the Climate Change Atlases do not only include projections for the future. Given the importance of precipitation, the past and present trends in precipitation, the most crucial variable for agriculture in a dryland region, are also analyzed.

To analyze potential impacts of climate change of on existing production systems, both atlases focus on a 'near' future (2010–2040). These impacts are analyzed through a relatively simple method of spatial downscaling of the coarse-resolution projections of GCMs. Using these downscaled projections of precipitation and temperature, anticipated changes in atmospheric water demand, climatic

zones, and growing periods are mapped. The atlases also contain a trend analysis of drought and wetness periods during 1901–2010, extrapolate the precipitation trends to 2010–2040, and compare these with GCM-derived change projections.

The objective of this working paper is not to reproduce information already provided in both atlas products, but rather to complement them by providing more details on the methods used to create the atlases, by synthesizing key results and suggesting follow-up actions.

Methods and key results for both countries are summarized through the following arrangement: current climate (1970–2000), historical climate (1901–2010), and change projections from the current climate to the near future (2010–2040). Focusing this study not only on expectations of future climate is justified by evidence that climate change has been happening for at least a century in both countries, in the form of a slow but inexorable trend of precipitation decline.

Conclusions are drawn on how these atlas products can serve farming communities in both countries, and what additional studies and research partnerships would be most useful for distilling from the map collections clear and location-specific messages to researchers, extension workers, and farmers on how to cope with the projected climatic changes. Representative maps from the Climate Change Atlases are included in an annex to this working paper; for the full sets refer to the Atlases proper.

2. THE ROLE OF CAPACITY-BUILDING IN THIS PROJECT

As mentioned in the Introduction, the Climate Change Atlases of Iraq and Jordan are products generated by National Agricultural Research Systems (NARS) under ICARDA technical coordination. These atlas products provide proof that, with a relatively small investment in capacity-building, skills for applying and adapting the findings from global climate change studies to country-level are well within NARS capabilities.

From the very beginning it was agreed that the objective of climate change assessment in Iraq and Jordan would have to be achieved by a division of labor, in which ICARDA would provide training to be followed by the NARS partners implementing most of the actual mapping activities. Since climate change was a new area of research for the NARS of Iraq and Jordan, it was obvious that the implementation of these activities would require much capacity-building. The capacity-building was very much driven by the specific questions that arose from the implementation needs of the particular mapping activities. Thus, as more questions arose more training sessions were organized to address these questions.

The capacity-building activities were ultimately organized around four major training events, the first three entirely under ICARDA support, and the last one with considerable input from the Cyprus Institute (CYI) in Nicosia.

Training Event 1
Period: November–December 2011 (eight working days)
Specific topics:

- Creating climate surfaces from station data through topography-guided spatial interpolation methods
- Creating downscaled climate change maps

Training Event 2
Period: May (six working days)
Specific topics:

- Methods for mapping potential evapotranspiration
- Downscaling historical precipitation data of the Global Precipitation Climatology Centre (GPCC)
- Mapping historical drought and wetness periods

Training Event 3
Period: March 2013 (five working days)
Specific topics:

- Generating downscaled change maps of climatic zones and growing periods
- Second session on mapping drought and wetness periods
- Introducing crop suitability mapping

Training Event 4
Period: July 2014 (eight working days)
Specific topics:

- Update on new IPCC report (AR5) and new datasets from IPCC and CCAFS (Climate Change, Agriculture and Food Security) Program
- Working with spatial data formats commonly used in climate change research
- Review of spatial downscaling methods
- Statistical analysis for characterizing extreme weather events
- Analyzing extreme weather events in the Middle East (CYI)
- Introduction to High-Performance Computing (CYI)

All training events were conducted in Amman and contained a session on project progress review and workplan adjustment. The last training event was specifically designed to ensure some degree of sustainability of the activities beyond the lifetime of the project. Overall the training sessions were successful. Each training event led to production of new maps and finally resulted in enough maps to bundle them into Climate Change Atlases for both Iraq and Jordan.

Staff of ICARDA's Geo-informatics Unit participated in all training events as lecturers. Their contributions, particularly of Mr. Wolfgang Göbel, Mr. Jalal Omary, and Ms. Layal Atassi, are gratefully acknowledged. In the last training course the following staff of the CYI conducted several important sessions: Mr. Andries De Vries, Mr. Hendrik Merx, Mr. Panayiotis Hadjinicolaou, Ms. Meryem Tanarhte, and Mr. Stelios Erotokritou.

3. METHODS

3.1. METHODS USED IN MAPPING CURRENT CLIMATE

3.1.1. Station data

The station data used to analyze current climatic conditions are an extract from a database of point climatic data, covering monthly averages of precipitation and minimum and maximum temperature, compiled by ICARDA's Geo-informatics Unit for 1911 main stations in the Central and West Asia and North Africa (CWANA) region and the countries covering the northern border of the Mediterranean. The location of these stations is shown in Figure 1, as well as the extraction window (in red) used in this report.

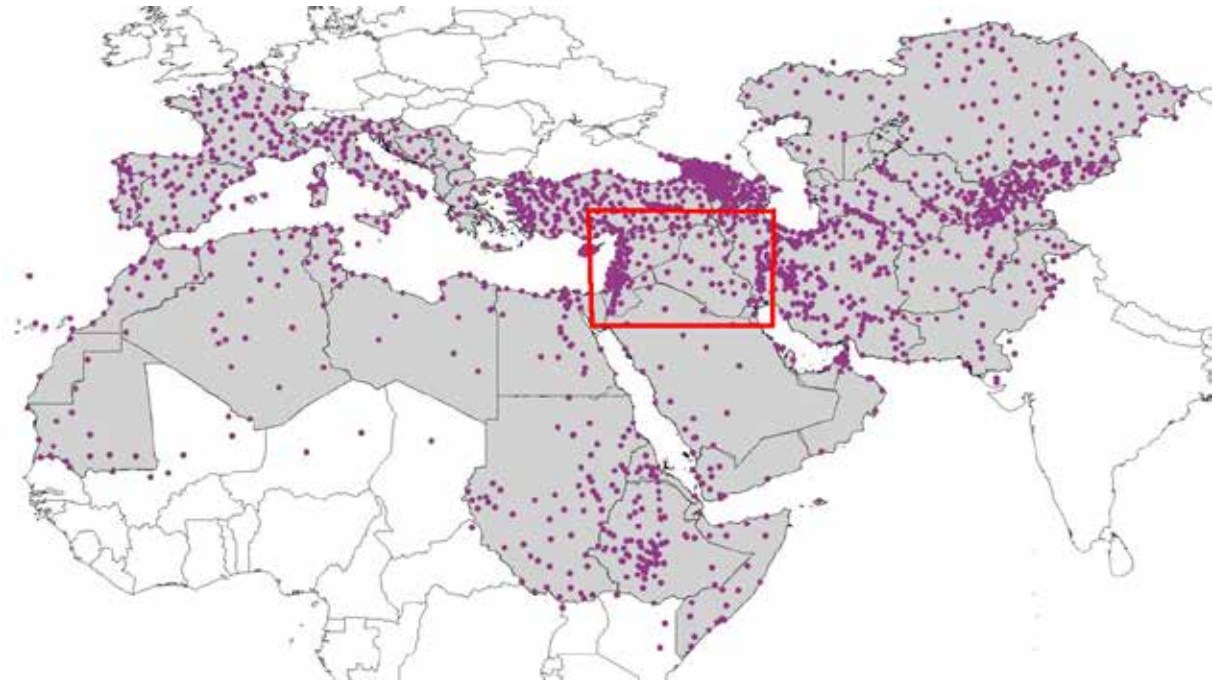

Figure 1. Location of climate stations in the CWANA and northern Mediterranean regions (with window of interest in red-bounded box)

Record length is variable for different stations and the data were not necessarily for the same period, but the averages were based on a m inimum of 20 years in the case of precipitation and 5 years in the case of temperature. The main sources were international, such as the Food and Agriculture Organization of the United Nations (FAO) (FAOCLIM database: FAO, 2002) and the National Climate Data Center of the US (NCDC database). For some countries, such as Iran, and the Central Asia and Caucasus countries the data came from national archives. In this study, maps that show current climate themes are confined to the window of interest (WOI). For the countries included in the WOI the data sources are mentioned in Table 1.

For the Climate Change Atlases of Iraq and Jordan use was made of the same international datasets, complemented with data from the national meteorological archives. The specific stations used for Jordan and Iraq, as well as those from some neighboring countries, are listed in Annex 1 of this report and are shown in Figure 2.

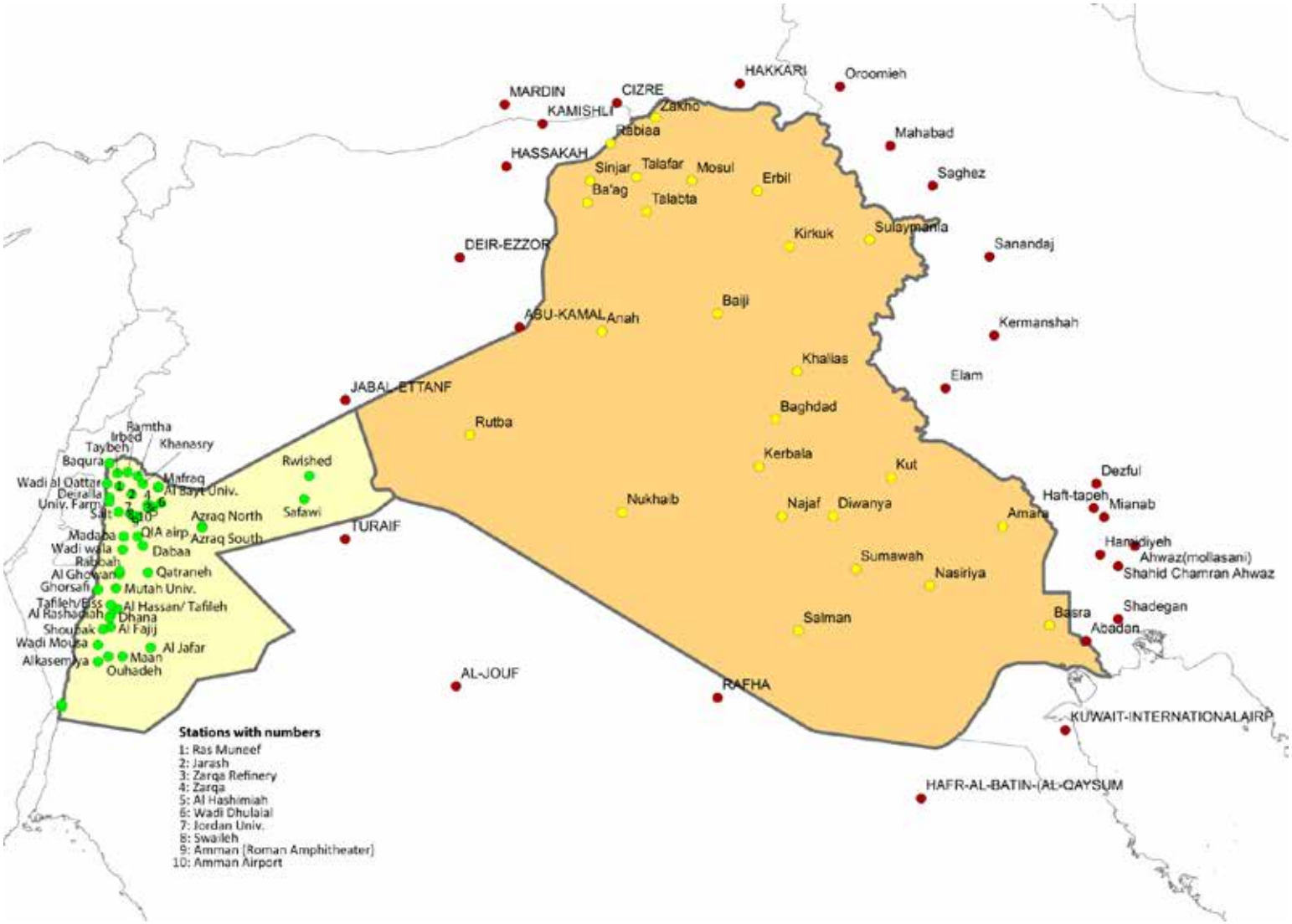

Figure 2. Location of meteorological stations used for generating surfaces of current climate in Jordan (green dots), Iraq (yellow dots), and neighboring countries (brown dots)

Table 1. Meteorological data sources

Element	Country	No. stations	Data source
Monthly average precipitation	Iran	126	Iran Meteorological Department
Monthly average precipitation	Iraq	37	FAOCLIM. Version 2. World-wide agroclimatic data
Monthly average precipitation	Israel	32	FAOCLIM. Version 2. World-wide agroclimatic data
Monthly average precipitation	Jordan	43	FAOCLIM. Version 2. World-wide agroclimatic data
Monthly average precipitation	Lebanon	31	FAOCLIM. Version 2. World-wide agroclimatic data
Monthly average precipitation	Saudi Arabia	39	FAOCLIM. Version 2. World-wide agroclimatic data
Monthly average precipitation	Syria	29	FAOCLIM. Version 2. World-wide agroclimatic data
Monthly average precipitation	Turkey	219	FAOCLIM. Version 2. World-wide agroclimatic data
Monthly mean maximum temperature	Iran	548	Iran Meteorological Department
Monthly mean maximum temperature	Iraq	20	FAOCLIM. Version 2. World-wide agroclimatic data
Monthly mean maximum temperature	Israel	7	FAOCLIM. Version 2. World-wide agroclimatic data
Monthly mean maximum temperature	Jordan	29	FAOCLIM. Version 2. World-wide agroclimatic data
Monthly mean maximum temperature	Lebanon	15	FAOCLIM. Version 2. World-wide agroclimatic data
Monthly mean maximum temperature	Saudi Arabia	23	FAOCLIM. Version 2. World-wide agroclimatic data
Monthly mean maximum temperature	Syria	45	FAOCLIM. Version 2. World-wide agroclimatic data
Monthly mean maximum temperature	Turkey	215	FAOCLIM. Version 2. World-wide agroclimatic data
Monthly mean minimum temperature	Iran	548	Iran Meteorological Department
Monthly mean minimum temperature	Iraq	20	FAOCLIM. Version 2. World-wide agroclimatic data
Monthly mean minimum temperature	Israel	7	FAOCLIM. Version 2. World-wide agroclimatic data
Monthly mean minimum temperature	Jordan	29	FAOCLIM. Version 2. World-wide agroclimatic data
Monthly mean minimum temperature	Lebanon	15	FAOCLIM. Version 2. World-wide agroclimatic data
Monthly mean minimum temperature	Saudi Arabia	23	FAOCLIM. Version 2. World-wide agroclimatic data
Monthly mean minimum temperature	Syria	45	FAOCLIM. Version 2. World-wide agroclimatic data
Monthly mean minimum temperature	Turkey	215	FAOCLIM. Version 2. World-wide agroclimatic data

3.1.2. Spatial interpolation

The 'thin-plate smoothing spline' method of Hutchinson (1995), as implemented in the ANUSPLIN software (Hutchinson, 2000), was used to convert this point database into 'climate surfaces'. These are raster-based files that are geographically referenced, contain continuous climatic values, and can be imported into a GIS system.

The Hutchinson method is a smoothing interpolation technique in which the degree of smoothness of the fitted function is determined automatically from the data by minimizing a measure of the predictive error of the fitted surface, as given by the generalized cross-validation (GCV). The GCV is calculated by removing each data-point and calculating the residual from the omitted data-point of a surface fitted to all other data points using the same smoothing parameter value. The GCV is then a suitably weighted sum of the squares of these residuals and can be approximated (Hutchinson, 2000) as:

$GCV = MSE + \sigma^2$

with MSE the mean square error of the fitted function and σ^2 the error variance.

Three independent spline variables were used: latitude, longitude, and altitude. The latter was input to the model in the form of a DEM ASCII grid file. The DEM used to generate the climate surfaces was SRTM30, a global DEM with resolution of 30 arc-second (approximately 1 km)[1]. Parameter estimation was undertaken over a regular grid with the same dimensions and resolution as the user-provided DEM. To automate the rather cumbersome process of climate surface generation, an auxiliary software product CLIMAP, developed by ICARDA's Geo-informatics Unit, was used. This Excel-based software provides a user-friendly interface for running ANUSPLIN and for generating derived surfaces

1 http://dds.cr.usgs.gov/srtm/version2_1/SRTM30/srtm30_documentation.pdf

using CLIMAP-provided models.

Applying the above spatial interpolation procedure on the station data of Table 1 and Annex 1, the following surfaces were generated with 30 arc-second resolution for the reference period:

- Mean monthly, seasonal, and annual precipitation totals
- Mean monthly and seasonal maximum and minimum temperature

The generated surfaces were then used to generate the following derived climatic variables:

- Köppen climatic zones
- Mean annual potential evapotranspiration
- Annual aridity index
- UNESCO agroclimatic zones
- Growing period durations

The procedures used to generate these variables are explained in the following sections.

3.1.3. Climatic zones according to the Köppen classification system

The Köppen climate classification system, devised by Waldimir Köppen (1846–1940), has the great advantage that it can build a classification of climates on the basis of annual and monthly averages of precipitation and temperature only. Initially published in 1918, the original Köppen classification system has been revised several times, especially by Geiger and Köppen himself (Köppen and Geiger, 1928). Despite its venerable age, the Köppen climate classification is still the most widely used to date. The system has five major subdivisions, designated by a capital letter:

A-climates: tropical moist climates

These climates have year-round temperatures above 18°C and abundant rainfall. Their general extent is north and south of the equator to about latitudes 15–25°. On the basis of seasonal distribution of precipitation, they can be subdivided into Af- (tropical wet), Am- (tropical monsoon, with moderate dry season), Aw- (tropical wet and dry, with winter drought), and As-climates (tropical wet and dry, with summer drought).

B-climates: dry climates

These climates are characterized by precipitation that is deficient compared to the water requirements of plants. Generally speaking, they occur in one of three situations: (i) subtropical deserts, within roughly 20–30° latitude; (ii) continental areas of mid-latitudes, far away from a moisture source; and (iii) rain-shadow effects caused by high mountains.

Depending on their degree of dryness Köppen subdivided dry climates into BS- (semi-arid or steppe climates) and BW-climates (arid or desert climates). Further differentiation of the BS- or BW-climates is done on the basis of the temperature regime and the seasonal characteristics of the dry period.

C-climates: moist climates with mild winters

These temperate and mild climates are characterized by adequate precipitation and distinct summer and winter seasons. Winters may be cold but are not severe. The C-climates occur mostly along both the eastern and western edges of continents, within roughly 20–40° latitude. Depending on the presence and timing of the dry season they are subdivided into Cw- (with dry period in winter), Cs- (with dry period in summer), and Cf-climates (without pronounced dry period). Köppen made a further differentiation on the basis of the summer temperature regime.

D-climates: moist climates with cold winters

These climates have warm to cool summers and cold winters, with persistent snow cover. They occur

within latitudes 40–70° and, as they are linked to the presence of large continental landmasses, only in the Northern Hemisphere. As for the C-climates, they are further subdivided in the Köppen classification according to the seasonality and occurrence of a dry period, and on the basis of the temperature regime of summer.

E-climates: arctic climates

These climates are characterized by year-round low temperatures and include the polar tundra (ET) and ice sheets (EF), as well as locations in high mountain ranges.

Despite the apparent simplicity of the climatic elements (monthly mean precipitation and temperature) that serve as input data, the system, once further subdivisions are considered, leads to surprisingly complex patterns[2]. For the detailed characteristics of these Köppen climatic zones in terms of annual and monthly precipitation and temperature variables refer to Annex 2.

3.1.4. Potential evapotranspiration

Potential evapotranspiration (PET) is the rate of evapotranspiration from an extensive surface of an 8–15-cm tall, green grass cover of uniform height, actively growing, completely shading the ground, and not short of water (Doorenbos and Pruitt, 1984).

The calculation of PET is a first step in the assessment of crop water requirements and irrigation needs. It is also essential for the calculation of the aridity index (see section 3.1.5.).

The recommended method for calculating PET is the Penman–Monteith method, with a calculation procedure for monthly data, as described in Allen et al. (1998). This method depends on the availability of the following meteorological data at station level: temperature, radiation, relative humidity, and wind speed. However, consistent long-term data on radiation and wind speed in particular, are available at only a few stations and therefore insufficient for reliable interpolation. Adding the fact that from the GCM models (see section 3.3.1.) we can obtain only precipitation and temperature consistently, it was clear that a method was needed for approximating the results of the Penman–Monteith PET method, while requiring only temperature data.

A suitable way to do this was to calculate PET according to the Hargreaves method (PET_{Har}), and subsequently to convert these values into Penman–Monteith estimates (PET_{Pen}), using a regression equation between monthly PET_{Har} and monthly PET_{Pen}. Experience in several ICARDA projects has indicated that this method works very well in dry areas, because in dryland regions the temperature is the main factor contributing to evapotranspiration.

From the FAOCLIM 2.0 global climate database monthly PET, calculated by the Penman–Monteith method (FAO, 2001), for 4253 stations from countries with dryland areas were extracted. For each of these stations the Köppen climatic zone was calculated in accordance with the criteria in Debaveye (1985). At the same time PET was calculated according to the Hargreaves method. This method is based on the combination of temperature data and calculated extraterrestrial radiation and has the following formula (Choisnel et al., 1992):

$$PET = 0.0023 \times Ra \times (T_{mean} + 17.8) \times \sqrt{(T_{max} - T_{min})}$$

with PET ($mm.d^{-1}$), Ra: extraterrestrial radiation ($mm.d^{-1}$), T_{mean}: mean monthly temperature, T_{max}: maximum monthly temperature, and T_{min}: minimum monthly temperature.

2 See the pattern of Köppen zones in the WOI (Fig. 13)

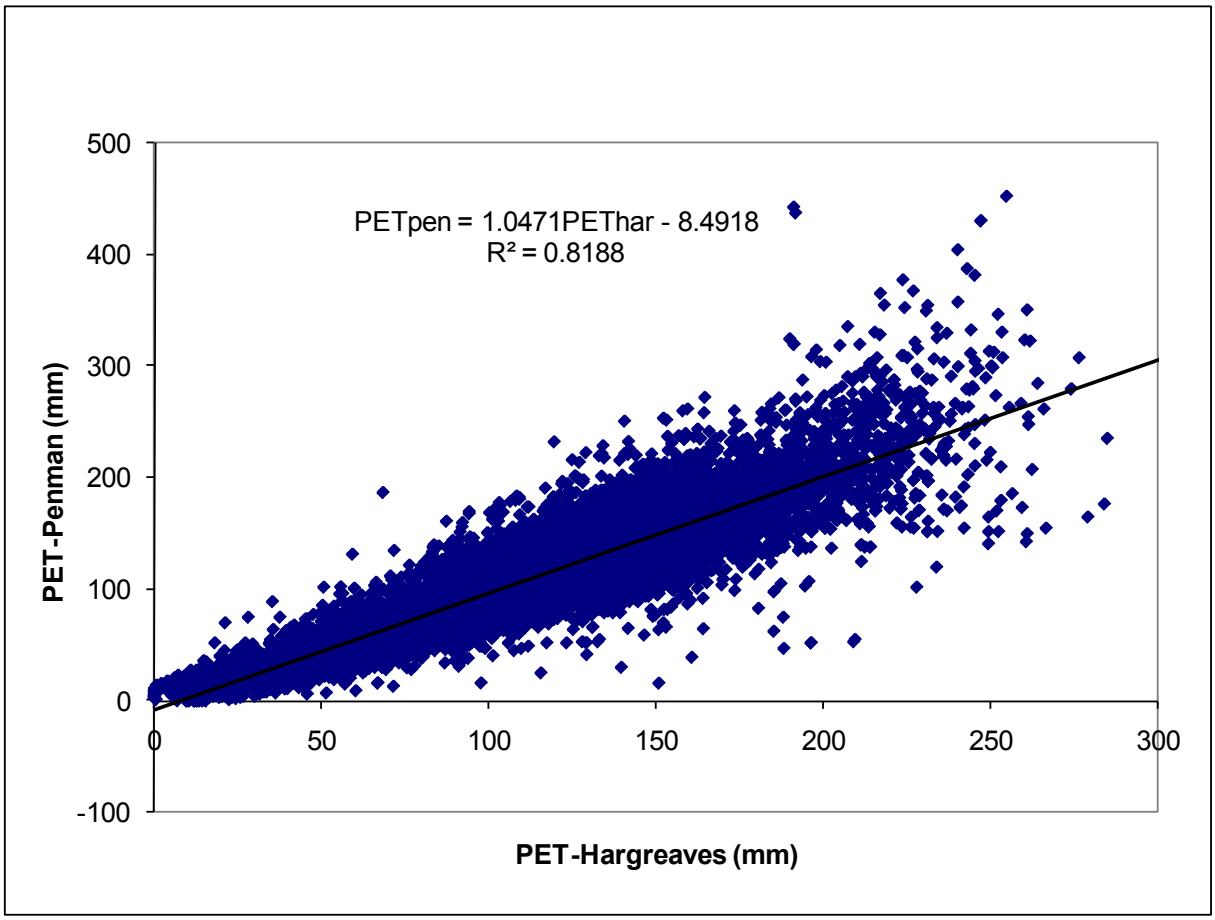

Figure 3. Correlation between monthly PET-Penman–Monteith and PET-Hargreaves (all climates combined except for the A, Cwc, Cfc, and Dw climatic zones)

Correlations were then established between the monthly values of PET_{Pen} and PET_{Har} that referred to a Köppen climatic zone that occurs in the study area[3]. Thus, for the climates within the West Asia window a highly predictive statistical relationship could be established between PET-Penman–Monteith and PET-Hargreaves (Fig. 3).

3.1.5. Aridity index

The aridity index is the ratio of the annual precipitation over the annual PET (UNESCO, 1979). The aridity index can thus be interpreted as a water balance in its most elementary form (on an annual basis) and takes account of higher moisture demand in hot climates, as well as differences in the effectiveness of precipitation for growth cycles that include a cold period versus those that do not.

3.1.6. Agroclimatic zones

The agroclimatic zones of the WOI were generated by the combination of climatic surfaces related to moisture regime, and winter and summer temperature regimes, in accordance with the criteria and class thresholds implemented in the UNESCO classification system for arid regions (UNESCO, 1979). The classes are shown in Tables 3–5. Figure 4 outlines the combination of basic and derived climatic surfaces used to generate the agroclimatic zones theme.

3 For more information on the Köppen climatic zones refer to section 3.1.3. and Annex

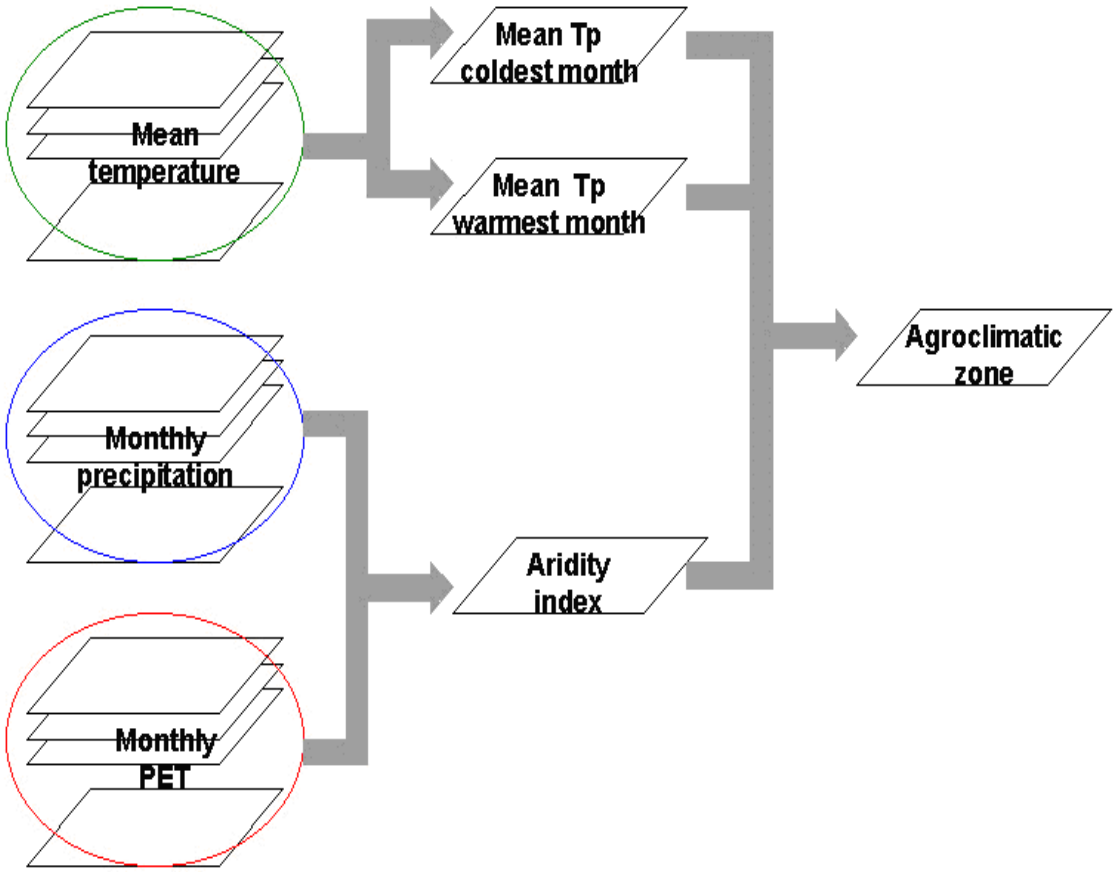

Figure 4. Developing the agroclimatic zones theme

In this classification system the moisture regime is determined by the ratio of annual rainfall over annual PET (also referred to as aridity index, see section 3.1.5.), calculated according to the Penman method[4]. It is therefore particular to the UNESCO system that in the definition of the moisture regime not only the water supply (precipitation) is considered, but also the water demand (evapotranspiration). Different classes may thus result from different values of the two terms (Table 2).

The winter type is determined by the mean temperature of the coldest month (Table 3). The summer type is determined by the mean temperature of the warmest month (Table 4).

Table 2. Classes for the moisture regime

Moisture regime	Hyper-arid (HA)	Arid (A)	Semi-arid (SA)	Sub-humid (SH)	Humid (H)	Per-humid (PH)
Aridity index	< 0.03	0.03–0.2	0.2–0.5	0.5–0.75	0.75–1	> 1

4 Penman values are approximated using the approach outlined in section 3.1.3.

Table 3. Classes for the winter type

Winter type	Warm (W)	Mild (M)	Cool (C)	Cold (K)
Mean temp. coldest month	> 20°C	> 10°C	> 0°C	≤ 0°C

Table 4. Classes for the summer type

Summer type	Very warm (VW)	Warm (W)	Mild (M)	Cool (C)
Mean temp. warmest month	> 30°C	> 20°C	> 10°C	≤ 10°C

The UNESCO system is basically open-ended and any particular climate can be simplified by the three attributes: moisture regime, winter type, and summer type. For example, the climate SA-C-VW is characterized by a semi-arid moisture regime, a cool winter type, and very warm summer type.

The UNESCO system is more geared than the Köppen classification to the broad suitability of various climates for agricultural uses because, in addition to its temperature range sensitivity, it allows a more precise appreciation of the balance between water input and loss conditions. In the WOI, 34 agroclimatic zones can be differentiated.

3.1.7. Growing periods

The concept of climatic growing period was developed to estimate the duration of the period during the year in which neither moisture nor temperature are limiting to plants. It is calculated by means of a model developed by the FAO (FAO, 1978). Under rainfed conditions, both moisture and temperature can be limiting. Under irrigated conditions, only temperature is considered a limiting factor. Thus the calculation of the growing period has two components: calculation of the moisture- and temperature-limiting growing periods separately, and their combination into a moisture–temperature-limiting growing period.

The criterion used for the definition of a moisture-limited growing period is the ratio of actual evapotranspiration (AET) to PET. If this ratio for any particular month is higher than a user-defined threshold (in this study 0.5), that month is part of a growing period. If it is not, that month is not part of the growing period. The start date of the growing period is obtained from linear interpolation of the AET/PET ratios between the last month that is part of the growing period, and the first month that is not part of the growing period. The end date, inversely, is obtained by linear interpolation of the AET/PET ratios between the last month that is part of the growing period, and the first one that is not part of the growing period.

The following equations were used for estimating the length, onset, and end of the moisture-limited growing period:

$$GP\_ON = M\_Start + NDays \frac{Thre - R_0}{R_1 - R_0}$$

$$GP\_END = M\_END + NDays2 \frac{Thre - R_{n-1}}{R_n - R_{n-1}}$$

$$LGP = GP\_END - GP\_ON$$

with GP_ON: growing period onset date
GP_END: growing period end date
LGP: length of growing period (d)
M_Start: number of days from 1 January to the end of the last month that is not part of the growing period

M_End: number of days from 1 January to the end of the month preceding the last month of the growing period

NDays: number of days in the first month of the growing period
NDays2: number of days in the last month of the growing period
Thre: AET/PET threshold for defining a growing period (user-defined; for this study set to 0 .5)
R_0: AET/PET ratio for the month preceding the first month of the growing period
R_1: AET/PET ratio for the first month of the growing period
R_{n-1}: AET/PET ratio for the month preceding the last month of the growing period
R_n: AET/PET ratio for the last month of the growing period.

Similarly, the temperature-limited growing period was calculated with reference to a temperature threshold, below which there is no growing period:

$$GP_{t,on} = M_{t,on} + NDays_t \frac{Thre_t - Temp_0}{Temp_1 - Temp_0}$$

$$GP_{t,end} = M_{t,end} + NDays2_t \frac{Thre_t - Temp_{n-1}}{Temp_n - Temp_{n-1}}$$

$$LGP_t = GP_{t,end} - GP_{t,on}$$

with $GP_{t,on}$: onset date of the temperature-limited growing period
$GP_{t,end}$: end date of the temperature -limited growing period
LGP_m: length of temperature-limited growing period
$M_{t,on}$: number of days from 1 January to the end of the last month that is not part of the temperature-limited growing period
$M_{t,end}$: number of days from 1 January to the end of the month preceding the last month of the temperature-limited growing period
$NDays_t$: number of days in the first month of the temperature-limited growing period
$NDays2_t$: number of days in the last month of the temperature-limited growing period
$Thre_t$: temperature threshold for defining a temperature-limited growing period (user-defined; for this study set to 5°C)
$Temp_0$: mean temperature for the month preceding the first month of the temperature-limited growing period
$Temp_1$: mean temperature for the first month of the moisture-limited growing period.

By combining the moisture-limited with the temperature-limited growing period, the length, onset, and end of the growing period, limited by both moisture and temperature, can be calculated.

The growing periods under current climatic conditions were mapped in three aspects: moisture-limited, temperature-limited, and moisture–temperature-limited growing periods.

3.2. METHODS USED IN MAPPING HISTORICAL CLIMATE

3.2.1. Mapping precipitation probabilities and trends during the period 1901–2010

3.2.1.1. Overview

Given the generally high temperatures and resulting evapotranspiration rates from crops and natural vegetation, precipitation is a key factor determining agricultural potential in drylands. A high degree of precipitation variability is the main constraint for agriculture in Iraq and Jordan, which, despite substantial irrigated areas, remains largely rainfed. Given this high rainfall variability, typical for all of West Asia, drought is a recurring shock for the cropping and livestock systems of both countries, and is an inherent feature of the climate.

A useful way to quantify these fluctuations is by expressing precipitation not in terms of averages, but

as probabilities of exceedance or non-exceedance. This way precipitation, on an annual basis, can be expressed as the probability of not exceeding a fixed amount (e.g. 100, 500, or 2000 mm) or as the amount likely to be exceeded (e.g. in three out of four, four out of five, or nine out of 10 years). The assessment of annual precipitation probabilities as a way to overcome the influence of the shorter-term fluctuations can be used to define 'reliable' rainfall and can thus serve as a simple adaptive capacity tool.

On top of the random variability has been a very consistent downward trend in precipitation since 1901 or even before, which implies that the average climate is not constant but actually changing over a longer period. Short-term fluctuations and long-term trends of precipitation are thus inter-related: if the long-term precipitation trend is one of decline, what would have been a normal precipitation 100 years ago, would now be considered unusually wet, and vice versa. For this reason, the longer-term precipitation trends also have to be examined. In addition, trend analysis can detect changes in the short-term fluctuations of precipitation and thus provide some guidance on whether in the medium-term that rainfall variability is likely to increase, decrease, or remain constant in the near future, and whether such changes can be considered significant or not.

3.2.1.2. Database

For the assessment of precipitation probabilities and trends the Full Data Reanalysis Product Version 6 of the GPCC of the Deutscher Wetterdienst was used. This dataset provides global grids of monthly precipitation at 0.5° × 0.5° (approximately 50 km × 50 km) resolution for every month from January 1901 to December 2010. It is based on the data of more precipitation stations (up to 45,000 globally) than any other gridded precipitation dataset. The 110-year record length, as well as because the dataset has no gaps in the record and that all station data have been thoroughly quality-controlled, makes this dataset very well suited for calculating long-term trends and evaluating the statistical significance of such trends. The dataset also has some drawbacks:

(i) The data have not been corrected for systematic gauge measurement errors. These are mainly due to losses from evaporation or wind drift and can reach up to about 30% in tropical and subtropical areas, much more at higher latitudes (see Figure 5 for average error values in West Asia). It must, however, be understood that practically all precipitation data from meteorological stations are subject to this error and it is not particular to gridded data. This error is particularly relevant when combining or comparing gauge- and satellite-based precipitation estimates, but is frequently ignored in practical applications of meteorological data.

(ii) The time-series grids were constructed as deviations from average monthly precipitation during the period 1951–2000. Although GPCC used more stations to construct these grids than have been used for any of the other gridded data sets available, the number of stations for Iraq and Jordan is still quite small in this part of West Asia, and especially contrasts with some neighboring countries, e.g. Iran and Turkey. This applies to the number of stations used to construct the grids of average precipitation for 1951–2000 (Fig. 6) and even more so to those used to construct the month-by-month deviations from average conditions during the first half of the twentieth century.

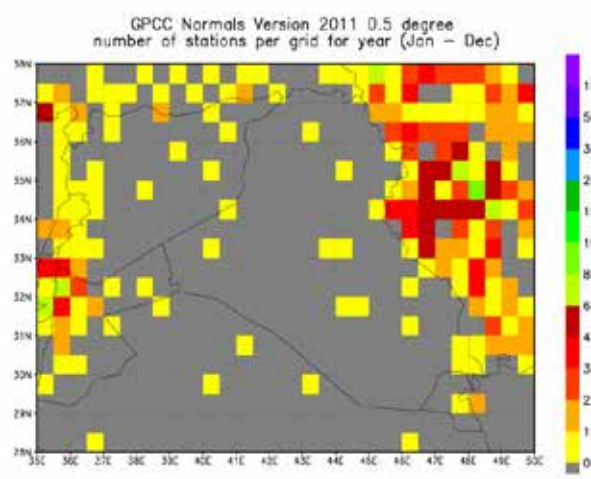

Figure 5. Relative gauge measuring error in % per month (average for the year). Source: GPCC

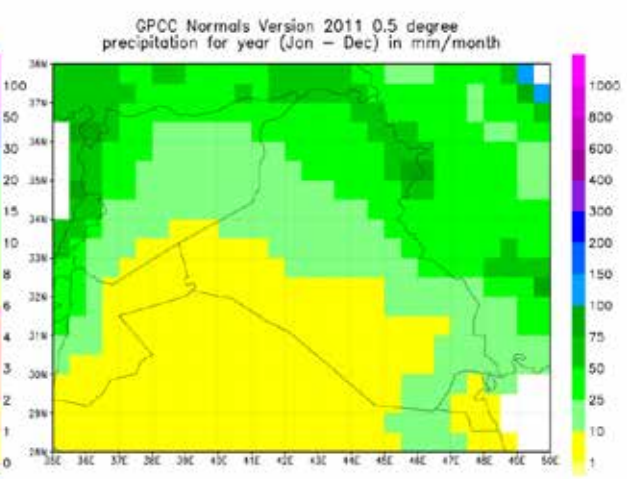

Figure 6. Mean annual precipitation during the period 1951–2000 (normals) in mm per month. Source: GPCC

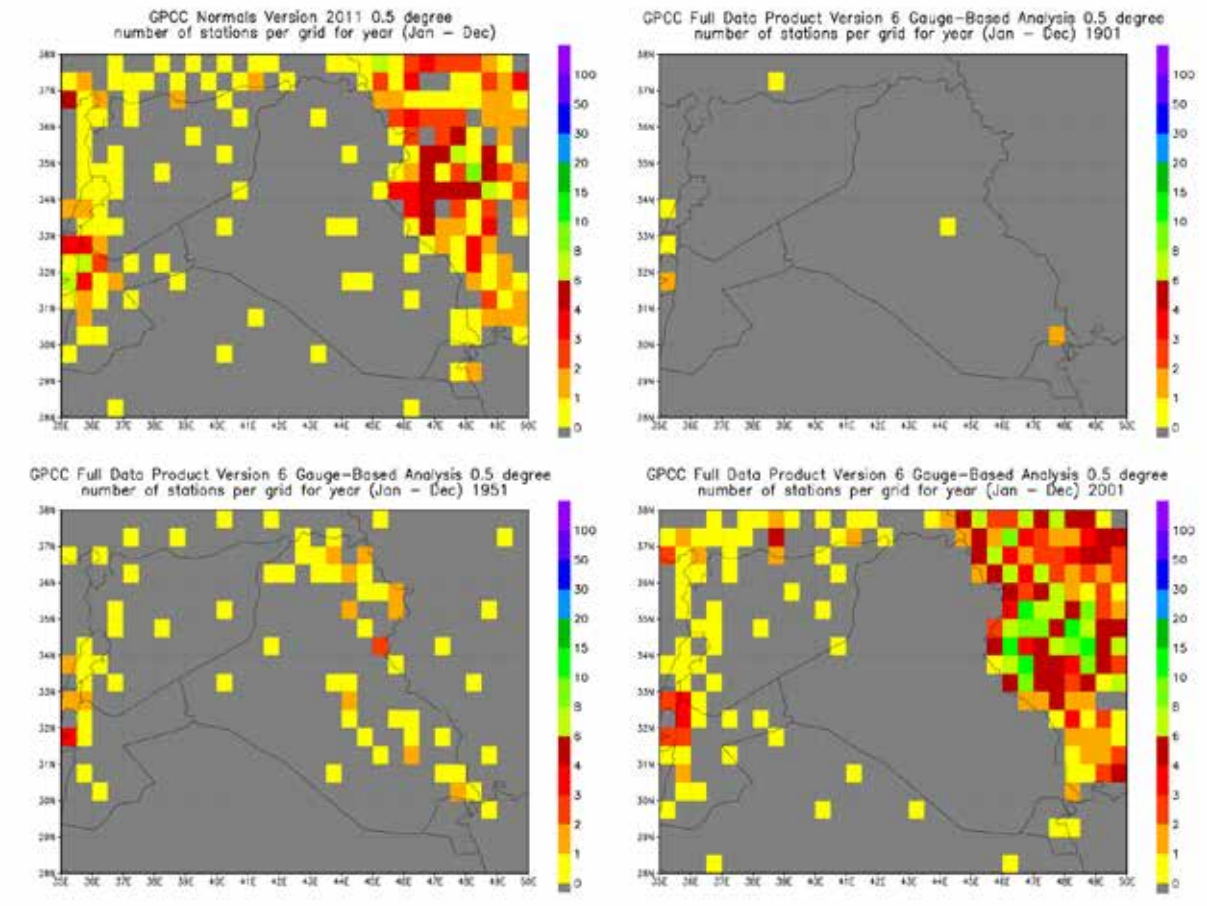

Figure 7. Density of station network in West Asia used for the construction of the grids of normals 1951–2000 (top left) and deviations for years 1901 (top right), 1951 (bottom left), and 2001 (bottom right). Source: GPCC

(iii) The number and spatial distribution of stations used for the construction of the surfaces varies over time (see Figure 7 for some examples). This may cause some local distortions in the time series, which have not been adjusted[5]. Noticeable in this respect are the particular developments of the station networks in neighboring countries Jordan, Iraq, and Iran (Fig. 3). Whereas Jordan and Iran witnessed a steady development of their meteorological networks, Iraq's network was almost entirely destroyed as a result of the first Gulf War (1990–1991) and is only now slowly recovering. The fragility of Iraq's meteorological network is certainly a factor that casts some doubts on the validity of the trend and drought analyses. Over larger areas, the general trends should, however, always be clear.

(iv) Because of the relatively small number of stations in desert regions, the limits of areas without or with very little rainfall during any particular month or year can be only approximated and are also affected by rounding errors. In areas with less than about 1 mm precipitation per month, this can cause visible spatial patterns and artefacts on maps of precipitation-derived indices, which magnify such subtle differences and are without any real meaning or consequence. For this reason all maps of Annex 7 related to aspects of the precipitation patterns have a mask that shows the spatial extent of the hyper-arid areas[6].

3.2.1.3. Annual precipitation probabilities

For each 0.5° grid cell the gridded annual precipitation data for 1901–2010 (with January as first and December as last month) were extracted using the GPCC Visualizer software in ArcView ASCII grid format[7]. This dataset was converted into an Excel spreadsheet containing 522 data points equally spaced across Iraq, Jordan, and neighboring areas. For each data-point the precipitation probabilities were calculated using the cumulative Gamma-distribution:

$$G(x) = \frac{1}{\beta^{\alpha}\Gamma\alpha}\int_0^x x^{\alpha-1}e^{\frac{-x}{\beta}}dx$$

in which α is a shape parameter and β is a scale parameter for the distribution. By modulating the shape and scale parameters, the Gamma-distribution allows an excellent fit to ranked precipitation data, as shown in Figure 8.

From Thom (1966) the following maximum likelihood estimators are used for α and β:

$$\hat{\alpha} = \frac{1}{4A}\left(1+\sqrt{1+\frac{4A}{3}}\right) \text{ and } \hat{\beta} = \frac{\bar{x}}{\hat{\alpha}} \qquad (1)$$

where

$$A = ln(\bar{x}) - \frac{\sum_{x=1}^{110} x}{n} \qquad (2)$$

and n is number of precipitation observations (here 110 years).

5 The Vasclimo dataset is a gridded precipitation dataset that has been corrected for this bias (see Schneider et al., 2008). Because of the requirement of using a temporally and spatially coherent network of stations, it covers only the period 1951–2000 and is based on data from < 10,000 stations worldwide.

6 Hyper-arid areas are defined as those areas with aridity index (annual precipitation/PET ratio) < 0.03.

7 http://kunden.dwd.de/GPCC/Visualizer

Since the Gamma function is undefined for x = 0 and in much of Africa zero values may occur in hyper-arid areas, the cumulative probability is adjusted as follows:

$$H(x) = q + (1 - q)G(x) \qquad (3)$$

where q is the probability of zero precipitation. If m is the number of zeros in a precipitation time series, Thom (1966) states that q can be estimated by m/n.

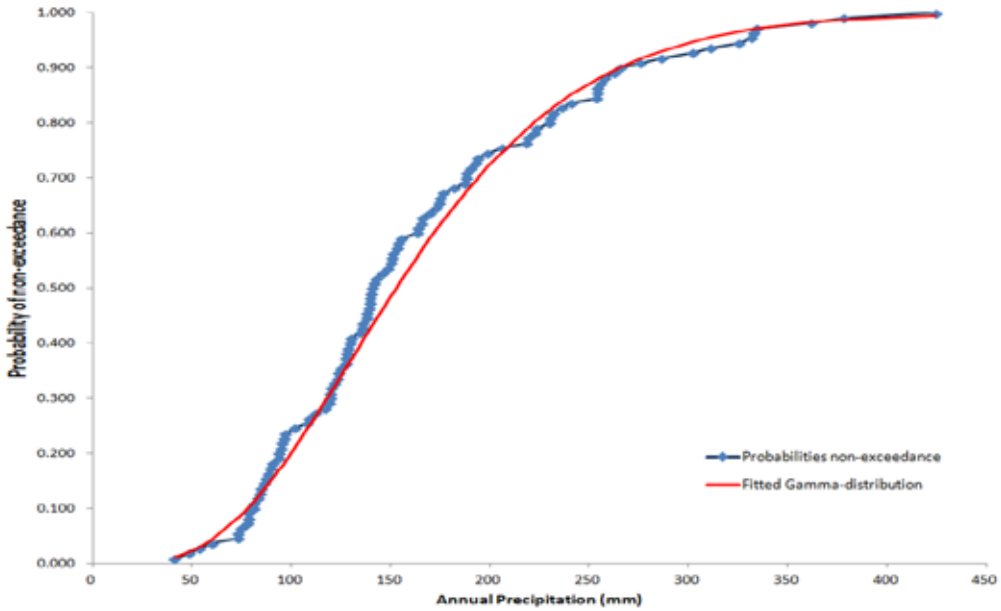

Figure 8. Probabilities of non-exceedance of annual precipitation in Location 276 (Iraq, 33.25°N and 44.25°E): observed (blue) versus modeled by the Gamma-distribution (red)

Using the estimates for α and β equation 1combined with equation 3, Excel allows calculation of cumulative probabilities for each data-point using the function GAMMADIST(x, α, β, cumulative) as follows:

$$P_y = p_{non-zero} * GAMMADIST(y, \alpha, \beta, cumulative) + p_{zero}$$

where
P_y is probability of not exceeding y mm, p_{zero} is probability of zero precipitation, and $p_{non-zero} = 1 - p_{zero}$

Similarly the function GAMMAINV(R,α,β) can be used to calculate the minimum precipitation amounts that can be expected within a given return period as follows:

$$Prec_{min,r} = GAMMAINV(R, \alpha, \beta)$$

where

$Prec_{min,r}$ = precipitation to be exceeded for a given probability of the Gamma function (e.g. 0.25, 0.2),

and R is probability of non-exceedance (e.g. 0.25: one out of four years; 0.1: one out of 10 years).

After calculation in Excel of these variables for each data-point, the relevant columns were imported in ArcGIS, and converted into point vector files. These vector files were then converted to raster with 0.5° resolution. The final maps were produced by resampling the low-resolution rasters to 0.0083333 (30 arc-second) resolution using simple bilinear interpolation.

3.2.1.4. Annual precipitation trends

Linear regression has been used to calculate the annual precipitation trends on the 0.5° grid cells using the following equations:

$$Y = a + bX$$

with

$$b = \frac{\sum_{i}^{N}(X_i - \bar{X})(Y_i - \bar{Y})}{\sum_{i}^{N}(X_i - \bar{X})^2} \text{ and } a = \bar{Y} - b\bar{X}$$

$$r = \frac{(N * \sum_{i}^{N} X_i Y_i) - (\sum_{i}^{N} X_i * \sum_{i}^{N} Y_i)}{\sqrt{(N * \sum_{i}^{N} X_i^2 - (\sum_{i}^{N} X_i)^2) * (N * \sum_{i}^{N} Y_i^2 - (\sum_{i}^{N} Y_i)^2)}}$$

with
X_i: year i
N: number of years
Y_i: precipitation in year i
$\overline{X}$: average of years over period 1901–2010
$\overline{Y}$: average of annual precipitation over period 1901–2010
r: correlation coefficient

Trend precipitation begin period (mm):$a + (b \times 1901$
Trend precipitation end period (mm): $a + (b \times 2010)$
Absolute change of trend precipitation (mm): $b \times 110$

Relative change of trend precipitation: $\frac{Trend\_PrecYr_{2010} - Trend\_PrecYr_{1901}}{Trend\_PrecYr_{2010}} x100$

Statistical significance testing

H0 hypothesis: the calculated value of the sample correlation coefficient is due to random variations in the population (population correlation coefficient ρ = 0)

H1 hypothesis: ρ ≠ 0

Fisher z-transform of the correlation coefficient (Sokal and Rohlf, 1981; REA, 2004):

Population correlation coefficient: $z_F = \frac{1}{2}\ln(\frac{1+r}{1-r})$
$\rho_{H0} = 0$

Population mean: $\mu_{H0} = \ln\frac{1+\rho_{H0}}{1-\rho_{H0}}$

Population standard deviation: $\sigma_{H0} = \sqrt{\frac{1}{N-3}}$

z-score: $Z = \frac{z_F - \mu_{H0}}{\sigma_{H0}}$

H0 is rejected at significance level 0.01 if z > 2.3263 or z < –2.3263

H0 is rejected at significance level 0.05 if z > 1.6449 or z < –1.6449

H0 is rejected at significance level 0.1 if z > 1.2816 or z < 1.2816

H0 is accepted if z ≤1.2816 and z ≥ –1.2816

3.2.1.5. Moving average of the standard deviation

Linear regression was also used to calculate changes in the variability of the annual precipitation. The standard deviation of the annual precipitation for a moving 30-year period was calculated with annual lag (1901–1930, 1902–1931, ...1981–2010). This generated a dataset of 81 data-pairs with the mid-year of each moving period (1916, 1917, ...1996) as X-values and the standard deviations in each period as Y-values.

To this dataset the same procedures for linear regression and statistical significance were applied as for the trend in annual precipitation.

Trend precipitation begin period (mm): $a + (b \times 1916)$

Trend precipitation end period (mm): $a + (b \times 1996)$

Absolute change of trend precipitation (mm): $b \times 81$

Relative change of trend precipitation:

$$\frac{Trend\_PrecYr_{1996} - Trend\_PrecYr_{1916}}{Trend\_PrecYr_{1996}} * 100$$

3.2.2. Drought and wetness periods

Due to the large precipitation variations in space and time an indicator is needed that can be interpreted uniformly across the two countries to assess whether precipitation conditions at any particular time are exceptional, unusual, or normal.

The Standardized Precipitation Index (SPI)[8] is a tool developed primarily for defining and monitoring drought. It allows determining the exceptionality of a drought at a given time scale of interest for

8 The first publication on the SPI was McKee et al. (1993). A good description of the methodology is in Edwards and McKee (1997).

any rainfall station with historic data. It can also be used to determine periods of anomalously wet events. The SPI makes the relative intensities of droughts and wet periods comparable across different climates. A drought condition identified by a certain value of SPI is expected to happen anywhere with comparable frequency. The SPI can be determined relatively easily as it is based on precipitation totals alone, but this is also its main weakness; the index does not take into account differences in evaporative demand or soil moisture storage.

The SPI is used for periods with lengths between one month and several years. For the current study, the annual SPI was mapped for each year of 1901–2010, the reference period for which data are available from the GPCC database (see section 2.2.1.). To compute the index, the same Gamma-distribution, as used for the calculation of precipitation probabilities (section 2.2.2.), is fitted to the non-zero precipitation totals of all the years of the reference period. The fitted distribution, together with the probability of precipitation being greater than zero, permits calculating the probability that a certain precipitation total is exceeded. This probability is then interpreted as applying to a standard normal distribution and converted into a deviation from the mean in multiples of the standard deviation: the SPI.

The SPI is thus created by transformation of the cumulative probability H(x) (equation 3) into a standard normal random variable Z with mean zero and variance of 1. The cumulative probability is transformed into the standard normal variable Z by an approximation method described by Abramowitz and Stegun (1965):

$$Z = SPI = -\left(t - \frac{c_0 + c_1 t + c_2 t^2}{1 + d_1 t + d_2 t^2 + d_3 t^3}\right) \qquad \text{for } 0 < H(x) \leq 0.5$$

$$Z = SPI = +\left(t - \frac{c_0 + c_1 t + c_2 t^2}{1 + d_1 t + d_2 t^2 + d_3 t^3}\right) \qquad \text{for } 0.5 < H(x) \leq 1.0$$

where

$$t = \sqrt{\ln\left(\frac{1}{(H(x))^2}\right)} \qquad \text{for } 0 < H(x) \leq 0.5$$

$$t = \sqrt{\ln\left(\frac{1}{(1-H(x))^2}\right)} \qquad \text{for } 0.5 < H(x) \leq 1$$

and

$c_0 = 2.515517$
$c_1 = 0.802853$
$c_2 = 0.010328$
$d_1 = 1.432788$
$d_2 = 0.189269$
$d_3 = 0.001308$

The transformation of cumulative probabilities, as derived by fitting to the incomplete Gamma function, into the standard normal distribution through the Z-score provides direct information on the expected frequencies of drought or high-rainfall events associated with a certain SPI value (see Table 5).

In practice, extremely dry or wet periods with SPI values < –2 or > +2 tend to occur more frequently than expected according to the theory. This can be due to the effect of years without any precipitation or to the tails of the empirical distribution of precipitation being thicker than those of the fitted Gamma-distribution. In extremely arid areas, with an average annual precipitation of about 10 mm or below, the SPI is without real meaning and spatial interpolation and rounding errors can cause artefacts and interference patterns around grid cells with zero precipitation during a particular year. As mentioned earlier, for this reason all the maps of Annex 7 related to aspects of precipitation patterns, have a mask that shows the spatial extent of the hyper-arid areas.

Table 5. Expected frequencies of SPI values

SPI value	Theoretical frequency from standard normal distribution	Approximate number of years expected for event to happen	SPI class description[9]
> +4.0	3.1671243×10^{-5}	31,574	Extremely wet
> +3.0	0.001349898	741	
> +2.0	0.022750132	44	
> +1.5	0.0668072	15	Very wet
> +1.0	0.15865526	6	Moderately wet
+1.0 to –1.0	0.6826895	2 out of 3	Near normal
< –1.0	0.15865526	6	Moderately dry
< –1.5	0.0668072	15	Very dry
< –2.0	0.022750132	44	Extremely dry
< –3.0	0.001349898	741	
< –4.0	3.1671243×10^{-5}	31,574	

3.3. METHODS USED IN MAPPING CLIMATE CHANGE

3.3.1. GCMs and greenhouse gas emission scenarios

Since the publication of the Fourth Assessment Report (AR4) of the Intergovernmental Panel on Climate Change (IPCC), a broad consensus has developed among the scientific community that climate change is real, has started to show in the current weather, and has a discernible human signature (IPCC, 2007).

GCMs – complex models that emulate the interactions between the atmosphere, land and ocean surfaces, geosphere, biosphere, and human interventions – have been at the forefront in making predictions about climate in a specified future (e.g. 2010–2040 and 2070–2100). These predictions, or rather projections, rely on the relationship between so-called greenhouse gas (GHG) emissions and global warming, and since these emissions depend largely on human 'behavior', it is standard practice to run the climate models under specific GHG emission assumptions.

The three most commonly used scenarios for assessing the impact of climate change are the SRES [10] scenarios A1b, A2, and B1 (IPCC, 2007). The following description of these scenarios is taken from the IPCC summary report.

A1. The A1 storyline and scenario family describes a future world of very rapid economic growth, global population that peaks in mid-century and declines thereafter, and the rapid introduction of

9 Drought/wetness class terminology follows the National Drought Monitoring Center classification of drought. Colors used in this table are the same as in the SPI maps (Annex 4)

10 SRES: Special Report on Emission Scenarios

new and more efficient technologies. Major underlying themes are convergence among regions, capacity-building, and increased cultural and social interactions, with a substantial reduction in regional differences in per capita income. The A1 scenario family develops into three groups that describe alternative directions of technological change in the energy system. The A1b scenario assumes a balance between fossil-intensive and non-fossil energy sources, where balance is defined as not relying too heavily on one particular energy source, on the assumption that similar improvement rates apply to all energy supply and end-use technologies.

A2. The A2 storyline and scenario family describes a very heterogeneous world. The underlying theme is self-reliance and preservation of local identities. Fertility patterns across regions converge very slowly, which results in continuously increasing population. Economic development is primarily regionally oriented and per capita economic growth and technological change more fragmented and slower than other storylines.

B1. The B1 storyline and scenario family describes a convergent world with the same global population, that peaks in mid-century and declines thereafter, as in the A1 storyline, but with rapid change in economic structures towards a service and information economy, with reductions in material intensity and the introduction of clean and resource-efficient technologies. The emphasis is on global solutions to economic, social, and environmental sustainability, including improved equity, but without additional climate initiatives.

A1b is the middle-of-the-road GHG emission scenario, A2 the more pessimistic, and B1 the more optimistic scenario. With no progress on reducing GHG emissions, the A2 scenario is now being considered more realistic, whereas A1b is slowly becoming the 'optimistic' scenario and B1 a kind of 'pie-in-the-sky' scenario. **For this reason only scenarios A1b and A2 were considered relevant to the studies in Iraq and Jordan.**

The IPCC's AR4 is based on simulations of 21 GCM models. Since the IPCC published its first Assessment Report in 1990, these three-dimensional mathematical representations of the processes responsible for climate have grown in complexity, and are now able to model the complex interactions between atmosphere, land surface, oceans, and sea ice (Fig. 9), and to simulate global distributions of temperature, winds, cloudiness, and precipitation.

Despite increasing sophistication, there are still considerable differences between the predictions of different models originating from different research groups. For this reason it is important to select those models considered the most appropriate for developing adaptation strategies or, alternatively, to apply a kind of averaging process of the output from different GCMs to obtain a middle-of-the-road prediction.

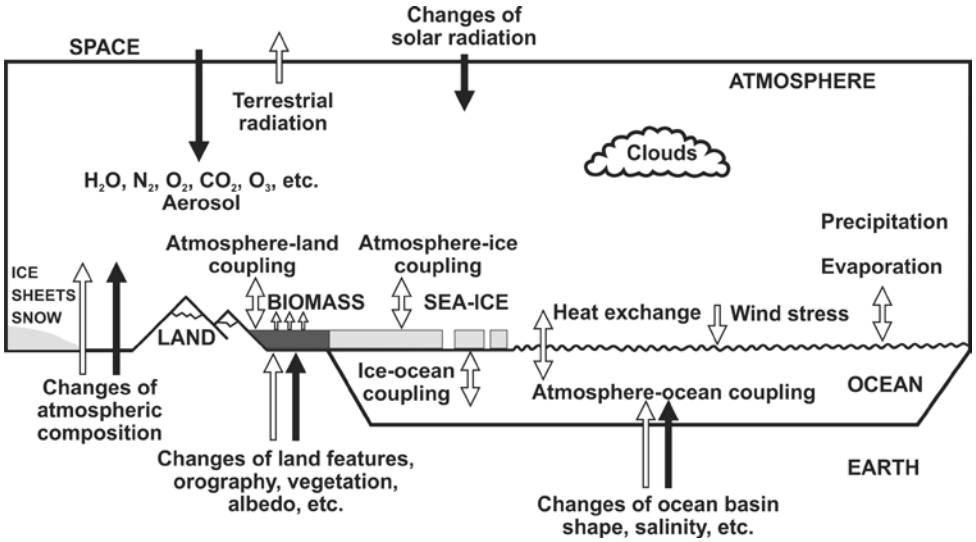

Figure 9. Schematic representation of a typical GCM

Given these divergences in output between individual GCMs, the choice was made to average the outputs from seven individual GCMs, selected on the basis of the following criteria: date of publication, spatial resolution, and public availability of datasets including precipitation and temperature for a 'near future' covering the period 2010–2040 (Table 6).

Table 6. GCM models used in the study

No.	Name	Country	Year	Resolution in degrees + (levels)	Source
01	BC-CR-BCM2.0	Norway	2005	2.8 × 2.8 (31)	http://www.ipcc-data.org/ https://esg.llnl.gov:8443/home/publicHomePage.do
02	CSIRO-MK3.0	Australia	2001	1.9 × 1.9 (18)	http://www.ipcc-data.org/ https://esg.llnl.gov:8443/home/publicHomePage.do
04	MIROC3.2	Japan	2004	2.8 × 2.8 (20)	http://www.ipcc-data.org/
08	CG-CM3.1(T63)	Canada	2005	2.8 × 2.8 (31)	http://www.ipcc-data.org/ http://www.cccma.ec.gc.ca/data/cgcm3/cgcm3.shtml
09	CNRM-CM3	France	2005	2.8 × 2.8 (45)	http://www.ipcc-data.org/ https://esg.llnl.gov:8443/home/publicHomePage.do http://www.mad.zmaw.de/projects-at-md/ensembles/experiment-list-for-stream-1/cnrm-cm3/
10	ECHAM5/MPI-OM	Germany	2003	1.9 × 1.9 (31)	http://www.ipcc-data.org/
12	GFDL-CM2.0	USA	2005	2 × 2.5 (24)	http://www.ipcc-data.org/

The 2010–2040 low-resolution climate change gridded datasets were downloaded from the IPCC Data Distribution Centre (http://www.ipcc-data.org/) in NetCDF format and were converted into formats suitable for processing in GIS.

3.3.2. Spatial downscaling

The coarse resolution of GCMs is perhaps the main bottleneck for planning of adaptation to climate change, as it prevents linkage to features with variability at much finer spatial variability, such as arable land, water resources, human settlements, agricultural production systems, and poverty hot-spots. Downscaling the output of GCMs is therefore extremely important for mainstreaming climate change projections into development planning. The specific approach to spatial downscaling is explained in this section.

3.3.2.1. GCM data processing

The transformation of GCM data into high-resolution climate maps is no trivial matter and required the following steps, as explained in the following sections:

- Data extraction procedures
- Change mapping at coarse resolution
- Resampling
- Correcting the precipitation maps
- Generating downscaled climate surfaces
- Calculating averages
- Calculating relative change
- Calculating change in seasonal precipitation

3.3.2.1.1. Data extraction procedures

Datasets for each GCM were retrieved from the sources mentioned above in a NetCDF format (.nc), a self-describing format for weather and climate data files, developed by UCAR[11]. 'Self-describing' means that a header describes the layout of the rest of the file, in particular the data arrays, as well as arbitrary file metadata in the form of name/value attributes. This file structure is particularly suitable for creating, accessing, and sharing array-oriented scientific data across networks with multiple platforms and software. The relevant data were extracted from these files using the program GrADS[12] (for Grid Analysis and Display System), which runs under Linux platforms.

The specific extraction procedure depended on the type of datasets. Data from the IPCC data portal website were merely extracted without any additional averaging. Monthly data from the ESG website were averaged over 30 years for the three periods of interest. Daily data were first averaged over the months of each year, and then averaged over each set of 30 years.

Some datasets had a calendar format incompatible with GrADS. This concerns (partly or entirely) the following GCMs: CSIRO-MK3.0, CGCM3.1 T47 and T63, PCM, and GISS-ER. To render them compatible, the descriptor files of these datasets were modified using the programs Ncdump and Ncgen[13]. Since the data extraction was based on day numbers rather than dates, calendar options could then be simply ignored.

For datasets containing different runs without average, averaging over the different runs was done in the GIS software ArcGIS[14].

11 http://www.unidata.ucar.edu/software/netcdf/
12 http://www.iges.org/grads/
13 http://www.unidata.ucar.edu/software/netcdf/workshops/2009/utilities/NcgenNcdump.html
14 http://www.esri.com/software/arcgis/index.html

To save downloading time and disk space, data were only downloaded for one-quarter of the globe (0–90°N, 0–180°E).

For precipitation and mean temperature the data were extracted for seven GCM models in Table 3: 01, 02, 04, 08, 09, 10, and 12.

For maximum and minimum temperature under GHG emission scenario A1b, data were used for GCM models 01, 02, 04, 08, and 09. No data were available for GCM model 12 and the data for GCM model 10 were unreliable. For maximum and minimum temperature under GHG scenario A2 data were used for GCM models 01, 02, 04, 08, and 09. No data were available for GCM models 10 and 12.

3.3.2.1.2. Change mapping at coarse resolution

After computing every monthly average for each climatic variable, GHG scenario and time horizon, the averages were subtracted by the grid of the period 1961–1990 (also a GCM output) in the case of temperature data. In the case of precipitation data, the ratio was computed.

For mean, minimum, and maximum temperature (°C): $\Delta T = T_{LR,21} - T_{LR,20}$

For precipitation (dimensionless): $r_{prec} = P_{LR,21} / P_{LR,20}$

with LR (low-resolution), 20: twentieth century data, and 21: twenty-first century data.

The change in temperature is thus expressed in absolute terms, while the change in precipitation is relative.

Change mapping was carried out in GrADS for compatible temperature data, and in ArcGIS in the case of non-compatible temperature formats and precipitation.

One GCM model (ECHAM5/MPI-OM) contained too many missing data in the area of interest during the months June–August. No grids were generated for this model during these months. For other GCMs missing data in particular pixels were filled up by using the mean of the surrounding pixels using the Neighborhood function in the ArcGIS software.

3.3.2.1.3. Resampling

To refine the coarse climate change raster maps, a resampling was carried out in ArcGIS down to a resolution of 0.008333 decimal degrees (about 1 km). This resolution corresponds to that of the reference climate maps of the study area.

The method for resampling was the cubic convolution method. With this method, new pixel values are computed based on a weighted average of the 16 nearest pixels of the original map (4 × 4 window). This method is relatively time-consuming but offers a smoother appearance than other available methods (nearest neighbor or bilinear interpolation). Possible edge effects (where the 16 pixel values are not all available) were avoided by selecting an area of interest larger than the study area. In our case the resampling of the climate change maps was carried out in ArcGIS over the rectangle 0–55°N × 3–64°E.

3.3.2.1.4. Corrections of precipitation maps

As we used a ratio to represent the change in precipitation, corrections of the coarse-gridded change maps were needed in two cases.

For some areas, GCMs regularly predicted an average of 0 mm of precipitation for both the reference

period and the future period under consideration. Calculating the precipitation ratio would therefore lead to indeterminate expressions. To counter this problem, precipitation was assumed not to be lower than a certain threshold value, which in our case was fixed at 0.0167 mm (or 6.43×10^{-8} kg m^{-2} s^{-1}), corresponding to a total amount of rainfall of 1 mm in 60 years. Values of simulations of both twentieth and twenty-first centuries that were < 0.0167 mm were raised to that value, to allow change to be computed.

A second issue is that the cubic convolution method for resampling sometimes produces negative values of relative change when the original values are close to 0 mm. The solution to obtain only positive values is to resample using the logarithm of the original values, and obtain the final change grids by exponential transformation of the latter layers.

3.3.2.1.5. Generating downscaled climate surfaces of precipitation and temperature

The process consisted of modifying the generated high-resolution surfaces of current climate (see section 3.2.) using the resampled change maps.

Downscaled high-resolution (1 km) monthly climate surfaces for the period 2010–2040 were thus obtained for each GCM and scenario by adding the resampled monthly change maps to the monthly high-resolution reference climate surfaces for temperature variables, and by multiplying for precipitation.

The calculations were performed in ArcGIS using simple raster algebra according to the formulas:

- For mean, minimum, and maximum temperature (°C): $T_{HR,2} = T_{HR,0} + \Delta T_{resampled}$
- For precipitation (mm): $P_{HR,2} = P_{HR,0} * r_{resampled}$
  with HR: high resolution.

3.3.2.1.6. Calculating averages

Given the vast amount of data generated and the divergence between the results from the selected GCMs, it made sense to create predictive maps based on the average of the selected GCMs.

Averages from the seven GCMs were computed for the resampled high-resolution change maps of precipitation and mean, maximum, and minimum temperature during each month and over the year, the winter, spring, summer, and autumn under the two emission scenarios A1b and A2. The winter period covers the months December–February, spring includes March–May, while summer covers June–August, and autumn September–November.

3.3.2.1.7. Relative change of precipitation

Based on the high-resolution maps of both current and future precipitation, high-resolution maps were prepared of the relative change between future and current precipitation, using ArcGIS raster algebra in accordance with the following formula:

$$relative\ change\ (\%) = \left(\frac{Prec_{cc}}{Prec_{cur}} - 1\right) * 100$$

with cc: climate change
cur: current climate.

Relative change maps were created on a monthly basis, for spring, summer, autumn, and winter and for the entire year.

3.3.2.1.8. Change in seasonal precipitation

The seasonal precipitation pattern can be represented as a percentage of the mean annual precipitation. If this percentage changes significantly, a shift in the pattern of seasonal precipitation can be deduced. Thus, to visualize changes in seasonal precipitation patterns, it is sufficient to take the difference in the percentage share of each season in the annual total. Such change in seasonal precipitation was calculated for winter, spring, summer, and autumn, as follows:

$$\left(\frac{Prec_{seas,cc}}{Prec_{yr,cc}} - \frac{Prec_{seas,cur}}{Prec_{yr,cur}}\right) * 100$$

with cc: climate change
cur: current climate
seas: the particular season (e.g. winter, spring...)
yr: annual total.

3.3.2.2. Derived climatic variables

The following derived variables were produced for the time frame 2010–2040 under the two GHG scenarios:

- Climatic zones according to the Köppen classification system
- PET (mm) on monthly and annual basis
- Aridity index on annual basis
- Agroclimatic zones
- Growing periods

3.3.2.2.1. Köppen zones

Using the projected precipitation and temperature values for 2010–2040 under scenarios A1b and A2, it was possible to map the Köppen zones for these futures.

3.3.2.2.2. PET

Using the projected temperatures for 2010–2040 and the same relationships between monthly Tmean, Tmax, Tmin, PET_{Har}, and PET_{Pen} as explained in section 3.1.4., it was possible to map the changes in PET_{Pen} for scenarios A1b and A2. The relative changes (%) between annual PET under current climatic conditions and PET under respective scenarios A1b and A2 were calculated as follows:

$$relative\ change\ (\%) = \left(\frac{PET_{cc}}{PET_{cur}} - 1\right) * 100$$

3.3.2.2.3. Aridity index

By taking the ratio of the projected annual precipitation and projected annual PET-Penman–Monteith in 2010–2040, the aridity index (for definition and calculation see section 3.1.5.) was mapped for scenarios A1b and A2.

The absolute changes in the aridity index between current conditions and 2010–2040 were calculated for each pixel by subtracting the aridity index for the current period from the aridity index for

2010–2040.

3.3.2.2.4. Agroclimatic zones

Changes in agroclimatic zones were assessed on the basis of changes in their defining criteria (moisture regime, winter type, and summer type) for both future scenarios.

3.3.2.2.5. Growing periods

The changes in these three growing period components were obtained by subtraction of the growing period lengths in the current climate from those in 2010–2040/scenario A1b and from those in 2010–2040/scenario A2.

4. RESULTS

4.1. CURRENT CLIMATE

4.1.1. Precipitation

Figure 10 shows the mean annual precipitation in the WOI.

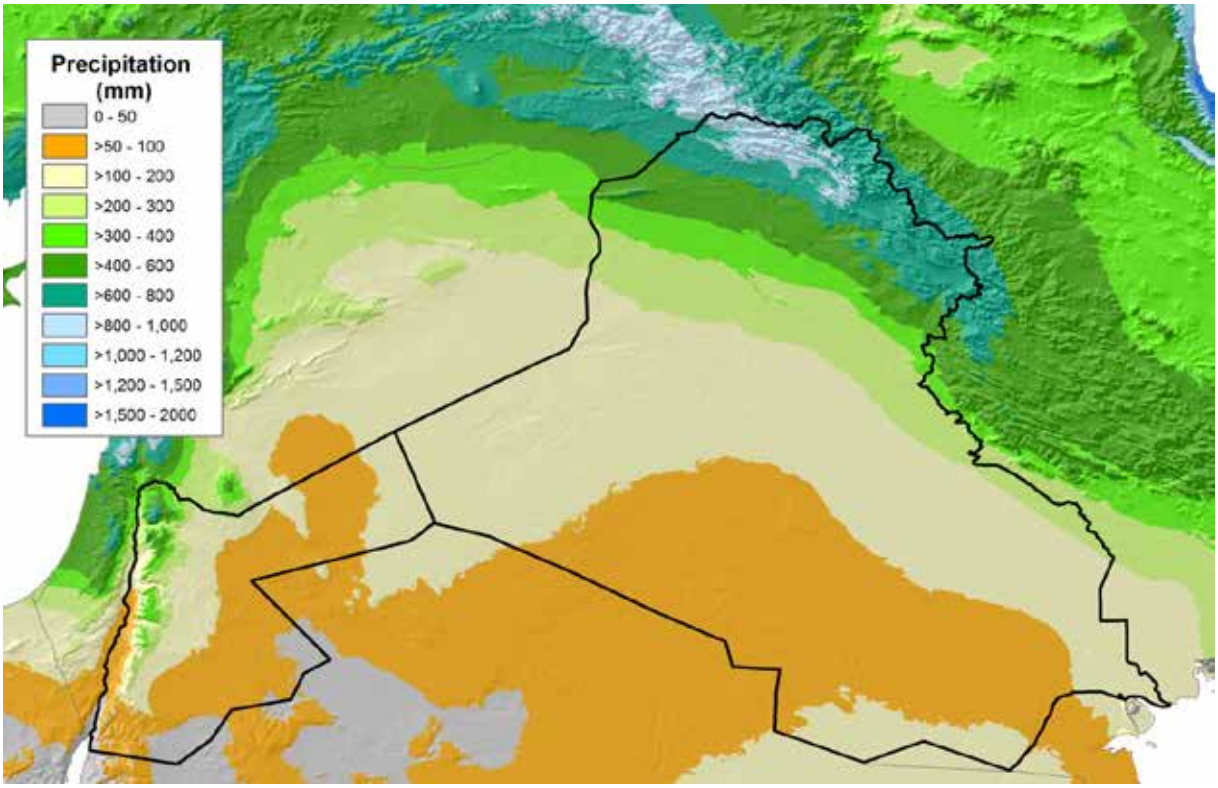

Figure 10. Mean annual precipitation (period 1970–2000)

Figure 11 presents the mean precipitations for winter (December–February), spring (March–May), summer (June–August), and autumn (September–November). The seasonal differences in precipitation are very obvious, with the highest levels in winter, followed by spring and autumn, and near zero levels in summer.

4.1.2. Temperature

The mean maximum and minimum temperatures for the four seasons are shown in Figures 12 and 13, respectively. The seasonal temperature patterns are typical for areas with a Mediterranean climate at low elevation (especially in Iraq) and medium elevation (especially in Jordan).

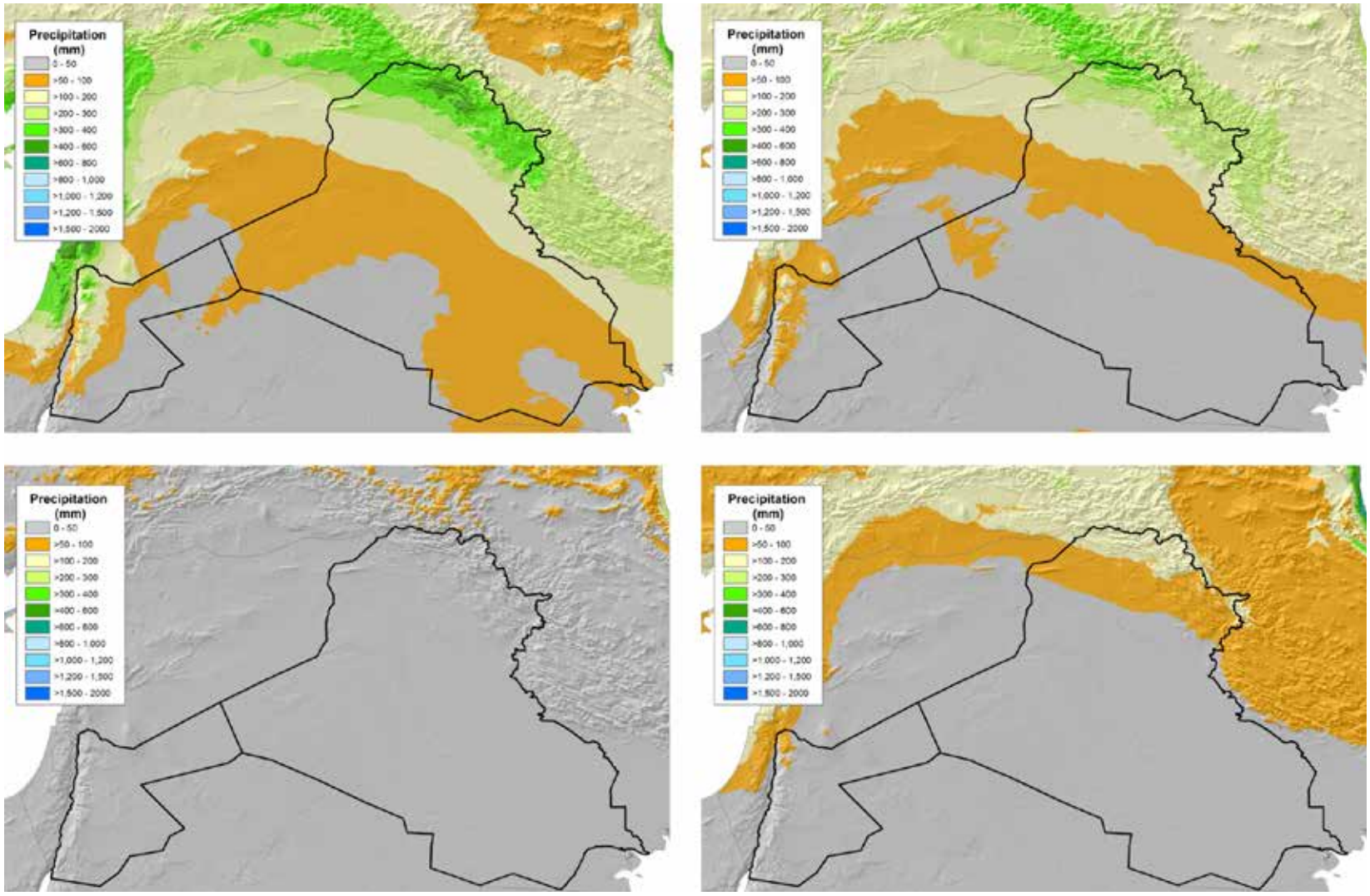

<u>Figure 11.</u> Seasonal mean precipitation (top left: winter; top right: spring; bottom left: summer; bottom right: autumn)

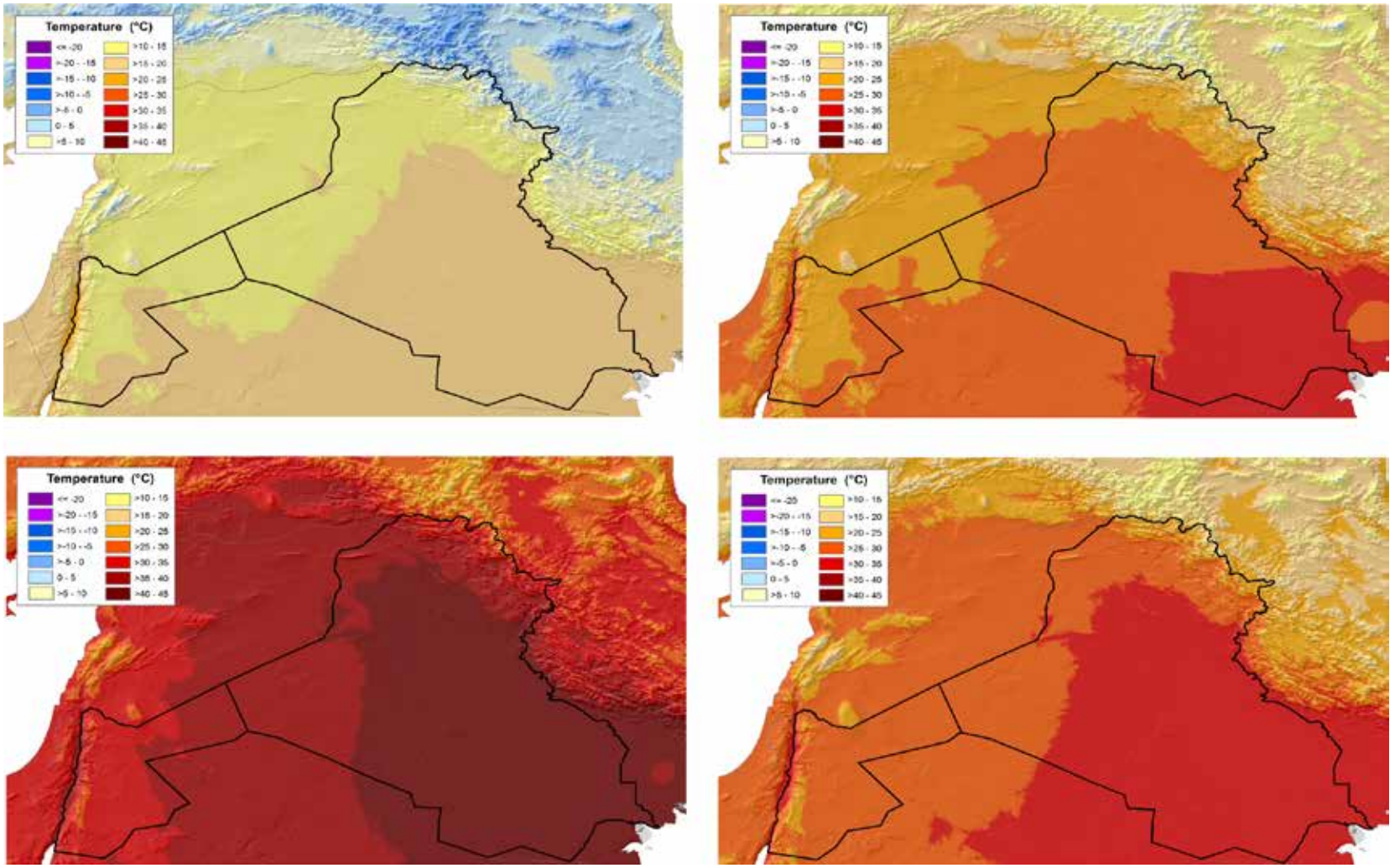

Figure 12. Seasonal mean maximum temperature (top left: winter; top right: spring; bottom left: summer; bottom right: autumn)

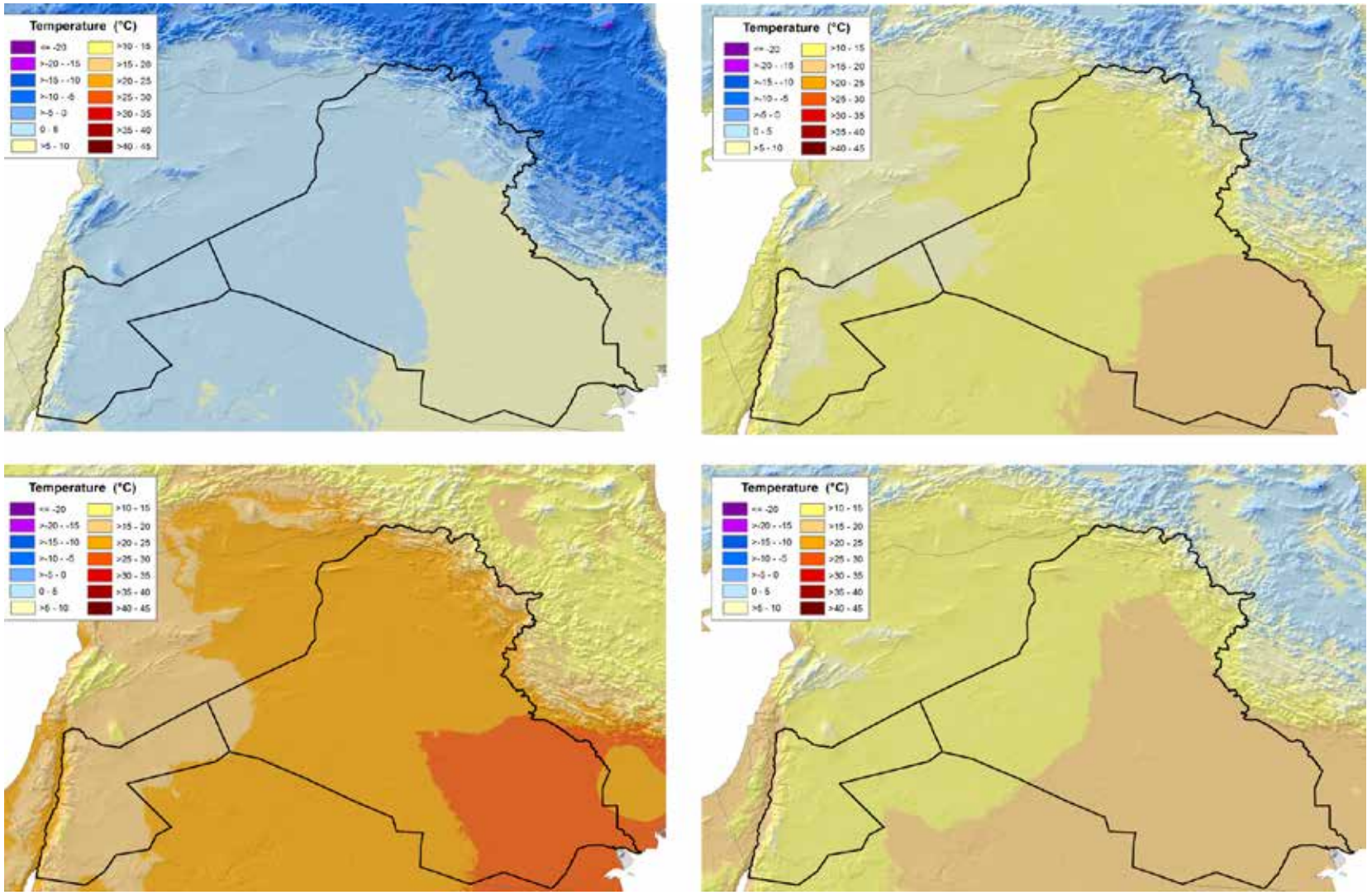

<u>Figure 13.</u> Seasonal mean minimum temperature (top left: winter; top right: spring; bottom left: summer; bottom right: autumn)

4.1.3. Climatic zones according to the Köppen system

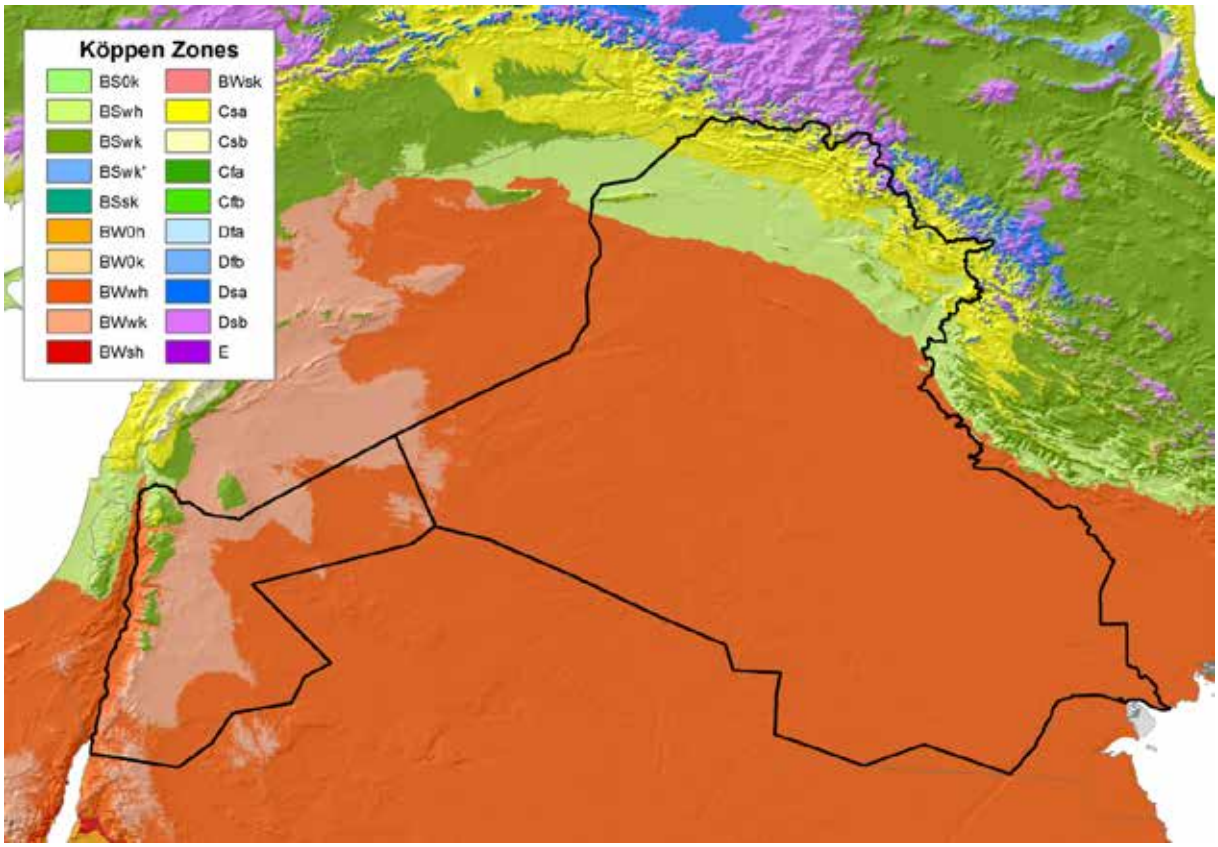

Figure 14. Köppen climatic zones

In the WOI, 20 Köppen zones can be differentiated (Fig. 14), showing the very diverse climatic conditions in this part of the world. However, for Iraq and Jordan proper, the picture is more homogeneous. Table 7 provides a listing and short description of all subdivisions of the Köppen system that currently occur within Iraq and Jordan. For the detailed characterization of all zones on the map of Figure 13, refer to Annex 2.

Table 7. Prevalence (%) of Köppen climatic zones in Iraq and Jordan

Zone	Map code	Description	Iraq	Jordan
BSwh	11	Hot semi-arid (steppe) climate, winter precipitation	9.0	1.0
BSwk	12	Cool semi-arid (steppe) climate, winter precipitation	0.3	3.7
BWwh	24	Hot arid (desert) climate, winter precipitation	83.0	57.2
BWwk	25	Cool arid (desert) climate, winter precipitation	0.7	37.8
Csa	36	Warm temperate rainy climate with dry and hot summer	6.4	0.3
Dsa	53	Subarctic climate with humid winter and hot summer	0.3	
Dsb	54	Subarctic climate with humid winter and warm summer	0.3	

4.1.4. PET

Annual PET patterns are shown in Figure 15 in the form of 10 classes. These patterns are strongly related to elevation, and therefore to temperature, as expected.

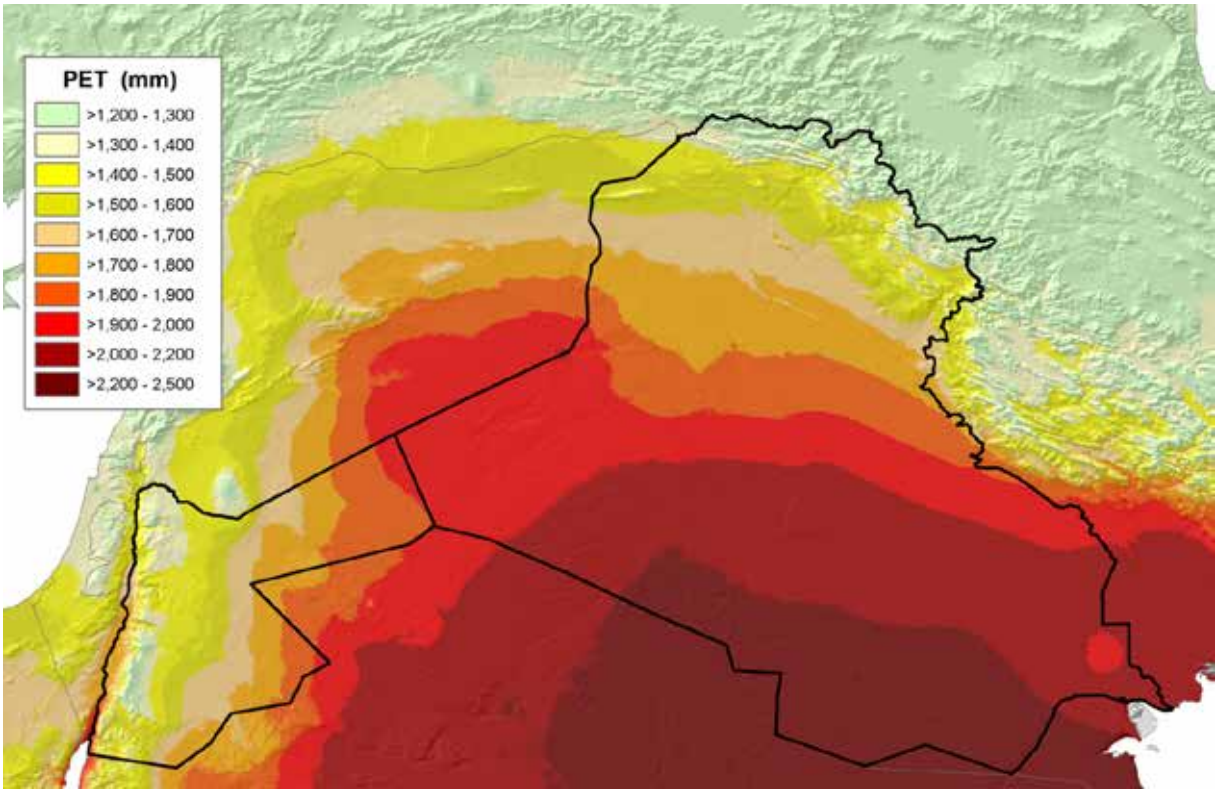

Figure 15. Annual potential evapotranspiration (PET)

The relative prevalence of different PET classes in Iraq and Jordan is shown in Table 8. These figures clearly indicate that the evaporative demand of the atmosphere, as expressed by PET, is significantly higher in Iraq than in Jordan. To produce the same crops, more water is therefore needed in Iraq, to be provided by either precipitation or irrigation.

Table 8. Prevalence (%) of annual PET classes in Iraq and Jordan

PET class	Iraq	Jordan
> 1200–1300	1.4	1.8
> 1300–1400	2.1	9.4
> 1400–1500	3.7	16.4
> 1500–1600	4.8	13.5
> 1600–1700	6.2	17.7
> 1700–1800	8.6	20.5
> 1800–1900	8.6	17.3
> 1900–2000	20.3	3.3
> 2000–2200	27.5	0.1
> 2200–2500	16.8	0.0

4.1.5. Aridity index

Figure 16 shows the pattern of aridity in Iraq and Jordan, expressed by the annual aridity index, in the form of five classes. Table 9 shows the estimates the share of each class in Iraq and Jordan.

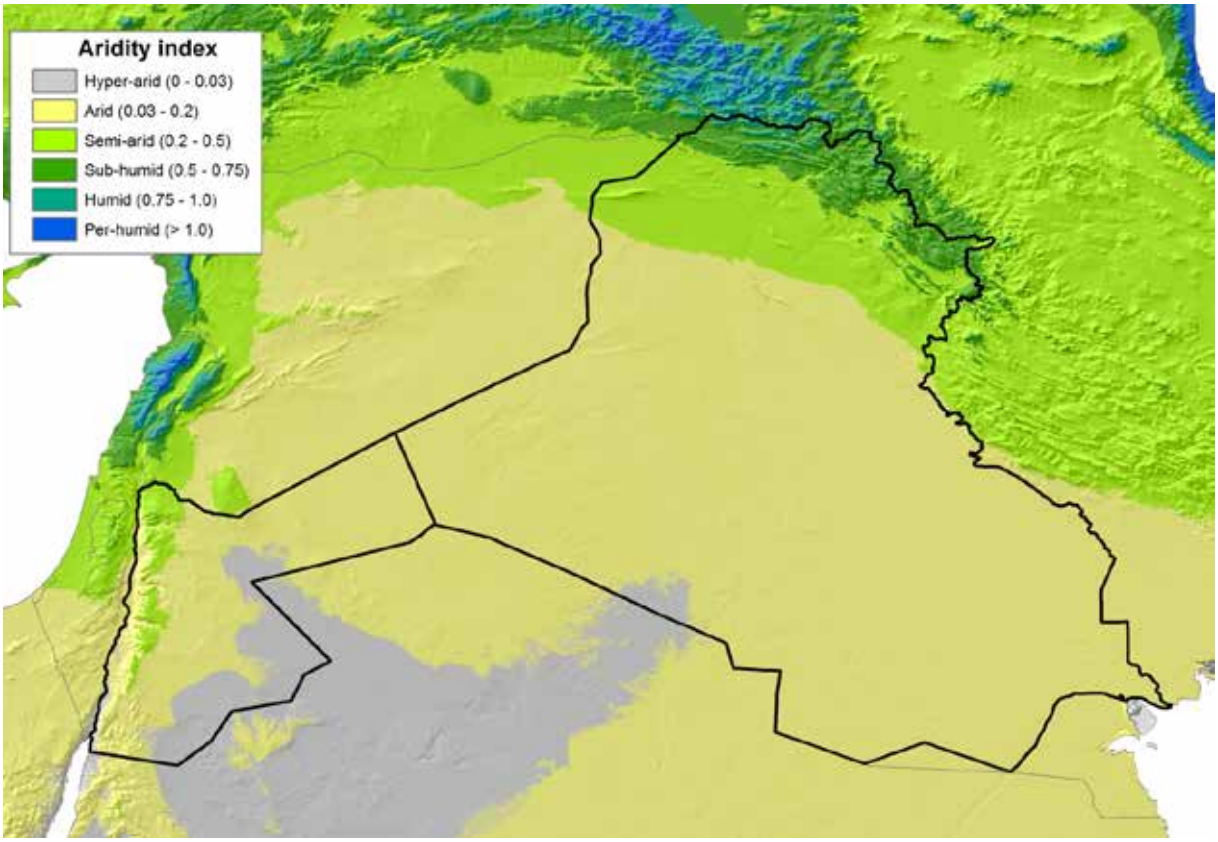

Figure 16. Aridity index classes

Table 9. Prevalence (%) of annual aridity index classes in Iraq and Jordan

Aridity index class	Jordan	Iraq
Hyper-arid (0–0.03)	0.8	24.3
Arid (0.03–0.2)	81.5	68.1
Semi-arid (0.2–0.5)	12.1	7.5
Sub-humid (0.5–0.75)	5.1	0.1
Humid (0.75–1.0)	0.5	0.0
Per-humid (> 1.0)	0.0	0.0

In both Iraq and Jordan aridity prevails, with the highest levels in Iraq. The share of land in which rain-fed agriculture is climatically feasible is therefore very low, with only 18% in Jordan and < 8% in Iraq. Much is of this land, moreover, is located in mountainous areas where other constraints prevail, such as steep slopes and shallow or stony soils.

4.1.6. Agroclimatic zones according to the UNESCO system

The complex nature of agricultural climates in the WOI is clear from Figure 17. Table 10 indicates that, of these, the most common agroclimatic zones in Iraq are A-C-VW and A-M-VW, together occupying 77% of the country, whereas in Jordan zones A-C-W and HA-C-W occupy 85%.

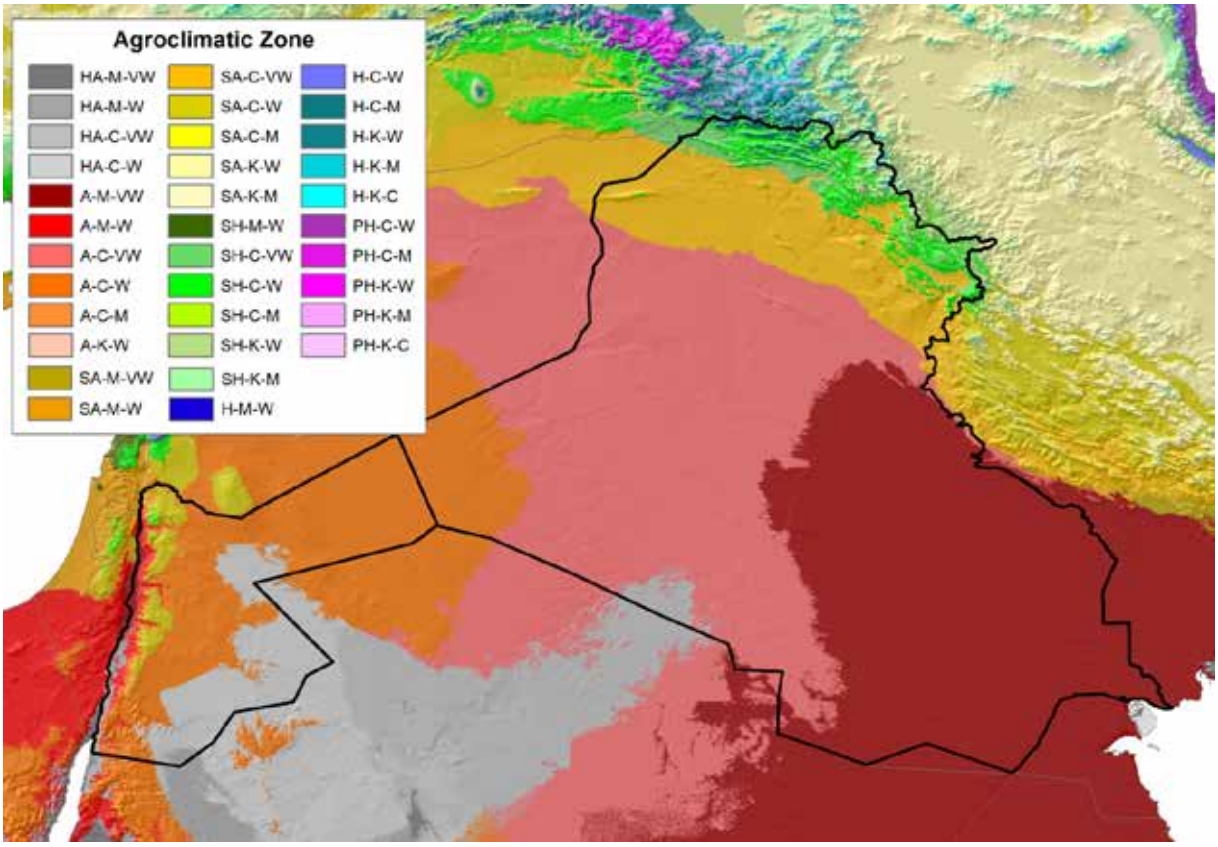

Figure 17. Agroclimatic zones

Table 10. Prevalence (%) of agroclimatic zones in Iraq and Jordan

Code	ACZ	Description	Iraq	Jordan
3	HA-M-VW	Hyper-arid climate with mild winters and very warm summers	0.0	0.4
4	HA-M-W	Hyper-arid climate with mild winters and warm summers	0.0	2.0
6	HA-C-VW	Hyper-arid climate with cool winters and very warm summers	1.0	0.0
7	HA-C-W	Hyper-arid climate with cool winters and warm summers	0.0	26.3
16	A-M-VW	Arid climate with mild winters and very warm summers	37.2	1.5
17	A-M-W	Arid climate with mild winters and warm summers	0.0	3.5
19	A-C-VW	Arid climate with cool winters and very warm summers	39.9	0.0
20	A-C-W	Arid climate with cool winters and warm summers	4.7	59.0
30	SA-M-W	Semi-arid climate with mild winters and warm summers	0.0	0.7
32	SA-C-VW	Semi-arid climate with cool winters and very warm summers	11.2	0.0
33	SA-C-W	Semi-arid climate with cool winters and warm summers	0.2	6.4
45	SH-C-VW	Sub-humid climate with cool winters and very warm summers	1.2	0.0
46	SH-C-W	Sub-humid climate with cool winters and warm summers	2.9	0.2
50	SH-K-W	Sub-humid climate with cold winters and warm summers	1.1	0.0
51	SH-K-M	Sub-humid climate with cold winters and mild summers	0.1	0.0
63	H-K-W	Humid climate with cold winters and warm summers	0.4	0.0
64	H-K-M	Humid climate with cold winters and mild summers	0.1	0.0
76	PH-K-W	Per-humid climate with cold winters and warm summers	0.0	0.0
77	PH-K-M	Per-humid climate with cold winters and warm summers	0.0	0.0

4.1.7. Growing periods

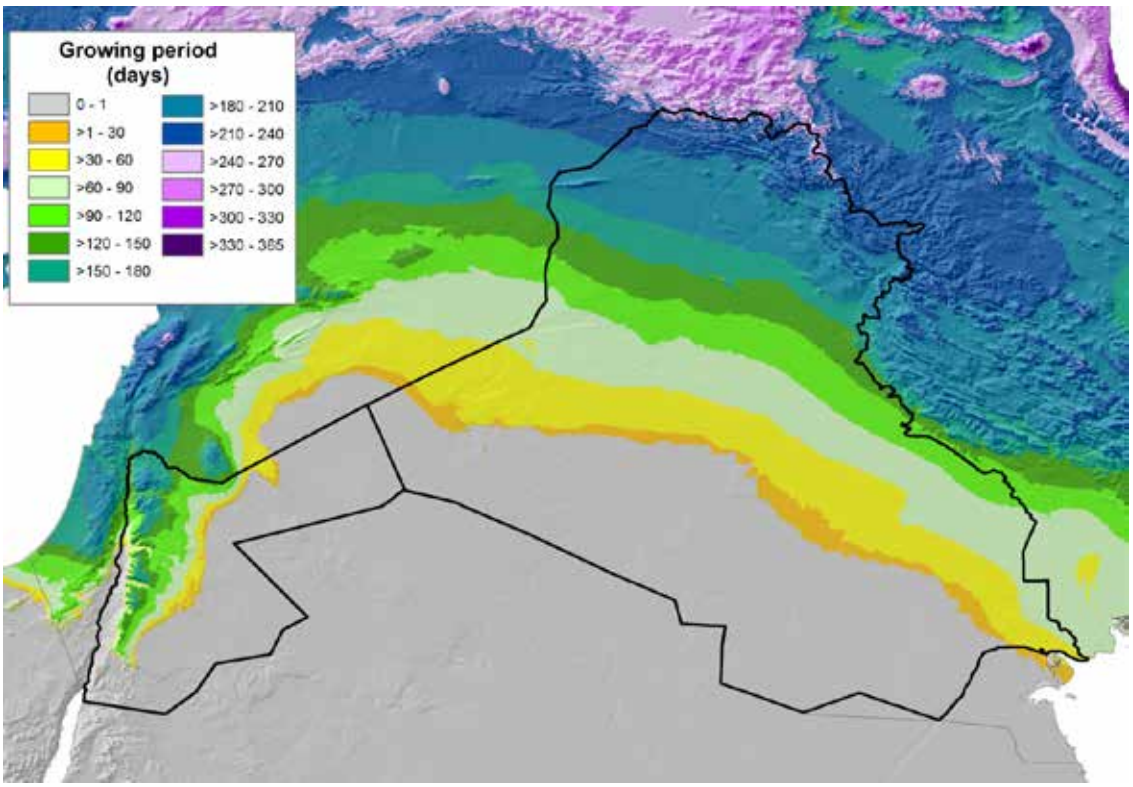

Figure 18. Moisture-limited growing period

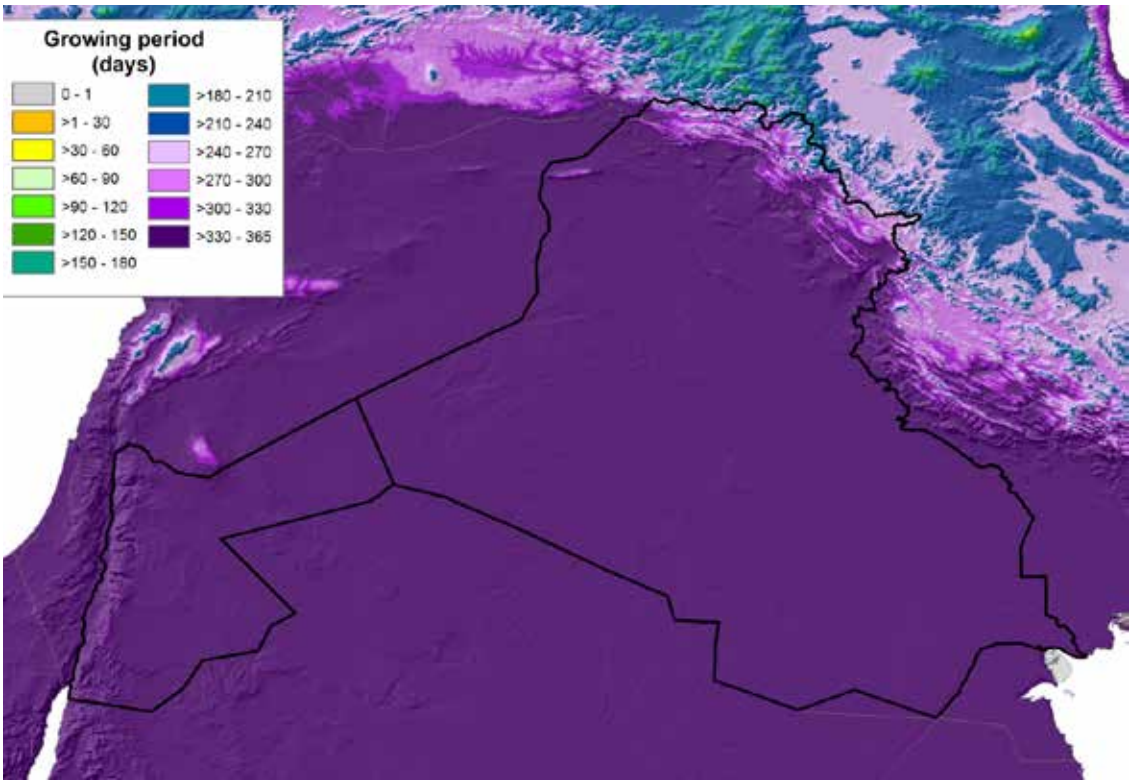

Figure 19. Temperature-limited growing period

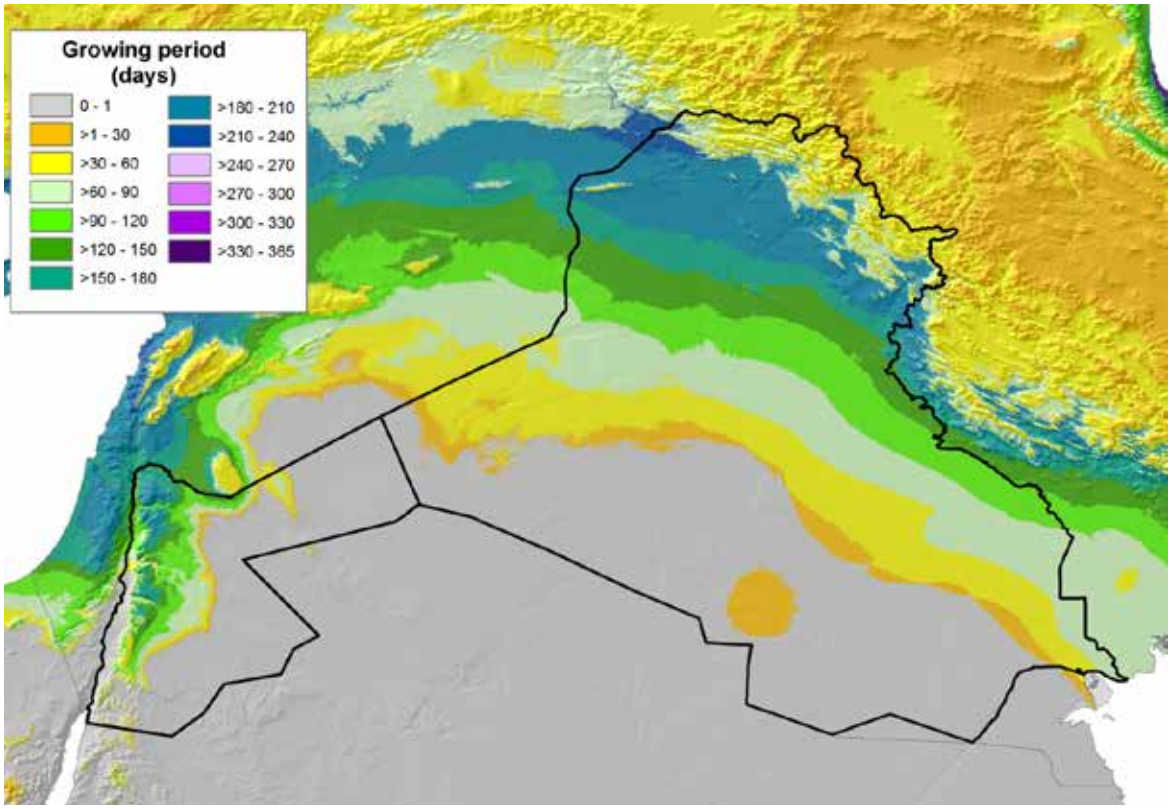

Figure 20. Main moisture- and temperature-limited growing period

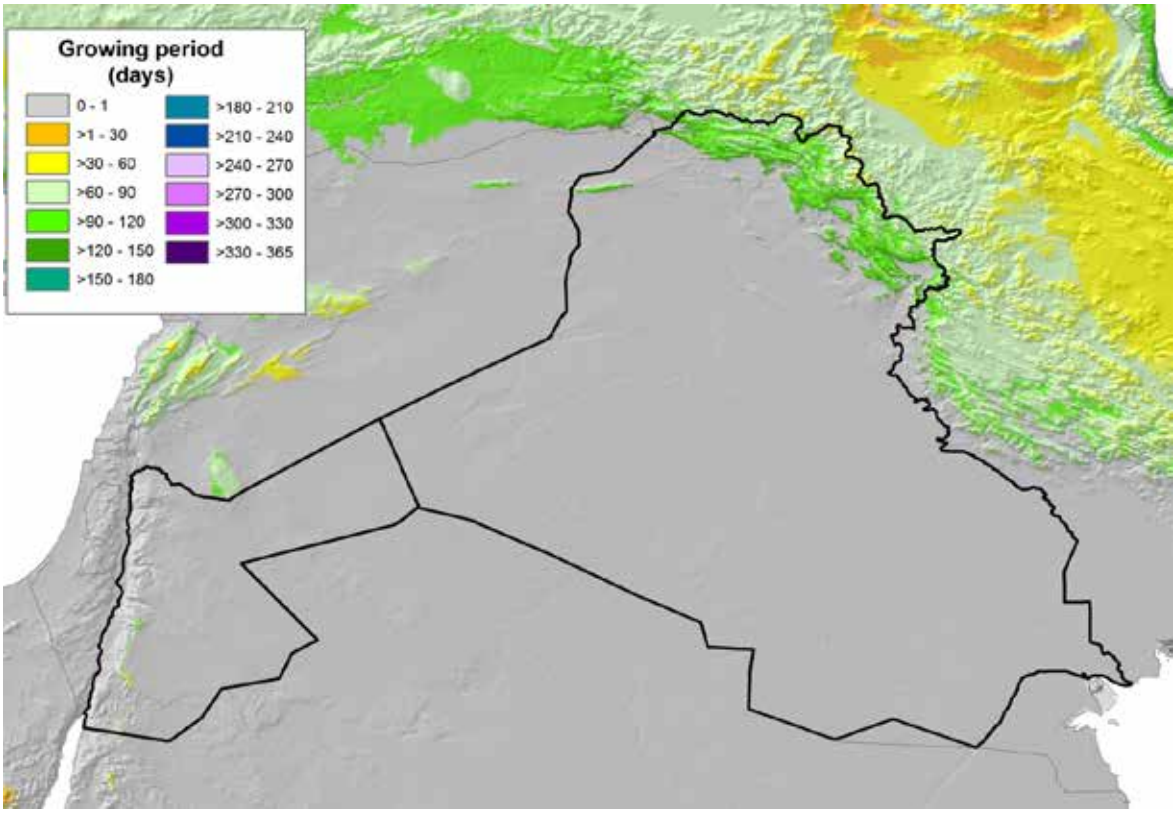

Figure 21. Secondary moisture- and temperature-limited growing period

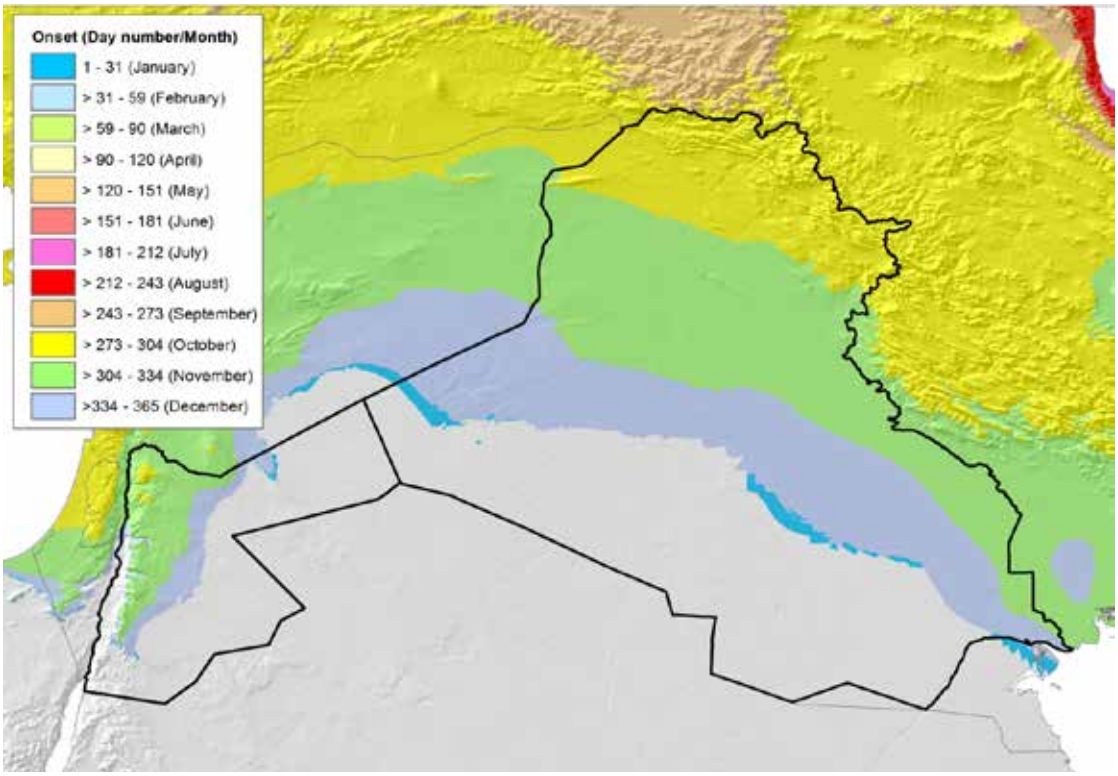

Figure 22. Onset month of the main moisture- and temperature-limited growing period

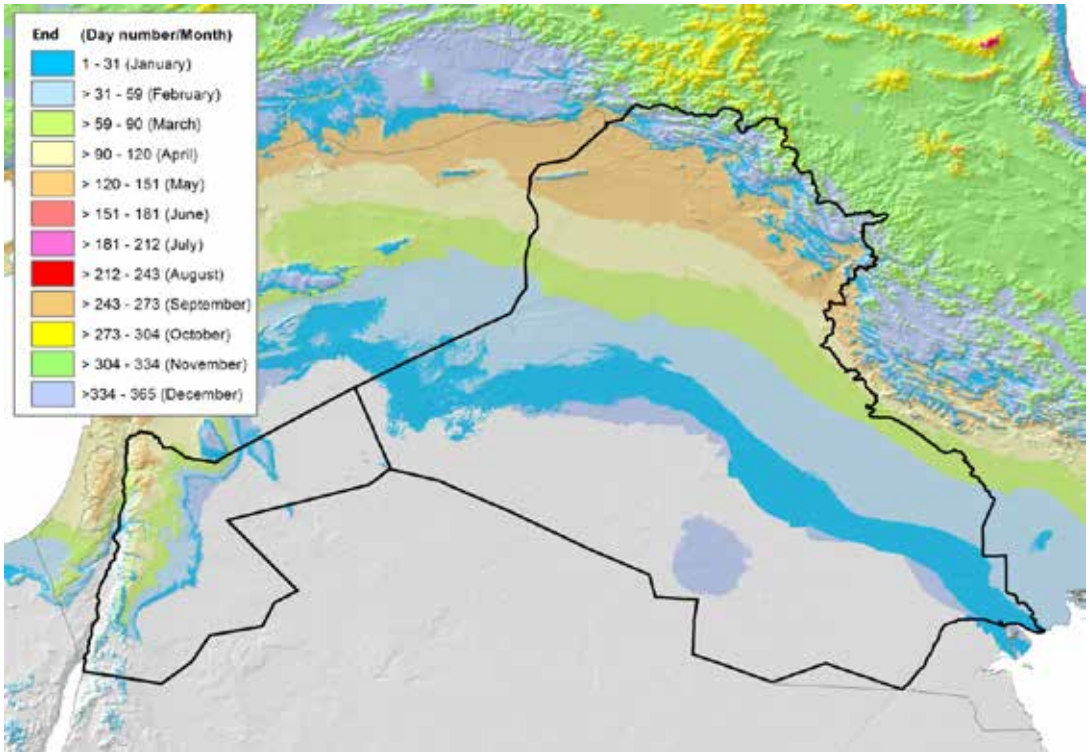

Figure 23. End month of the main moisture- and temperature-limited growing period

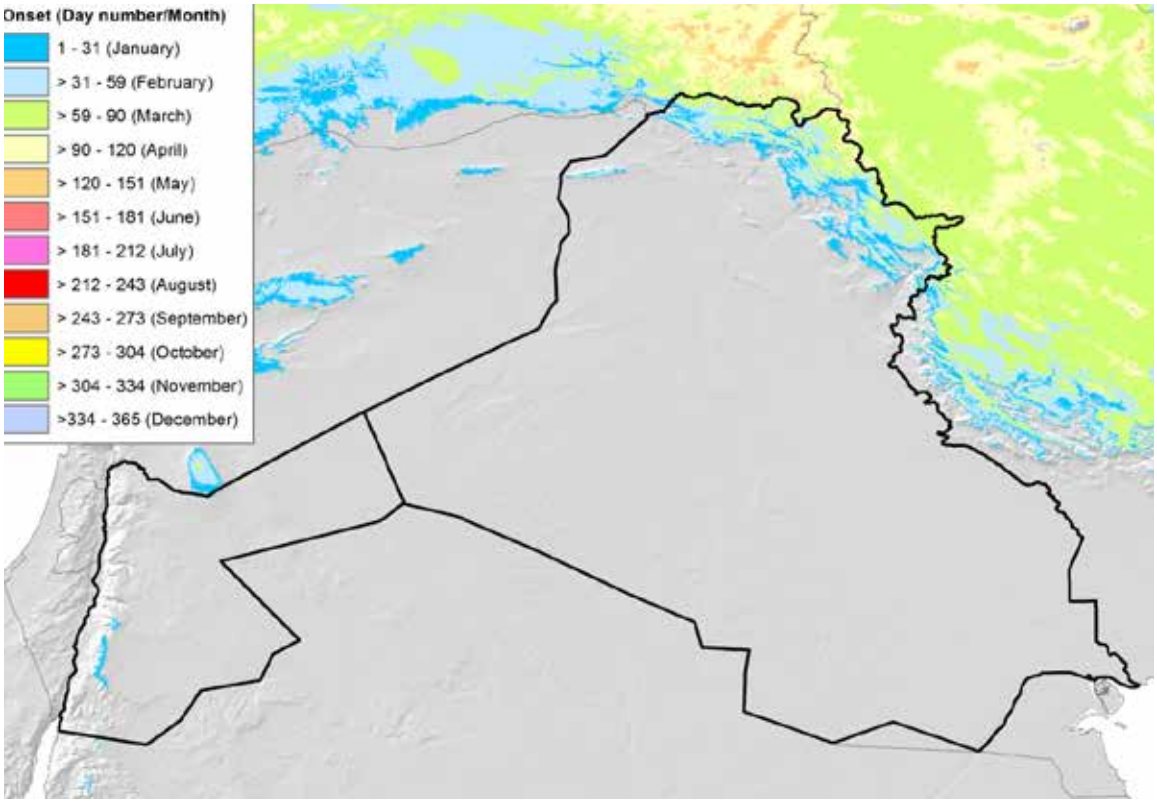

Figure 24. Onset month of the secondary moisture- and temperature-limited growing period

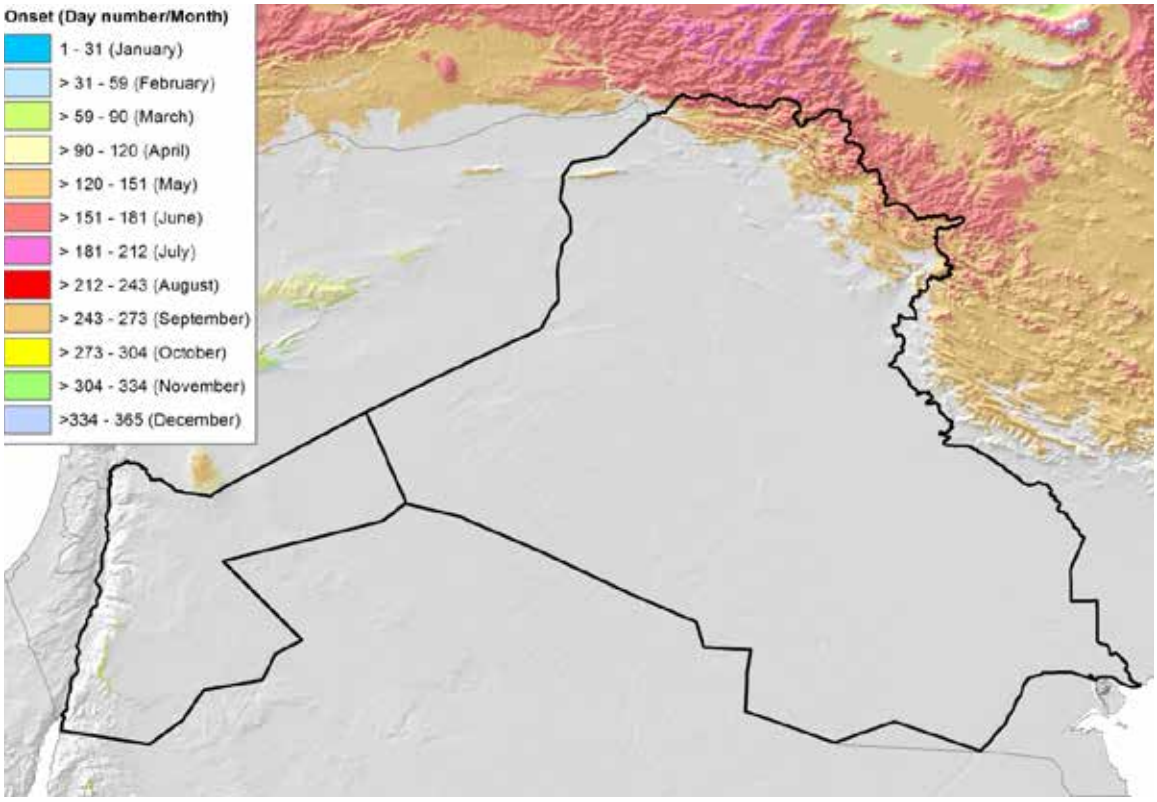

Figure 25. End month of the secondary moisture- and temperature-limited growing period

The growing period conditions in the WOI are mapped in Figures 18–25 and summarized in Table 11.

The moisture-limited growing period (Fig. 18) shows the north-south curved gradient of declining precipitation, typical of the Fertile Crescent. Roughly two-thirds of Jordan does not have a moisture-limited growing period that exceeds 90 days, which can be considered the minimum for rainfed agriculture; in Iraq the share of the country where moisture limits rainfed agriculture is up to 80%.

Temperature, on the other hand, is generally not a limiting factor, except in high-altitude mountainous areas. Therefore the temperature-limited growing period (Fig. 19) is almost unlimited in more than 95% of Iraq and Jordan. Since moisture is the main constraint in both countries, it is not surprising that the main moisture- and temperature-limited growing period (Fig. 20) is nearly identical to the moisture-limited growing period.

Table 11. Prevalence (%) of growing period classes in Iraq and Jordan

LGP-class	LGP-m		LGP-t		LGP-mt1		LGP-mt2	
	Iraq	Jordan	Iraq	Jordan	Iraq	Jordan	Iraq	Jordan
0–1	35.3	68.5	0.0	0.0	34.1	66.6	93.7	99.3
> 1–30	3.5	2.2	0.0	0.0	5.7	1.9	0.0	0.0
> 30–60	14.7	4.4	0.0	0.0	17.2	4.7	0.1	0.1
> 60–90	13.5	5.9	0.0	0.0	15.6	7.7	2.2	0.5
> 90–120	7.6	8.6	0.0	0.0	8.3	8.3	3.1	0.1
> 120–150	5.4	5.1	0.0	0.0	5.6	5.2	1.0	0.0
> 150–180	4.4	4.2	0.0	0.0	3.9	4.0	0.0	0.0
> 180–210	9.8	1.2	0.1	0.0	9.3	1.6	0.0	0.0
> 210–240	5.3	0.0	0.5	0.0	0.5	0.0	0.0	0.0
> 240–270	0.5	0.0	1.0	0.0	0.0	0.0	0.0	0.0
> 270–300	0.0	0.0	1.6	0.0	0.0	0.0	0.0	0.0
> 300–330	0.0	0.0	1.3	0.1	0.0	0.0	0.0	0.0
> 330–365	0.0	0.0	95.5	99.9	0.0	0.0	0.0	0.0

Notes:

LGP-m: moisture-limited growing period; LGP-t: temperature-limited growing period; LGP-mt1: main moisture- and temperature-limited growing period; LGP-mt2: secondary moisture- and temperature-limited growing period.

The main difference is in the mountain areas of Iraqi Kurdistan, where the growing period is split into two sub-periods, owing to an intermediate cold period: this is about the only area in the country with a secondary moisture- and temperature-limited growing period. In Jordan, a similar but much smaller area exists at high altitude on the Rift Valley escarpment. The onset and end months for the secondary growing periods in these high-elevation areas are shown in Figures 24 and 25.

In most of Iraq and Jordan, however, there is only one growing period, for which onset and end months are mapped in Figures 22 and 23.

4.2. PRECIPITATION: PAST AND PRESENT (1901–2010)

4.2.1. Annual precipitation probabilities

Using the methods explained in section 3.2.1.3., the following precipitation probability themes were calculated and mapped on the basis of the GPCC data for the period 1901–2010:

- Probability of not exceeding 100 mm per year (Annex 4, Fig. 35)
- Probability of not exceeding 200 mm per year (Annex 4, Fig. 36)
- Probability of not exceeding 300 mm per year (Annex 4, Fig. 37)
- Probability of not exceeding 400 mm per year (Annex 4, Fig. 38)
- Probability of not exceeding 600 mm per year (Annex 4, Fig. 39)
- Probability of not exceeding 800 mm per year (Annex 4, Fig. 40)
- Probability of not exceeding 1000 mm per year (Annex 4, Fig. 41)
- Annual precipitation likely to be exceeded in three out of four years (Annex 4, Fig. 42)
- Annual precipitation likely to be exceeded in four out of five years (Annex 4, Fig. 43)
- Annual precipitation likely to be exceeded in nine out of 10 years (Annex 4, Fig. 44).

These maps are summarized in Tables 12 and 13. Table 12 shows for Iraq and Jordan a breakdown of the probability of not exceeding a total amount (100, 200, …1000 mm) by probability class. The interpretation of this table is both straightforward and multiple: e.g. in Table 12, for Iraq the probability that annual precipitation will not exceed 200 mm is > 80% in 53.9% of the country; the probability that annual precipitation will not exceed 300 mm is > 80% in 68.8% of the country, and more than 50% in 74.9% of the country.

Table 13 shows for both countries a breakdown of the annual precipitation classes (0–50, > 50–100, ... > 800–1000 mm) that are likely to be exceeded with given return periods: three out of four, four out of five, and nine out of 10 years. The interpretation of this table is similarly clear-cut: e.g. annual precipitation in Jordan should exceed 200 mm in four out of five years in only 6.9% of the country.

4.2.2. Trends of annual precipitation

The trend mapping undertaken as part of this study confirms the usefulness of this tool to analyze the patterns of spatial and temporal variation in precipitation across Iraq and Jordan that can be discerned over the reference period, and, moreover, how statistically significant these trends are. Using the equations and transformations explained in section 3.2.1.4., the following elements of the annual precipitation trend were mapped:

- Correlation coefficient (Fig. 21)
- Absolute change (in mm) (Fig. 22)
- Relative change (in %) (Fig. 23)
- Correlation coefficient of the standard deviation (Fig. 24)
- Absolute change of the standard deviation (in mm) (Fig. 25)
- Absolute change of the SPI between 1901 and 2010 (Fig. 26)

A grid mask representing the significance of the particular trend element is present on most of these maps, with the densest grid indicative of the highest significance level, and the most open grid indicative of the lowest significance level. Where no mask appears in these maps, the trend is non-significant.

Table 12. Summary of precipitation probabilities 1901–2010: 1. Probability of non-exceedance classes

Country	Theme	0	> 0–0.1	> 0.1–0.2	> 0.2–0.3	> 0.3–0.4	> 0.4–0.5	> 0.5–0.6	> 0.6–0.7	> 0.7–0.8	> 0.8–0.9	> 0.9–0.99	> 0.99 - 1
Iraq	Prob_nexc100[15]	6.2	27.3	5.6	9.2	25.9	10.2	7.8	5.5	2.3	0.0	0.0	0.0
Iraq	Prob_nexc200	0.6	23.3	2.9	2.1	1.8	1.9	2.1	2.8	8.7	29.7	24.2	0.0
Iraq	Prob_nexc300	0.0	9.9	3.5	7.1	2.6	2.1	1.9	2.0	2.2	3.5	39.9	25.4
Iraq	Prob_nexc400	0.0	6.1	1.8	1.3	1.5	1.7	4.2	4.6	3.3	3.5	9.1	62.9
Iraq	Prob_nexc600	0.0	0.6	1.3	0.9	1.0	1.4	1.3	1.2	1.3	2.4	12.7	75.8
Iraq	Prob_nexc800	0.0	0.0	0.0	0.2	0.2	0.2	0.3	0.8	1.4	1.7	5.5	89.6
Iraq	Prob_nexc1000	0.0	0.0	0.0	0.0	0.0	0.0	0.0	0.1	0.4	0.5	3.7	95.3
Jordan	Prob_nexc100	0.0	13.7	6.6	6.2	7.9	35.8	11.2	14.1	3.6	0.7	0.0	0.0
Jordan	Prob_nexc200	0.0	3.0	2.9	2.7	3.3	3.5	4.3	6.0	9.1	57.1	8.0	0.0
Jordan	Prob_nexc300	0.0	0.0	1.0	1.3	1.5	1.8	2.3	3.2	4.6	9.0	73.4	1.8
Jordan	Prob_nexc400	0.0	0.0	0.0	0.0	0.1	0.8	1.4	1.8	2.5	5.6	39.5	48.4
Jordan	Prob_nexc600	0.0	0.0	0.0	0.0	0.0	0.0	0.0	0.0	0.0	0.7	9.9	89.4
Jordan	Prob_nexc800	0.0	0.0	0.0	0.0	0.0	0.0	0.0	0.0	0.0	0.0	0.8	99.2
Jordan	Prob_nexc1000	0.0	0.0	0.0	0.0	0.0	0.0	0.0	0.0	0.0	0.0	0.0	100.0

Table 13. Summary of precipitation probabilities 1901–2010: 2. Minimum annual precipitation at specified return periods

Country	Theme	0–50	> 50–100	> 100–200	> 200–300	> 300–400	> 400–600	> 600–800	> 800–1000
Iraq	Prob_minpr75	2.9	53.8	14.5	10.4	9.2	6.4	2.6	0.2
Iraq	Prob_minpr80	6.0	54.2	11.9	13.9	5.4	6.3	2.3	0.0
Iraq	Prob_minpr90	18.9	45.8	10.0	14.2	3.8	6.4	1.0	0.0
Jordan	Prob_minpr75	24.8	50.6	16.3	6.2	2.1	0.0	0.0	0.0
Jordan	Prob_minpr80	31.0	47.2	14.8	5.6	1.3	0.0	0.0	0.0
Jordan	Prob_minpr90	69.2	14.9	11.5	4.4	0.1	0.0	0.0	0.0

15 Prob_nexc100: probability annual precipitation will not exceed 100 mm. Prob_nexc_200...Prob_nexc1000: similar themes for 200, 300, ... 1000 mm.
Prob_min75: annual precipitation to be exceeded in three out of four years. Prob_min80: similar in eight out of 10 years; Prob_min90: similar in nine out of 10 years.

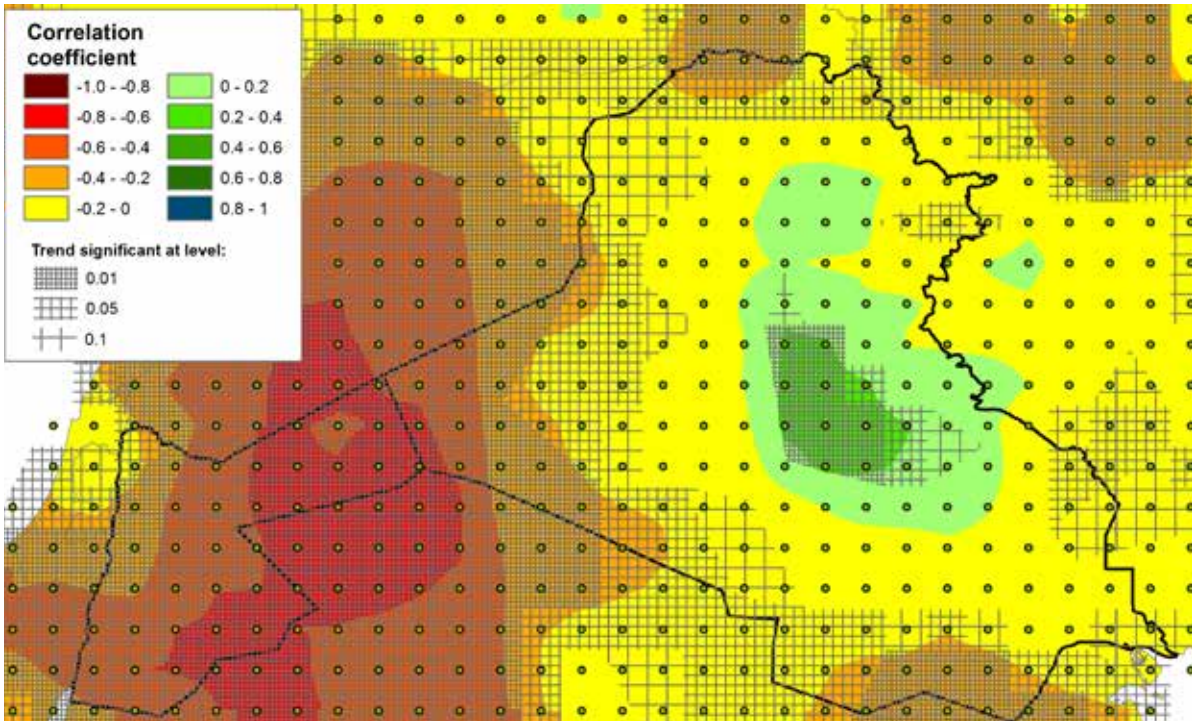

Figure 26. Correlation coefficient of the trend precipitation 1901–2010

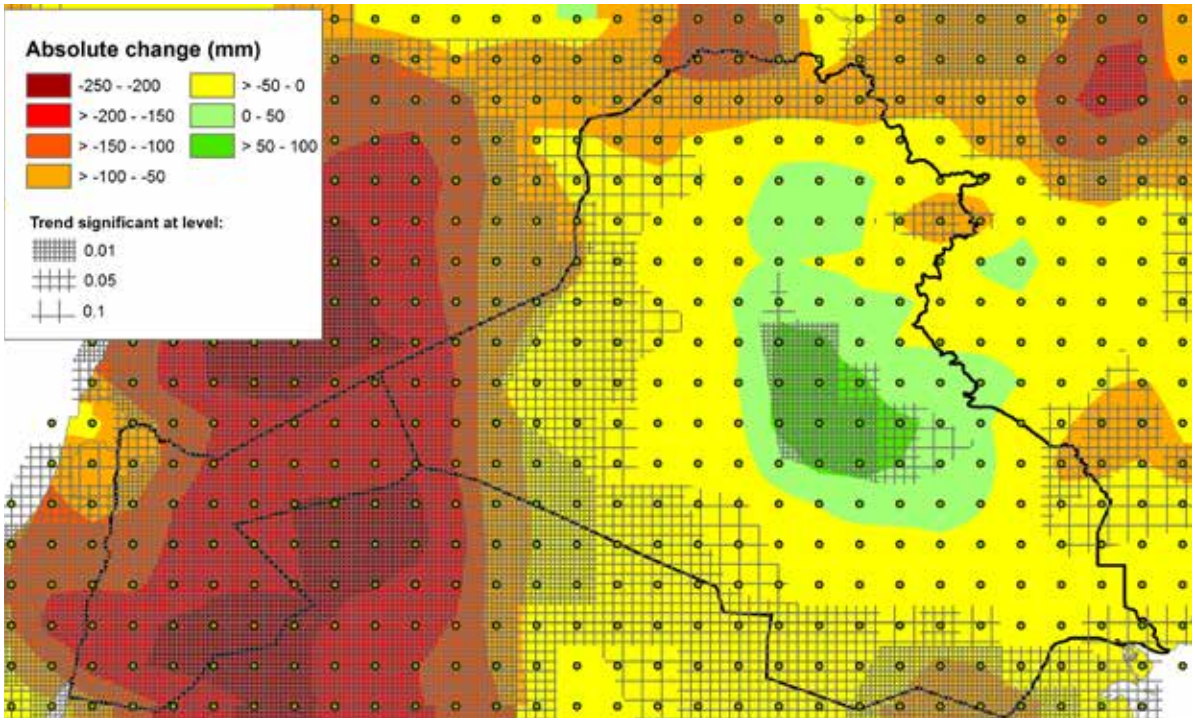

Figure 27. Absolute change of the trend precipitation 1901–2010

The correlation coefficient of the annual precipitation (Fig. 26) quantifies the relationship between precipitation and time and measures the strength of the trend in either a positive or negative direction. The correlation coefficient of the standard deviation is a measure of the strength of the changes in the short-term precipitation variability in either a positive (variability increases) or a negative direction (variability decreases).

The significance level assesses the probability that the observed trend, for the annual precipitation and the standard deviation, is entirely random: at value 0.01 that probability is 1%, at 0.05 it is 5%, and at 0.1 it is 10%.

The absolute change of the trend precipitation (Fig. 27) is the difference in precipitation that would exist between the first and last year of the reference period 1901–2010 if the annual precipitation entirely followed the trend line.

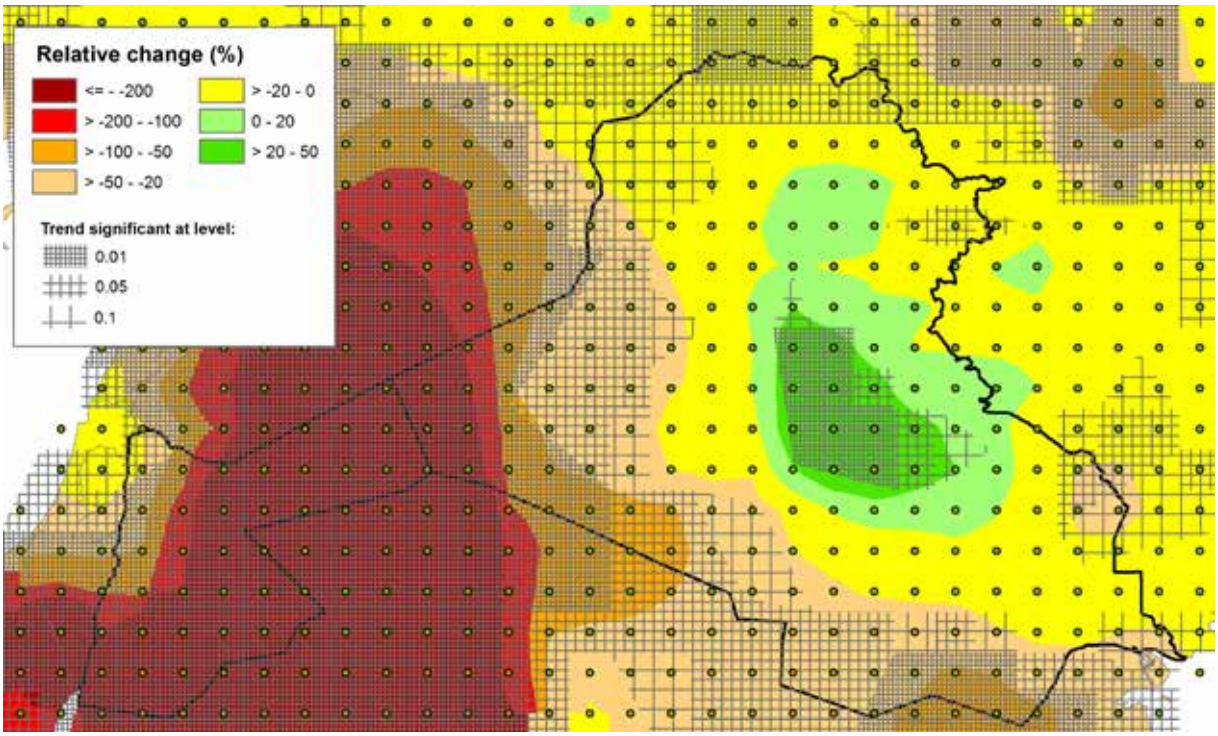

Figure 28. Relative change of the trend precipitation 1901–2010

The relative change of the trend precipitation (Fig. 28) relates this absolute difference to the annual precipitation of the first year. Both indicators are therefore also measures of the strength of the trend in either a positive or negative direction. Similar interpretations are possible with the absolute and relative changes of the trend standard deviation.

Figures 26–28 clearly show a general trend of declining annual precipitation. That decline is strongest in Jordan but less severe in Iraq, where a central region is even observed, in which annual precipitation has increased. However, given the fluctuations in the number of precipitation stations in Iraq that contributed to the GPCC database (see section 3.2.1.2.), caution should be exercised in accepting such a positive trend as an anomaly in a region otherwise characterized by a very large, and also statistically significant, precipitation drop.

Figures 29 and 30 make it clear that where precipitation declines, the absolute variability tends to decline, and vice versa. The variability of annual precipitation significantly declines during the period 1901–2010 in all of Jordan and west and southwest Iraq. However, it also increases significantly in north and northeast Iraq.

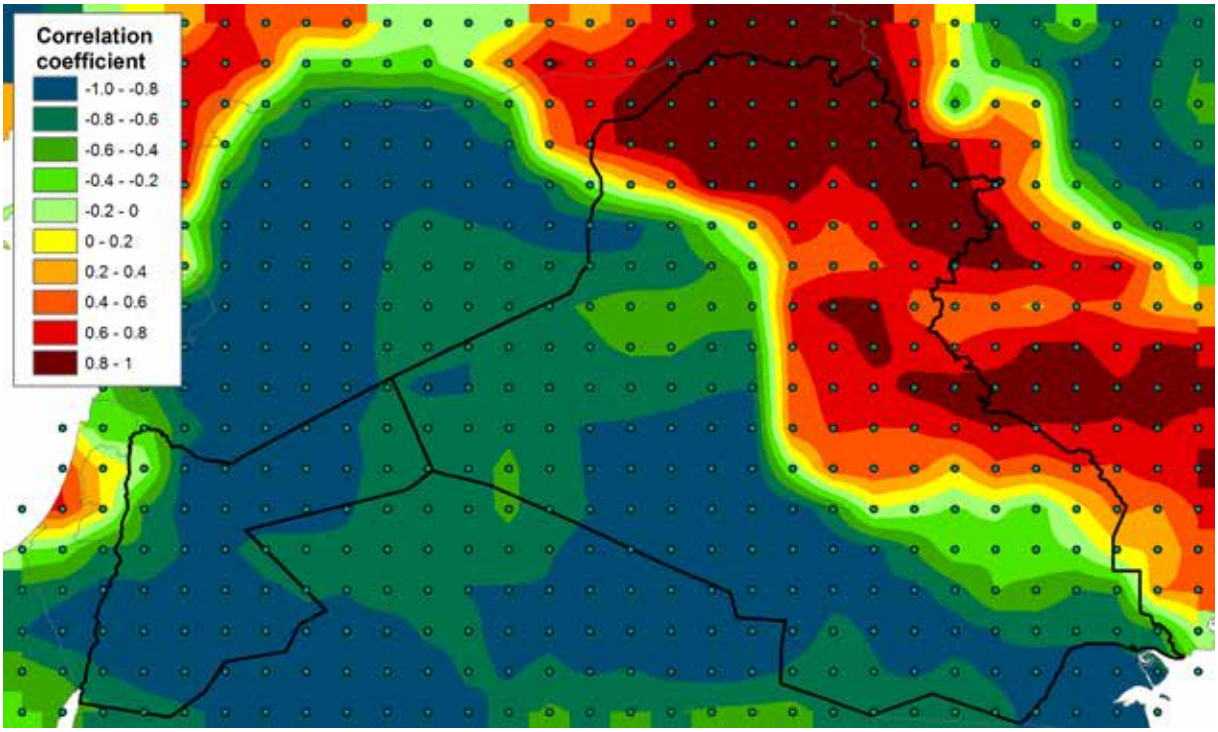

Figure 29. Correlation coefficient in the trend of the standard deviation of annual precipitation 1901–2010

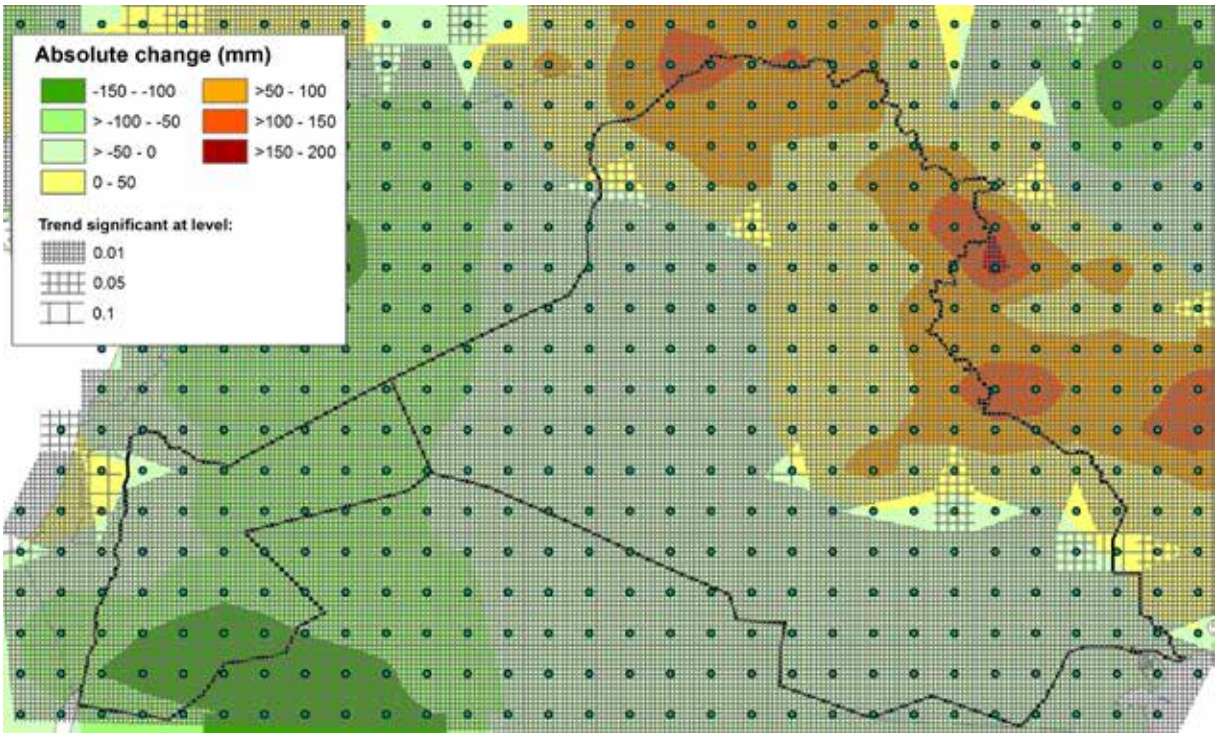

Figure 30. Absolute change in the standard deviation of annual precipitation 1901–2010

4.2.3. Drought and wetness periods

The history of surges and declines of droughts, wetness anomalies, and episodes of near normal precipitation conditions in Iraq and Jordan is well represented by the annual SPI maps (see Annex 5).

Table 14 summarizes these maps in the form of percentages of each country occupied by the individual SPI-classes, established in Table 5.

Maps and tables indicate that, consistent with statistical expectations, conditions were normal in most of both countries. Major droughts (occupying > 50% of the country) occurred in Iraq during the years 1901, 1905, 1932, 1964, 1973, 1990, and 2008–2010. The years in which above-normal precipitation conditions prevailed in > 50% of Iraq were 1907, 1911, 1914, 1916, 1918–1919, 1926, 1938, 1946, 1954, 1957, 1974, and 1982.

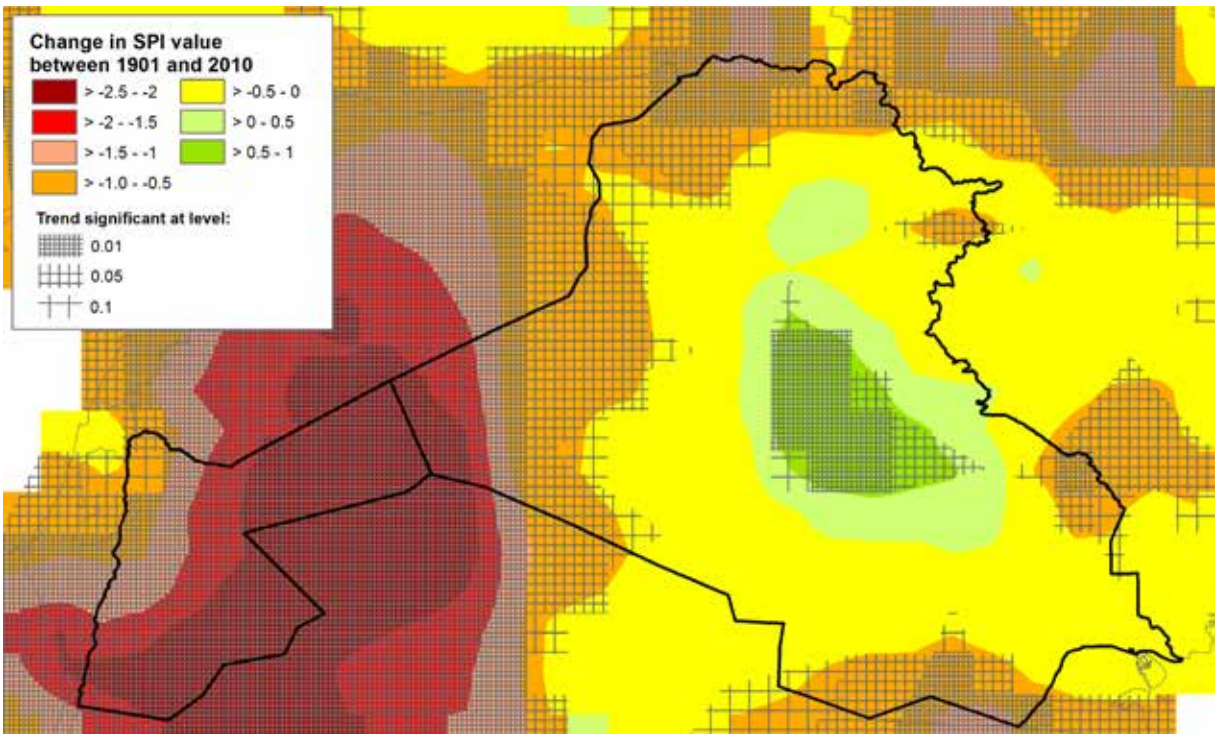

Figure 31. Absolute change of the trend SPI value between 1901 and 2010 (cross-shading indicates significance level of the trend)

In Jordan the major drought years were 1932–1933, 1958, 1960, 1962, 1973, 1978, 1981, 1995, 1999–2000, and 2008–2009; and the wetter years were 1902, 1904–1906, 1908, 1910-1911, 1914, 1918–1921, and 1944. Thus, in the second half of the twentieth century and later, Jordan did not experience years of above-normal precipitation compared to the first half of the twentieth century. The patterns of precipitation variations, as expressed in periods of drought and wetness, are therefore not the same in Iraq and Jordan. This is confirmed by the trend analysis of the SPI for the period 1901–2010: Figure 31 indicates a very strong and highly negative trend in Jordan, but a less negative trend in Iraq (with even a positive anomaly in the center of the country). There is definitely a different pattern, but care is needed with over-interpretation given the instability of the meteorological network in Iraq (see section 3.2.1.2.).

4.3. PROJECTED CHANGES FROM CURRENT CLIMATE TO 2010–2040

The climate change projections for Iraq and Jordan are summarized in Tables 15–22 of Annex 6 for the following climate themes:

- Relative changes in annual and seasonal precipitation
- Change in annual maximum and minimum temperature, and mean seasonal temperatures
- Change in annual PET
- Changes in Köppen climatic zones
- Changes in annual aridity index
- Changes in moisture-limited, temperature-limited, and moisture- and temperature-limited growing periods.

Representative change maps for Jordan, related to the above themes, are provided in Annex 7. Similar maps for Iraq will be added at a later stage.

4.3.1. Precipitation changes

A first observation is the similarity in patterns of precipitation between scenarios A1b and A2, at all time-scales: monthly, seasonal, and annual. This is certainly evident from Table 15 and the precipitation maps in Annex 7. This is no surprise, as 2010–2040 represents a 'near' future and global GHG emissions start to diverge significantly only from 2030 (Fig. 32).

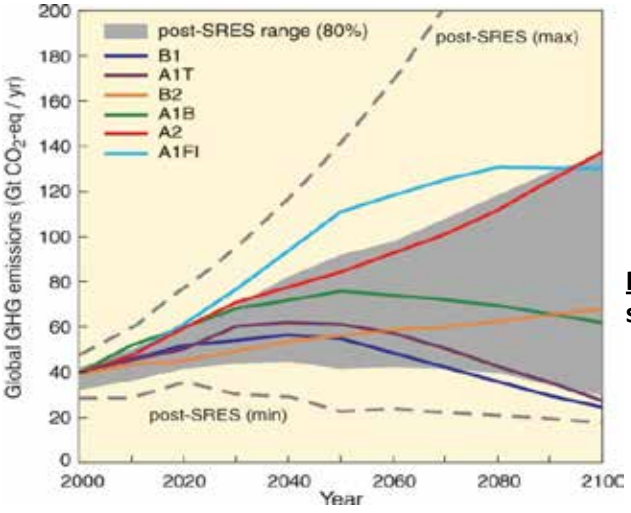

Figure 32. Evolution of global GHG emissions by scenario (source: IPCC, 2007)

It is noteworthy that in areas with very low rainfall, relative changes in precipitation, compared to the current climate, are also the result of artefacts: a 2 mm increase in precipitation, where the annual total is 10 mm represents a relative increase of 20%; whereas the same increase in an area with 100 mm annual total would represent only a 2% relative increase. For this reason the change estimates of Table 15 exclude the hyper-arid areas of Iraq and Jordan (see column '% of area excluded').

There is clear indication of considerable precipitation decline in spring in both Iraq and Jordan, with little difference between scenarios A1b and A2. In almost 70% of the area the decline is in the range 10–20%, in the remainder in 0–10%. The erratic patterns in loss/gain of summer precipitation are probably artefacts, owing to the fact that in areas under Mediterranean influence the summer precipitation is very low. Nevertheless, in the eastern part of the area, particularly in Iraq and to a lesser extent in Jordan and Syria (scenario A1b), there are gains of > 20% in summer precipitation.

The same trend of increase (> 20%) extends into the autumn in Iraq, whereas gains of 0–10% are observed in eastern Jordan. Scattering of gain/loss patterns is somewhat more pronounced under the A2 than the A1b scenario. In winter very clear losses (5–20%) occur in both Iraq and Jordan, more pronounced under scenario A1b than A2.

Under both scenarios the annual precipitation is set to decline significantly, but here the outcomes

from scenarios A1b and A2 differ substantially. A decline of 5–20% is expected in > 90% of Iraq and Jordan under scenario A1b; the same decline is anticipated in only 18% of Iraq under scenario A2, whereas it remains > 90% in Jordan. The main factors contributing to the annual precipitation decline are the clearly discernible losses in winter and spring precipitation, which are obviously the largest components of annual precipitation. These losses are very serious, as they are predicted to occur in the 'near' future and during the growth cycle of winter crops.

4.3.2. Temperature changes

Table 16 in Annex 6 summarizes the expected increases in temperature for Iraq and Jordan under both scenarios. As in the case of precipitation, monthly and annual temperature and change maps are very similar, if not nearly identical, between scenarios A1b and A2. The changes in mean annual temperature between current climate and those for 2010–2040 across the study area are in the range 1–1.5°C. Seasonal differences can be expected in the temperature increase. In winter (December–February) nearly all of Iraq and Jordan can expect a temperature increase in the range of 0.5–1.0°C. The temperature increases in spring and autumn are expected to be higher than in winter: about 80% of Iraq and even 100% of Jordan in the range of 1.0–1.5°C increase for scenario A1b, and 50% of Iraq even in the range 1.5–2°C. Still higher increases (1.5–2°C) can be expected in summer particularly in Iraq (100% under both scenario A1b and A2) and parts of Jordan.

4.3.3. Changes in PET and aridity

Table 17 in Annex 6 summarizes the changes in annual PET under both scenarios A1b and A2 compared to the current climate. Generally a 3–4% increase is expected in annual PET, with little difference between the two scenarios. However, overall the expected increase in PET represents a very modest increase in the crop water requirements and irrigation demand.

Table 19 in Annex 6 summarizes the change in aridity index under both scenarios: negative values indicate a trend towards more arid conditions, positive values towards more humid conditions. Across both Iraq and Jordan a trend towards more arid conditions prevails, and this trend is similar under A1b and A2. It is to be noted that these trends are in most cases the result of both declining precipitation and higher PET.

4.3.4. Changes in climatic zones

Table 18 in Annex 6 summarizes the current distribution of the Köppen climatic zones in Iraq and Jordan and the estimated changes under respective scenarios A1b and A2. It is expected that the vast majority of Iraq (> 95%) will retain the same climatic zone as now under both scenarios. However, it is expected that in about one-third of Jordan a shift in climatic zone may occur, in the form of a change from a steppe (BS) climate to a desert (BW) climate. Given the general nature of the Köppen classification, this is obviously a very significant development, as it is likely to occur in a very near future, and there is an intimate linkage between climate and biodiversity.

4.3.5. Changes in growing period conditions

Changes in the three aspects of the growing period theme (moisture-limited, temperature-limited, and moisture–temperature-limited) are summarized in Tables 20–22 of Annex 6. There is very little difference in changes in growing period duration between the A1b and A2 scenarios. In the vast majority of Iraq and Jordan (about 90%) a decline in the range of 0–15 days is expected in the moisture-limited growing period. Scenario A1b predicts stronger reductions, mostly in the range 15–30 days, in almost 20% of Iraq whereas under scenario A2 such drastic reductions affect only a small part (5–10%) of both countries.

Changes in the temperature-limited growing period are expected to affect small high-altitude areas, particularly in Iraq with about 6% expected to have an increase in the temperature-limited growing period of 1–30 days.

The net effect on the moisture- and temperature-limited growing period would be a reduction of 0–15 days in the vast majority of each country (70–90%), with an increase of 0–30 days in a maximum of 8% of Iraq.

4.4. FARMER PERCEPTIONS OF CLIMATE CHANGE

The previous sections of this report focused on the actual climatic conditions, their trends, and future projections. We looked at how rainfall amounts or patterns have changed and whether growing seasons became shorter (or longer in some high-altitude locations). The actual climatic data of the past allowed us to establish trends of climatic change that could be linked to projections for the future.

The indicators of climatic change included in this working paper are strong and alarming enough to necessitate appropriate actions of mitigation or adaptation in the two countries concerned. By necessity, adaptation measures will be required by the farmers of both countries.

What particular adaptation measures would be most appropriate is not a difficult issue since the most fundamental change expected is a further drying of the climate, consistent with the trend of the last 100 years, accompanied by further warming in most of Iraq and Jordan of the order of 1–1.5°C over the entire period. The agricultural techniques for adapting to such changes already exist in the region, and a summary can be found in De Pauw and Göbel (2011). Some of these techniques are being tested in the current IFAD project.

An apparently more subtle bottleneck is the issue of perception of climate change by farmers. The limited evidence available points to confusion among farmers about what climate change means, and what impacts it may have in the two countries. The sad truth is that if farmers have no or limited perception of climate change, as aligned with the scientific outlook, there is no way they can adapt their farming practices to that reality.

Investigating farmer perceptions of climate change should therefore be a priority for researchers and decision-makers alike. By directly linking questionnaire-based interviews and focus group discussions to actual meteorological data, one can get some measure of how good the match is between reality and perception. The trends in the meteorological data can be considered a measure of past change and this reality can then be compared with the perceptions of (older) farmers about how climate has changed in the relatively recent past (e.g. 20–30 years ago). This is the theoretical basis of farmer perception surveys and in theory this is a legitimate approach since farmers, being so dependent for their livelihood on the weather, are much more likely to look for, and possibly detect, patterns of change in the weather than individuals whose livelihoods do not depend on weather.

In this section we look at the realities of past climatic change and compare these with the results of a farmer perception survey among older farmers that was conducted, as part of this project, in the Karak area of southern Jordan by an NCARE team, led by Dr. Samia Akroush and Ms. Muna Saba.
To address this issue, a survey was conducted by the socioeconomic group in cooperation with the climate change component team in Jordan and Iraq. To assess farmers' perceptions on climate change and the development priorities in communities they developed a questionnaire, with which they interviewed farmers. In addition, focus group discussions with farmers were conducted to capture their understanding of climate change based on memories and past experience.

The 'Climate Change Living Memory Survey', as it was officially called, came to the following synthesis of farmer perceptions of changes in the rainy season and rainfall:

- A general decrease in total rainfall amounts
- A delay in the beginning of rainy season, which used to start in September, October, and mostly November, and currently is being delayed until January and February
- The rainy season is stopping by March and no rainfall is received in April (although this rainfall period is regarded as crucial for crop production)
- Whereas rainfall used to be well distributed all over the season, currently most is concentrated in January and February.

By looking at trends of precipitation during the period 1975–2007 for two stations in the Karak area, Hassan/Tafileh (Fig. 33) and Rabbah (Fig. 34), it was possible to match farmer perceptions of change with reality.

Farmer perception 1: Decrease in rainfall amounts.

There is a decline of annual precipitation in Rabbah and Tafileh.

Farmer perception 2: A delay in the beginning of rainy season which used to start in September, October, and mostly November and currently is being delayed until January and February.

There is a decline in the October–December precipitation in Tafileh. However, there is no evidence of decline in Rabbah.

Farmer perception 3: Rainy season stopping by March and no rainfall is received in April (although this rainfall period is regarded as crucial for the crop production).

A decline of April precipitation can be observed in both Rabbah and Tafileh

Farmer perception 4: Rainfall used to be distributed all over the season, currently most is concentrated in January and February.

There is no evidence of such a trend. In fact, January–March rainfall has remained stable in Rabbah and Tafileh.

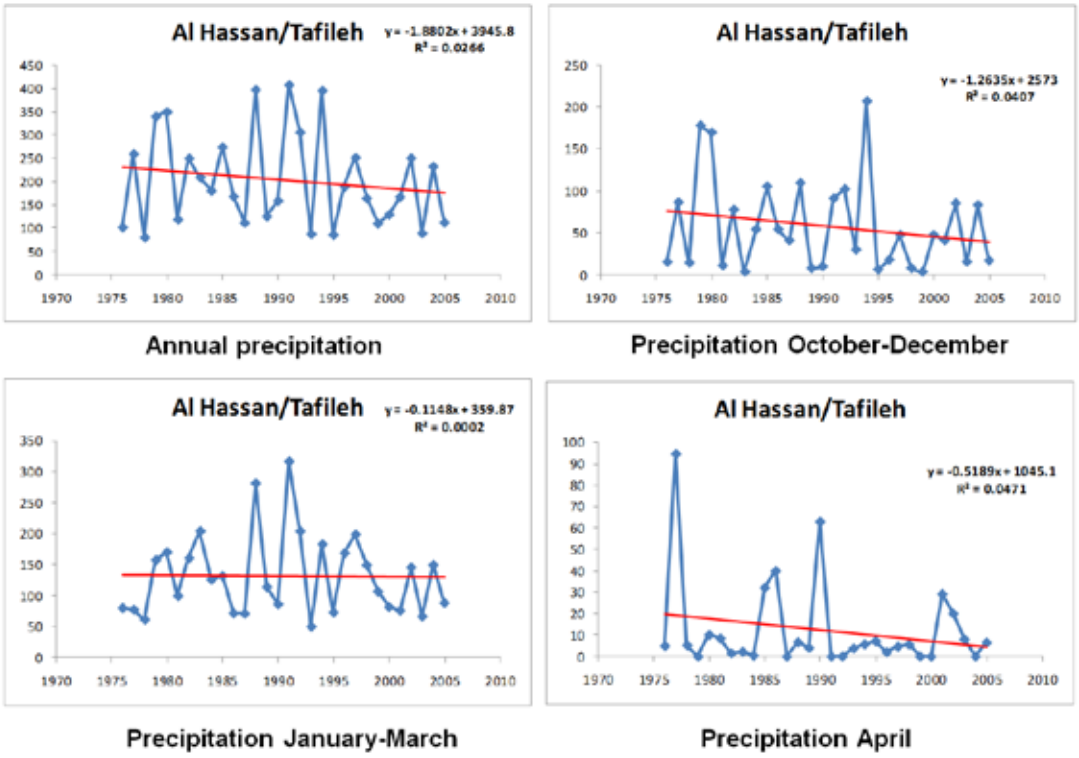

Figure 33. Precipitation variations and trends in Hassan/Tafileh (Jordan) 1975–2007

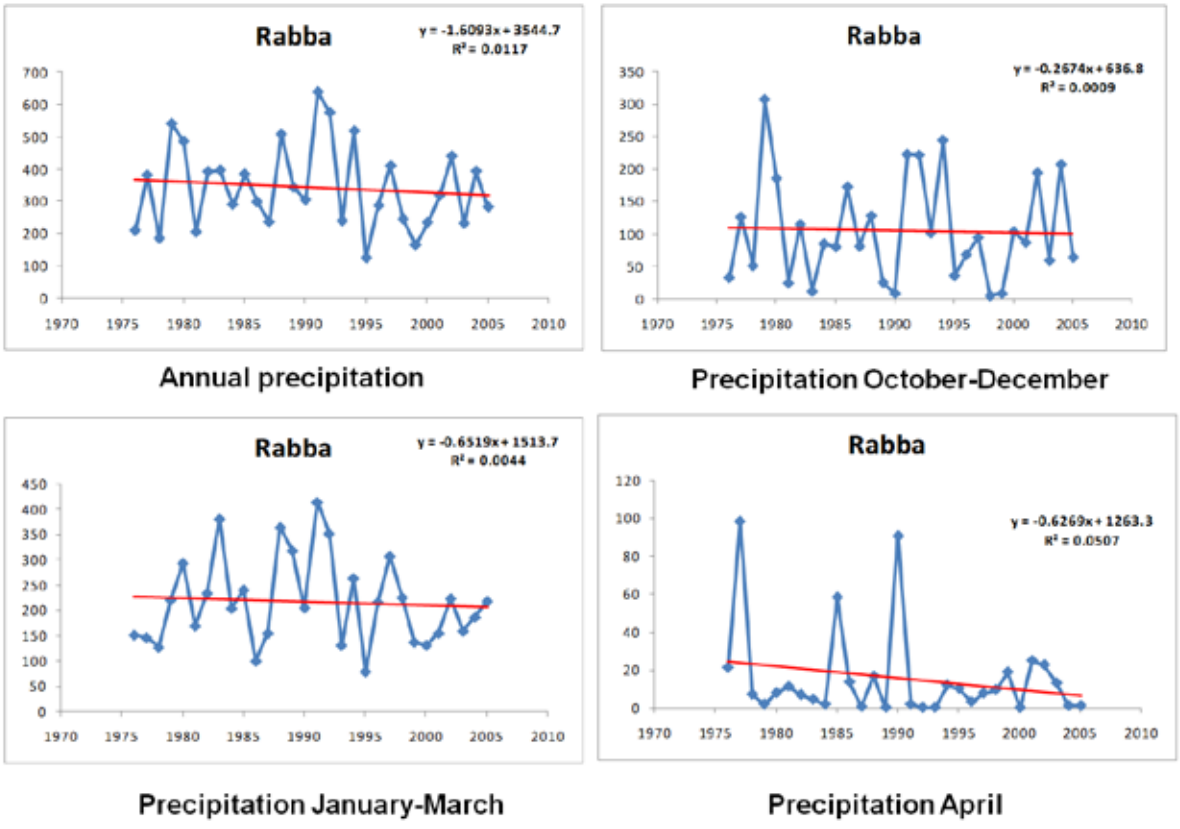

Figure 34. Precipitation variations and trends in Rabba (Jordan) 1975–2007

It is noteworthy that none of the observed precipitation trends are statistically significant. However, that does not mean that these trends are not real: even the stronger trends are masked by the large inter-annual variability. It is therefore all the more remarkable that farmers did indeed recognize some major precipitation trends. At the same time it is not surprising that farmers saw some trends where none exist, since the large precipitation variability is likely to evoke the natural response of looking only at the more recent past.

The point here is that a problem has to be recognized first and analyzed correctly before it can be addressed through appropriate extension work. As this particular survey indicates an agreement between what farmers see as a general drying of the climate and the observed trend of precipitation decline, it will be possible to introduce some techniques related to soil moisture conservation. For more detailed packages to work with the farmers, a better understanding of in-season changes will be required.

A similar study, undertaken by Ms. Auerbach with Bedouins in southern Jordan, similarly identifies misperceptions of the essence and causes of climate change, which lead to fatalistic attitudes and explains the absence of plans to manage risk and why farmers do not recognize appropriate adaptation strategies. Generally speaking, any significant gap between perceptions and understanding of climatic change will make it difficult to promote appropriate adaptation measures. More investment in public awareness campaigns is likely to be money well spent.

4.5. COMMUNICATING CLIMATE CHANGE THROUGH PUBLIC AWARENESS WORKSHOPS: THE CASE OF PROJECT TARGET VILLAGES IN JORDAN

The main benefit of the downscaling of coarse-resolution climate change projections is that it facilitates the communication of the potential effects of the latter to local stakeholder audiences. This is illustrated by a case study of how key messages from the downscaled climate change maps were communicated to the community members during the public awareness workshops conducted in the target communities of Karak Governorate.

4.5.1. Precipitation changes

As indicated in Figure 35, the winter season (December–February), is the season where the highest rain is received in this area and in all Jordan, followed by spring (March–May). The downscaled projections indicate that in winter in the three villages, precipitation decline is estimated by both emission scenarios A1b and A2 at about 15 mm in Samakiyyah, 25 mm in Ader, and 20 mm in Sul. The same trend is observed in spring, with expected reductions in precipitation in the three villages of 12, 13, and 12 mm, respectively, using emission scenario A1b. Using emission scenario A2 the estimated values are slightly higher.

These results are very important for local farming communities, since reduction in rainfall of this magnitude will seriously affect crops, surface and ground water, and livestock in these villages. In turn the expected effects of climate change will affect community livelihoods and food security, if no measures are taken to reduce these effects. This is where the project technologies and other climate change proofing technologies become so important to assist in the adaptation of the system to this change.

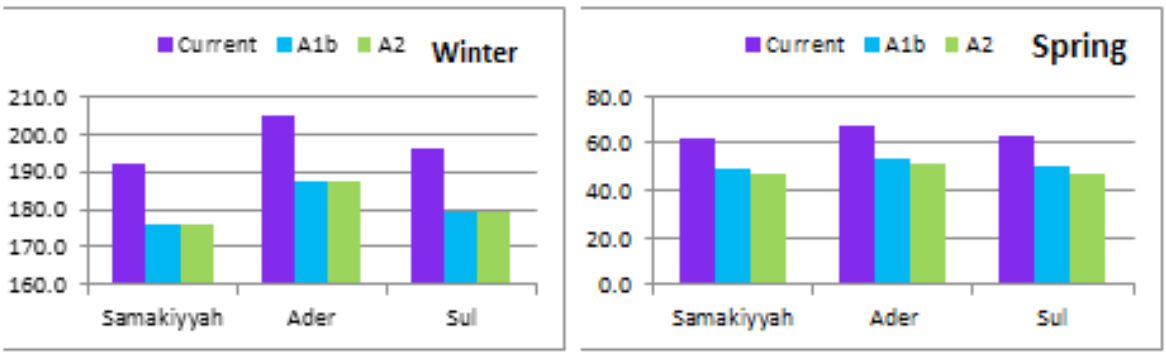

Figure 35. Comparison of current precipitation with winter and spring precipitation (mm) scenarios for three villages targeted by the project in Karak, south Jordan

4.5.2. Temperature changes

As in the case of precipitation, monthly and annual temperature and change maps are very similar for the Karak area, if not nearly identical, between scenarios A1b and A2. The expected change in the maximum temperature in the villages studied by the project in Jordan (Fig. 36) is in the range of 1.0–1.5°C.

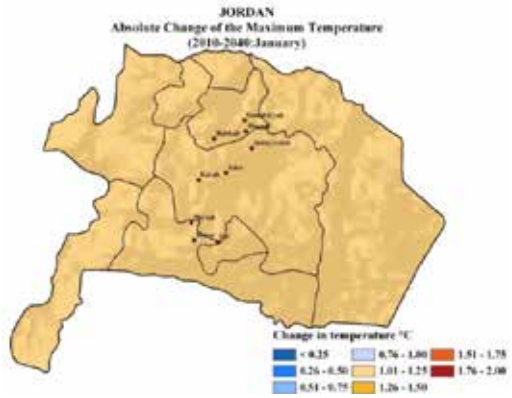

Figure 36. Expected change in the maximum temperature in the project villages in Karak, south Jordan

4.5.3. Changes in growing period conditions

Moisture and temperature-limited growing periods were mapped for the target project area in Karak under current and future scenarios. Changes in growing period show a delay in onset date (up to 5 days), whereas the end of the growing period is likely to be 5–15 days earlier. The change in the onset, end, and length of the growing periods are similar for both scenarios and estimated at 15–30 days (Figures 37 and 38).

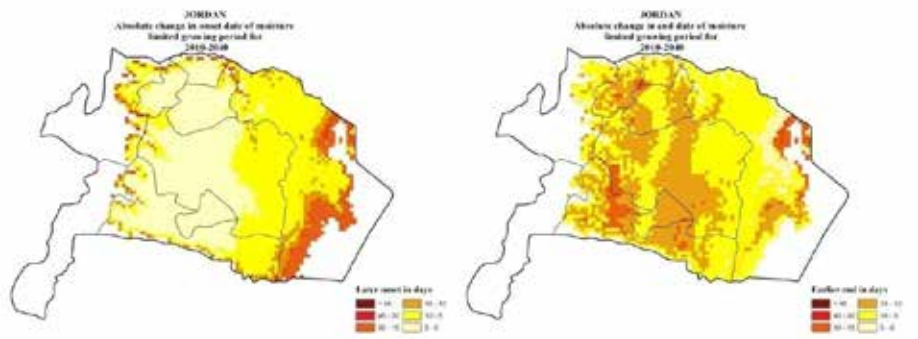

Figure 37. Expected changes in the onset and end of the growing period in Karak, south Jordan

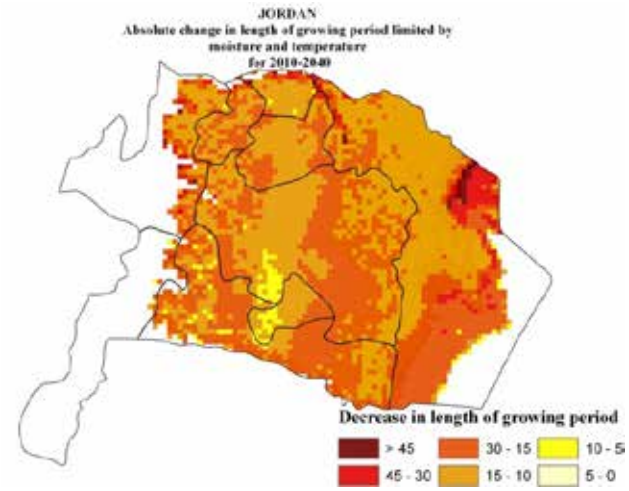

Figure 38. Expected change in length of growing period in Karak, south Jordan

5. CONCLUSIONS AND RECOMMENDATIONS FOR FOLLOW-UP

In both Iraq and Jordan there has been good progress in the characterization of climate change within the current knowledge as made available through the IPCC AR4.

The key change indicators (absolute change in seasonal precipitation, minimum and maximum temperature, and annual PET, and changes in climatic zone, agroclimatic zones, and growing periods) indicate that in both Iraq and Jordan the climate should become drier, with reduced growing periods, shifts in climatic zones, and higher temperatures and water requirements than currently. These changes are quantified in the Atlases in terms of the areas affected.

It was also confirmed that the trend of declining precipitation that emerges from the comparison of the current climate with the future one projected by the GCMs, is very much in line with the trend of the past. The results of a trend analysis of coarse-gridded precipitation data for the period 1901–2010, obtained from the GPCC, indicates that annual precipitation has been declining for a long time and that these trends are significant in all of Jordan and most of Iraq. The anticipated changes are quite remarkable given that the future conditions evaluated in the project are very near.

Much effort has been dedicated in this project towards capacity-building, which has paid off. In the last year of the project the teams of Iraq and Jordan have committed themselves to consolidate their rich datasets into Climate Change Atlases and the fruits of their efforts are available.

Two main lessons could be drawn:

1) The model of capacity-building that was adopted, consisting of relatively short training courses, focusing on precisely defined outcomes, with 'home-work' after each training event, can definitely be outscaled to other countries.
2) The target of producing an atlas as a deliverable is a very good way to introduce climate change assessment capabilities within NARS.

These atlas publications could well be very useful in distilling clear and location-specific messages to researchers, extension workers, and farmers on how to cope with the projected climatic changes. However, this has not happened yet. The main reason is that the Climate Atlases are certainly good in the characterization of future conditions at the level of the actual climatic changes and setting the scene for the general management principles to be adopted, but not very good at predicting what the impact would be on the systems of the region. For the latter objective we need more sophisticated tools. ICARDA already has some tools available that could be adapted to the needs of climate change research.

Whereas in the current project most attention has been given to describing the state of the general climate in the medium future, it is clear that climate change will be characterized by changes in the frequency and intensity of extreme events (e.g. heat waves and droughts). Such changes can be captured through specialized models that generate artificial daily weather data, which can then be analyzed in terms of changes in probabilities through standard statistical techniques.

The USDA Agricultural Research Service in Lubbock, Texas, and ICARDA jointly developed a GIS-based tool, the 'ICARDA Agro-Climate Tool', which can be downloaded (http://www.lbk.ars.usda.gov/wewc/icarda%20agro-climate%20tool.aspx) and installed on individual PCs. The tool allows estimating the probabilities of dry spells, hot or cold spells, as well as irrigation needs for a wide range of crops in different locations in the CWANA region, for specified time periods during the year, under current climatic conditions.

This tool, fed with downscaled data produced by different GCM models, can be adapted with limited resources to estimate, for various time horizons and emission scenarios, the probabilities of dry or

hot spells and their impacts on crops in the future. Therefore it will be very useful to develop concrete recommendations for farmer adaptation to climate change.

A very important issue is the perspective of sustainability beyond the lifetime of the current IFAD-supported project. This issue is basically about maintaining and updating the skills in climate change assessment that were transferred to the national programs of Iraq and Jordan through this project. Sustainability, in all likelihood, will only be possible by maintaining or developing suitable partnerships that ensure some continuity in the support to the national programs engaged in the project.

From the very beginning it was clear that a project dealing with climate change would face the challenge of coping with the inherent uncertainties of climate change research. A typical example of uncertainty is the issue of how different models give different predictions. Another important uncertainty is that climate change projections are linked to the outcomes of energy–population–development interactions that are difficult to predict and are therefore presented in the form of scenarios. In other words, what may appear a sensible basis for interpreting climate change today could become outdated in the near future. Therefore there is a need for continuity into the future, beyond the lifetime of the IFAD project, and this continuity can only be ensured by strategic partnerships[15].

In the course of this project new datasets were made available through the CCAFS Program[16], which is the CGIAR CRP mandated to provide the entire system with new data and tools for climate change research. CCAFS is therefore a logical partner in any research activities related to climate change to be undertaken after the end of the project.

Another very useful partnership which should be further explored is with the CYI in Nicosia. Whereas CCAFS' mandate is global, the CYI's is the Near East neighborhood and CYI is perhaps the most suitable partner to assist national programs in the region through their climate-change related research[17] and high-performance-computing facility. They were heavily involved in the last ICARDA course and would be very happy to assist Jordan and Iraq (as well as other countries of WANA) with training and research collaboration. Training opportunities that could be explored concretely could cover extreme-events-analysis and high-performance-computing.

16 http://ccafs.cgiar.org/
17 http://www.cyi.ac.cy/eewrc/eewrc-research-projects/climate-change-and-impact.html

REFERENCES

Abramowitz, M. and I.A. Stegun. 1964. Handbook of mathematical functions. National Bureau of Standards, Applied Mathematics Series 55, US Department of Commerce, 470 pp.

Allen, R.G., L.S. Pereira, D. Raes and M. Smith. 1998. Crop evapotranspiration. Guidelines for computing crop water requirements. FAO Irrigation and Drainage Paper 56. FAO, Rome. (Link: http://www.kimberly.uidaho.edu/water/fao56/fao56.pdf)

Choisnel, E., O. de Villele and F. Lacroze. 1992. Une approche uniformisée du calcul de l'évapotranspiration potentielle pour l'ensemble des pays de la Communauté Européenne. Centre Commun de Recherche, Commission des Communautés Européennes. (Link: http://bookshop.europa.eu/en/une-approche-uniformis-e-du-calcul-de-l-evapotranspiration-potentielle-pour-l-ensemble-des-pays-de-la-communaut-europ-enne-pbEUNA14223/downloads/EU-NA-14-223-FR-C/EUNA14223FRC_001.pdf;pgid=y8dIS7GUWMdSR0EAlMEUUsWb0000FbkZxmTq;sid=qMrDMfYx-LbDJaU4oN5dlpQUrx-nF4rtStrg=?FileName=EUNA14223FRC_001.pdf&SKU=EUNA14223FRC_PDF&CatalogueNumber=EU-NA-14-223-FR-C)

CMIP. 2007. Climate Model Documentation, References, and Links. (Link: http://www-pcmdi.llnl.gov/ipcc/model_documentation/ipcc_model_documentation.php)

Debaveye, J. 1985. Soil survey technical documents. Vol. 2: Handbook for data interpretation. Soil Survey and Assessment Project. Department of Development Cooperation, Min. Foreign Trade and Foreign Affairs, Belgium.

De Pauw, E. 2010. Agroecological zoning of the CWANA region. Pages 335–348 *in* Sustainable Development in Drylands – Meeting the Challenge of Global Climate Change (A. El-Beltagy and M.C. Saxena, ed.). Proc. 9th International Conference on Development of Drylands, 7–10 November 2008, IDDC, ICARDA. (Link: https://dl.dropboxusercontent.com/u/33140444/Publications/AEZ_CWANA_all_pages_color.pdf)

De Pauw, E. and W. Göbel. 2011. Climate change in drylands: from assessment methods to adaptation strategies. Pages 15–36 *in* Crop Stress Management & Global Climate Change (J.L. Araus and G.A. Slafer, ed.). CABI Climate Change Series 2 (Link: http://bookshop.cabi.org/?site=191&page=2633&pid=2259)

Doorenbos, J., and W.O. Pruitt. 1984. Guidelines for predicting crop water requirements. FAO Irrigation and Drainage Paper 24. FAO, Rome. (Link: http://www.fao.org/docrep/018/s8376e/s8376e.pdf)

Edwards, D.C., and T.B. McKee. 1997. Characteristics of 20th century drought in the United States at multiple time scales. Climatology Report 97-2. Dept. of Atmos. Sci., CSU, Fort Collins, CO, USA. (Link: http://ccc.atmos.colostate.edu/edwards.pdf)

FAO. 2001. FAOCLIM, a CD-ROM with world-wide agroclimatic data, version 2. Environment and Natural Resources Service (SDRN) Working Paper No.5. FAO, Rome. (Link: http://unfccc.int/adaptation/nairobi_work_programme/knowledge_resources_and_publications/items/5370.php)

Hutchinson, M.F. 1995. Interpolating mean rainfall using thin plate smoothing splines. *International Journal of Geographical Information Systems* 9: 385–403. (Link: http://www.tandfonline.com/doi/pdf/10.1080/02693799508902045)

Hutchinson, M.F. 2000. ANUSPLIN version 4.1. User Guide. Center for Resource and Environmental Studies, Australian National University, Canberra.

IPCC. 2007. Summary for policymakers *in* Climate Change 2007: The Physical Science Basis. Contribu-

tion of Working Group I to the Fourth Assessment Report of the Intergovernmental Panel on Climate Change (S. Solomon, D. Qin, M. Manning, Z. Chen, M. Marquis, K.B. Averyt, M. Tignor and H.L. Miller, ed.). Cambridge University Press, Cambridge, UK and New York, USA. (Link: https://www.ipcc.ch/pdf/assessment-report/ar4/wg1/ar4-wg1-spm.pdf)

IPCC. 2007. Regional climate projections *in* Climate Change 2007: The Physical Science Basis. Contribution of Working Group I to the Fourth Assessment Report of the Intergovernmental Panel on Climate Change. (S. Solomon, D. Qin, M. Manning, Z. Chen, M. Marquis, K.B. Averyt, M. Tignor and H.L. Miller, ed.). Cambridge University Press, Cambridge, UK and New York, USA. (Link: https://www.ipcc-wg1.unibe.ch/publications/wg1-ar4/ar4-wg1-chapter11.pdf)

Köppen, W., and H. Geiger. 1928. Handbuch der Klimatkunde. Berlin, Germany.

McKee, T.B., N.J. Doesken and J. Kleist. 1993. The relationship of drought frequency and duration of time scales. Eighth Conference on Applied Climatology, 17–22 January 1993, Anaheim, California. (Link: http://clima1.cptec.inpe.br/~rclima1/pdf/paper_spi.pdf)

Research and Education Association (REA). 2004. The Statistics Problem Solver. REA, New Jersey, USA, 1045 pp.

Schneider, U., T. Fuchs, A. Meyer-Christoffer and B. Rudolf. 2008. Global precipitation analysis products of the GPCC. GPCC, DWD, Germany. (Link: ftp://ftp.dwd.de/pub/data/gpcc/PDF/GPCC_intro_products_v2011.pdf)

Sokal R.R. and F.J. Rohlf. 1981. Biometry. Freeman, USA, 859 pp.

Thom, H.C.S. 1966. Some methods of climatological analysis. WMO Technical Note 81, Secretariat of the WMO, Switzerland, 53 pp.

UNESCO. 1979. Map of the world distribution of arid regions. Map at scale 1:25,000,000 with explanatory note. UNESCO, Paris.

LIST OF ACRONYMS

Acronym	Meaning
A1b	a middle-of-the-road SRES greenhouse gas emission scenario
A2	a pessimistic SRES greenhouse gas emission scenario
AET	Actual evapotranspiration
AR4	Fourth Assessment Report of the IPCC
AR5	Fifth Assessment Report of the IPCC
B1	an optimistic SRES greenhouse gas emission scenario
CCAFS	Climate Change, Agriculture and Food Security Program of the CGIAR
CGIAR	Consultative Group on International Agricultural Research
CRP	CGIAR Research Program
CWANA	Central Asia, West Asia and North Africa regions
CYI	Cyprus Institute
DEM	Digital elevation model
FAO	Food and Agriculture Organization of the United Nations
GCM	Global circulation model
GCV	Generalized cross-validation
GHG	Greenhouse gas
GIS	Geographic Information Systems
GPCC	Global Precipitation Climatology Centre
ICARDA	International Center for Agricultural Research in Dry Areas
IFAD	International Fund for Agricultural Development
IPCC	Intergovernmental Panel on Climate Change
NARS	National Agricultural Research System
NCARE	National Center for Agricultural Research and Extension, Jordan
NCDC	National Climate Data Center
PET	Potential evapotranspiration
SPI	Standardized Precipitation Index
SRES	GHG emission scenarios published in the IPCC 2000 ‘Special Report on Emission Scenarios (SRES)’
WANA	West Asia and North Africa

ANNEX 1

AVAILABILITY OF LONG-TERM STATION MEANS FOR PRECIPITATION AND TEMPERATURE

1. JORDAN[18]

Station	Long.	Lat.	Alt.	Prec	Tmax	Tmin
Al_ Al_Bayt_Univ	36.250000	32.350000	686	1995–2003	1995–2003	1995–2003
Al_Fajij	35.633333	30.550000	1263	2001–2003	2001–2003	2001–2003
Al_Ghowair	35.750000	31.233333	980	1980–2003	1980–2003	1980–2003
Al_Hashimiah	36.183333	32.100000	575	1998–2003	1998–2003	1998–2003
Al_Jafar	36.150000	30.283333	865	1938–2003	1965–2003	1965–2003
Al_Rashadiah	35.633333	30.700000	1500	2001–2003	2001–2003	2001–2003
Alhasan_Tafilah	35.716667	30.783333	1200	1971–2003	1973–2003	1973–2003
Alkasemiya	35.466667	30.100000	1510	1967–2003	1967–2003	1967–2003
Amman_Airport	35.983333	31.983333	781	1922–2003	1923–2003	1923–2003
Aqaba_ port	35.000000	29.516667	2	1966–2003	1966–2003	1966–2003
Azraq_ North	36.816667	31.850000	533	1967–2003	1967–2003	1967–2003
Azraq_South	36.816667	31.833333	521	1981–2003	1980–2003	1980–2003
Baqura	35.616667	32.666667	–170	1967–2003	1967–2003	1967–2003
Dabaa	36.050000	31.600000	750	1967–2003	1967–2003	1967–2003
Deiralla	35.616667	32.216667	–224	1952–2003	1952–2003	1952–2003
Dhana	35.616667	30.666667	1250	1998–2003	1998–2003	1998–2003
Ghorsafi	35.466667	31.033333	–350	1974–2003	1974–2003	1974–2003
Irbed	35.850000	32.550000	616	1937–2003	1955–2003	1955–2003
Jarash	35.900000	32.266667	540	1995–2003	1995–2003	1995–2003
Jordan_univ	35.883333	32.016667	980	1938–2003	1960–2003	1960–2003
Khanasry	36.050000	32.400000	863	1998–2003	1998–2003	1998–2003
King_Hussien_Int	35.000000	29.550000	51	1946–2003	1959–2003	1959–2003
Maan	35.783333	30.166667	1069	1938–2003	1959–2003	1959–2003
Madaba	35.800000	31.716667	785	1938–2003	1969–2003	1969–2003
Mafraq	36.250000	32.366667	686	1942–2003	1953–2003	1953–2003
Mutah_Univ	35.700000	31.050000	1105	1986–2003	1985–2003	1985–2003
Ouhadeh	35.600000	30.166667	1293	2001–2003	2001–2003	2001–2003
QAI_airport	35.983333	31.716667	722	1952–2003	1970–2003	1970–2003
Qatraneh	36.116667	31.250000	768	1938–2003	1984–2003	1984–2003
Rabbah	35.750000	31.266667	920	1952–2003	1961–2003	1961–2003
Ramtha	35.983333	32.500000	590	1976–2003	1976–2003	1976–2003
Ras_Muneef	35.750000	32.366667	1150	1961–2003	1976–2003	1976–2003
Roman_Ampt_Amman	35.950000	31.950000	750	1974–2003	1974–2003	1974–2003
Rwished	38.200000	32.500000	683	1942–2003	1961–2003	1961–2003
Safawi	38.133333	32.200000	674	1943–2003	1943–2003	1943–2003
Salt	35.733333	32.033333	796	1960–2003	1991–2003	1991–2003
Shoubak	35.533333	30.516667	1365	1938–2003	1960–2003	1960–2003
Swaileh	35.900000	32.000000	1050	1981–2003	1985–2003	1985–2003
Tafileh/Eiss	35.633333	30.833333	1260	1999–2003	1999–2003	1999–2003
Taybeh	35.716667	32.533333	373	1971–2003	1973–2003	1973–2003
University_farm	35.616667	32.166667	–230	1986–2003	1985–2003	1985–2003
Wadi al_Qattar	35.583333	32.400000	–200	1998–2003	1998–2003	1998–2003
Wadi_Dhulaial	36.283333	32.150000	580	1968–2003	1968–2003	1968–2003
Wadi_Mousa	35.466667	30.316667	1115	1976–2003	1984–2003	1984–2003

18 data provided by Jordan Meteorological Department

Wadi_wala	35.783333	31.550000	450	1962–2003	1961–2003	1961–2003
Zarqa	36.116667	32.133333	644	2002–2003	2002–2003	2002–2003
Zarqa_refinery	36.116667	32.083333	555	1966–2003	1966–2003	1966–2003

2. IRAQ[19]

Station	Long.	Lat.	Alt.	Prec	Tmax	Tmin
Amara	47.170000	31.850000	9	1980–2009	1980–2009	1980–2009
Anah	41.985000	34.370000	175	1980–2009	1980–2009	1980–2009
Baghdad	44.230000	33.230000	34	1980–2009	1980–2009	1980–2009
Baiji	43.483340	34.600000	115	1980–2009	1980–2009	1980–2009
Basra	47.780000	30.570000	2	1980–2008	1980–2008	1980–2008
Diwanya	44.980000	31.980000	20	1980–2008	1980–2008	1980–2008
Erbil	44.000000	36.183330	420	1980–2002	1980–2002	1980–2002
Kerbala	44.020000	32.620000	29	1980–2008	1980–2008	1980–2008
Khalias	44.510000	33.850000	50	1980–2009	1991–2009	1991–2009
Kirkuk	44.416670	35.466670	331	1980–2008	1980–2008	1980–2008
Kut	45.730000	32.480000	17	1980–2004	1988–2002	1988–2002
Mosul	43.150000	36.316670	223	1980–2008	1980–2008	1980–2008
Najaf	44.320000	31.980000	32	1975–2006	1975–2006	1975–2006
Nasiriya	46.230000	31.080000	3	1991–2008	1980–2008	1980–2008
Nukhaib	42.250000	32.030000	305	1980–2009	1980–1994	1980–1994
Rutba	40.280000	33.030000	615	1980–2008	1971–2002	1971–2002
Sinjar	41.833340	36.316670	465	1980–2009	1980–2008	1980–2008
Sulaymania	45.450000	35.550000	853	1980–2008	1981–1990	1980–1990
Sumawah	45.270000	31.300000	6	1980–2009	1980–2008	1980–2008
Zakho	42.683330	37.133330	443	1980–1990	1981–1990	1981–1990

19 data from Iraq Meteorological Department, provided by Iraq project team

3. NEIGHBORING COUNTRIES

Station	Long.	Lat.	Alt.	Country	Source Data
Abadan	48.25	30.37	7	Iran	Iran Met. Dept.
Ahwaz (Mollasani)	48.88	31.60	50	Iran	Iran Met. Dept.
Dezful	48.38	32.40	143	Iran	Iran Met. Dept.
Elam	46.43	33.63	1319	Iran	Iran Met. Dept.
Haft-tapeh	48.35	32.08	80	Iran	Iran Met. Dept.
Hamidiyeh	48.43	31.48	53	Iran	Iran Met. Dept.
Kermanshah	47.06	34.32	1322	Iran	Iran Met. Dept.
Mahabad	45.72	36.77	1385	Iran	Iran Met. Dept.
Mianab	48.48	31.97	50	Iran	Iran Met. Dept.
Oroomieh	45.07	37.53	1313	Iran	Iran Met. Dept.
Saghez	46.27	36.25	1523	Iran	Iran Met. Dept.
Sanandaj	47.00	35.33	1373	Iran	Iran Met. Dept.
Shadegan	48.67	30.65	6	Iran	Iran Met. Dept.
Shahid Chamran Ahwaz	48.67	31.33	18	Iran	Iran Met. Dept.
Kuwait Int. Airport	47.98	29.22	55	Kuwait	FAOCLIM2
Al Jouf	40.10	29.78	689	Saudi Arabia	FAOCLIM2
Hafr Al Batin	46.12	28.33	360	Saudi Arabia	FAOCLIM2
Rafha	43.48	29.63	447	Saudi Arabia	FAOCLIM2
Turaif	38.67	31.68	818	Saudi Arabia	FAOCLIM2
Abu-Kamal	40.92	34.42	182	Syria	FAOCLIM2
Deir-Ezzor	40.15	35.32	212	Syria	FAOCLIM2
Hassakah	40.75	36.50	296	Syria	FAOCLIM2
Jebel Atanf	38.67	33.48	708	Syria	FAOCLIM2
Kamishli	41.22	37.05	455	Syria	FAOCLIM2
Cizre	42.18	37.32	400	Turkey	FAOCLIM2
Hakkari	43.77	37.57	1720	Turkey	FAOCLIM2
Mardin	40.73	37.30	1050	Turkey	FAOCLIM2

ANNEX 2

CHARACTERISTICS OF THE KÖPPEN CLIMATIC ZONES[20]

Zone BS0k: Cool semi-arid (steppe) climate, neither winter nor summer drought
$Prec_{May–Sep} < 1.2 \times Prec_{Nov–Mar}$ **or** $Prec_{Nov–Mar} < 1.2 \times Prec_{May–Sep}$ and
$Prec_{year} \geq 10 \times (Temp_{year} + 7)$ and
$Temp_{year} < 18°C$ and $Temp_{warmest} \geq 18°C$

Zone BSwh: Hot semi-arid (steppe) climate, winter precipitation
$Temp_{year} \geq 18°C$ and
$Prec_{year} \leq 20 \times (Temp_{year} + 14)$ and
$Prec_{year} \geq 10 \times (Temp_{year} + 14)$ and
$Prec_{Nov–Mar} \geq 1.2 \times Prec_{May–Sep}$

Zone BSwk: Cool semi-arid (steppe) climate, winter precipitation
$Temp_{year} < 18°C$ and $Temp_{warmest} \geq 18°C$ and
$Prec_{year} \leq 20 \times (Temp_{year} + 14)$ and
$Prec_{year} \geq 10 \times (Temp_{year} + 14)$ and
$Prec_{Nov–Mar} \geq 1.2 \times Prec_{May–Sep}$

Zone BSwk': Cold semi-arid (steppe) climate, winter precipitation
$Prec_{Nov–Mar} \geq 1.2 \times Prec_{May–Sep}$ and
$Prec_{year} \geq 10 \times (Temp_{year} + 14)$ and
$Temp_{year} < 18°C$ and $Temp_{warmest} < 18°C$ and

Zone BSsk: Cool semi-arid (steppe) climate, summer precipitation
$Prec_{May–Sep} \geq 1.2 \times Prec_{Nov–Mar}$ and
$Prec_{year} \geq 10 \times Temp_{year}$ and
$Temp_{year} < 18°C$ and $Temp_{warmest} \geq 18°C$

Zone BW0h: Hot arid (desert) climate, neither winter nor summer drought
$Prec_{Nov–Mar} < 1.2 \times Prec_{May–Sep}$ and
$Prec_{year} < 10 \times (Temp_{year} + 7)$ and
$Temp_{year} \geq 18°C$

Zone BW0k: Cool arid (desert) climate, neither winter nor summer drought
$Prec_{Nov–Mar} < 1.2 \times Prec_{May–Sep}$ and
$Prec_{year} < 10 \times (Temp_{year} + 7)$ and
$Temp_{year} < 18°C$ and $Temp_{warmest} \geq 18°C$

Zone BWwh: Hot arid (desert) climate, winter precipitation
$Temp_{year} \geq 18°C$ and
$Prec_{year} < 10 \times (Temp_{year} + 14)$ and
$Prec_{Nov–Mar} \geq 1.2 \times Prec_{May–Sep}$

Zone BWwk: Cool arid (desert) climate, winter precipitation
$Temp_{year} < 18°C$ and $Temp_{warmest} \geq 18°C$ and
$Prec_{year} < 10 \times (Temp_{year} + 14)$ and
$Prec_{Nov–Mar} \geq 1.2 \times Prec_{May–Sep}$

20 The location of the Köppen climatic zones is shown in Figure 14.

Zone BWsh: Hot arid (desert) climate, summer precipitation
$Prec_{May–Sep} \geq 1.2 \times Prec_{Nov–Mar}$ and
$Temp_{year} \geq 18°C$

Zone BWsk: Cool arid (desert) climate, summer precipitation
$Prec_{May–Sep} \geq 1.2 \times Prec_{Nov–Mar}$ and
$Temp_{year} < 18°C$ and $Temp_{warmest} \geq 18°C$

Zone Csa: Warm temperate rainy climate with dry and hot summers
Not a B-climate and
$Temp_{coldest} \leq 18°C$ and $Temp_{coldest} \geq –3°C$ and
$Temp_{warmest} \geq 22°C$ (hot summer) and
$Precip_{wettest\ Dec–Feb} > 3 \times Prec_{driest\ Jun–Aug}$ (summer drought)

Zone Csb: Warm temperate rainy climate with dry and warm summers
Not a B-climate and
$Temp_{coldest} \leq 18°C$ and $Temp_{coldest} \geq –3°C$ and
$Temp_{warmest} < 22°C$ and (no.of months with Tmean > 10°C) ≥ 4 (warm summer) and
$Precip_{wettest\ Dec–Feb} > 3 \times Prec_{driest\ Jun–Aug}$ (summer drought)

Zone Cfa: Warm temperate rainy climate without dry season and hot summers
not B-climate) and
$Temp_{coldest} \leq 18°C$ and $Temp_{coldest} \geq –3°C$ and
'no dry season': neither winter drought nor summer drought and
'hot summer': $Temp_{warmest} \geq 22°C$

Zone Cfb: Warm temperate rainy climate without dry season and warm summers
not B-climate) and
$Temp_{coldest} \leq 18°C$ and $Temp_{coldest} \geq –3°C$ and
'no dry season': neither winter drought nor summer drought and
'warm summer': $Temp_{warmest} < 22°C$ and (no. of months with Tmean > 10°C) ≥ 4

Zone Dfa: Continuously humid subarctic climate with hot summer
not B-climate and
$Temp_{warmest} > 10°C$ and $Temp_{coldest} < –3°C$ and
'no dry season': neither winter drought nor summer drought and
'hot summer': $Temp_{warmest} \geq 22°C$

Zone Dfb: Continuously humid subarctic climate with warm summer
not B-climate and
$Temp_{warmest} > 10°C$ and $Temp_{coldest} < –3°C$ and
'no dry season': neither winter drought nor summer drought and
'warm summer': $Temp_{warmest} < 22°C$ and (no. of months with Tmean > 10°C) ≥ 4

Zone Dsa: Subarctic climate with humid winter and hot summer
Not a B-climate and
$Temp_{warmest} > 10°C$ and $Temp_{coldest} < –3°C$
$Temp_{warmest} \geq 22°C$ (hot summer) and
$Precip_{wettest\ Dec–Feb} > 3 \times Prec_{driest\ Jun–Aug}$ (summer drought)

Zone Dsb: Subarctic climate with humid winter and warm summer
Not a B-climate and
$Temp_{warmest}$ > 10°C and $Temp_{coldest}$ < –3°C
$Temp_{warmest}$ < 22°C and (no.of months with Tmean > 10°C) ≥ 4 (warm summer) and
$Precip_{wettest\ Dec–Feb}$ > 3 × $Prec_{driest\ Jun–Aug}$ (summer drought)

Zone E: Arctic climate
not B-climate and
$Temp_{warmest}$ (≤ 10°C and > 0°C) and $Temp_{coldest}$ $< -3°C$

Explanation of symbols
$Temp_{year}$: Mean annual temperature
$Temp_{coldest}$: Mean temperature of the coldest month of the year ($Temp_{coldest}$)

$Temp_{warmest}$: Mean temperature of the warmest month of the year
$Prec_{year}$: Mean annual precipitation total
$Prec_{Nov–Mar}$: Mean precipitation total for November–March
$Prec_{May–Sep}$: Mean precipitation total for May–September
$Prec_{wettestJun–Aug}$: Mean precipitation of the wettest month during June–August
$Prec_{driestJun–Aug}$: Mean precipitation of the driest month during June–August
$Prec_{wettestDec–Feb}$: Mean precipitation of the wettest month during December–February
$Prec_{driestDec–Feb}$: Mean precipitation of the driest month during December–February

ANNEX 3

CHARACTERISTICS OF THE UNESCO AGROCLIMATIC ZONES[21]

Agroclimatic zone	Moisture regime	Aridity index	Winter type	Winter temp.	Summer type	Summer temp.
HA-M-VW	Hyper-arid	< 0.03	Mild	10–20°C	Very warm	> 30°C
HA-M-W	Hyper-arid	< 0.03	Mild	10–20°C	Warm	20–30°C
HA-C-VW	Hyper-arid	< 0.03	Cool	0–10°C	Very warm	> 30°C
HA-C-W	Hyper-arid	< 0.03	Cool	0–10°C	Warm	20–30°C
A-M-VW	Arid	0.03–0.2	Mild	10–20°C	Very warm	> 30°C
A-M-W	Arid	0.03–0.2	Mild	10–20°C	Warm	20–30°C
A-C-VW	Arid	0.03–0.2	Cool	0–10°C	Very warm	> 30°C
A-C-W	Arid	0.03–0.2	Cool	0–10°C	Warm	20–30°C
A-C-M	Arid	0.03–0.2	Cool	0–10°C	Mild	10–20°C
A-K-W	Arid	0.03–0.2	Cold	≤ 0°C	Warm	20–30°C
SA-M-VW	Semi-arid	0.2–0.5	Mild	10–20°C	Very warm	> 30°C
SA-M-W	Semi-arid	0.2–0.5	Mild	10–20°C	Warm	20–30°C
SA-C-VW	Semi-arid	0.2–0.5	Cool	0–10°C	Very warm	> 30°C
SA-C-W	Semi-arid	0.2–0.5	Cool	0–10°C	Warm	20–30°C
SA-C-M	Semi-arid	0.2–0.5	Cool	0–10°C	Mild	10–20°C
SA-K-W	Semi-arid	0.2–0.5	Cold	≤ 0°C	Warm	20–30°C
SA-K-M	Semi-arid	0.2–0.5	Cold	≤ 0°C	Mild	10–20°C
SH-M-W	Sub-humid	0.5–0.75	Mild	10–20°C	Warm	20–30°C
SH-C-VW	Sub-humid	0.5–0.75	Cool	0–10°C	Very warm	> 30°C
SH-C-W	Sub-humid	0.5–0.75	Cool	0–10°C	Warm	20–30°C
SH-C-M	Sub-humid	0.5–0.75	Cool	0–10°C	Mild	10–20°C
SH-K-W	Sub-humid	0.5–0.75	Cold	≤ 0°C	Warm	20–30°C
SH-K-M	Sub-humid	0.5–0.75	Cold	≤ 0°C	Mild	10–20°C
H-M-W	Humid	0.75–1	Mild	10–20°C	Warm	20–30°C
H-C-W	Humid	0.75–1	Cool	0–10°C	Warm	20–30°C
H-C-M	Humid	0.75–1	Cool	0–10°C	Mild	10–20°C
H-K-W	Humid	0.75–1	Cold	≤ 0°C	Warm	20–30°C
H-K-M	Humid	0.75–1	Cold	≤ 0°C	Mild	10–20°C
H-K-C	Humid	0.75–1	Cold	≤ 0°C	Cool	≤ 10°C
PH-C-W	Per-humid	> 1	Cool	0–10°C	Warm	20–30°C
PH-C-M	Per-humid	> 1	Cool	0–10°C	Mild	10–20°C
PH-K-W	Per-humid	> 1	Cold	≤ 0°C	Warm	20–30°C
PH-K-M	Per-humid	> 1	Cold	≤ 0°C	Mild	10–20°C
PH-K-C	Per-humid	> 1	Cold	≤ 0°C	Cool	≤ 10°C

21 The location of the UNESCO agroclimatic zones is shown in Figure 17.

ANNEX 4.

MAPS OF PRECIPITATION PROBABILITIES (1901–2010)

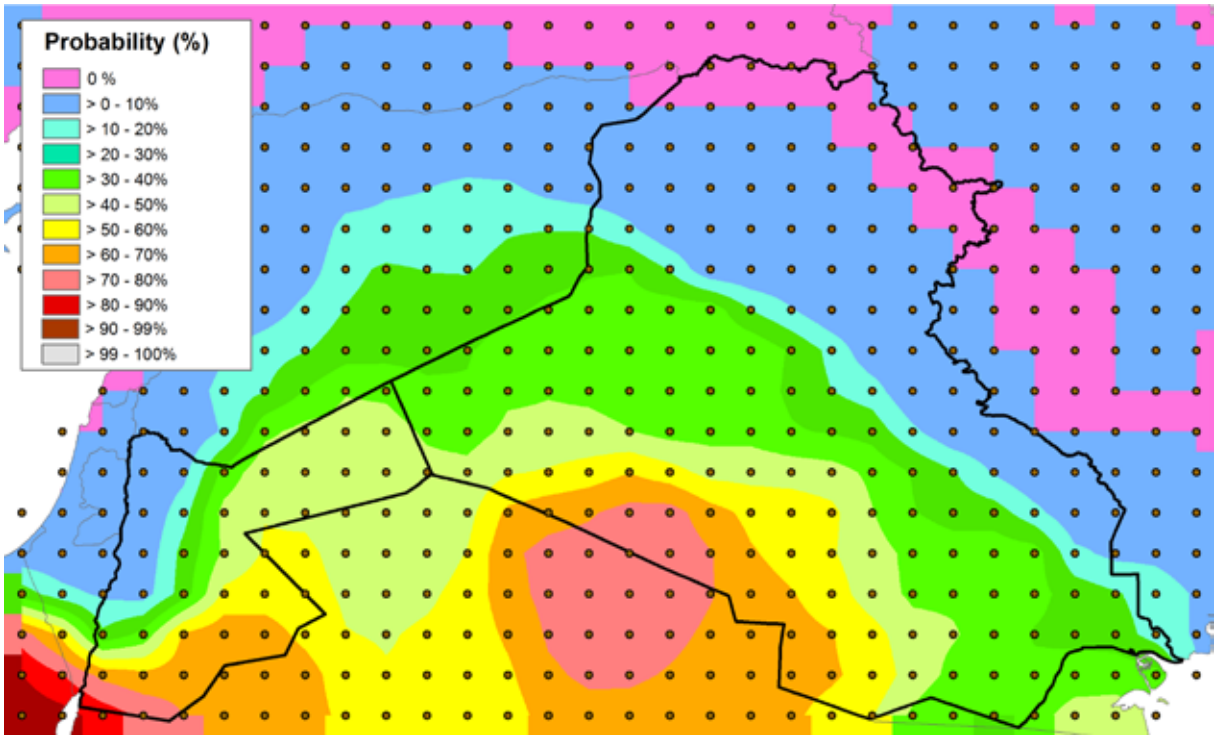

Figure 39. Probability of annual precipitation not exceeding 100 mm

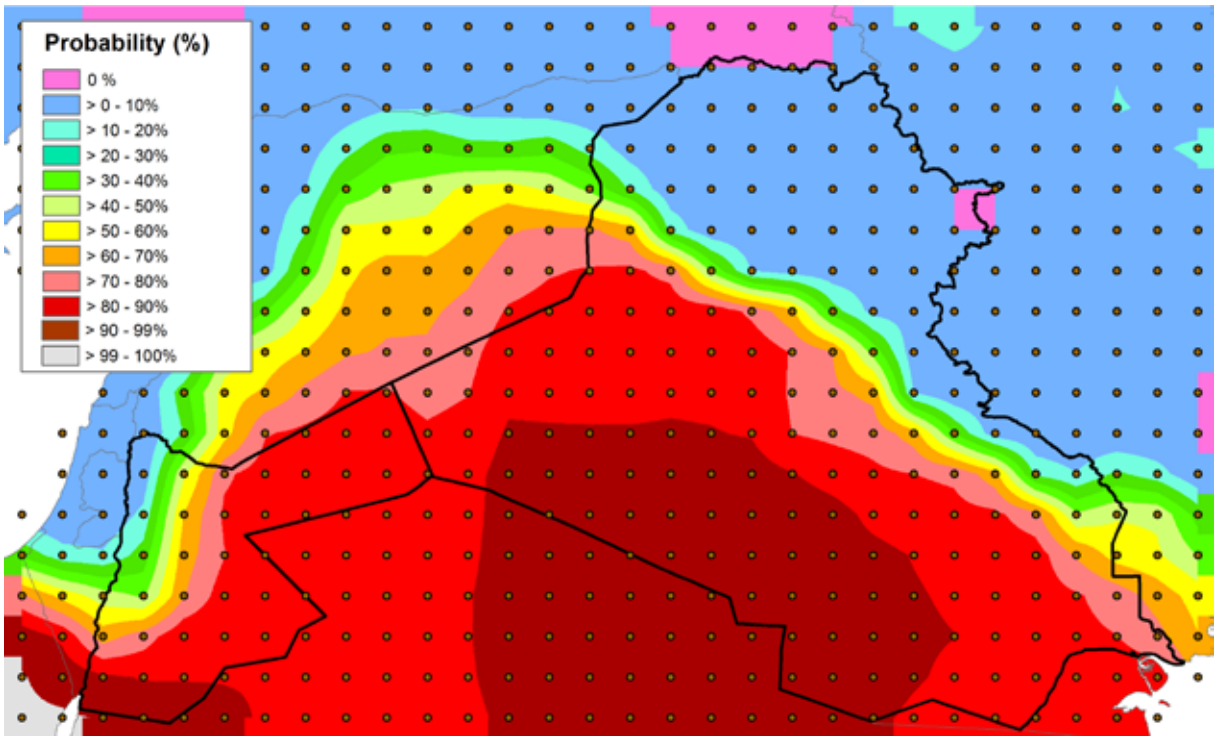

Figure 40. Probability of annual precipitation not exceeding 200 mm

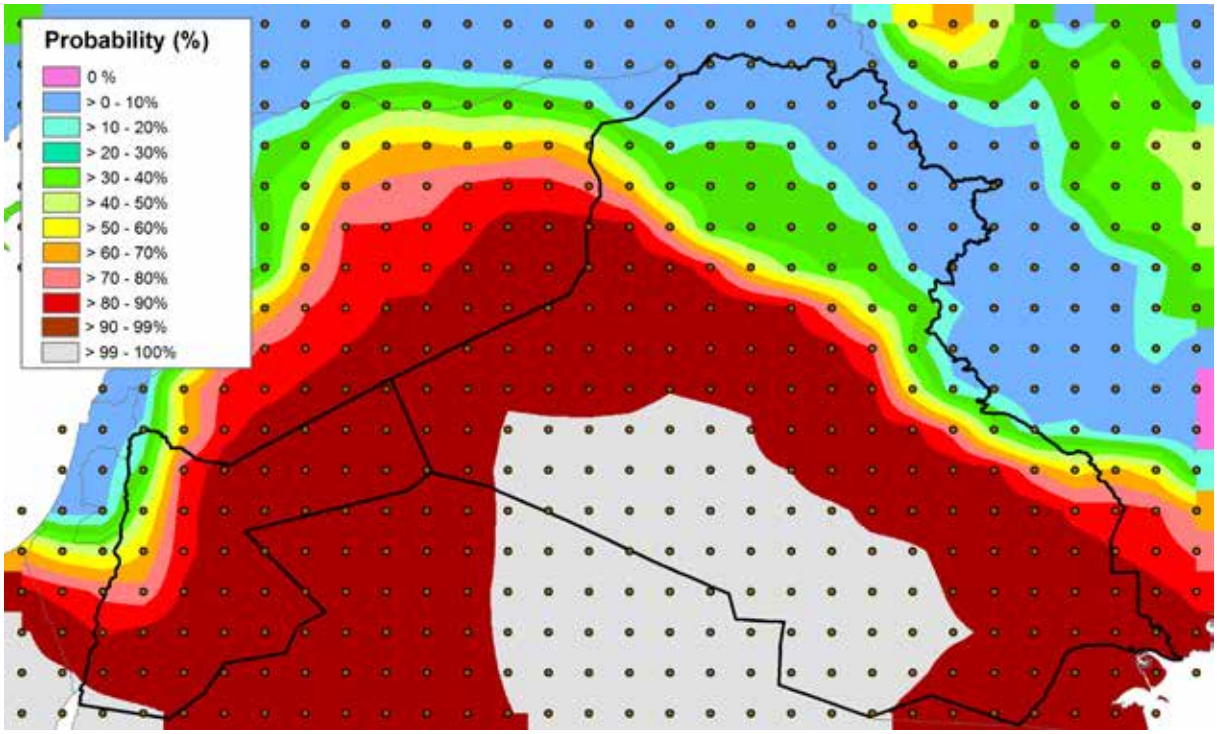

Figure 41. Probability of annual precipitation not exceeding 300 mm

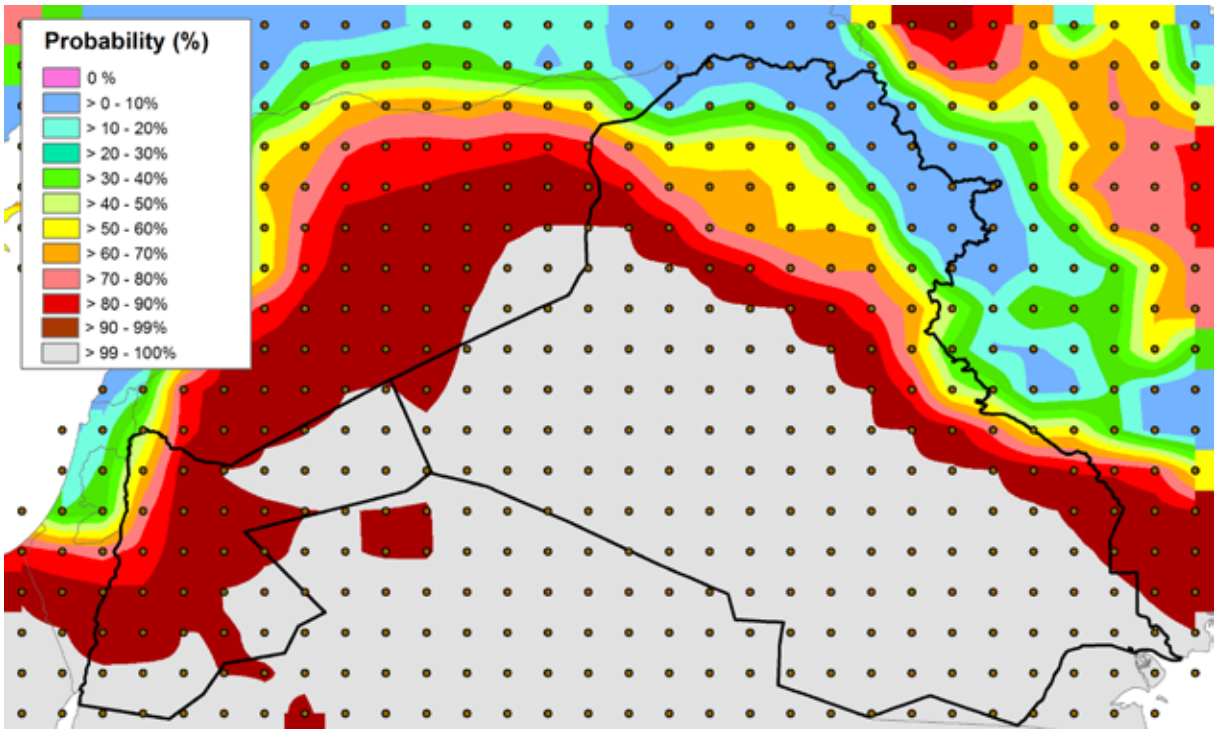

Figure 42. Probability of annual precipitation not exceeding 400 mm

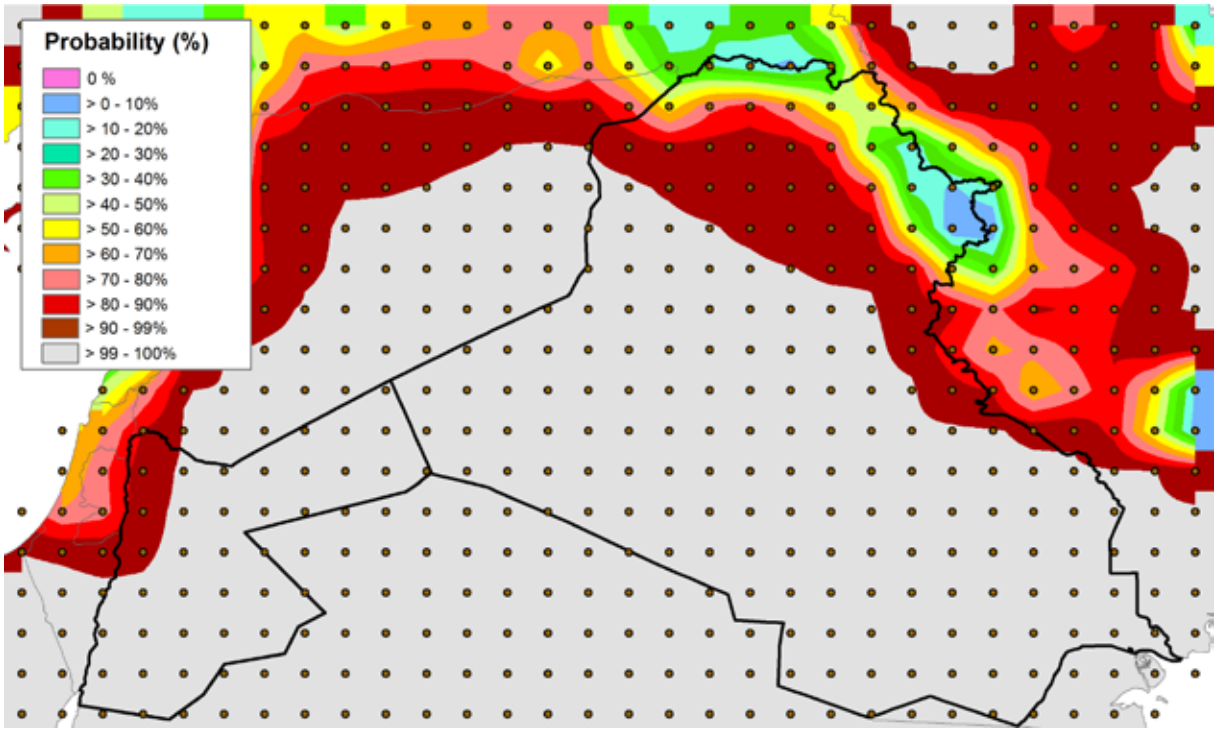

Figure 43. Probability of annual precipitation not exceeding 600 mm

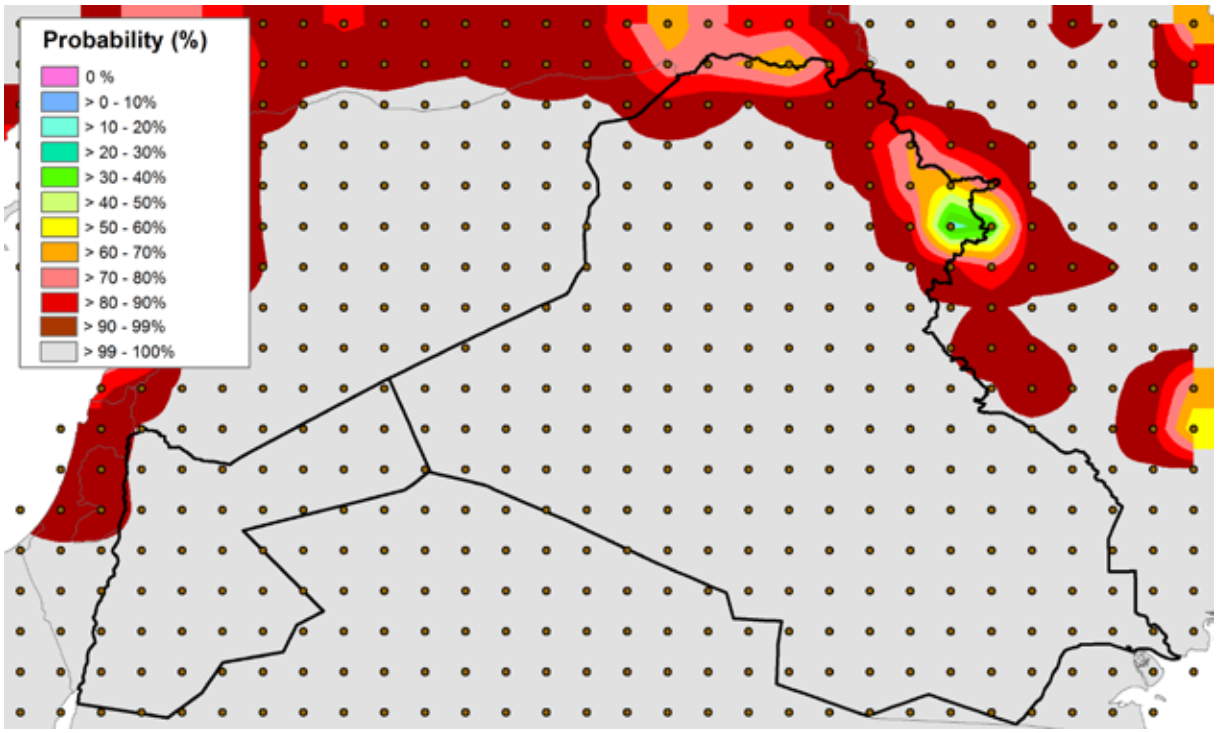

Figure 44. Probability of annual precipitation not exceeding 800 mm

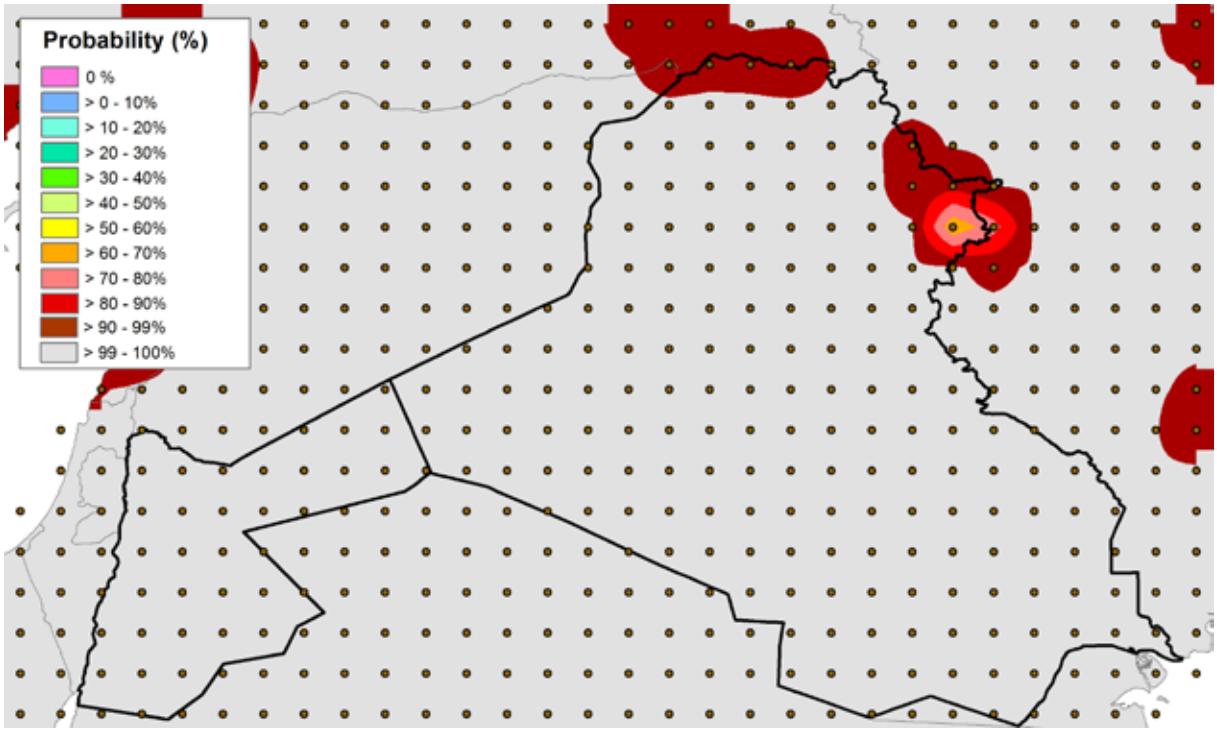

Figure 45. Probability of annual precipitation not exceeding 1000 mm

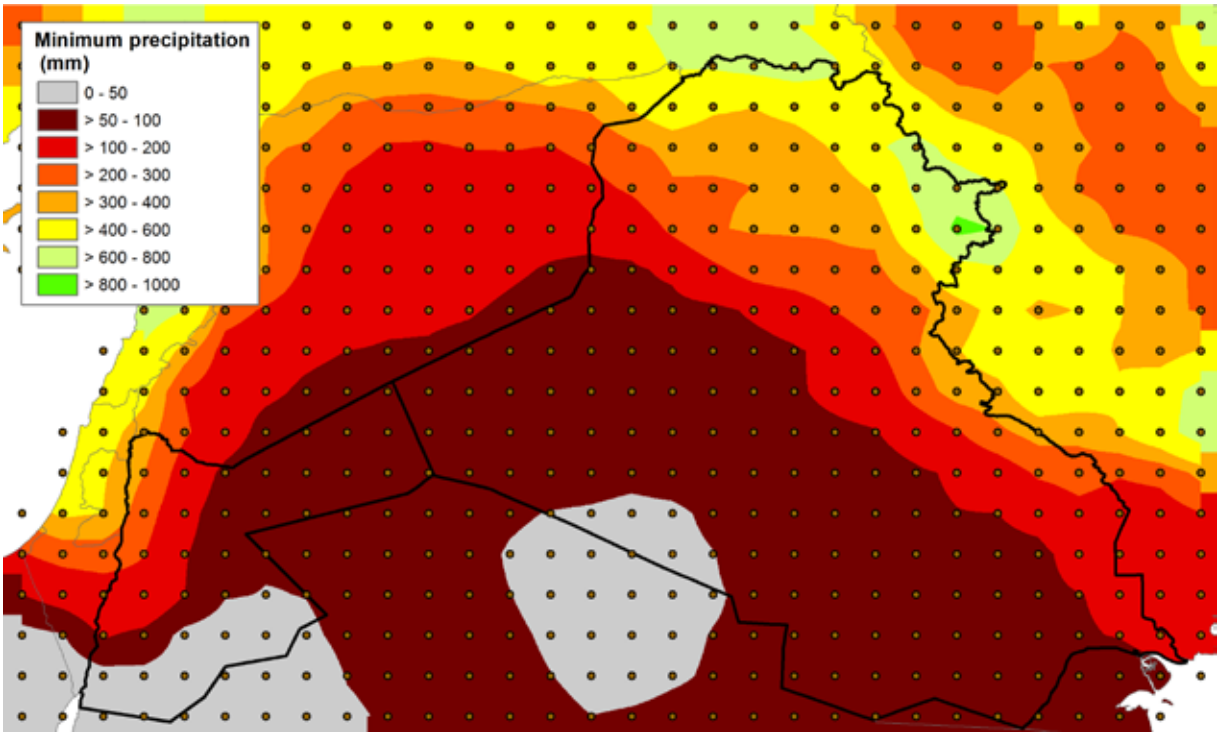

Figure 46. Minimum annual precipitation likely to be exceeded in three out of four years

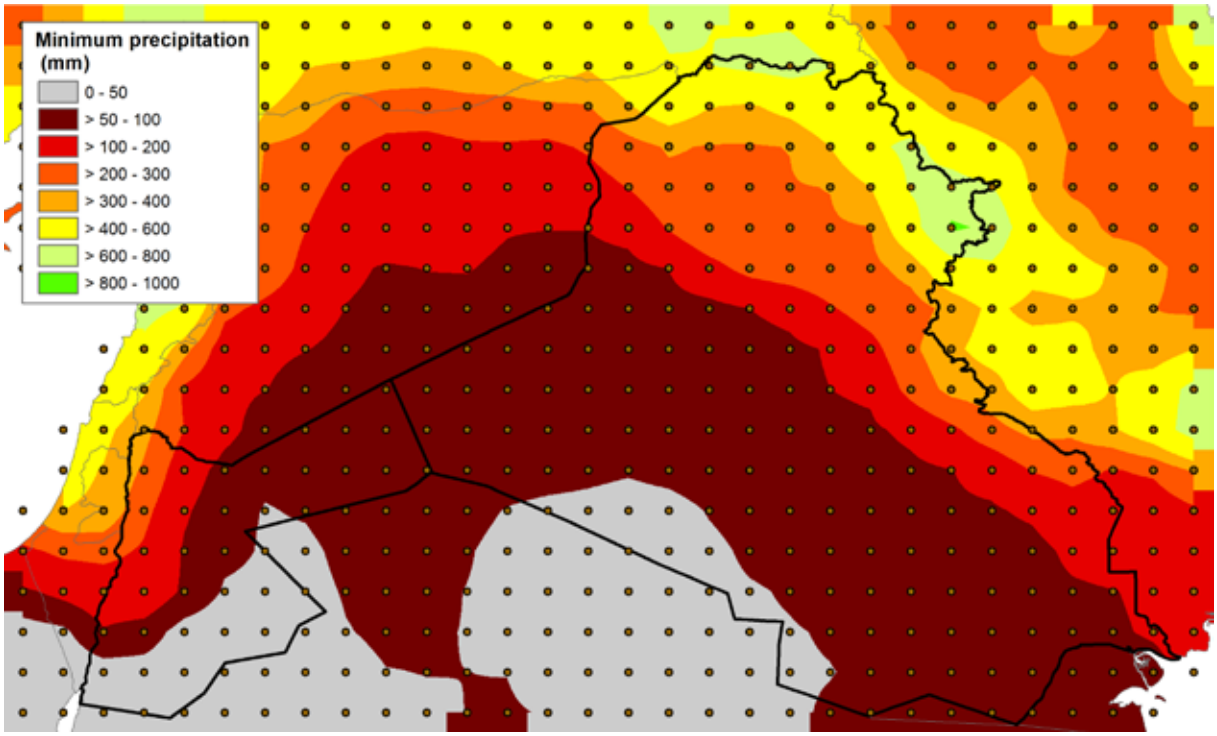

Figure 47. Minimum annual precipitation likely to be exceeded in four out of five years

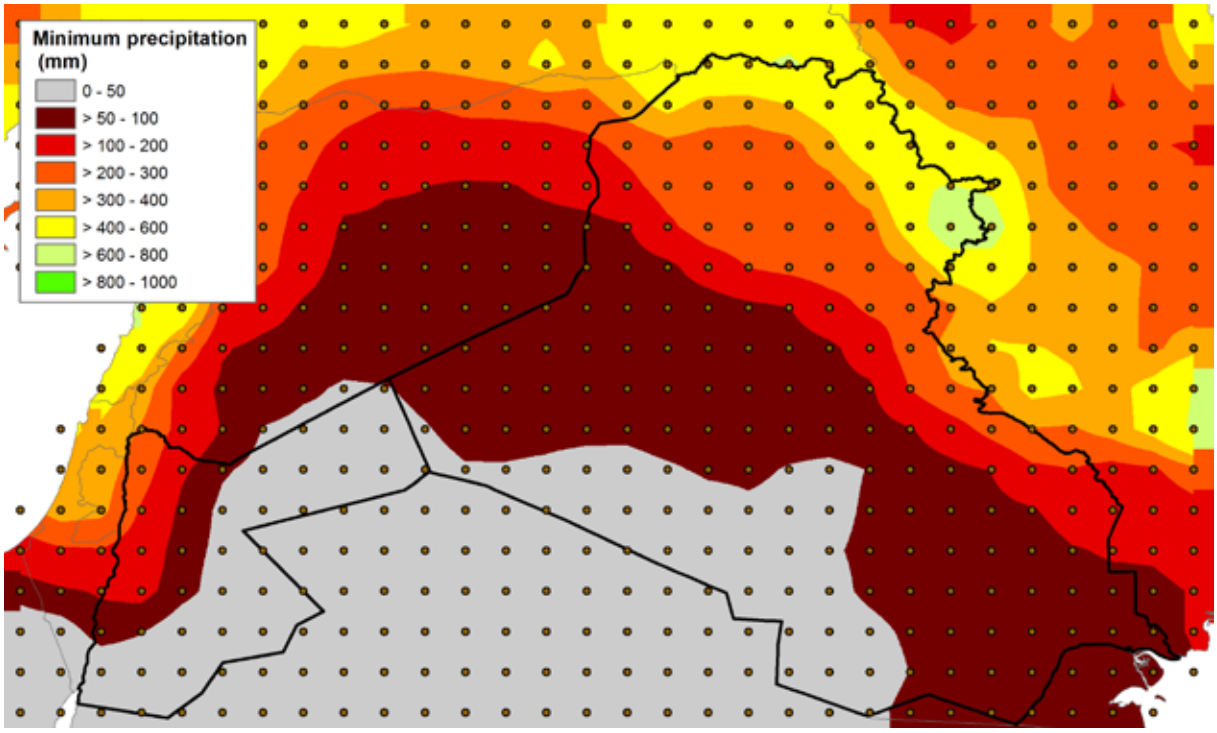

Figure 48. Minimum annual precipitation likely to be exceeded in nine out of 10 years

ANNEX 5.

MAPS OF HISTORICAL DROUGHT AND WETNESS PERIODS (1901–2010)

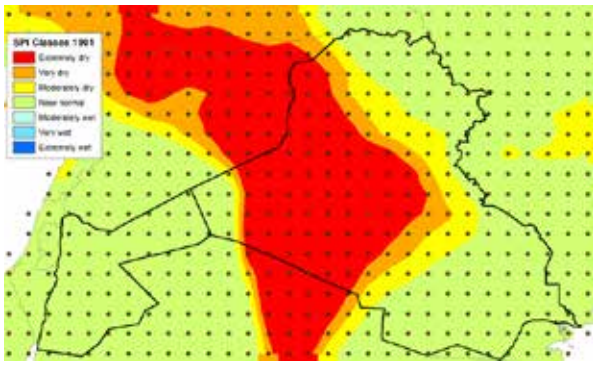

Figure 49. Annual Standardized Precipitation Index in 1901

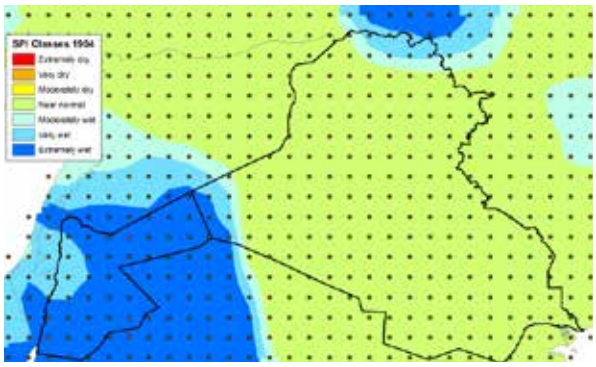

Figure 52. Annual Standardized Precipitation Index in 1904

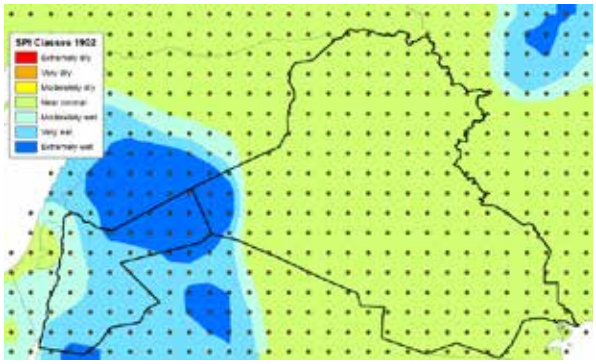

Figure 50. Annual Standardized Precipitation Index in 1902

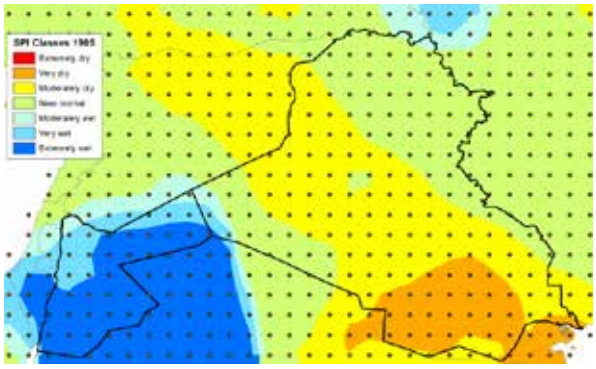

Figure 53. Annual Standardized Precipitation Index in 1905

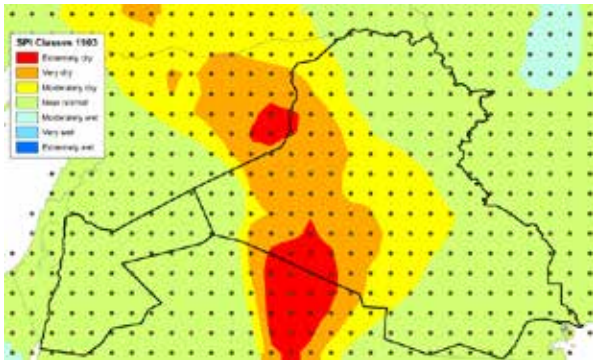

Figure 51. Annual Standardized Precipitation Index in 1903

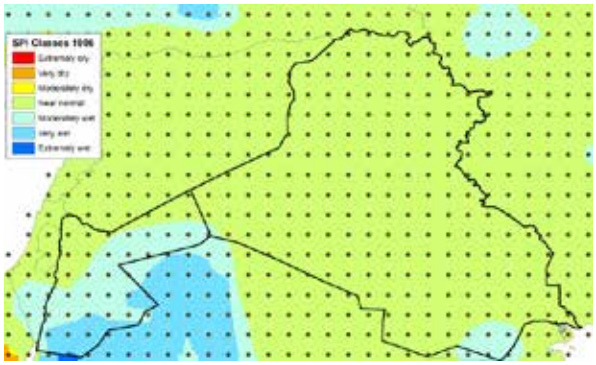

Figure 54. Annual Standardized Precipitation Index in 1906

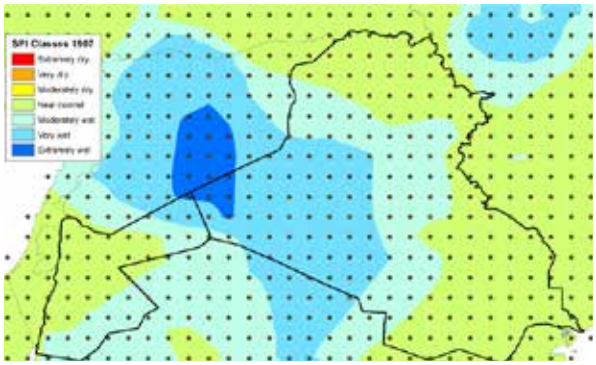

Figure 55. Annual Standardized Precipitation Index in 1907

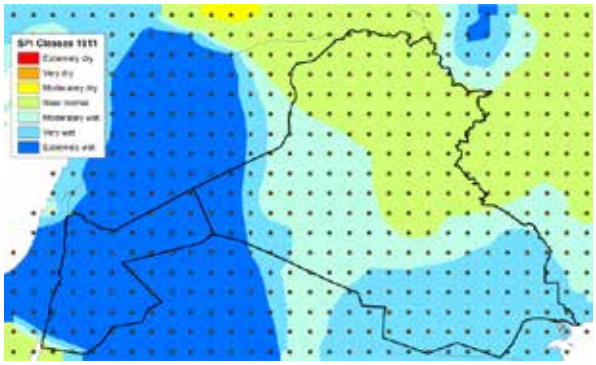

Figure 59. Annual Standardized Precipitation Index in 1911

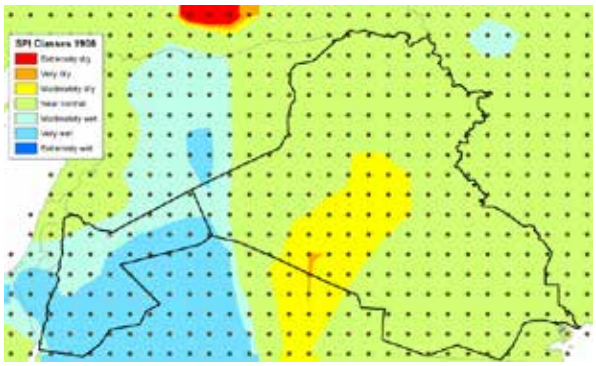

Figure 56. Annual Standardized Precipitation Index in 1908

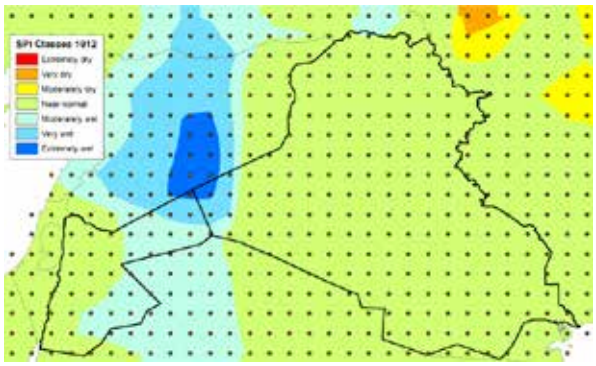

Figure 60. Annual Standardized Precipitation Index in 1912

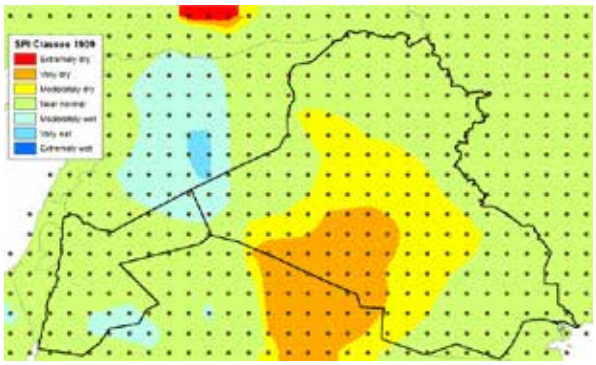

Figure 57. Annual Standardized Precipitation Index in 1909

Figure 61. Annual Standardized Precipitation Index in 1913

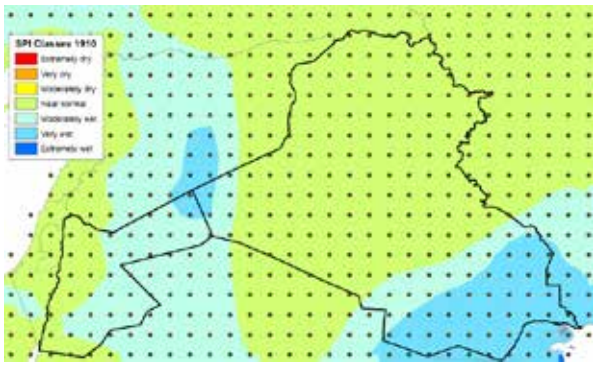

Figure 58. Annual Standardized Precipitation Index in 1910

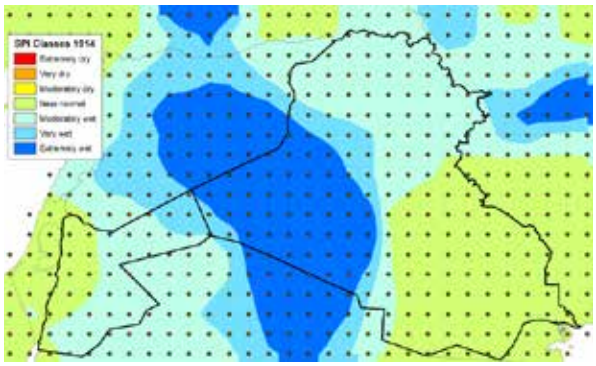

Figure 62. Annual Standardized Precipitation Index in 1914

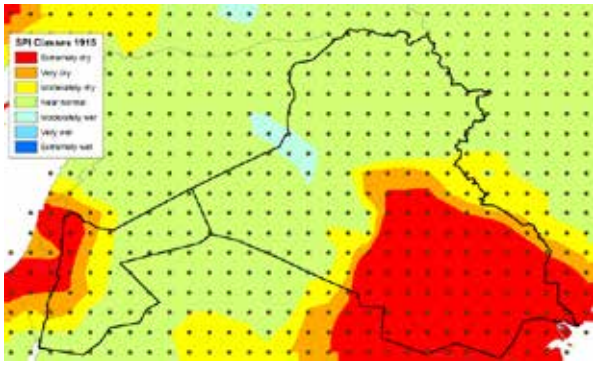

Figure 63. Annual Standardized Precipitation Index in 1915

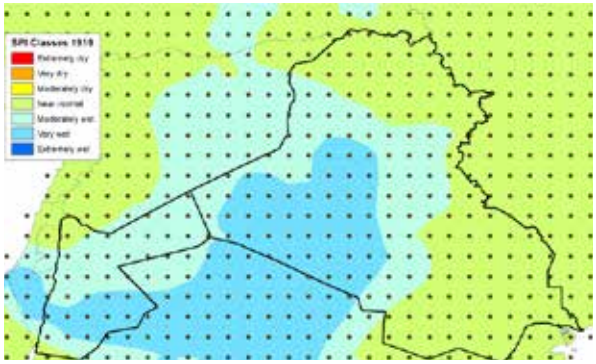

Figure 67. Annual Standardized Precipitation Index in 1919

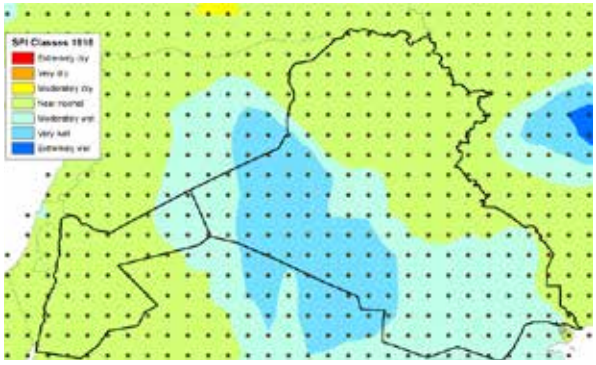

Figure 64. Annual Standardized Precipitation Index in 1916

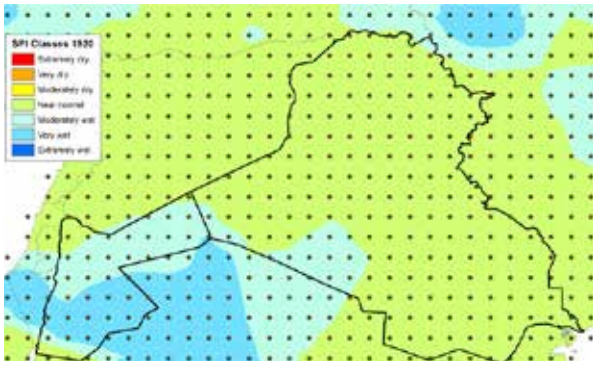

Figure 68. Annual Standardized Precipitation Index in 1920

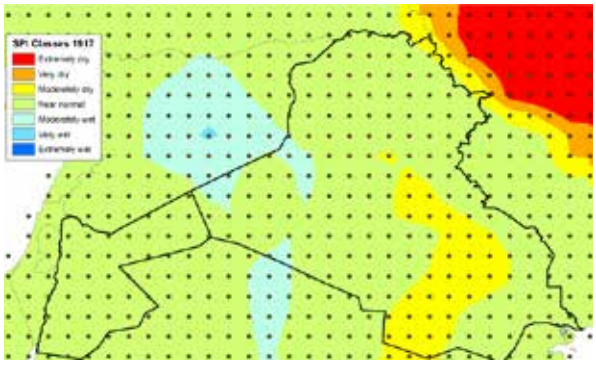

Figure 65. Annual Standardized Precipitation Index in 1917

Figure 69. Annual Standardized Precipitation Index in 1921

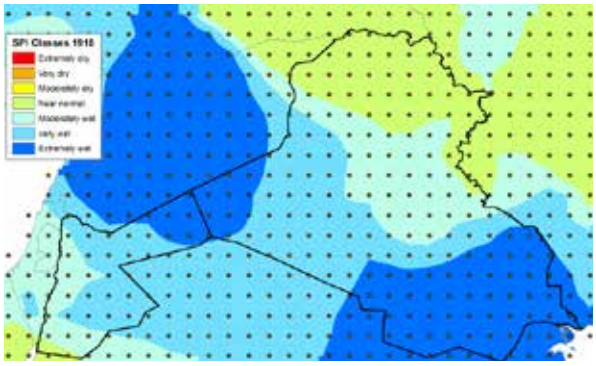

Figure 66. Annual Standardized Precipitation Index in 1918

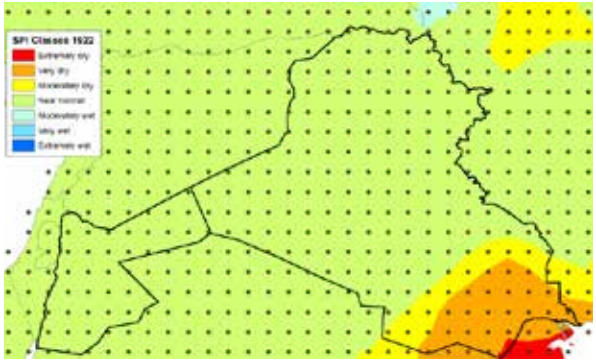

Figure 70. Annual Standardized Precipitation Index in 1922

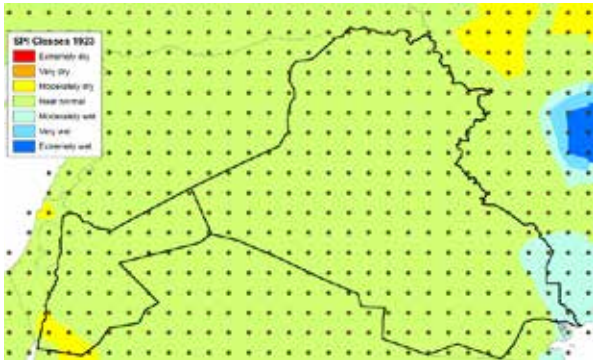

Figure 71. Annual Standardized Precipitation Index in 1923

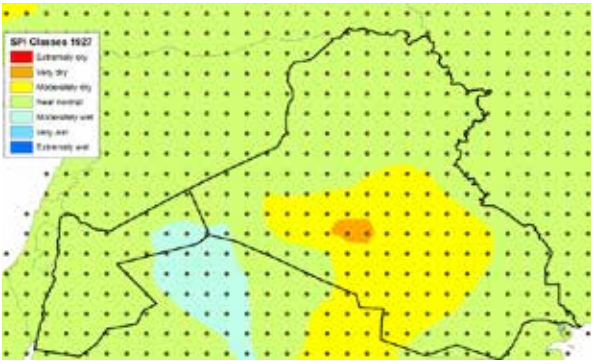

Figure 75. Annual Standardized Precipitation Index in 1927

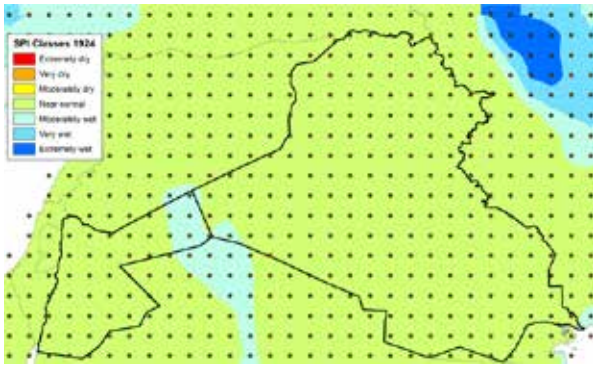

Figure 72. Annual Standardized Precipitation Index in 1924

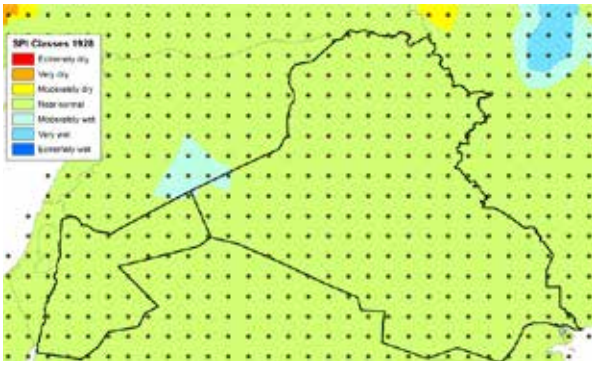

Figure 76. Annual Standardized Precipitation Index in 1928

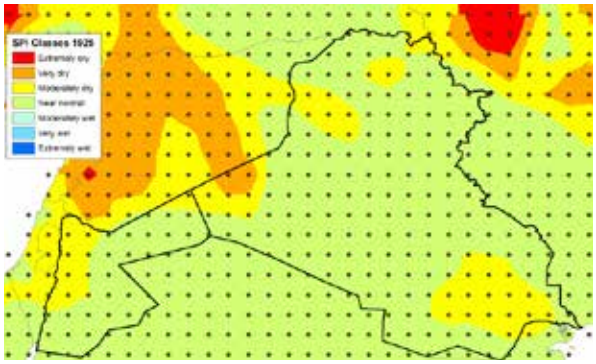

Figure 73. Annual Standardized Precipitation Index in 1925

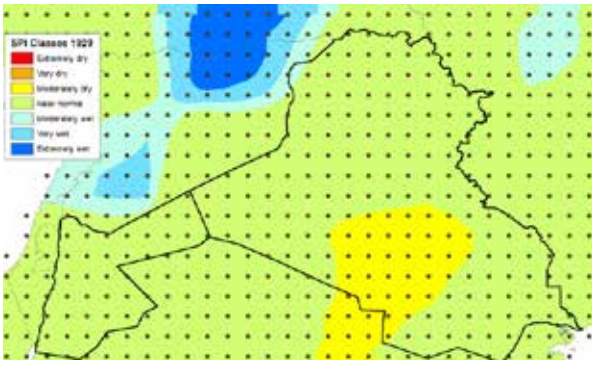

Figure 77. Annual Standardized Precipitation Index in 1929

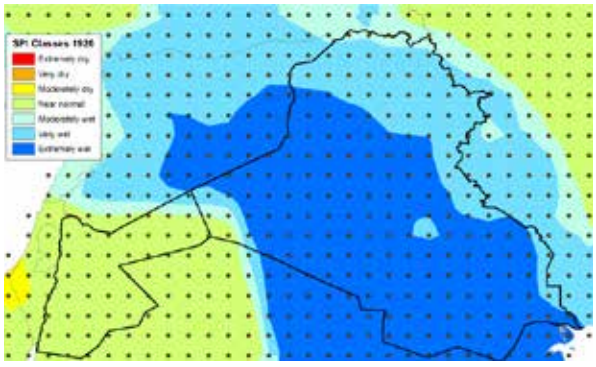

Figure 74. Annual Standardized Precipitation Index in 1926

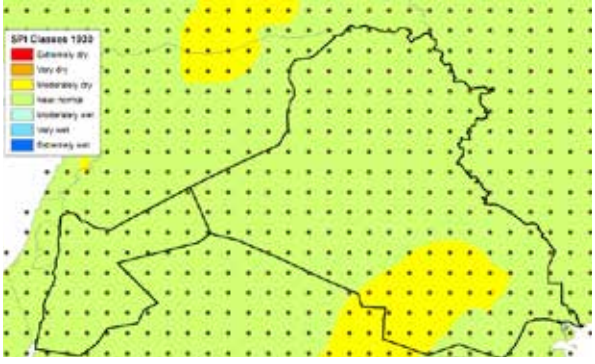

Figure 78. Annual Standardized Precipitation Index in 1930

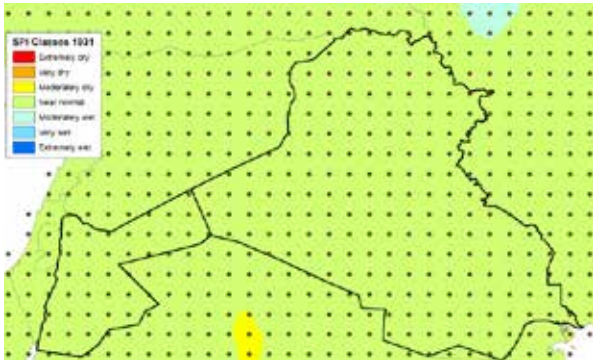

Figure 79. Annual Standardized Precipitation Index in 1931

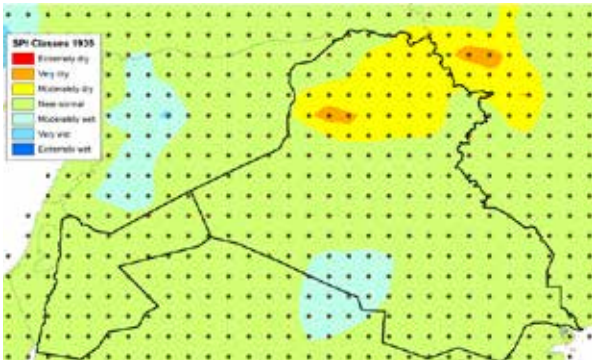

Figure 83. Annual Standardized Precipitation Index in 1935

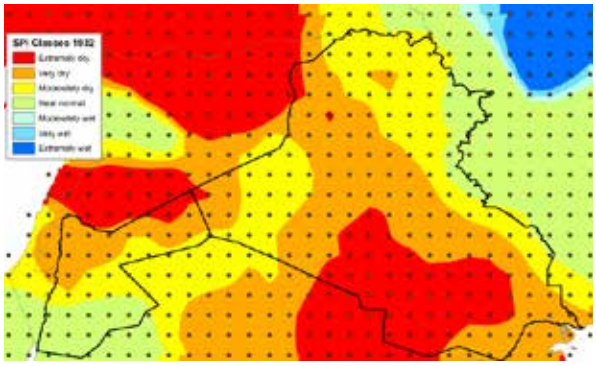

Figure 80. Annual Standardized Precipitation Index in 1932

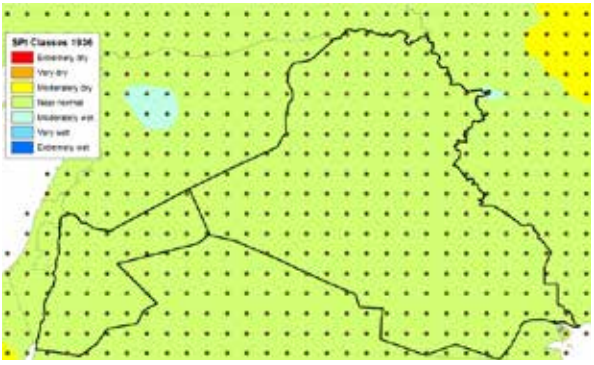

Figure 84. Annual Standardized Precipitation Index in 1936

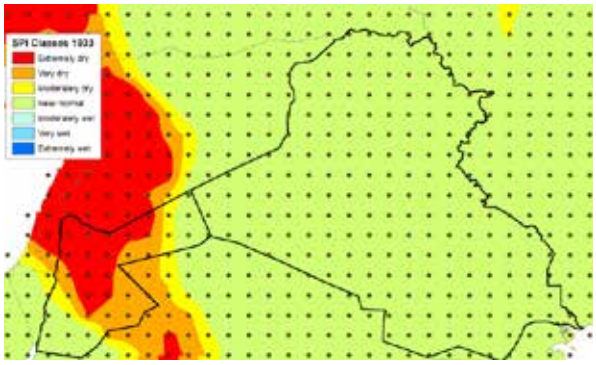

Figure 81. Annual Standardized Precipitation Index in 1933

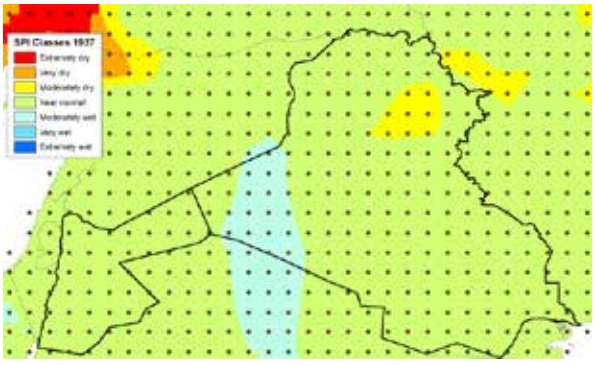

Figure 85. Annual Standardized Precipitation Index in 1937

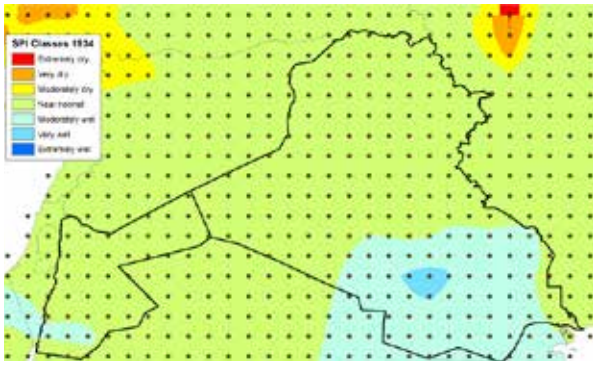

Figure 82. Annual Standardized Precipitation Index in 1934

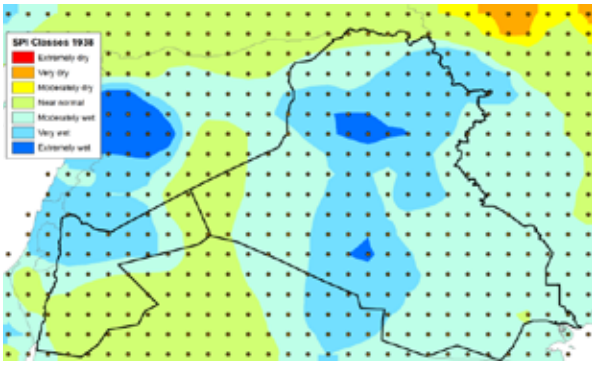

Figure 86. Annual Standardized Precipitation Index in 1938

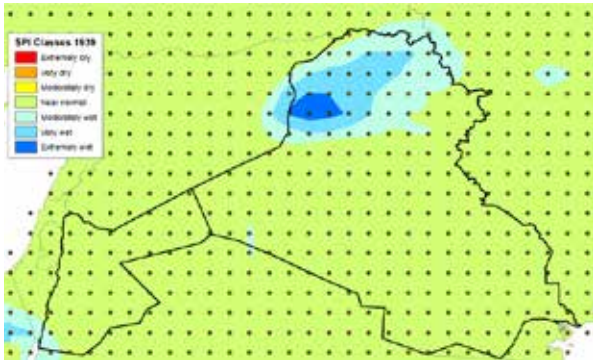

Figure 87. Annual Standardized Precipitation Index in 1939

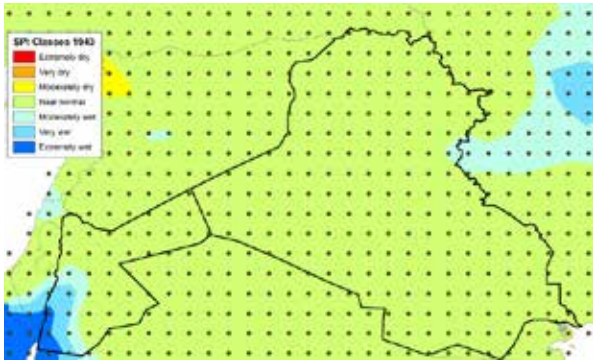

Figure 91. Annual Standardized Precipitation Index in 1943

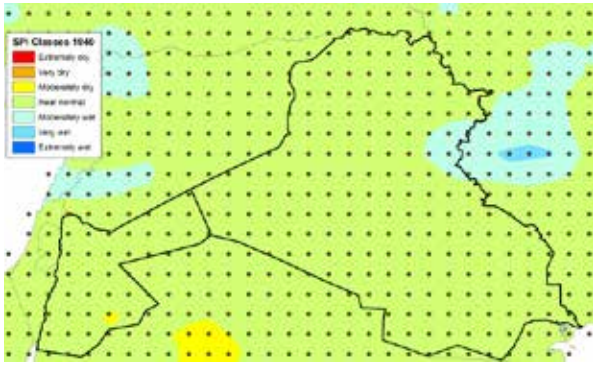

Figure 88. Annual Standardized Precipitation Index in 1940

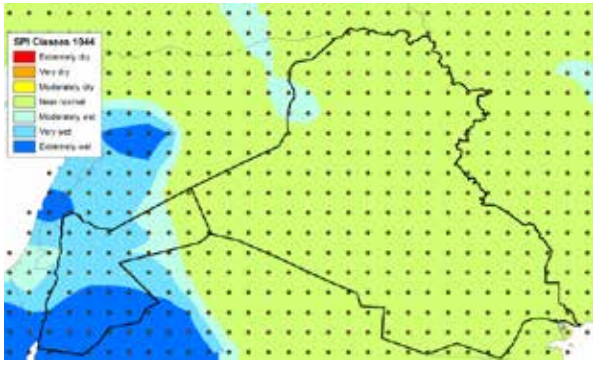

Figure 92. Annual Standardized Precipitation Index in 1944

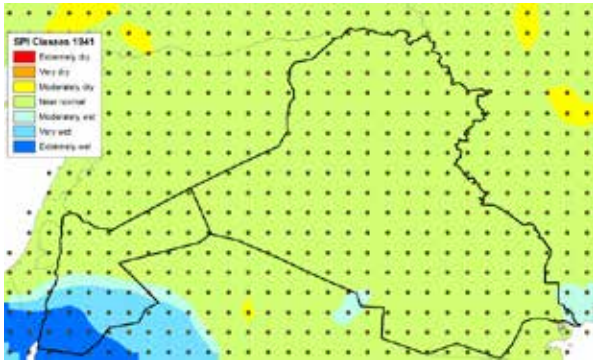

Figure 89. Annual Standardized Precipitation Index in 1941

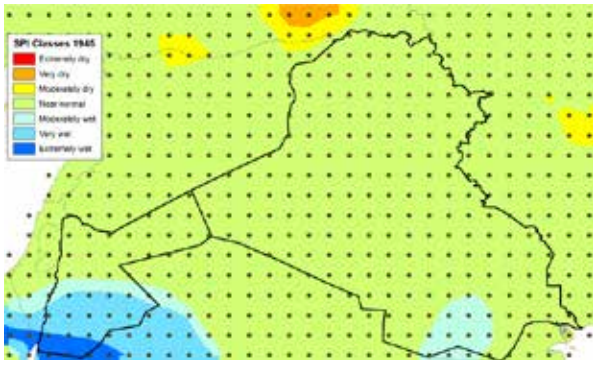

Figure 93. Annual Standardized Precipitation Index in 1945

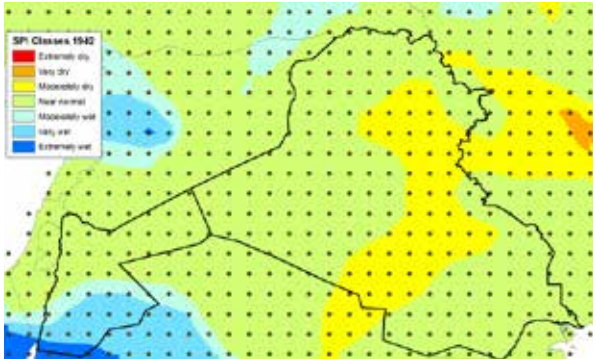

Figure 90. Annual Standardized Precipitation Index in 1942

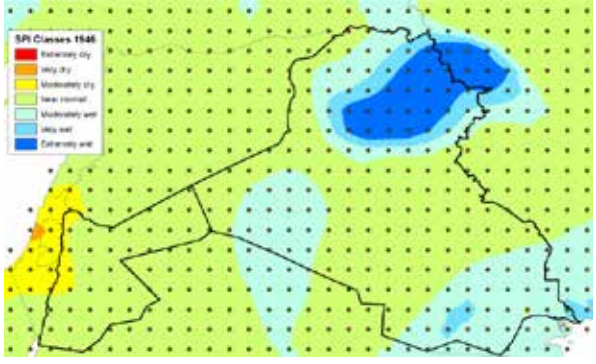

Figure 94. Annual Standardized Precipitation Index in 1946

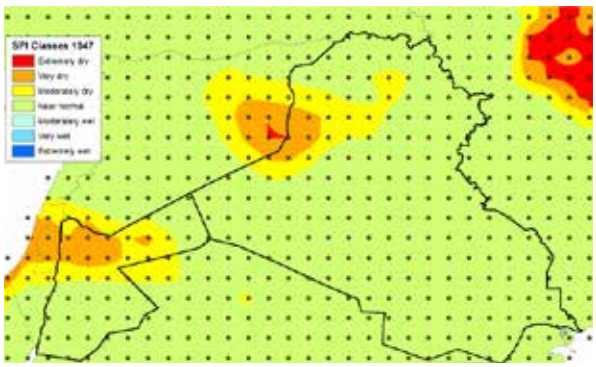

Figure 95. Annual Standardized Precipitation Index in 1947

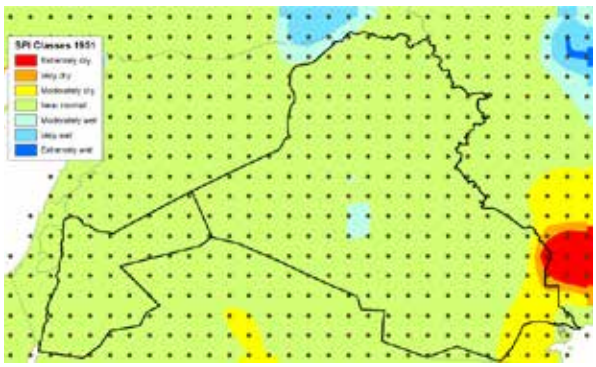

Figure 99. Annual Standardized Precipitation Index in 1951

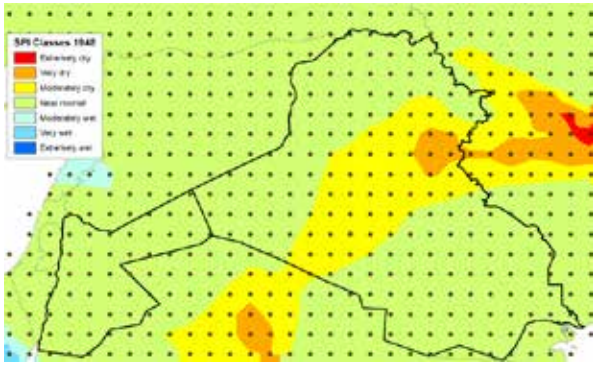

Figure 96. Annual Standardized Precipitation Index in 1948

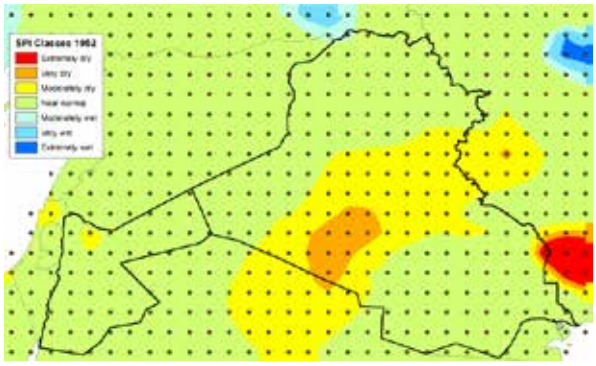

Figure 100. Annual Standardized Precipitation Index in1952

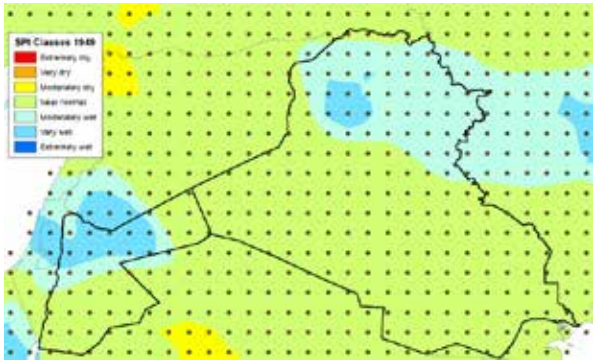

Figure 97. Annual Standardized Precipitation Index in 1949

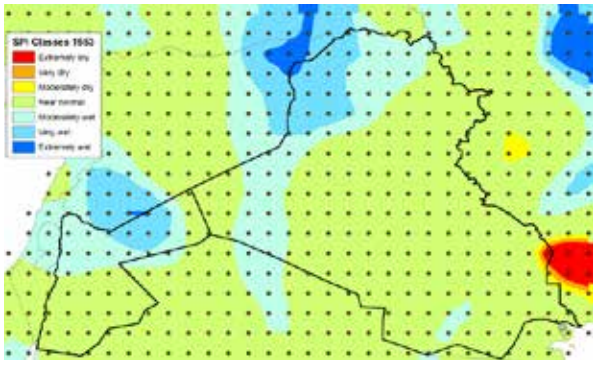

Figure 101. Annual Standardized Precipitation Index in1953

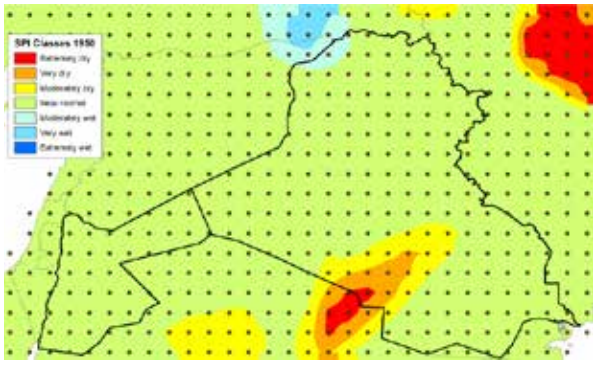

Figure 98. Annual Standardized Precipitation Index in 1950

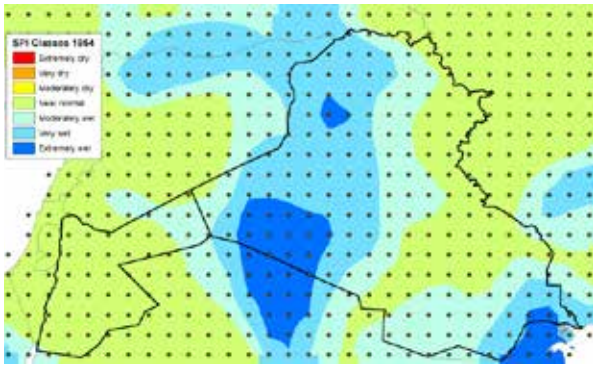

Figure 102. Annual Standardized Precipitation Index in1954

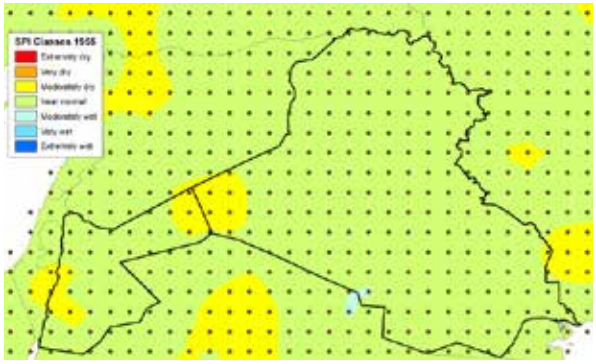

Figure 103. Annual Standardized Precipitation Index in1955

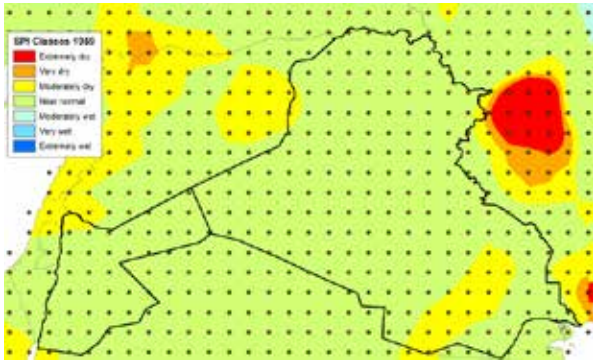

Figure 107. Annual Standardized Precipitation Index in1959

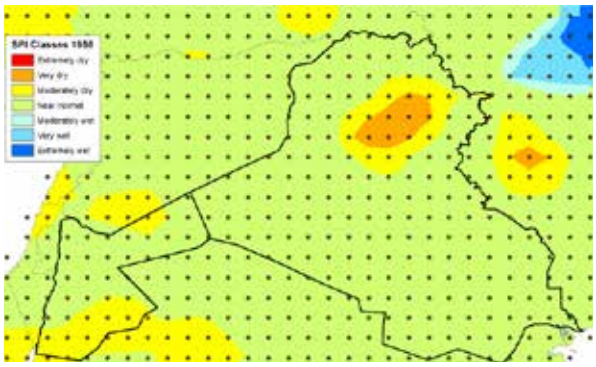

Figure 104. Annual Standardized Precipitation Index in1956

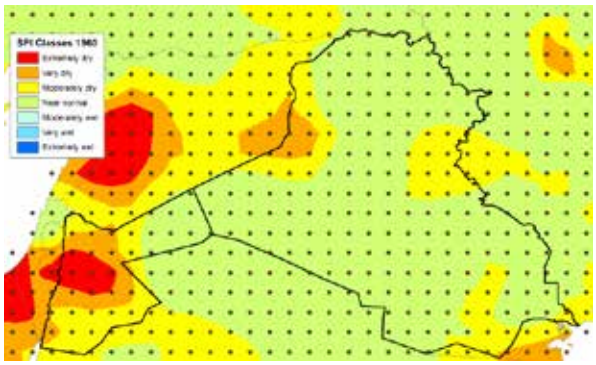

Figure 108. Annual Standardized Precipitation Index in1960

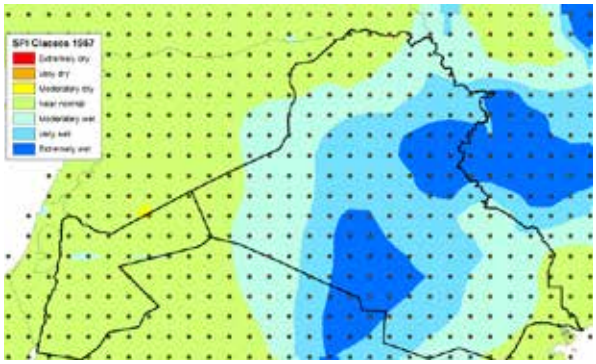

Figure 105. Annual Standardized Precipitation Index in1957

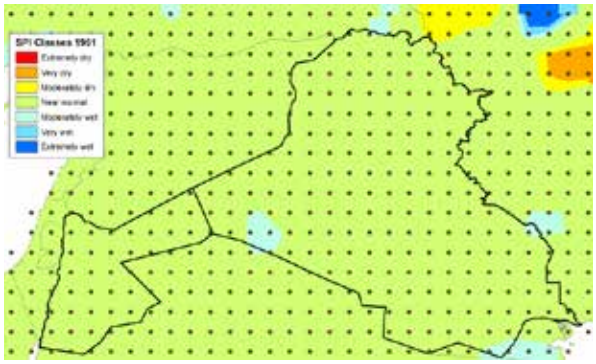

Figure 109. Annual Standardized Precipitation Index in1961

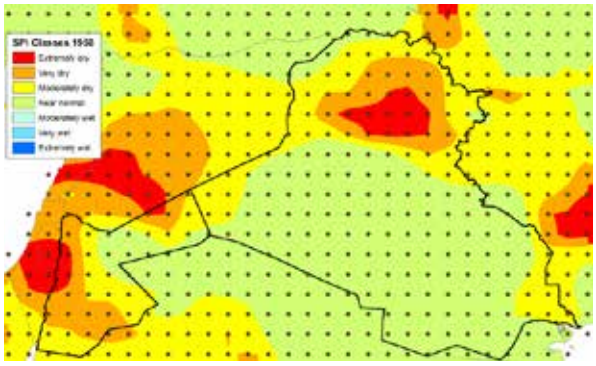

Figure 106. Annual Standardized Precipitation Index in1958

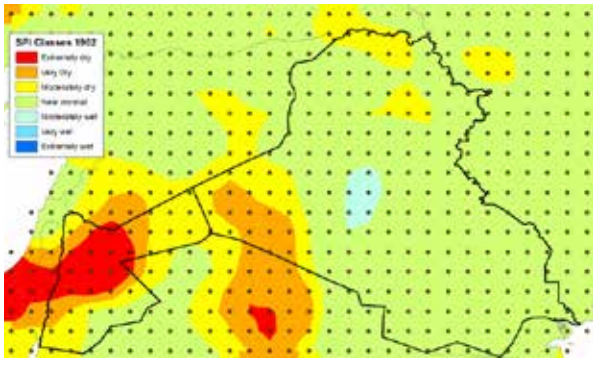

Figure 110. Annual Standardized Precipitation Index in1962

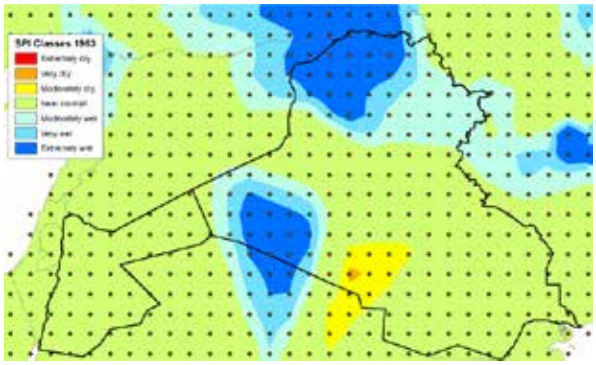

Figure 111. Annual Standardized Precipitation Index in1963

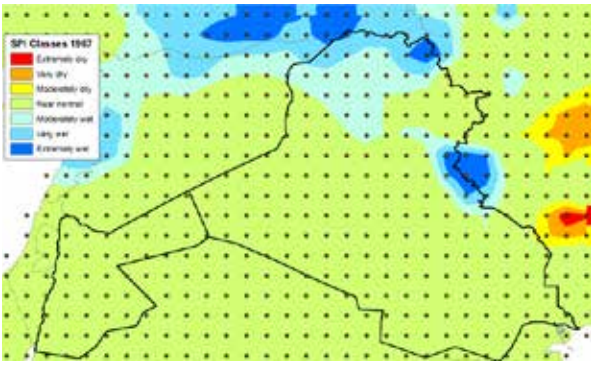

Figure 115. Annual Standardized Precipitation Index in1967

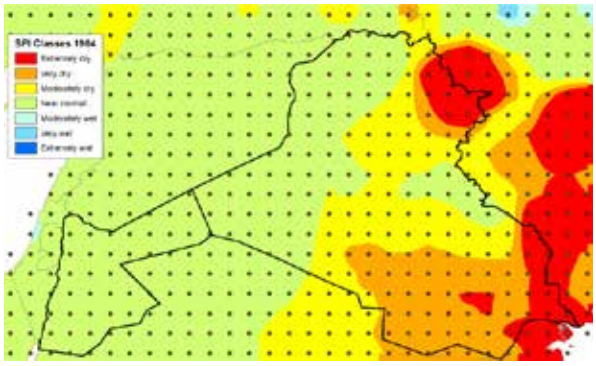

Figure 112. Annual Standardized Precipitation Index in1964

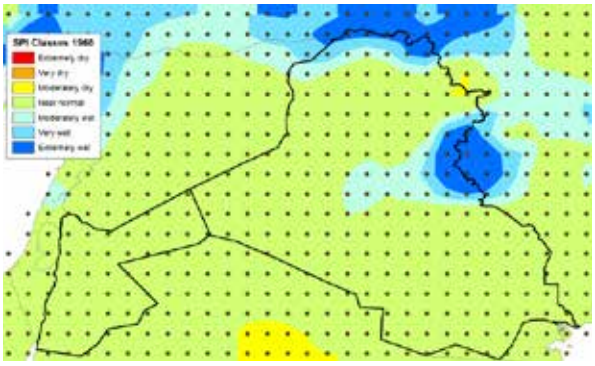

Figure 116. Annual Standardized Precipitation Index in1968

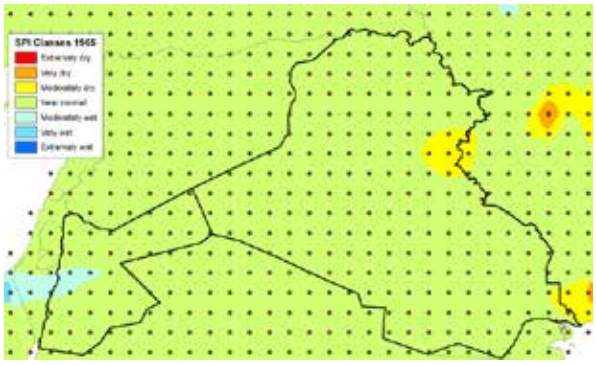

Figure 113. Annual Standardized Precipitation Index in1965

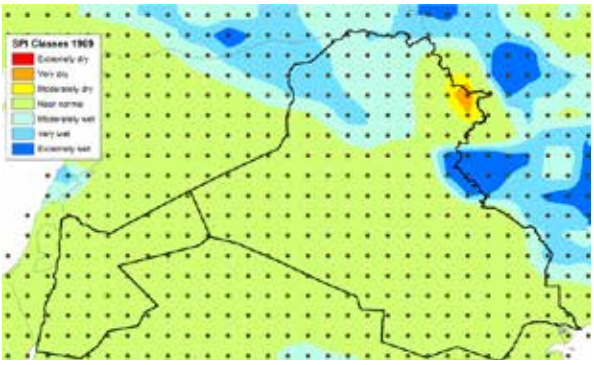

Figure 117. Annual Standardized Precipitation Index in1969

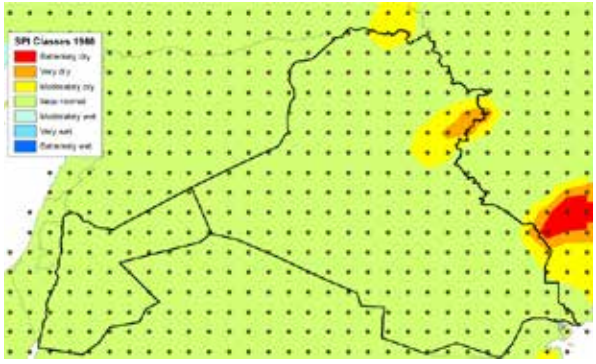

Figure 114. Annual Standardized Precipitation Index in1966

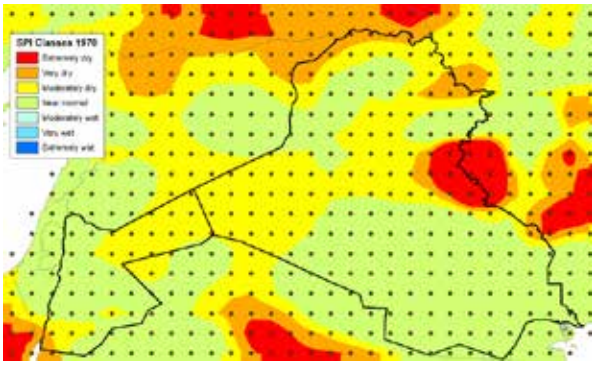

Figure 118. Annual Standardized Precipitation Index in1970

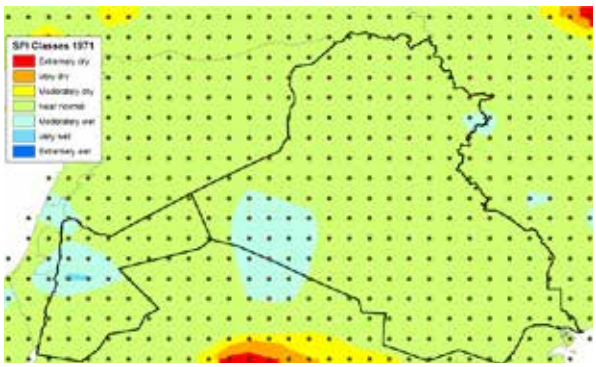

Figure 119. Annual Standardized Precipitation Index in1971

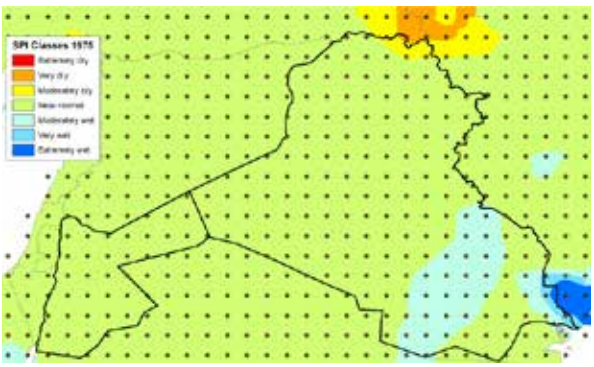

Figure 123. Annual Standardized Precipitation Index in1975

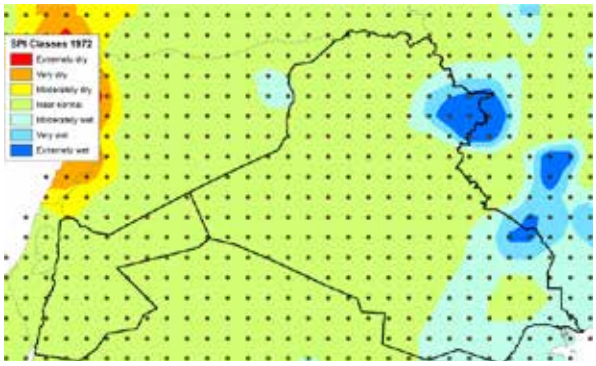

Figure 120. Annual Standardized Precipitation Index in1972

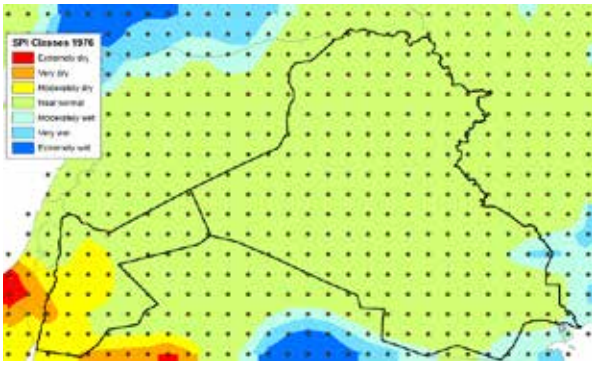

Figure 124. Annual Standardized Precipitation Index in1976

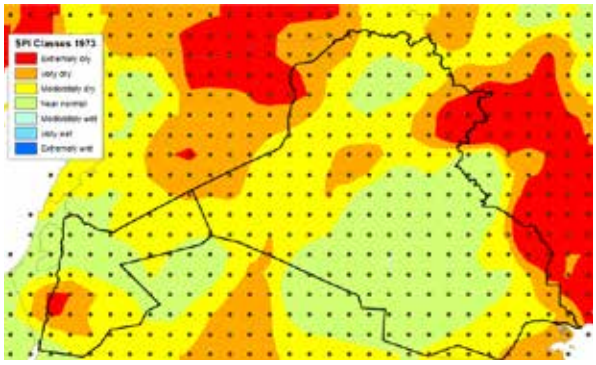

Figure 121. Annual Standardized Precipitation Index in1973

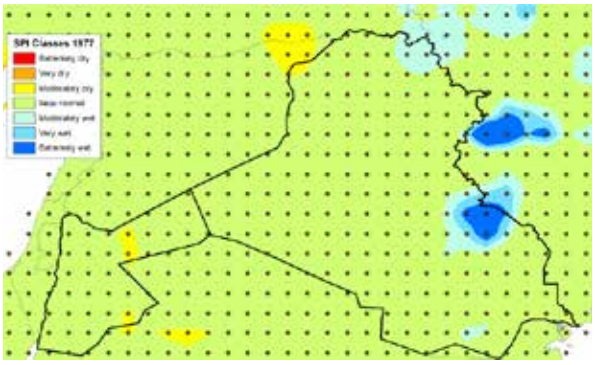

Figure 125. Annual Standardized Precipitation Index in1977

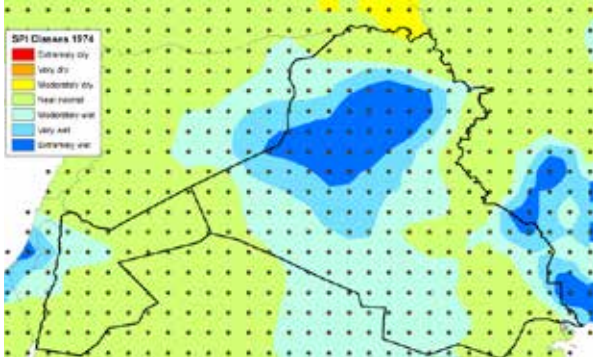

Figure 122. Annual Standardized Precipitation Index in1974

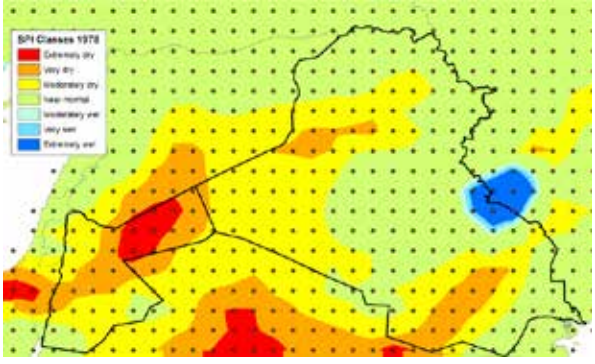

Figure 126. Annual Standardized Precipitation Index in1978

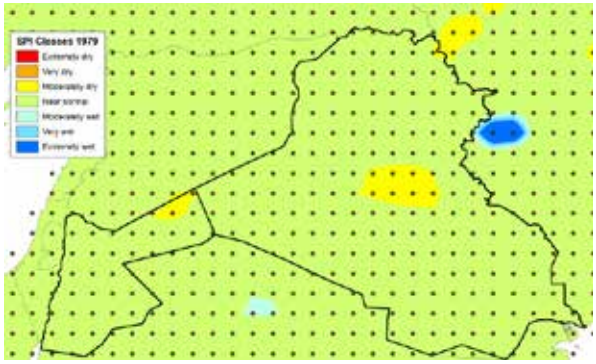

Figure 127. Annual Standardized Precipitation Index in1979

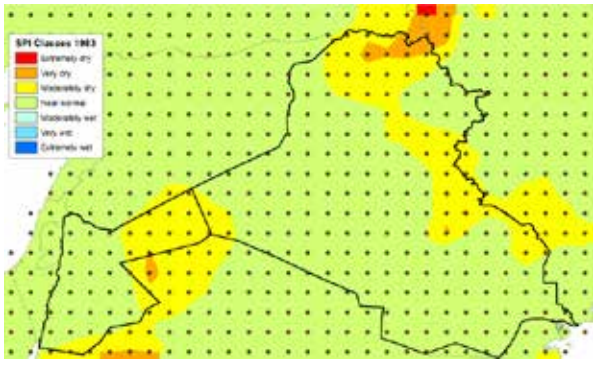

Figure 131. Annual Standardized Precipitation Index in1983

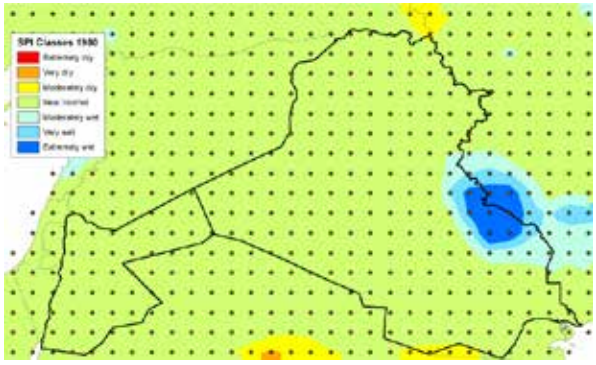

Figure 128. Annual Standardized Precipitation Index in1980

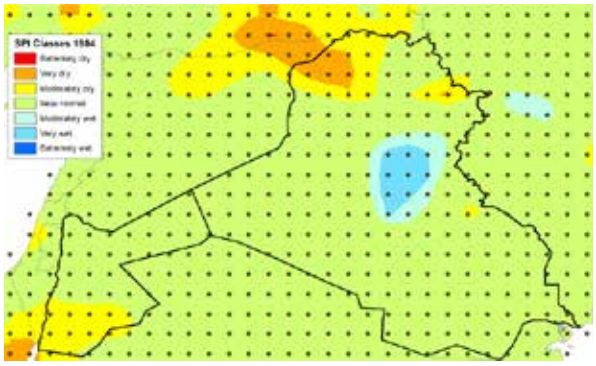

Figure 132. Annual Standardized Precipitation Index in1984

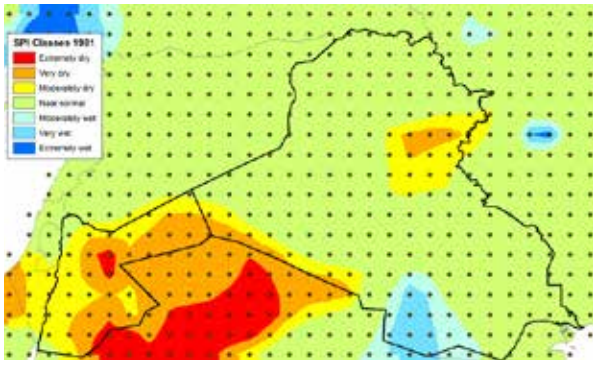

Figure 129. Annual Standardized Precipitation Index in1981

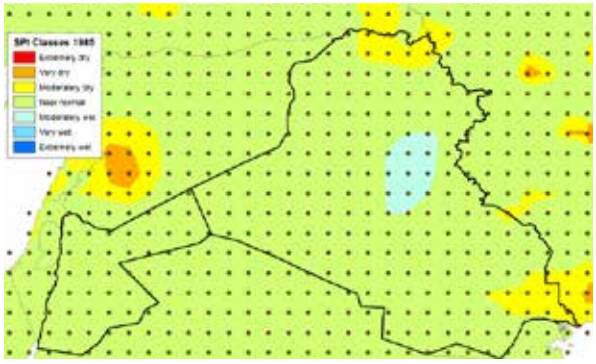

Figure 133. Annual Standardized Precipitation Index in1985

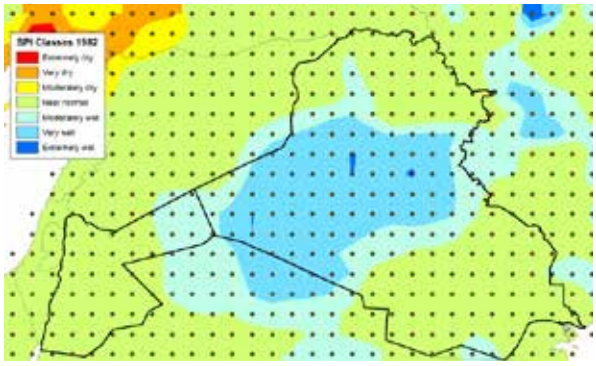

Figure 130. Annual Standardized Precipitation Index in1982

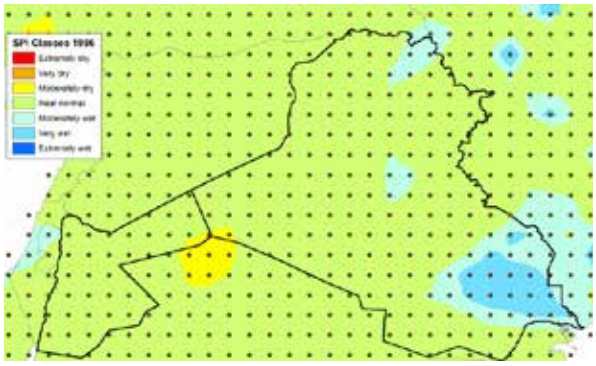

Figure 134. Annual Standardized Precipitation Index in1986

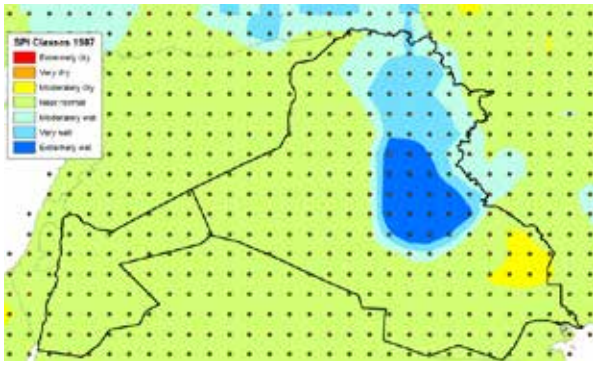

Figure 135. Annual Standardized Precipitation Index in1987

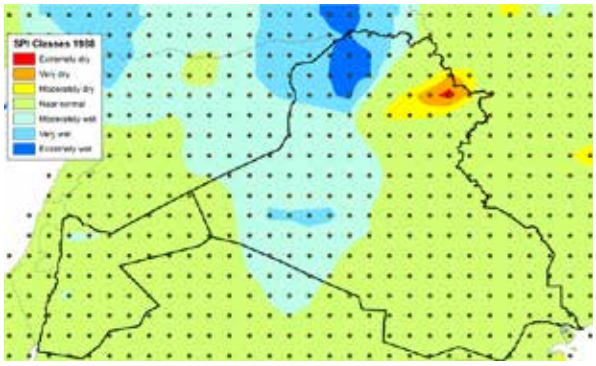

Figure 136. Annual Standardized Precipitation Index in1988

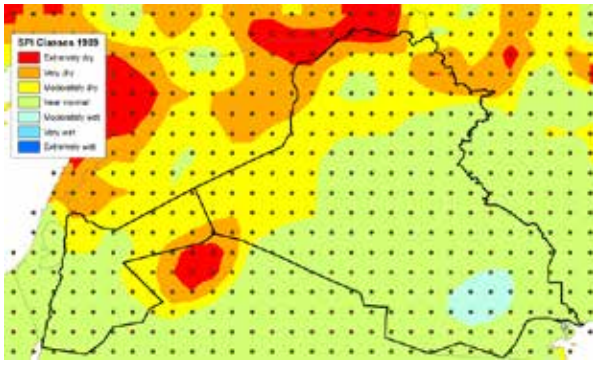

Figure 137. Annual Standardized Precipitation Index in1989

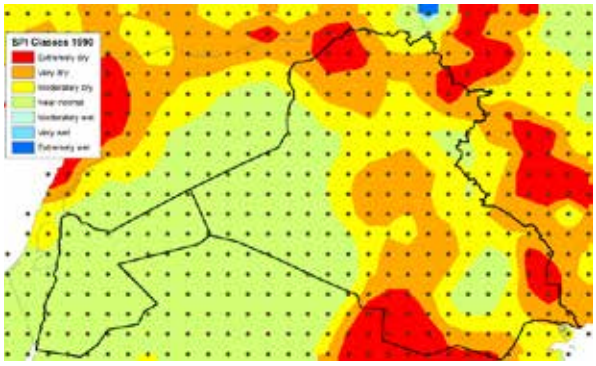

Figure 138. Annual Standardized Precipitation Index in1990

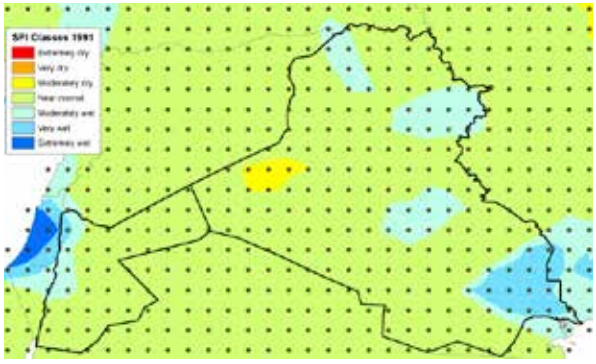

Figure 139. Annual Standardized Precipitation Index in1991

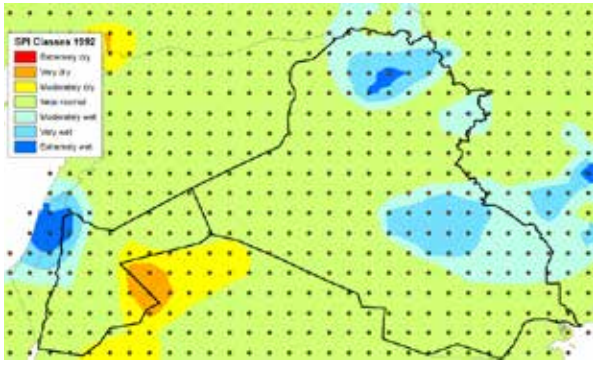

Figure 140. Annual Standardized Precipitation Index in1992

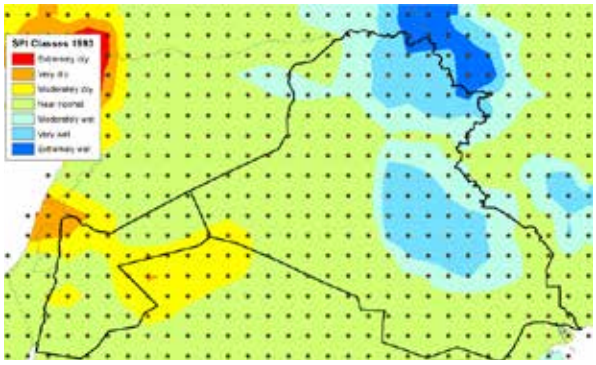

Figure 141. Annual Standardized Precipitation Index in1993

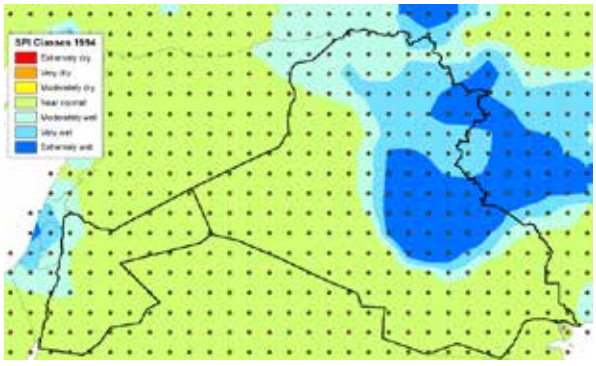

Figure 142. Annual Standardized Precipitation Index in1994

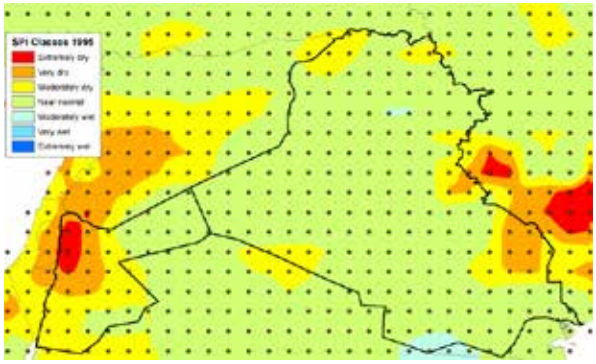

Figure 143. Annual Standardized Precipitation Index in1995

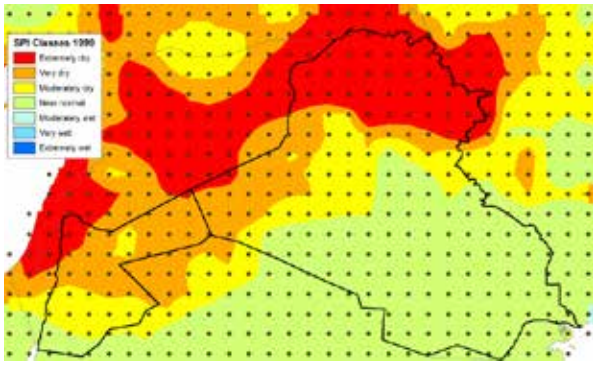

Figure 147. Annual Standardized Precipitation Index in1999

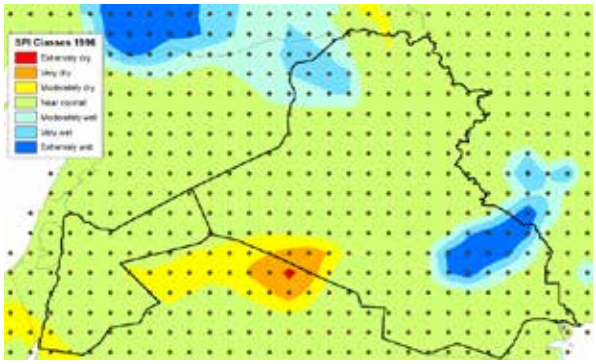

Figure 144. Annual Standardized Precipitation Index in1996

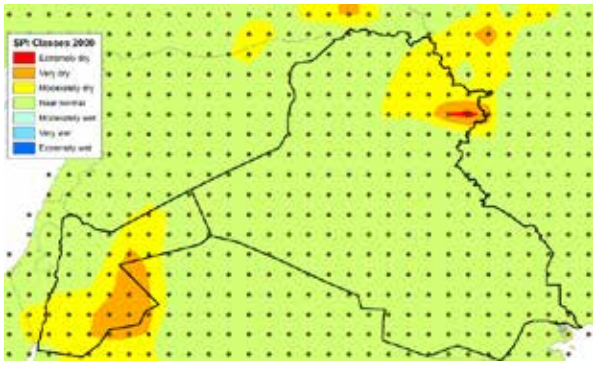

Figure 148. Annual Standardized Precipitation Index in2000

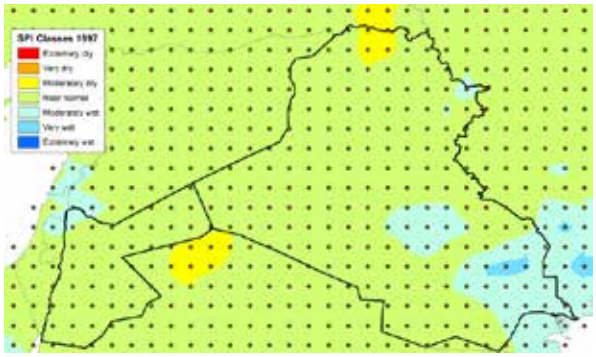

Figure 145 Annual Standardized Precipitation Index in1997

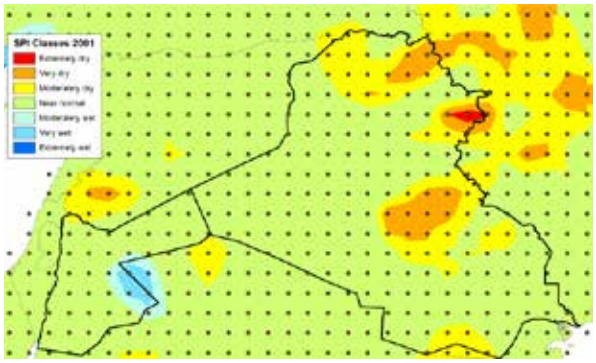

Figure 149. Annual Standardized Precipitation Index in2001

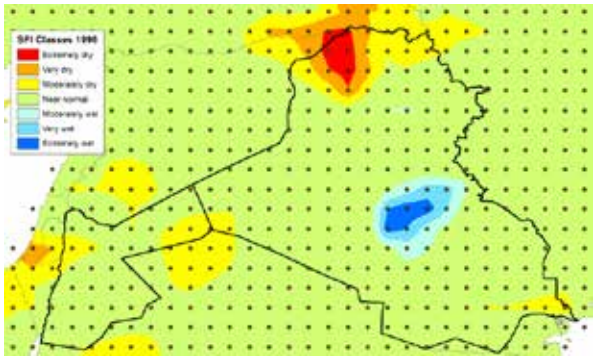

Figure 146. Annual Standardized Precipitation Index in1998

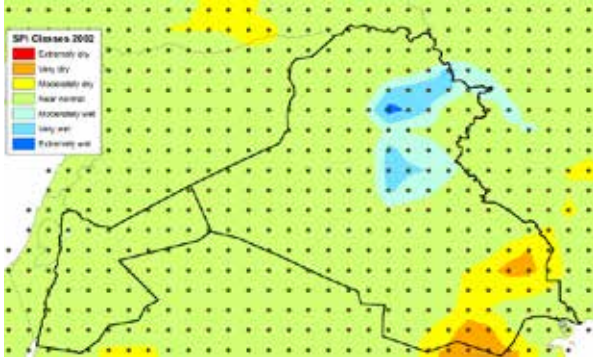

Figure 150. Annual Standardized Precipitation Index in2002

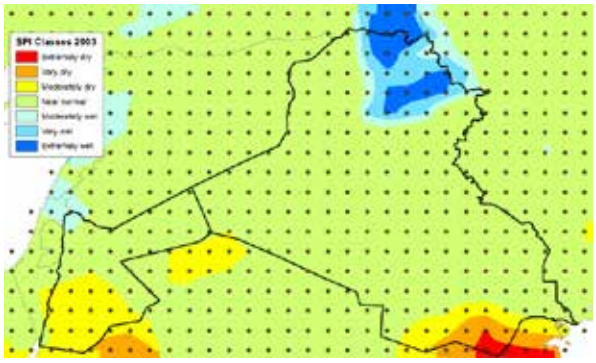

Figure 151. Annual Standardized Precipitation Index in2003

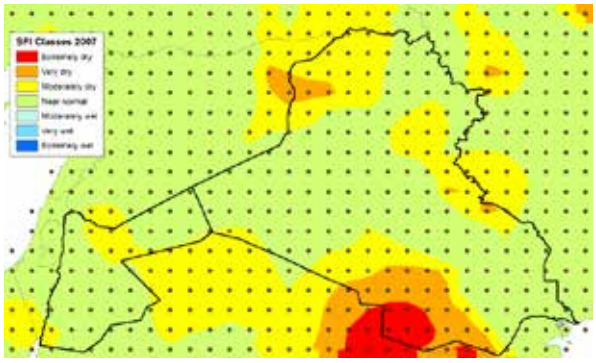

Figure 155. Annual Standardized Precipitation Index in2007

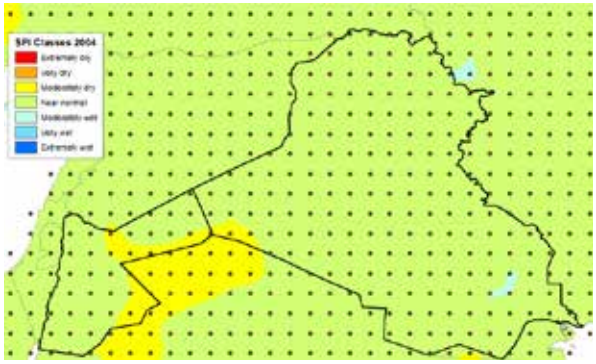

Figure 152. Annual Standardized Precipitation Index in2004

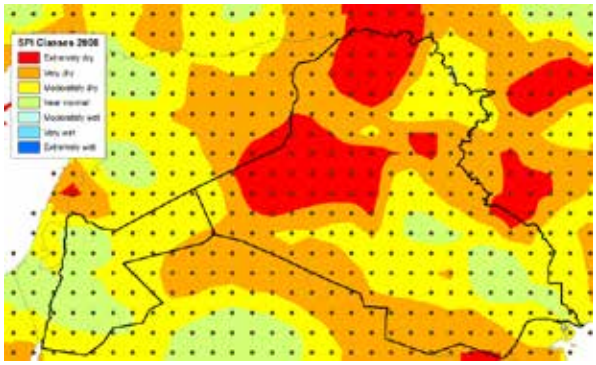

Figure 156. Annual Standardized Precipitation Index in2008

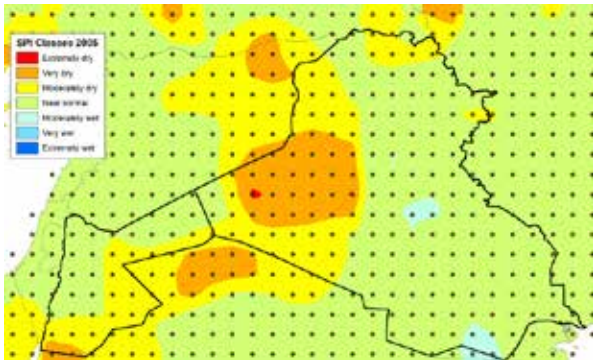

Figure 153. Annual Standardized Precipitation Index in2005

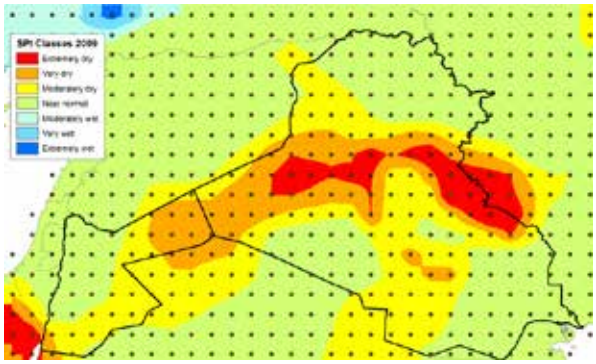

Figure 157. Annual Standardized Precipitation Index in2009

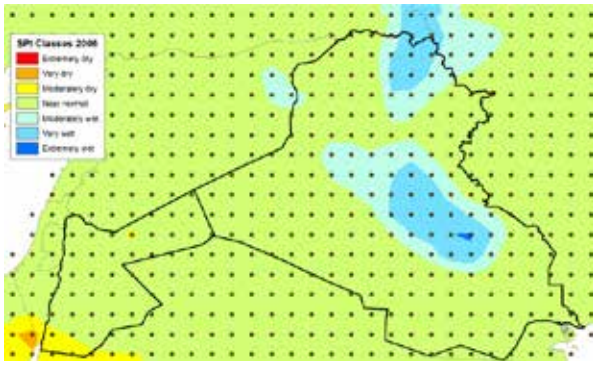

Figure 154. Annual Standardized Precipitation Index in2006

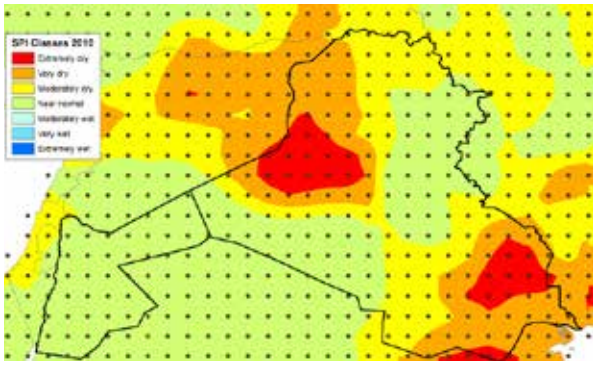

Figure 158. Annual Standardized Precipitation Index in2010

Table 14. Percentages of drought/wetness classes in Iraq and Jordan (1901–2010)

Year	SPI-classes Iraq (%)[22]							SPI-classes Jordan (%)						
	ExtrDry	Vdry	ModDry	Normal	ModWet	Vwet	ExtrWet	ExtrDry	Vdry	ModDry	Normal	ModWet	Vwet	ExtrWet
1901	36.2	8.7	13.4	41.6	0.0	0.0	0.0	0.0	0.0	0.0	100.0	0.0	0.0	0.0
1902	0.0	0.0	0.0	95.9	0.8	0.7	2.6	0.0	0.0	0.0	0.0	18.4	52.4	29.2
1903	3.4	21.1	22.4	53.1	0.0	0.0	0.0	0.0	0.0	0.0	100.0	0.0	0.0	0.0
1904	0.0	0.0	0.0	92.5	2.9	3.3	1.2	0.0	0.0	0.0	0.0	0.0	10.9	89.1
1905	0.0	15.5	46.1	36.1	1.4	0.7	0.1	0.0	0.0	0.0	0.0	3.4	24.6	72.0
1906	0.0	0.0	0.0	97.5	2.5	0.0	0.0	0.0	0.0	0.0	27.8	53.3	18.6	0.2
1907	0.0	0.0	0.0	45.1	25.8	27.4	1.7	0.0	0.0	0.0	53.5	38.7	7.3	0.5
1908	0.0	0.2	14.9	82.2	2.4	0.2	0.0	0.0	0.0	0.0	2.4	33.5	64.0	0.0
1909	0.0	12.1	29.5	56.6	1.8	0.0	0.0	0.0	0.0	0.0	85.3	14.7	0.0	0.0
1910	0.0	0.0	0.0	71.2	10.1	18.7	0.0	0.0	0.0	0.0	36.6	59.4	4.0	0.0
1911	0.0	0.0	0.0	36.6	30.2	29.3	4.0	0.0	0.0	0.0	0.2	1.0	1.9	96.9
1912	0.0	0.0	0.0	96.8	1.1	1.6	0.5	0.0	0.0	0.0	50.7	41.4	7.2	0.7
1913	0.0	0.0	0.0	76.4	10.4	13.3	0.0	0.0	0.0	0.0	99.2	0.8	0.0	0.0
1914	0.0	0.0	0.0	35.9	30.3	7.8	26.1	0.0	0.0	0.0	29.3	58.9	11.8	0.0
1915	30.2	6.2	6.6	55.1	1.9	0.0	0.0	9.6	12.8	16.4	61.2	0.0	0.0	0.0
1916	0.0	0.0	0.0	42.2	34.7	23.1	0.0	0.0	0.0	0.0	84.0	16.0	0.0	0.0
1917	0.0	0.0	18.3	77.8	3.9	0.0	0.0	0.0	0.0	0.0	100.0	0.0	0.0	0.0
1918	0.0	0.0	0.0	20.1	20.2	27.8	31.9	0.0	0.0	0.0	2.8	27.1	53.4	16.7
1919	0.0	0.0	0.0	47.4	27.9	24.7	0.0	0.0	0.0	0.0	7.4	65.6	27.0	0.0
1920	0.0	0.0	0.0	92.6	7.4	0.0	0.0	0.0	0.0	0.0	10.3	53.6	36.1	0.0
1921	0.0	0.0	0.0	69.8	26.1	4.1	0.0	0.0	0.0	0.0	31.9	68.1	0.0	0.0
1922	0.2	11.9	7.3	80.6	0.0	0.0	0.0	0.0	0.0	0.0	100.0	0.0	0.0	0.0

22 ExtrDry: extremely dry; Vdry: very dry; ModDry: moderately dry; Normal: near normal; ModWet: moderately wet; Vwet: very wet; ExtrWet: extremely wet

Year	SPI-classes Iraq (%)							SPI-classes Jordan (%)						
	ExtrDry	Vdry	ModDry	Normal	ModWet	Vwet	ExtrWet	ExtrDry	Vdry	ModDry	Normal	ModWet	Vwet	ExtrWet
1923	0.0	0.0	0.0	97.2	2.8	0.0	0.0	0.0	0.0	7.7	92.3	0.0	0.0	0.0
1924	0.0	0.0	0.0	99.2	0.8	0.0	0.0	0.0	0.0	0.0	87.0	13.0	0.0	0.0
1925	0.0	1.4	18.7	79.8	0.0	0.0	0.0	0.0	0.0	25.0	75.0	0.0	0.0	0.0
1926	0.0	0.0	0.0	0.8	2.2	25.0	72.0	0.0	0.0	0.0	95.1	3.2	1.7	0.0
1927	0.0	1.3	33.5	64.8	0.4	0.0	0.0	0.0	0.0	0.0	90.6	9.4	0.0	0.0
1928	0.0	0.0	0.0	99.5	0.5	0.0	0.0	0.0	0.0	0.0	99.6	0.4	0.0	0.0
1929	0.0	0.0	18.1	81.5	0.3	0.0	0.0	0.0	0.0	0.0	100.0	0.0	0.0	0.0
1930	0.0	0.0	14.8	85.2	0.0	0.0	0.0	0.0	0.0	0.0	100.0	0.0	0.0	0.0
1931	0.0	0.0	0.0	100.0	0.0	0.0	0.0	0.0	0.0	0.0	100.0	0.0	0.0	0.0
1932	23.1	42.5	29.7	4.7	0.0	0.0	0.0	5.6	36.5	26.0	31.9	0.0	0.0	0.0
1933	0.0	0.0	0.0	100.0	0.0	0.0	0.0	34.6	29.1	9.9	26.4	0.0	0.0	0.0
1934	0.0	0.0	0.0	68.8	29.6	1.6	0.0	0.0	0.0	0.0	92.7	7.2	0.0	0.0
1935	0.0	0.7	16.5	77.5	5.3	0.0	0.0	0.0	0.0	0.0	100.0	0.0	0.0	0.0
1936	0.0	0.0	0.0	99.9	0.1	0.0	0.0	0.0	0.0	0.0	100.0	0.0	0.0	0.0
1937	0.0	0.0	4.2	86.7	9.1	0.0	0.0	0.0	0.0	0.0	100.0	0.0	0.0	0.0
1938	0.0	0.0	0.0	5.4	54.0	37.9	2.7	0.0	0.0	0.0	51.8	20.7	27.6	0.0
1939	0.0	0.0	0.0	79.7	11.2	7.5	1.6	0.0	0.0	0.0	97.6	2.4	0.0	0.0
1940	0.0	0.0	0.0	97.3	2.7	0.0	0.0	0.0	0.0	1.1	98.9	0.0	0.0	0.0
1941	0.0	0.0	0.0	99.4	0.6	0.0	0.0	0.0	0.0	0.0	53.4	7.9	22.2	16.5
1942	0.0	0.0	26.4	73.6	0.0	0.0	0.0	0.0	0.0	0.0	57.4	12.6	25.5	4.4
1943	0.0	0.0	0.0	99.5	0.5	0.0	0.0	0.0	0.0	0.0	76.9	9.7	9.2	4.2
1944	0.0	0.0	0.0	98.6	1.4	0.0	0.0	0.0	0.0	0.0	11.8	10.9	39.9	37.3
1945	0.0	0.0	0.0	95.4	4.6	0.0	0.0	0.0	0.0	0.0	53.7	9.8	28.7	7.8
1946	0.0	0.0	0.0	49.7	33.1	7.2	10.0	0.0	0.0	7.5	92.5	0.0	0.0	0.0
1947	0.0	2.4	8.0	89.7	0.0	0.0	0.0	0.0	15.5	23.1	61.4	0.0	0.0	0.0

1948	0.0	2.5	24.3	73.2	0.0	0.0	0.0	0.0	0.0	0.0	100.0	0.0	0.0	0.0
1949	0.0	0.0	0.0	75.1	22.2	2.8	0.0	0.0	0.0	0.0	60.5	16.1	23.4	0.0
1950	0.3	3.2	6.8	88.4	1.3	0.0	0.0	0.0	0.0	0.0	100.0	0.0	0.0	0.0
1951	0.2	0.6	4.0	93.8	1.4	0.0	0.0	0.0	0.0	0.0	100.0	0.0	0.0	0.0
1952	0.2	5.6	26.3	67.8	0.2	0.0	0.0	0.0	0.0	2.5	97.5	0.0	0.0	0.0
1953	0.1	0.1	0.3	74.5	17.6	7.1	0.2	0.0	0.0	0.0	57.3	29.3	13.2	0.2
1954	0.0	0.0	0.0	26.4	29.5	35.1	9.0	0.0	0.0	0.0	86.1	13.9	0.0	0.0
1955	0.0	0.0	4.0	95.8	0.2	0.0	0.0	0.0	0.0	18.5	81.5	0.0	0.0	0.0
Year	SPI-classes Iraq (%)							SPI-classes Jordan (%)						
	ExtrDry	Vdry	ModDry	Normal	ModWet	Vwet	ExtrWet	ExtrDry	Vdry	ModDry	Normal	ModWet	Vwet	ExtrWet
1956	0.0	3.9	7.3	88.8	0.0	0.0	0.0	0.0	0.0	31.5	68.5	0.0	0.0	0.0
1957	0.0	0.0	0.0	12.8	36.4	35.6	15.3	0.0	0.0	0.2	97.7	2.1	0.0	0.0
1958	4.3	9.5	20.7	65.5	0.0	0.0	0.0	5.6	34.6	40.6	19.2	0.0	0.0	0.0
1959	0.0	0.0	8.7	91.3	0.0	0.0	0.0	0.0	0.0	2.9	97.1	0.0	0.0	0.0
1960	0.0	2.2	16.2	81.6	0.0	0.0	0.0	14.6	26.3	35.9	23.2	0.0	0.0	0.0
1961	0.0	0.0	0.0	97.6	2.4	0.0	0.0	0.0	0.0	0.0	100.0	0.0	0.0	0.0
1962	0.0	5.5	12.1	79.7	2.7	0.0	0.0	29.7	18.4	39.4	12.5	0.0	0.0	0.0
1963	0.0	0.2	4.3	58.5	14.6	7.9	14.4	0.0	0.0	0.0	100.0	0.0	0.0	0.0
1964	8.9	24.5	28.0	38.6	0.0	0.0	0.0	0.0	0.0	0.0	100.0	0.0	0.0	0.0
1965	0.0	0.0	2.8	97.2	0.0	0.0	0.0	0.0	0.0	0.0	93.5	6.5	0.0	0.0
1966	0.0	1.3	4.8	93.9	0.0	0.0	0.0	0.0	0.0	0.0	100.0	0.0	0.0	0.0
1967	0.0	0.0	0.0	81.8	12.1	4.6	1.5	0.0	0.0	0.0	100.0	0.0	0.0	0.0
1968	0.0	0.0	0.2	82.9	9.1	4.1	3.8	0.0	0.0	0.0	100.0	0.0	0.0	0.0
1969	0.0	0.4	1.0	77.6	14.9	5.0	1.0	0.0	0.0	0.0	100.0	0.0	0.0	0.0
1970	3.0	5.6	35.0	56.4	0.0	0.0	0.0	0.0	1.6	42.8	55.6	0.0	0.0	0.0
1971	0.0	0.0	0.0	91.9	8.0	0.0	0.0	0.0	0.0	0.0	79.6	19.2	1.2	0.0
1972	0.0	0.0	0.0	77.2	16.9	3.1	2.8	0.0	0.0	0.2	99.8	0.0	0.0	0.0

1973	5.0	13.1	41.0	40.8	0.1	0.0	0.0	2.8	13.1	51.1	33.0	0.0	0.0	0.0
1974	0.0	0.0	0.3	27.7	40.2	17.6	14.2	0.0	0.0	0.0	86.3	13.7	0.0	0.0
1975	0.0	0.1	1.1	82.4	15.6	0.7	0.1	0.0	0.0	0.0	100.0	0.0	0.0	0.0
1976	0.0	0.0	0.0	97.1	2.6	0.3	0.0	0.0	2.2	39.6	58.2	0.0	0.0	0.0
1977	0.0	0.0	0.3	92.1	4.8	1.3	1.5	0.0	0.0	4.6	95.4	0.0	0.0	0.0
1978	0.0	8.4	38.0	50.9	0.7	0.6	1.5	16.2	34.2	37.2	12.4	0.0	0.0	0.0
1979	0.0	0.0	4.2	95.7	0.1	0.0	0.0	0.0	0.0	4.5	95.4	0.1	0.0	0.0
1980	0.0	0.0	0.4	90.9	3.8	2.0	2.8	0.0	0.0	0.0	99.9	0.1	0.0	0.0
1981	0.0	3.3	10.0	79.1	4.1	3.4	0.0	4.3	51.3	39.0	5.4	0.0	0.0	0.0
1982	0.0	0.0	0.0	47.4	16.1	36.2	0.3	0.0	0.0	0.0	81.4	18.5	0.1	0.0
1983	0.0	1.8	20.8	77.4	0.0	0.0	0.0	0.0	0.0	35.5	64.5	0.0	0.0	0.0
1984	0.0	2.4	6.4	82.7	4.6	3.9	0.0	0.0	0.0	25.8	74.2	0.0	0.0	0.0
Year	SPI-classes Iraq (%)							SPI-classes Jordan (%)						
	ExtrDry	Vdry	ModDry	Normal	ModWet	Vwet	ExtrWet	ExtrDry	Vdry	ModDry	Normal	ModWet	Vwet	ExtrWet
1985	0.0	0.0	6.8	87.9	5.3	0.0	0.0	0.0	0.0	0.0	100.0	0.0	0.0	0.0
1986	0.0	0.0	0.4	81.7	11.0	6.9	0.0	0.0	0.0	1.6	98.3	0.0	0.0	0.0
1987	0.0	0.0	3.4	63.8	10.5	12.6	9.7	0.0	0.0	0.0	100.0	0.0	0.0	0.0
1988	0.1	1.3	2.4	60.0	26.9	6.3	2.8	0.0	0.0	0.0	97.6	2.4	0.0	0.0
1989	0.9	6.9	25.4	62.5	4.3	0.0	0.0	0.0	5.2	37.2	57.7	0.0	0.0	0.0
1990	9.6	31.4	29.4	29.6	0.0	0.0	0.0	0.0	0.0	0.0	100.0	0.0	0.0	0.0
1991	0.0	0.0	2.1	77.3	14.7	5.9	0.0	0.0	0.0	0.0	87.0	11.1	2.0	0.0
1992	0.0	0.0	0.0	69.6	17.9	11.7	0.7	0.0	4.1	10.5	74.2	6.1	3.3	1.9
1993	0.0	0.0	1.1	57.7	20.2	20.3	0.7	0.0	2.2	31.7	66.1	0.0	0.0	0.0
1994	0.0	0.0	0.0	55.1	13.5	14.8	16.7	0.0	0.0	0.0	90.4	9.6	0.1	0.0
1995	0.0	3.6	11.1	84.0	1.3	0.0	0.0	7.5	16.9	37.8	37.7	0.0	0.0	0.0
1996	0.0	1.4	2.6	80.7	6.3	4.9	4.1	0.0	0.0	4.2	95.8	0.0	0.0	0.0
1997	0.0	0.0	1.8	82.7	14.6	0.9	0.0	0.0	0.0	0.0	97.4	2.6	0.0	0.0

1998	1.8	2.6	6.8	80.6	4.1	2.7	1.5	0.0	0.0	14.0	86.0	0.0	0.0	0.0
1999	20.9	13.9	14.5	50.7	0.0	0.0	0.0	6.7	53.2	30.9	9.1	0.0	0.0	0.0
2000	0.2	1.2	6.9	91.7	0.0	0.0	0.0	0.0	18.0	42.9	39.1	0.0	0.0	0.0
2001	0.4	7.1	18.4	74.1	0.0	0.0	0.0	0.0	0.0	0.7	88.5	6.6	4.2	0.0
2002	0.0	2.6	8.9	75.0	8.7	4.6	0.2	0.0	0.0	0.0	99.7	0.3	0.0	0.0
2003	0.7	2.1	3.7	81.8	2.8	5.1	3.8	0.0	0.0	36.0	61.9	2.1	0.0	0.0
2004	0.0	0.0	1.1	98.4	0.6	0.0	0.0	0.0	0.0	19.4	80.6	0.0	0.0	0.0
2005	0.1	13.7	18.9	64.9	2.4	0.0	0.0	0.0	2.8	44.1	53.2	0.0	0.0	0.0
2006	0.0	0.0	0.0	73.1	15.7	11.1	0.1	0.0	0.0	6.9	93.1	0.0	0.0	0.0
2007	2.9	9.4	25.2	62.5	0.0	0.0	0.0	0.0	0.0	16.3	83.7	0.0	0.0	0.0
2008	23.5	38.5	30.4	7.6	0.0	0.0	0.0	0.0	2.8	55.9	41.3	0.0	0.0	0.0
2009	9.3	19.1	30.9	40.7	0.0	0.0	0.0	0.0	21.3	39.4	39.3	0.0	0.0	0.0
2010	13.4	25.9	27.2	33.4	0.0	0.0	0.0	0.0	0.0	0.5	99.5	0.0	0.0	0.0

ANNEX 6.

CLIMATE CHANGE PROJECTIONS: SUMMARY TABLES

Table 15. Projected precipitation changes

Theme	Scenario	Country	% of area excluded	Percent of each class							
				< –20	–20 to –10	–10 to –5	–5 to 0	0–5	5–10	10–20	> 20
1	A1b	Iraq	15	0	66	20	12	2	0	0	0
		Jordan	25	10	90	0	0	0	0	0	0
	A2	Iraq	15	0	66	16	9	4	2	2	1
		Jordan	25	1	88	6	2	2	1	0	0
2	A1b	Iraq	15	0	0	0	1	2	1	2	94
		Jordan	25	1	3	5	7	13	12	25	35
	A2	Iraq	15	0	0	0	9	9	8	12	61
		Jordan	25	0	51	28	8	6	4	2	0
3	A1b	Iraq	15	0	0	0	2	23	13	18	44
		Jordan	25	0	0	13	45	41	1	0	0
	A2	Iraq	15	0	0	0	1	2	2	28	68
		Jordan	25	0	21	24	30	22	3	0	0
4	A1b	Iraq	15	15	54	15	16	0	0	0	0
		Jordan	25	0	7	88	5	0	0	0	0
	A2	Iraq	15	0	4	40	51	5	0	0	0
		Jordan	25	0	7	67	26	1	0	0	0
5	A1b	Iraq	15	0	29	67	3	0	0	0	0
		Jordan	25	0	69	31	0	0	0	0	0
	A2	Iraq	15	0	2	16	66	14	3	0	0
		Jordan	25	0	43	48	7	1	0	0	0

Notes:

Theme 1: Relative change (%) of spring precipitation from current climate to 2010–2040, scenarios A1b and A2

Theme 2: Relative change (%) of summer precipitation from current climate to 2010–2040, scenarios A1b and A2

Theme 3: Relative change (%) of autumn precipitation from current climate to 2010–2040, scenarios A1b and A2

Theme 4: Relative change (%) of winter precipitation from current climate to 2010–2040, scenarios A1b and A2

Theme 5: Relative change (%) of annual precipitation from current climate to 2010–2040, scenarios A1b and A2

Table 16. Projected temperature changes

Theme	Country	Percent of each change class					
		Scenario A1b			Scenario A2		
		0.5–1°C	1–1.5°C	1.5–2°C	0.5–1°C	1–1.5°C	1.5–2°C
1	Iraq	0	100	0	0	100	0
	Jordan	55	45	0	48	52	0
2	Iraq	0	100	0	0	100	0
	Jordan	55	45	0	48	52	0
3	Iraq	0	100	0	0	100	0
	Jordan	3	97	0	0	100	0
4	Iraq	85	15	0	24	76	0
	Jordan	91	9	0	86	14	0
5	Iraq	0	80	20	0	49	51
	Jordan	0	100	0	0	100	0
6	Iraq	0	0	100	0	0	100
	Jordan	0	72	28	0	53	47
7	Iraq	0	80	20	0	66	34
	Jordan	0	100	0	0	99	1

Notes:

Theme 1: Absolute change (°C) of the annual maximum temperature from current climate to 2010–2040, scenarios A1b and A2

Theme 2: Absolute change (°C) of the annual minimum temperature from current climate to 2010–2040, scenarios A1b and A2

Theme 3: Absolute change (°C) of the annual mean temperature from current climate to 2010–2040, scenarios A1b and A2

Theme 4: Absolute change (°C) of the annual winter temperature from current climate to 2010–2040, scenarios A1b and A2

Theme 5: Absolute change (°C) of the annual spring temperature from current climate to 2010–2040, scenarios A1b and A2

Theme 6: Absolute change (°C) of the annual summer temperature from current climate to 2010–2040, scenarios A1b and A2

Theme 7: Absolute change (°C) of the annual autumn temperature from current climate to 2010–2040, scenarios A1b and A2

Table 17. Projected changes in annual potential evapotranspiration

Country	Percent of each change class							
	A1b				A2			
	2–3%	3–4%	4–5%	5–6%	2–3%	3–4%	4–5%	5–6%
Iraq	0	89	11	1	0	79	21	1
Jordan	6	94	0	0	2	94	4	0

Table 18. Composition (%) and changes (%) in Köppen climatic zones

Koeppen zone	Current climate		Changes (scenario A1b)			Changes (scenario A2)		
	Iraq	Jordan		Iraq	Jordan		Iraq	Jordan
			Stable	95	68	Stable	96	66
BSwh	9	1	-> BSwh	2	1	-> BSwh	2	1
BSwk	0	4						
BWwh	83	57	-> BWwh	2	30	-> BWwh	1	32
BWwk	0	38	-> BWwk	0	1	-> BWwk	0	1
Csa	6	0						

Table 19. Changes in aridity index

Scenario	Country	Percent of each aridity class					
		–1.0 to –0.2	–0.2 to –0.1	–0.1 to –0.05	–0.05 to 0	0–0.05	0.05–0.1
A1b	Iraq	0	0	7	93	0	0
	Jordan	0	0	1	99	0	0
A2	Iraq	0	0	1	95	4	0
	Jordan	0	0	1	94	5	0

Table 20. Changes in the moisture-limited growing period

Scenario	Country	Percent of each LGP change class					
		–60 to –45	–45 to –30	–30 to –15	–15 to 0	0–15	15–30
A1b	Iraq	2	7	12	79	1	0
	Jordan	1	2	5	92	0	0
A2	Iraq	0	1	4	90	5	0
	Jordan	1	1	8	90	0	0

Table 21. Changes in the temperature-limited growing period

Scenario	Country	Percent of each LGP change class				
		0–1	1–15	15–30	30–45	45–75
A1b	Iraq	93	4	2	0	0
	Jordan	99	0	0	0	0
A2	Iraq	93	4	2	1	0
	Jordan	99	0	0	0	0

Table 22. Changes in the moisture- and temperature-limited growing period

Scenario	Country	Percent of each LGP change class							
		–60 to –45	–45 to –30	–30 to –15	–15 to 0	0–15	15–30	30–45	45–75
A1b	Iraq	2	6	12	72	6	2	0	1
	Jordan	1	2	5	91	0	0	0	0
A2	Iraq	0	1	4	84	6	2	1	2
	Jordan	1	1	7	90	0	0	0	0

ANNEX 7

REPRESENTATIVE MAPS FROM THE CLIMATE CHANGE ATLAS OF JORDAN

1. Precipitation changes

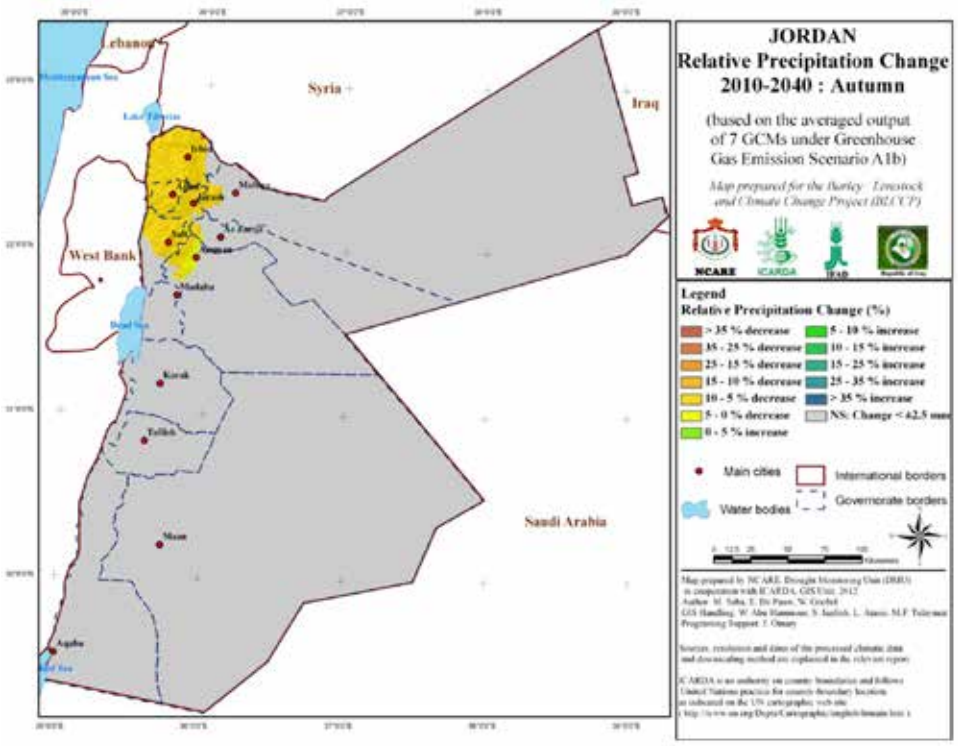

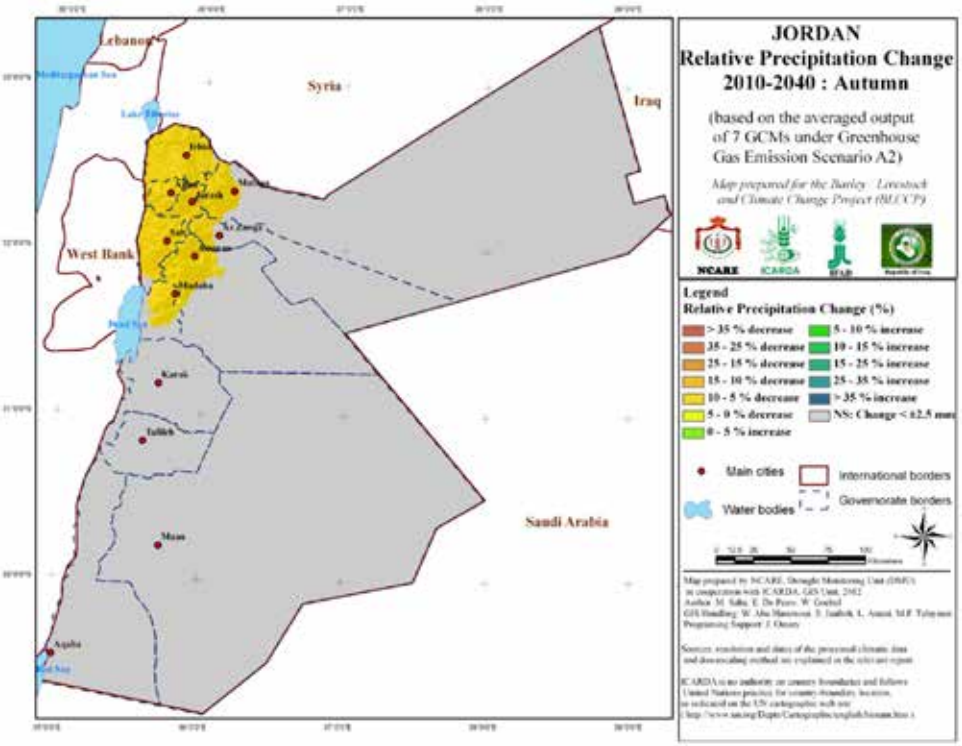

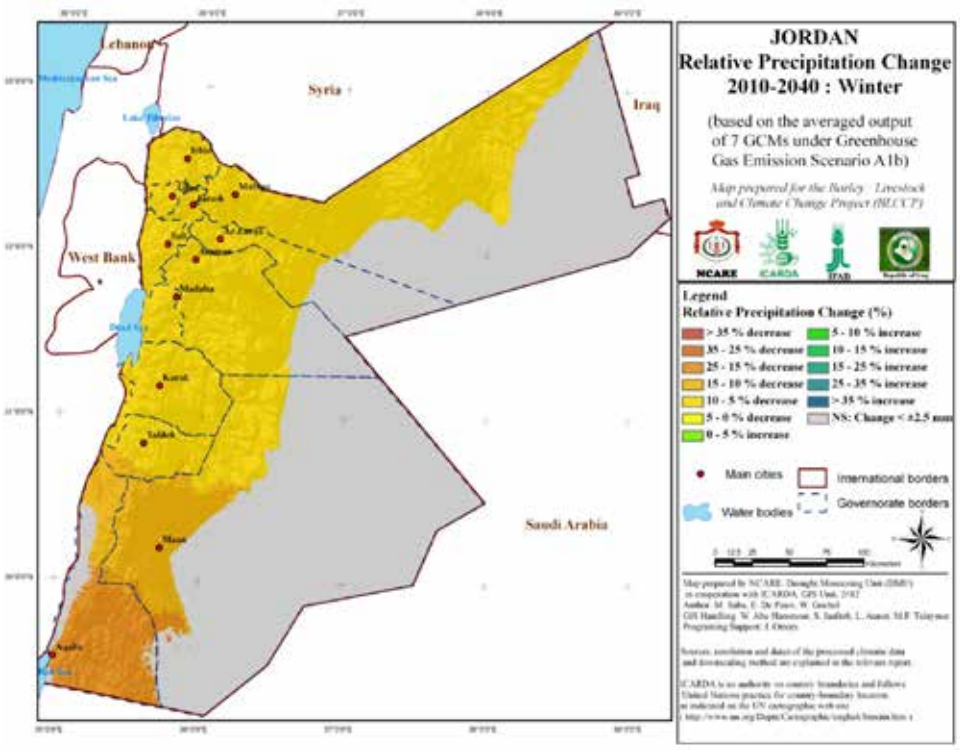
Lebanon
Syria
Iraq
West Bank
Saudi Arabia
JORDAN
Relative Precipitation Change
2010-2040 : Winter
(based on the averaged output
of 7 GCMs under Greenhouse
Gas Emission Scenario A1b)
Maps prepared for the Barley - Livestock and Climate Change Project (BLCCP)
NCARE
ICARDA
IFAD
Legend
Relative Precipitation Change (%)
> 35 % decrease
35 - 25 % decrease
25 - 15 % decrease
15 - 10 % decrease
10 - 5 % decrease
5 - 0 % decrease
0 - 5 % increase
5 - 10 % increase
10 - 15 % increase
15 - 25 % increase
25 - 35 % increase
> 35 % increase
NS: Change < ±2.5 mm
Main cities
International borders
Water bodies
Governorate borders

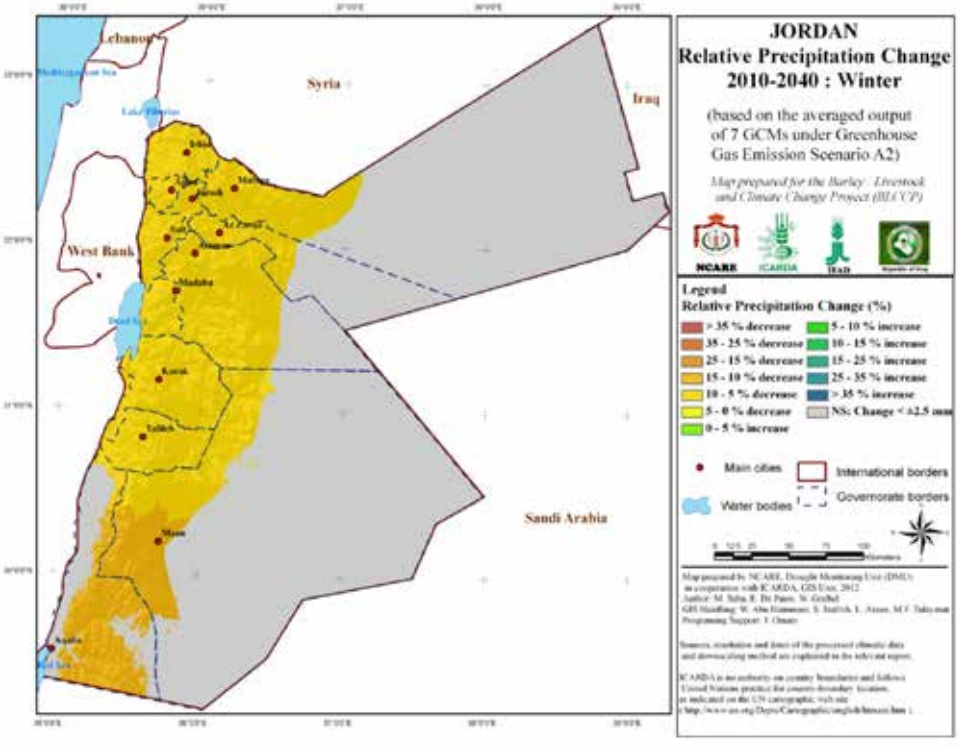
Lebanon
Syria
Iraq
West Bank
Saudi Arabia
JORDAN
Relative Precipitation Change
2010-2040 : Winter
(based on the averaged output
of 7 GCMs under Greenhouse
Gas Emission Scenario A2)
Maps prepared for the Barley - Livestock and Climate Change Project (BLCCP)
NCARE
ICARDA
IFAD
Legend
Relative Precipitation Change (%)
> 35 % decrease
35 - 25 % decrease
25 - 15 % decrease
15 - 10 % decrease
10 - 5 % decrease
5 - 0 % decrease
0 - 5 % increase
5 - 10 % increase
10 - 15 % increase
15 - 25 % increase
25 - 35 % increase
> 35 % increase
NS: Change < ±2.5 mm
Main cities
International borders
Water bodies
Governorate borders

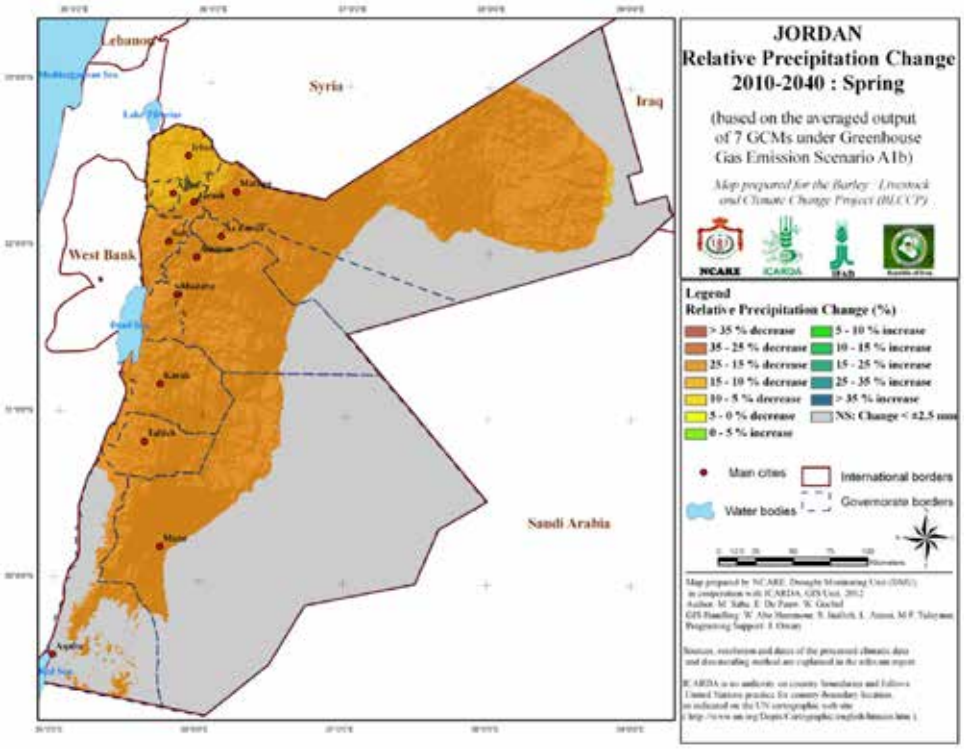
Lebanon
Syria
Iraq
West Bank
Saudi Arabia
JORDAN
Relative Precipitation Change
2010-2040 : Spring
(based on the averaged output
of 7 GCMs under Greenhouse
Gas Emission Scenario A1b)
Map prepared for the Barley : Livestock
and Climate Change Project (BLCCP)
NCARE
ICARDA
IFAD
Legend
Relative Precipitation Change (%)
> 35 % decrease
35 - 25 % decrease
25 - 15 % decrease
15 - 10 % decrease
10 - 5 % decrease
5 - 0 % decrease
0 - 5 % increase
5 - 10 % increase
10 - 15 % increase
15 - 25 % increase
25 - 35 % increase
> 35 % increase
NS: Change < ±2.5 mm
Main cities
International borders
Water bodies
Governorate borders

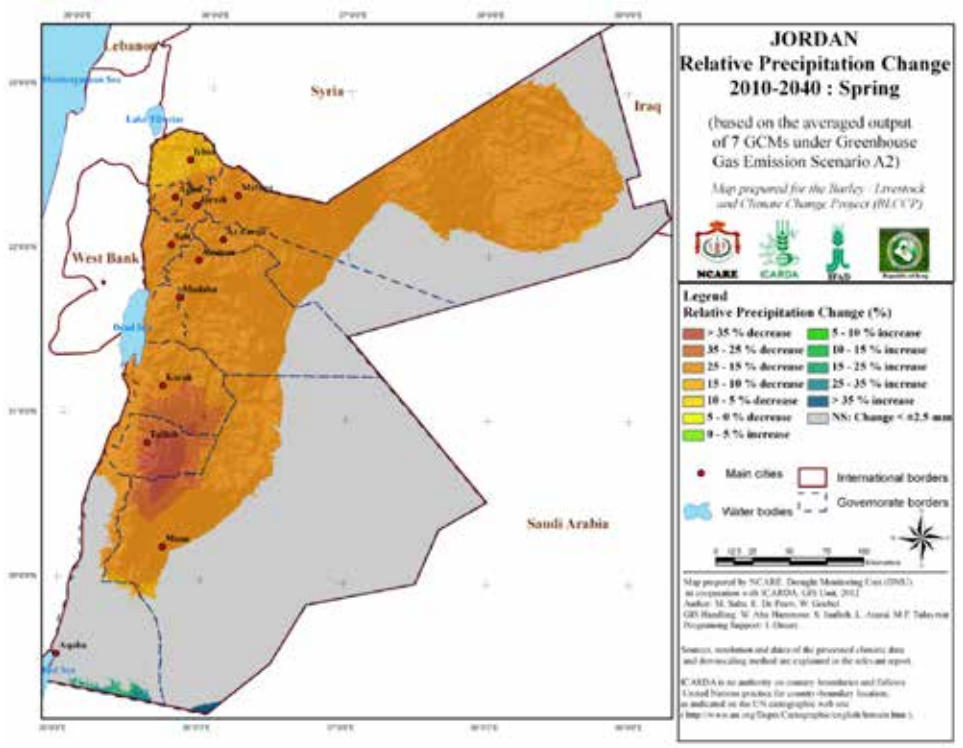
Lebanon
Syria
Iraq
West Bank
Saudi Arabia
JORDAN
Relative Precipitation Change
2010-2040 : Spring
(based on the averaged output
of 7 GCMs under Greenhouse
Gas Emission Scenario A2)
Map prepared for the Barley : Livestock
and Climate Change Project (BLCCP)
NCARE
ICARDA
IFAD
Legend
Relative Precipitation Change (%)
> 35 % decrease
35 - 25 % decrease
25 - 15 % decrease
15 - 10 % decrease
10 - 5 % decrease
5 - 0 % decrease
0 - 5 % increase
5 - 10 % increase
10 - 15 % increase
15 - 25 % increase
25 - 35 % increase
> 35 % increase
NS: Change < ±2.5 mm
Main cities
International borders
Water bodies
Governorate borders

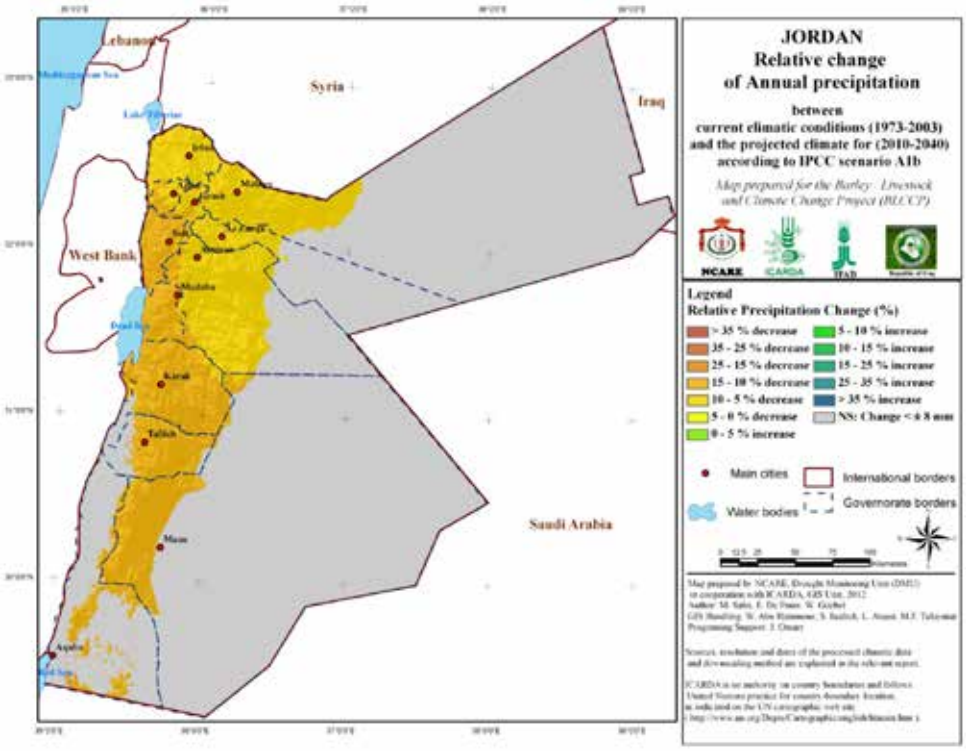
Lebanon
Syria
Iraq
West Bank
Saudi Arabia
JORDAN
Relative change
of Annual precipitation
between
current climatic conditions (1973-2003)
and the projected climate for (2010-2040)
according to IPCC scenario A1b
Maps prepared for the Barley: Livestock and Climate Change Project (BLCCP)
NCARE
ICARDA
IFAD
Legend
Relative Precipitation Change (%)
> 35 % decrease
35 - 25 % decrease
25 - 15 % decrease
15 - 10 % decrease
10 - 5 % decrease
5 - 0 % decrease
0 - 5 % increase
5 - 10 % increase
10 - 15 % increase
15 - 25 % increase
25 - 35 % increase
> 35 % increase
NS: Change < ± 8 mm
Main cities
International borders
Water bodies
Governorate borders

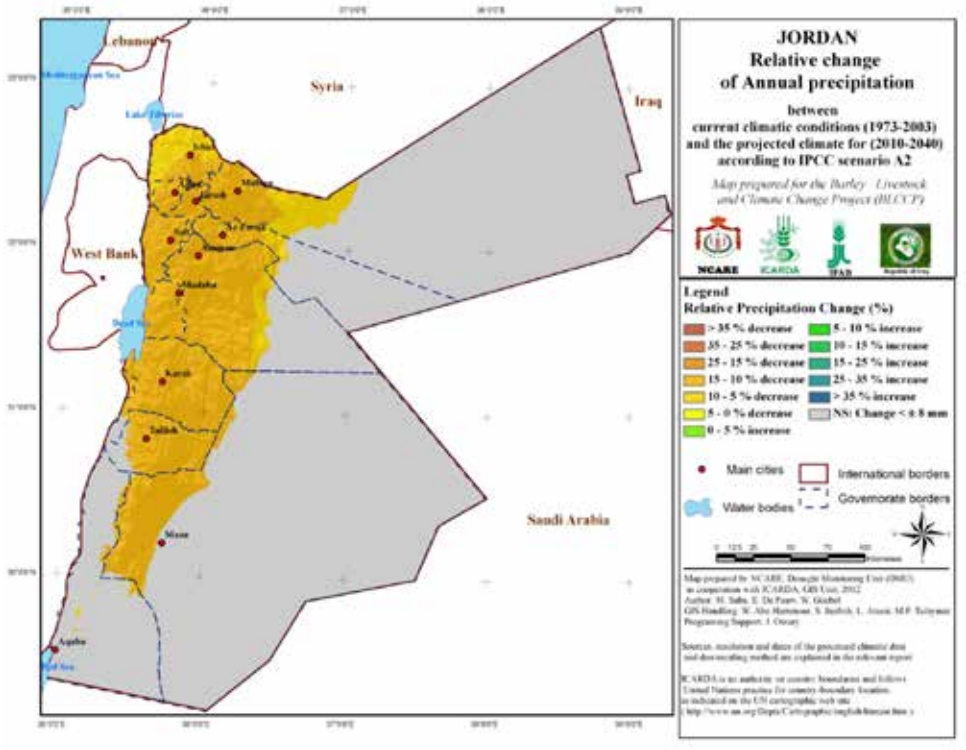
Lebanon
Syria
Iraq
West Bank
Saudi Arabia
JORDAN
Relative change
of Annual precipitation
between
current climatic conditions (1973-2003)
and the projected climate for (2010-2040)
according to IPCC scenario A2
Maps prepared for the Barley: Livestock and Climate Change Project (BLCCP)
NCARE
ICARDA
IFAD
Legend
Relative Precipitation Change (%)
> 35 % decrease
35 - 25 % decrease
25 - 15 % decrease
15 - 10 % decrease
10 - 5 % decrease
5 - 0 % decrease
0 - 5 % increase
5 - 10 % increase
10 - 15 % increase
15 - 25 % increase
25 - 35 % increase
> 35 % increase
NS: Change < ± 8 mm
Main cities
International borders
Water bodies
Governorate borders

2. Temperature changes

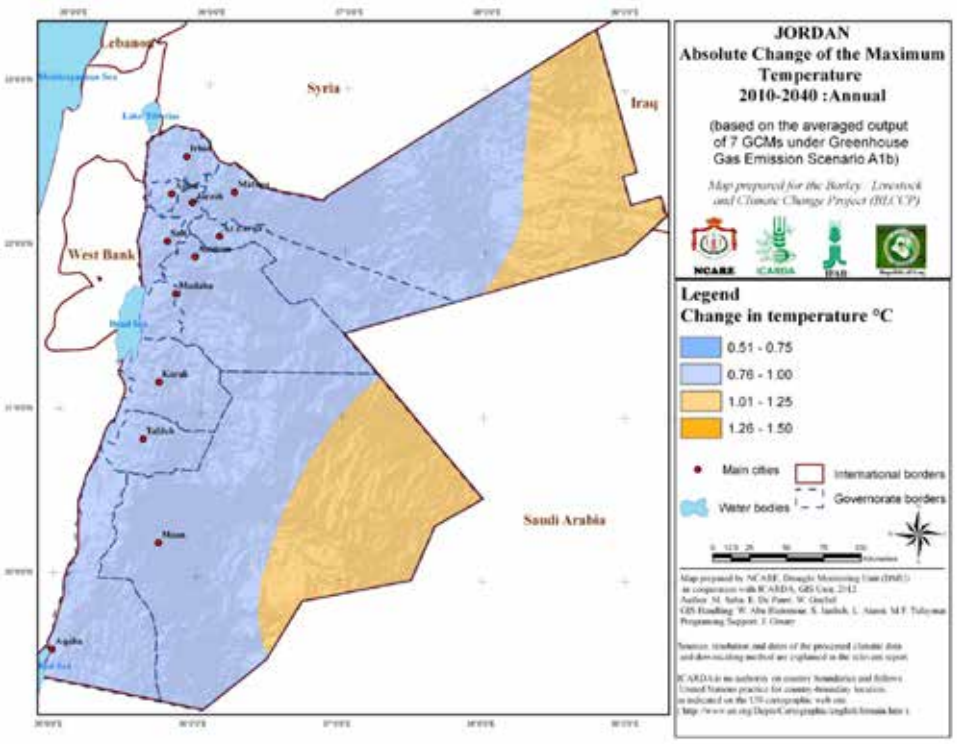

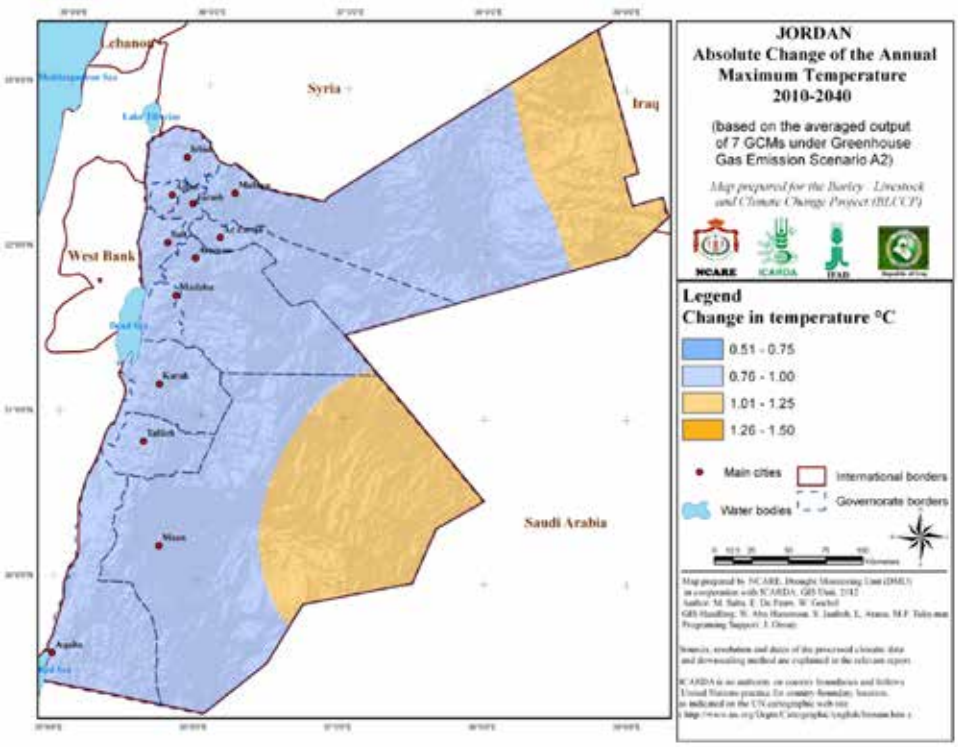

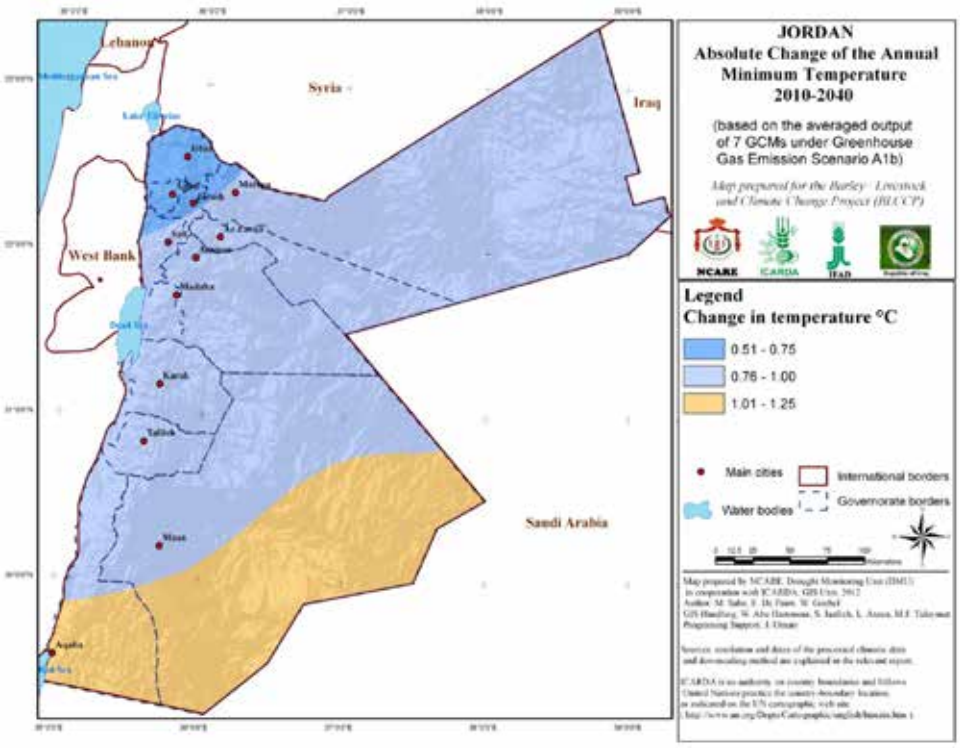
Lebanon
Syria
Iraq
West Bank
Saudi Arabia
JORDAN
Absolute Change of the Annual Minimum Temperature 2010-2040
(based on the averaged output of 7 GCMs under Greenhouse Gas Emission Scenario A1b)
Maps prepared for the Barley - Livestock and Climate Change Project (BLCCP)
NCARE
ICARDA
IFAD
Legend
Change in temperature °C
0.51 - 0.75
0.76 - 1.00
1.01 - 1.25
Main cities
International borders
Water bodies
Governorate borders

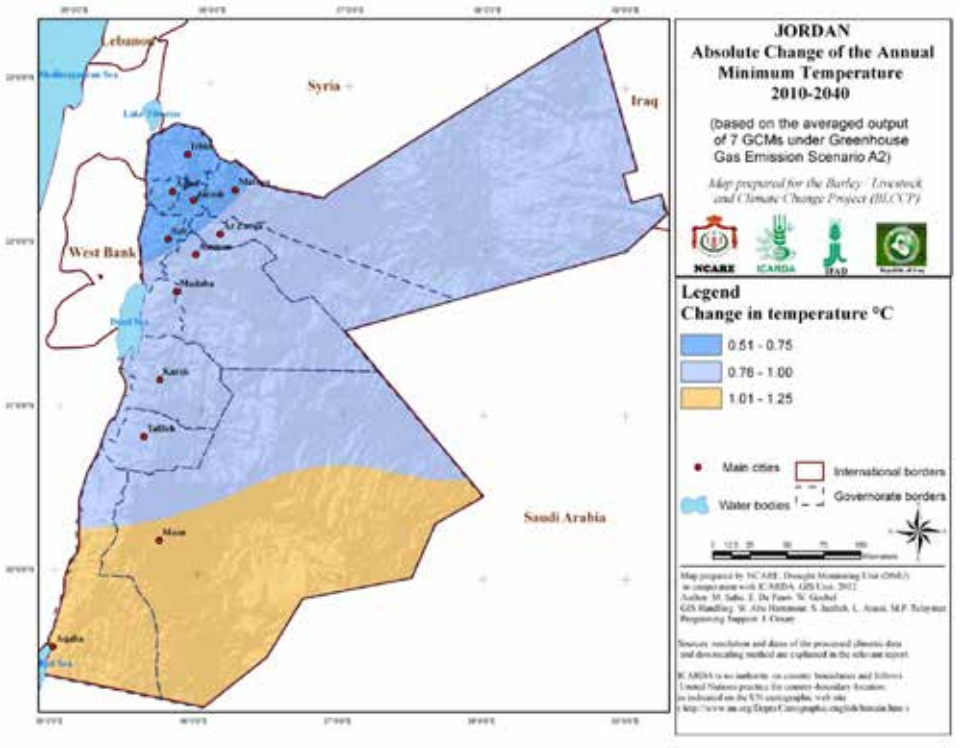
Lebanon
Syria
Iraq
West Bank
Saudi Arabia
JORDAN
Absolute Change of the Annual Minimum Temperature 2010-2040
(based on the averaged output of 7 GCMs under Greenhouse Gas Emission Scenario A2)
Maps prepared for the Barley - Livestock and Climate Change Project (BLCCP)
NCARE
ICARDA
IFAD
Legend
Change in temperature °C
0.51 - 0.75
0.76 - 1.00
1.01 - 1.25
Main cities
International borders
Water bodies
Governorate borders

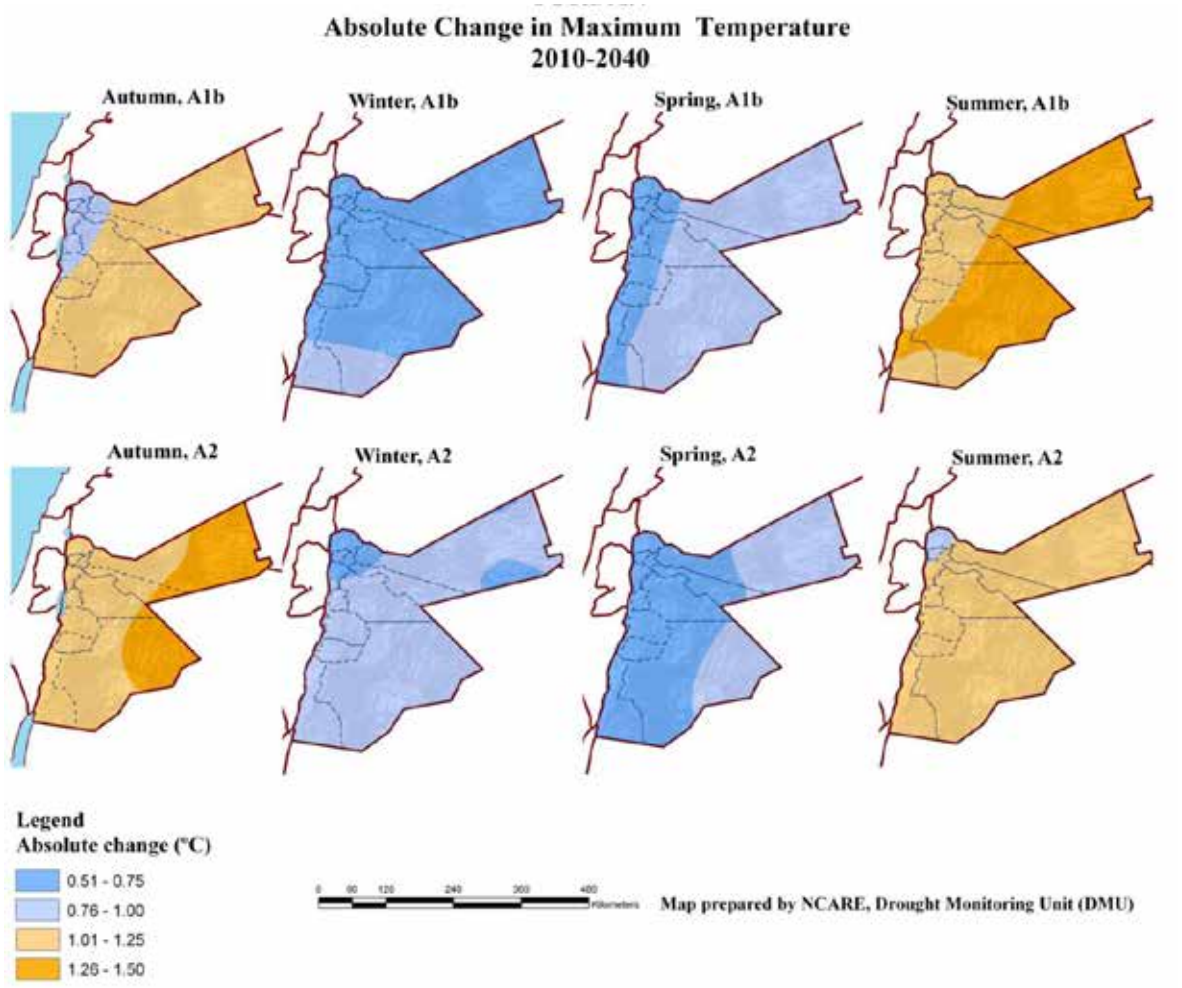
Absolute Change in Maximum Temperature
2010-2040
Autumn, A1b
Winter, A1b
Spring, A1b
Summer, A1b
Autumn, A2
Winter, A2
Spring, A2
Summer, A2
Legend
Absolute change (°C)
0.51 - 0.75
0.76 - 1.00
1.01 - 1.25
1.26 - 1.50
Map prepared by NCARE, Drought Monitoring Unit (DMU)

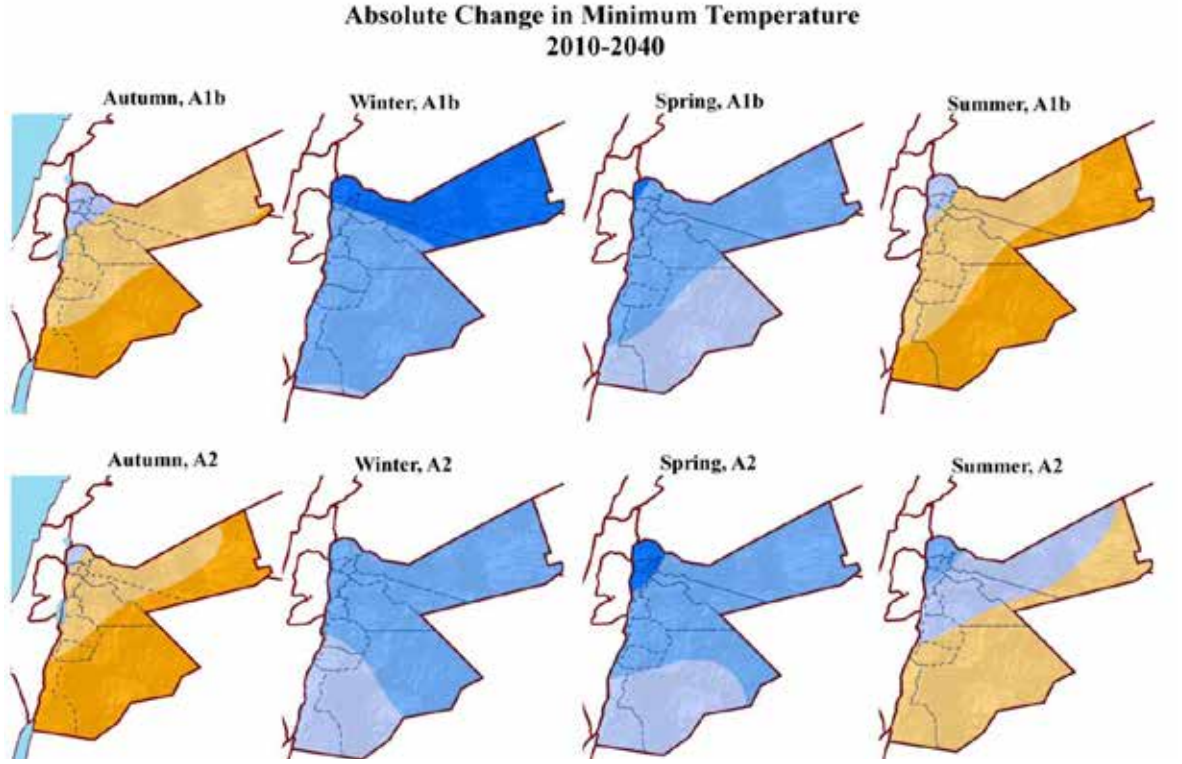
Absolute Change in Minimum Temperature
2010-2040
Autumn, A1b
Winter, A1b
Spring, A1b
Summer, A1b
Autumn, A2
Winter, A2
Spring, A2
Summer, A2

3. Changes in potential evapotranspiration and aridity index

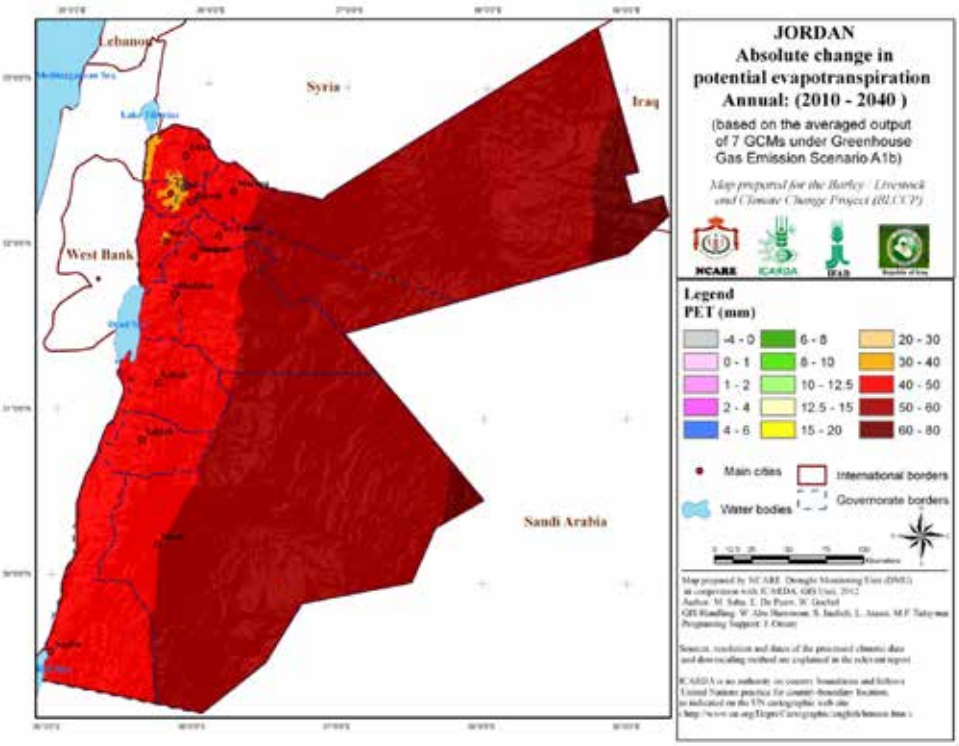

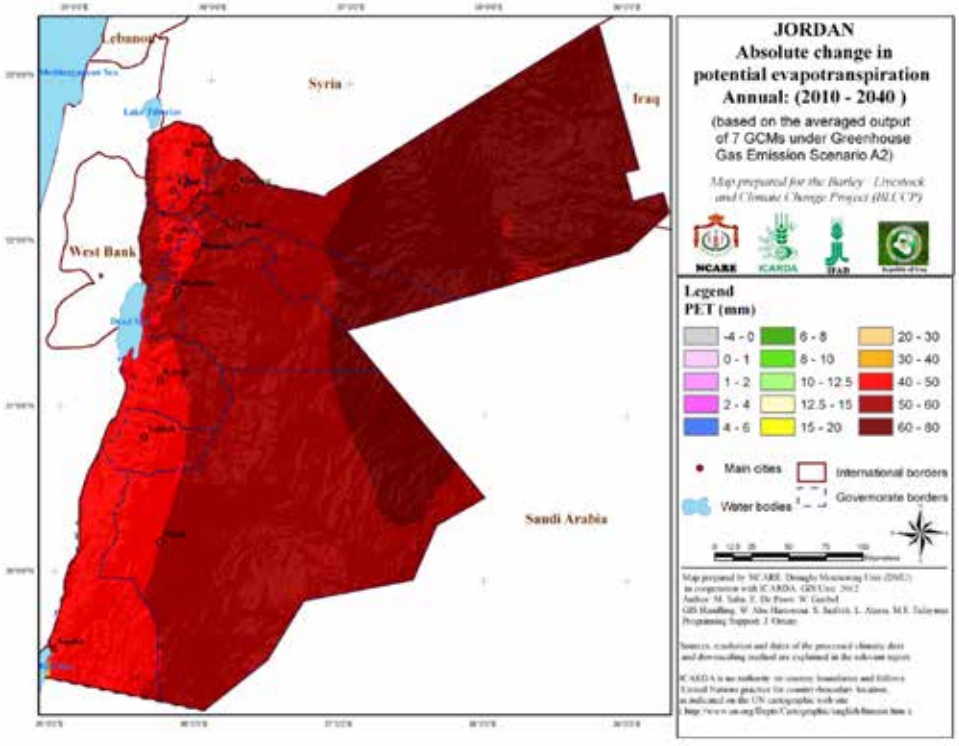

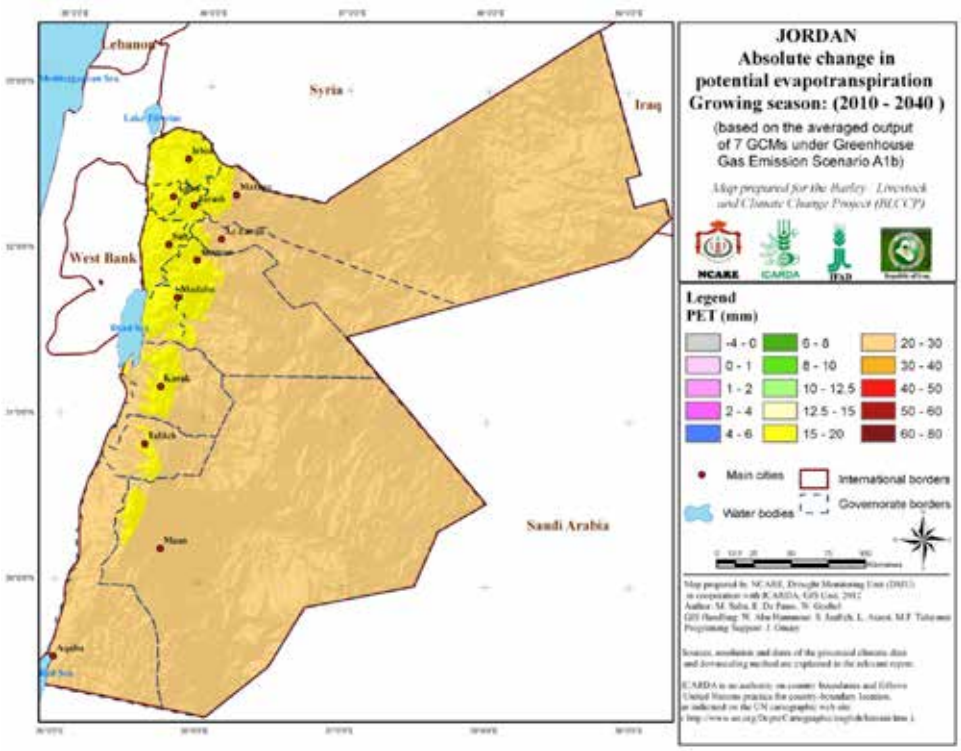
Lebanon
Syria
Iraq
West Bank
Saudi Arabia
Irbid
Jerash
Madaba
Karak
Tafilah
Ma'an
Aqaba
JORDAN
Absolute change in potential evapotranspiration Growing season: (2010 - 2040)
(based on the averaged output of 7 GCMs under Greenhouse Gas Emission Scenario A1b)
Map prepared for the Barley - Livestock and Climate Change Project (BLCCP)
NCARE
ICARDA
IFAD
Legend
PET (mm)
-4 - 0
0 - 1
1 - 2
2 - 4
4 - 6
6 - 8
8 - 10
10 - 12.5
12.5 - 15
15 - 20
20 - 30
30 - 40
40 - 50
50 - 60
60 - 80
Main cities
International borders
Governorate borders
Water bodies

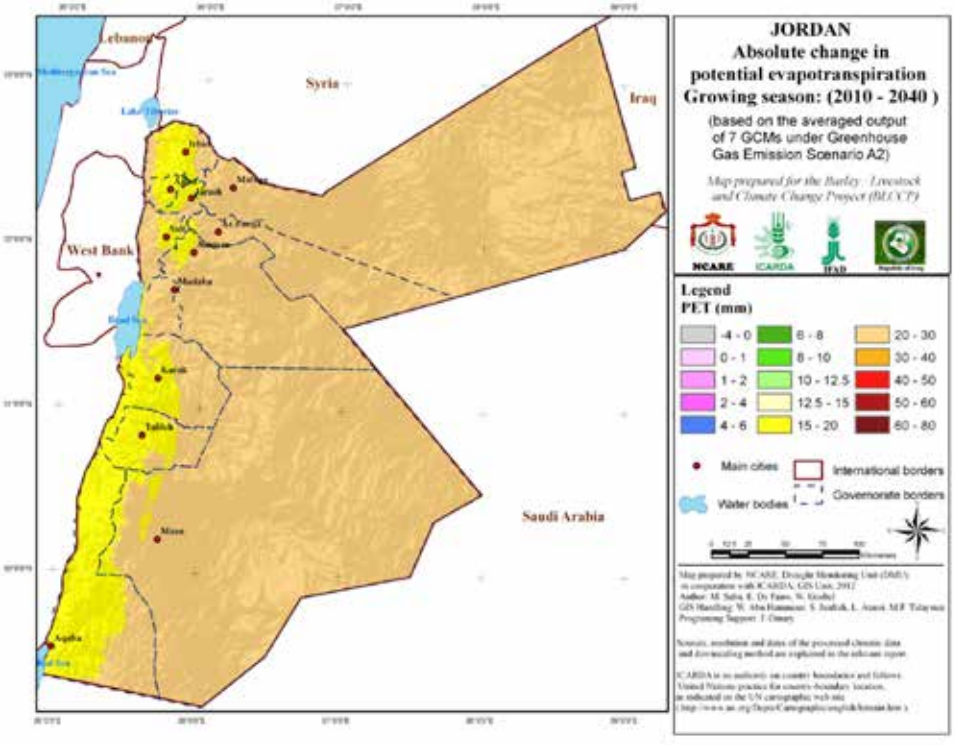
Lebanon
Syria
Iraq
West Bank
Saudi Arabia
Irbid
Jerash
Madaba
Karak
Tafilah
Ma'an
Aqaba
JORDAN
Absolute change in potential evapotranspiration Growing season: (2010 - 2040)
(based on the averaged output of 7 GCMs under Greenhouse Gas Emission Scenario A2)
Map prepared for the Barley - Livestock and Climate Change Project (BLCCP)
NCARE
ICARDA
IFAD
Legend
PET (mm)
-4 - 0
0 - 1
1 - 2
2 - 4
4 - 6
6 - 8
8 - 10
10 - 12.5
12.5 - 15
15 - 20
20 - 30
30 - 40
40 - 50
50 - 60
60 - 80
Main cities
International borders
Governorate borders
Water bodies

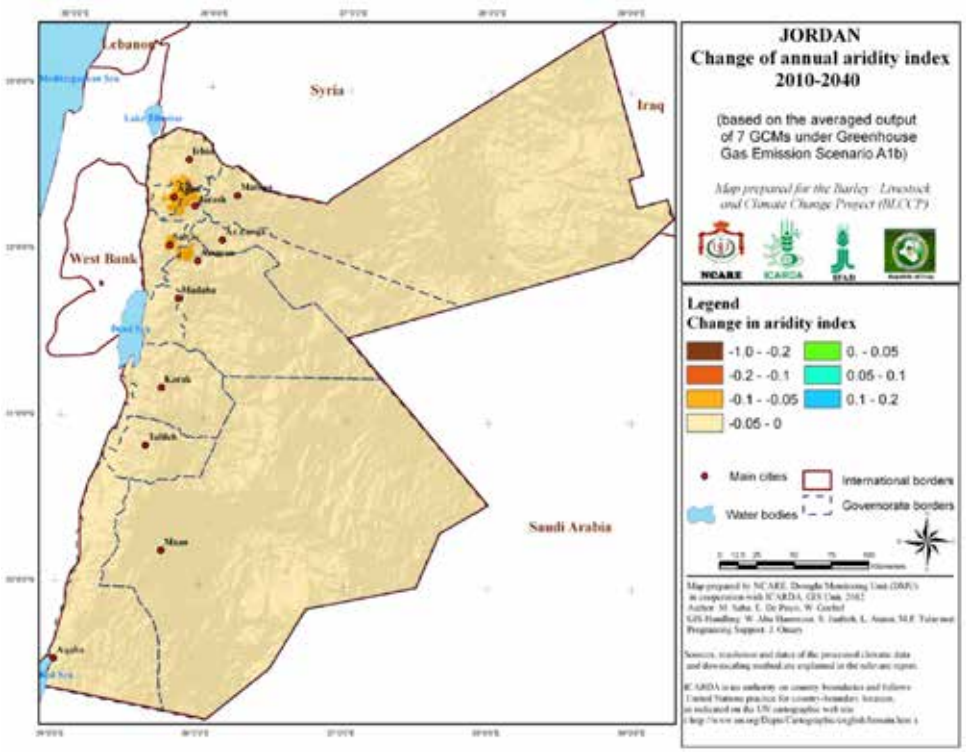
JORDAN
Change of annual aridity index
2010-2040
(based on the averaged output
of 7 GCMs under Greenhouse
Gas Emission Scenario A1b)
Map prepared for the Barley : Livestock
and Climate Change Project (BLCCP)
NCARE
ICARDA
IFAD
Legend
Change in aridity index
-1.0 - -0.2
-0.2 - -0.1
-0.1 - -0.05
-0.05 - 0
0. - 0.05
0.05 - 0.1
0.1 - 0.2
Main cities
International borders
Governorate borders
Water bodies
Lebanon
Syria
Iraq
West Bank
Saudi Arabia

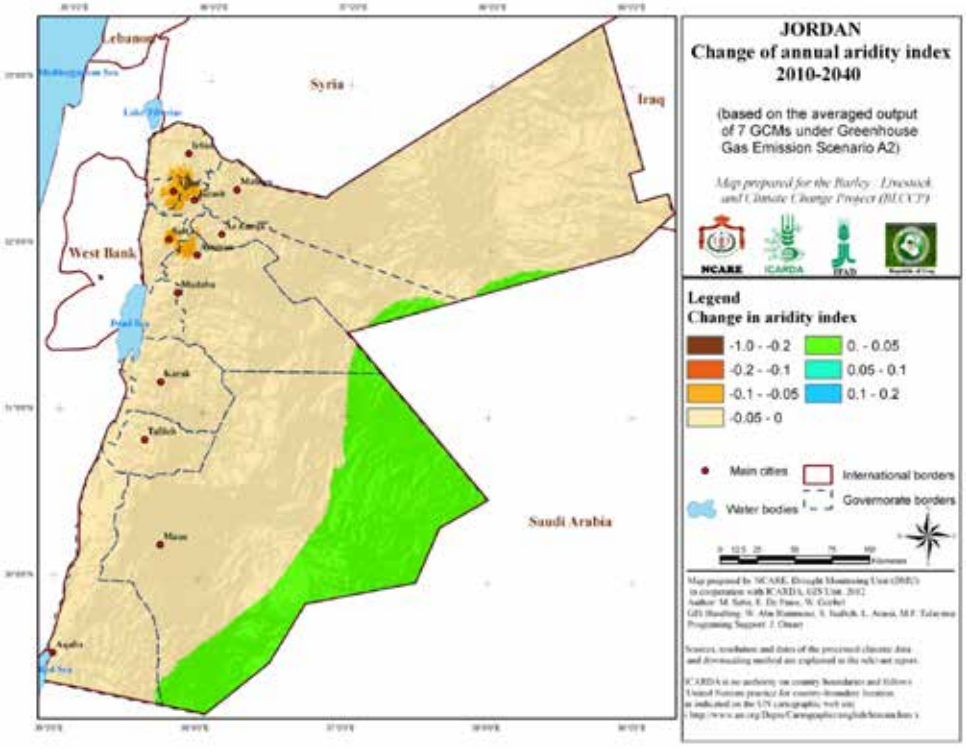
JORDAN
Change of annual aridity index
2010-2040
(based on the averaged output
of 7 GCMs under Greenhouse
Gas Emission Scenario A2)
Map prepared for the Barley : Livestock
and Climate Change Project (BLCCP)
NCARE
ICARDA
IFAD
Legend
Change in aridity index
-1.0 - -0.2
-0.2 - -0.1
-0.1 - -0.05
-0.05 - 0
0. - 0.05
0.05 - 0.1
0.1 - 0.2
Main cities
International borders
Governorate borders
Water bodies
Lebanon
Syria
Iraq
West Bank
Saudi Arabia

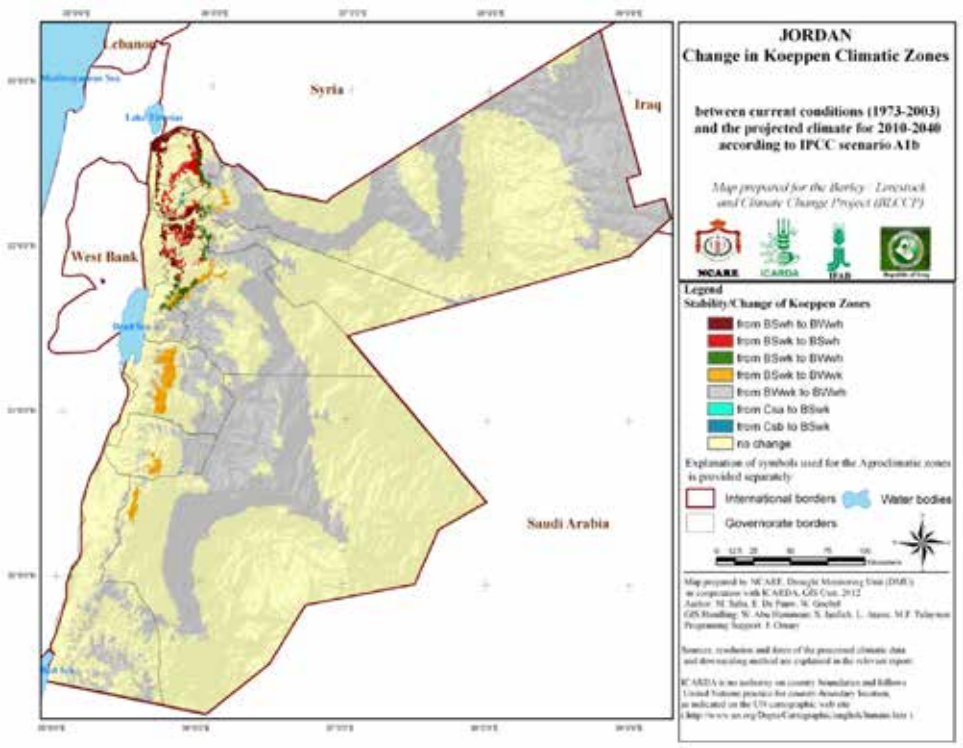
Lebanon
Syria
Iraq
West Bank
Saudi Arabia
JORDAN
Change in Koeppen Climatic Zones
between current conditions (1973-2003) and the projected climate for 2010-2040 according to IPCC scenario A1b
Map prepared for the Barley - Livestock and Climate Change Project (BLCCP)
NCARE
ICARDA
IFAD
Legend
Stability/Change of Koeppen Zones
from BSwh to BWwh
from BSwk to BSwh
from BSwk to BWwh
from BSwk to BWwk
from BWwk to BWwh
from Csa to BSwk
from Csb to BSwk
no change
Explanation of symbols used for the Agroclimatic zones is provided separately
International borders
Water bodies
Governorate borders

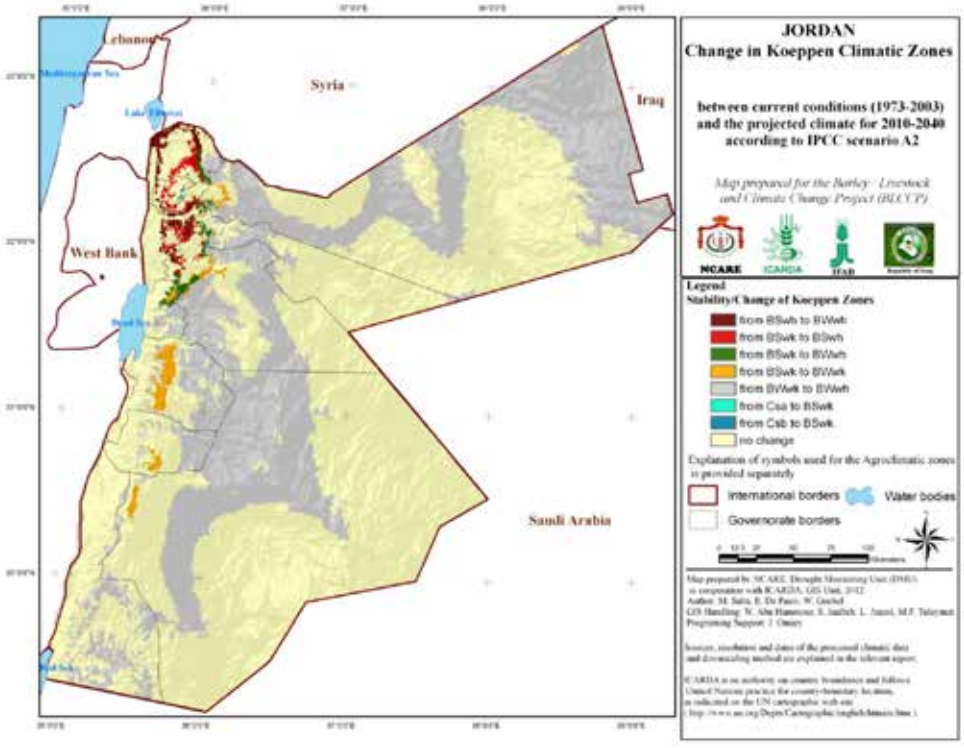
Lebanon
Syria
Iraq
West Bank
Saudi Arabia
JORDAN
Change in Koeppen Climatic Zones
between current conditions (1973-2003) and the projected climate for 2010-2040 according to IPCC scenario A2
Map prepared for the Barley - Livestock and Climate Change Project (BLCCP)
NCARE
ICARDA
IFAD
Legend
Stability/Change of Koeppen Zones
from BSwh to BWwh
from BSwk to BSwh
from BSwk to BWwh
from BSwk to BWwk
from BWwk to BWwh
from Csa to BSwk
from Csb to BSwk
no change
Explanation of symbols used for the Agroclimatic zones is provided separately
International borders
Water bodies
Governorate borders

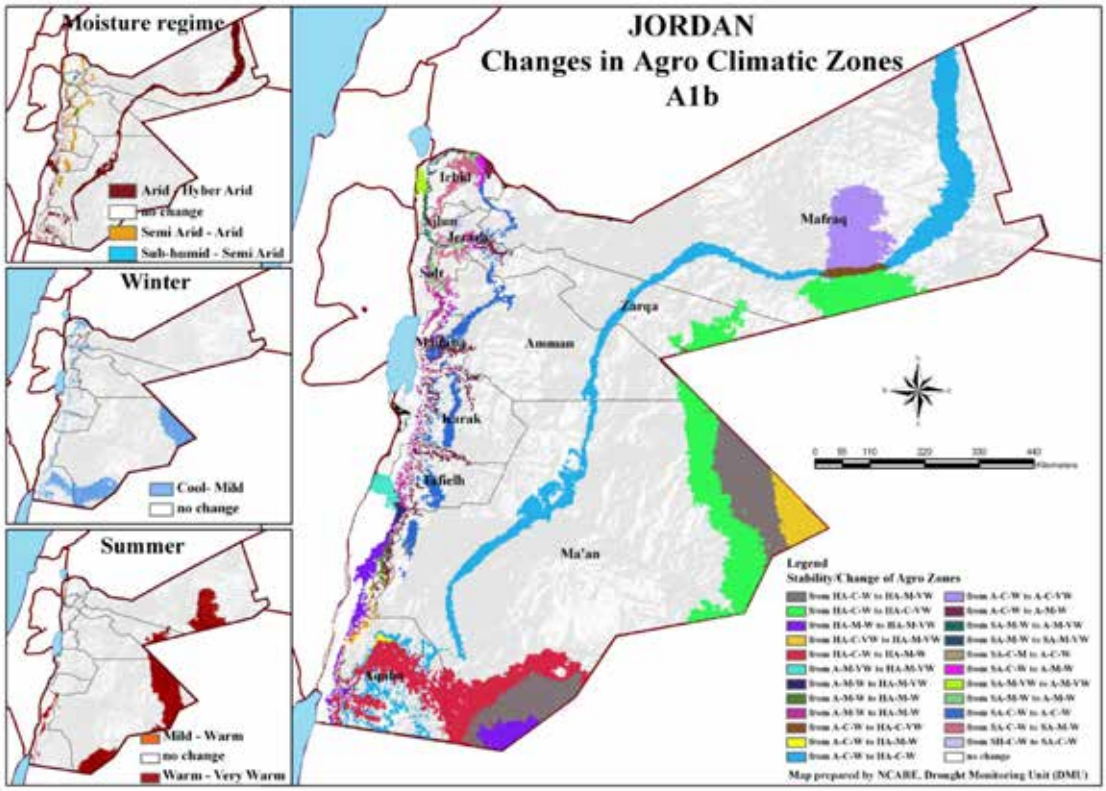
Moisture regime
Arid - Hyber Arid
no change
Semi Arid - Arid
Sub-humid - Semi Arid
Winter
Cool- Mild
no change
Summer
Mild - Warm
no change
Warm - Very Warm
JORDAN
Changes in Agro Climatic Zones
A1b
Irbid
Jerash
Salt
Zarqa
Amman
Karak
Tafielh
Ma'an
Mafraq
Legend
Stability/Change of Agro Zones
Map prepared by NCARE, Drought Monitoring Unit (DMU)

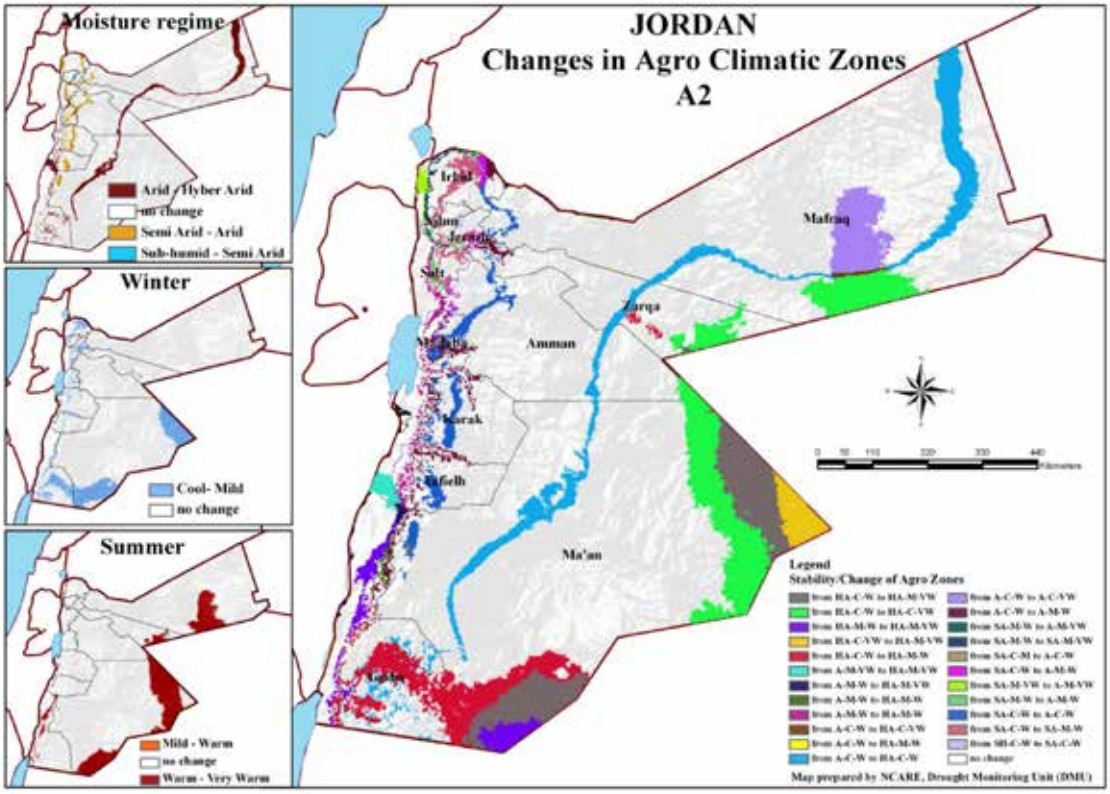
Moisture regime
Arid - Hyber Arid
no change
Semi Arid - Arid
Sub-humid - Semi Arid
Winter
Cool- Mild
no change
Summer
Mild - Warm
no change
Warm - Very Warm
JORDAN
Changes in Agro Climatic Zones
A2
Irbid
Jerash
Salt
Zarqa
Amman
Karak
Tafielh
Ma'an
Mafraq
Legend
Stability/Change of Agro Zones
Map prepared by NCARE, Drought Monitoring Unit (DMU)

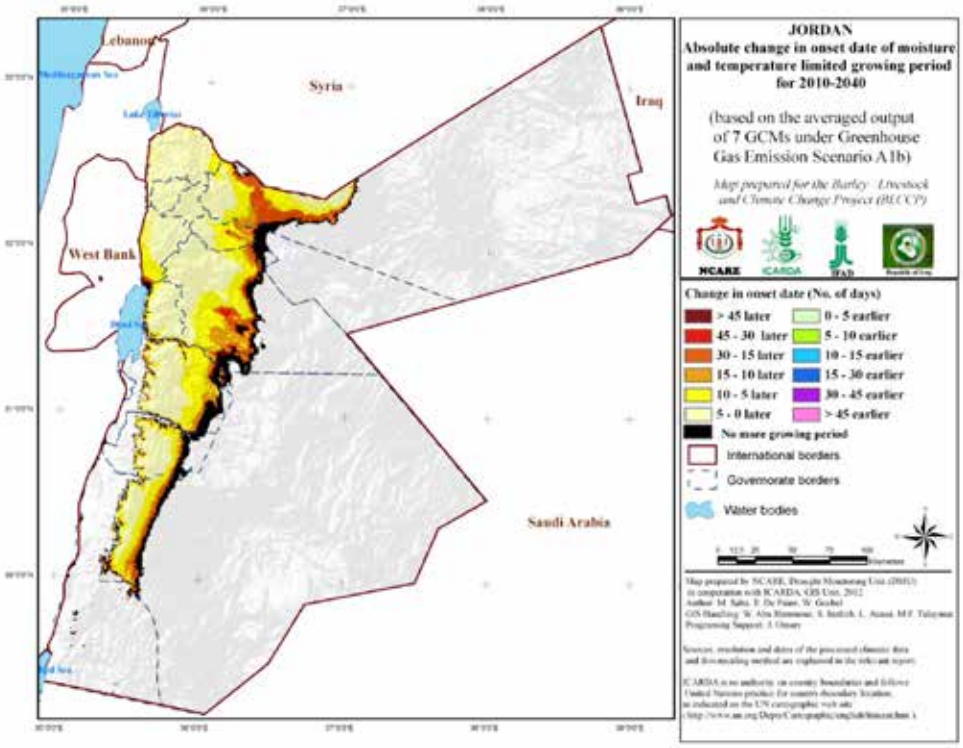
Lebanon
Syria
Iraq
West Bank
Saudi Arabia
JORDAN
Absolute change in onset date of moisture and temperature limited growing period for 2010-2040
(based on the averaged output of 7 GCMs under Greenhouse Gas Emission Scenario A1b)
Map prepared for the Barley : Livestock and Climate Change Project (BLCCP)
NCARE
ICARDA
IFAD
Change in onset date (No. of days)
> 45 later
45 - 30 later
30 - 15 later
15 - 10 later
10 - 5 later
5 - 0 later
0 - 5 earlier
5 - 10 earlier
10 - 15 earlier
15 - 30 earlier
30 - 45 earlier
> 45 earlier
No more growing period
International borders
Governorate borders
Water bodies

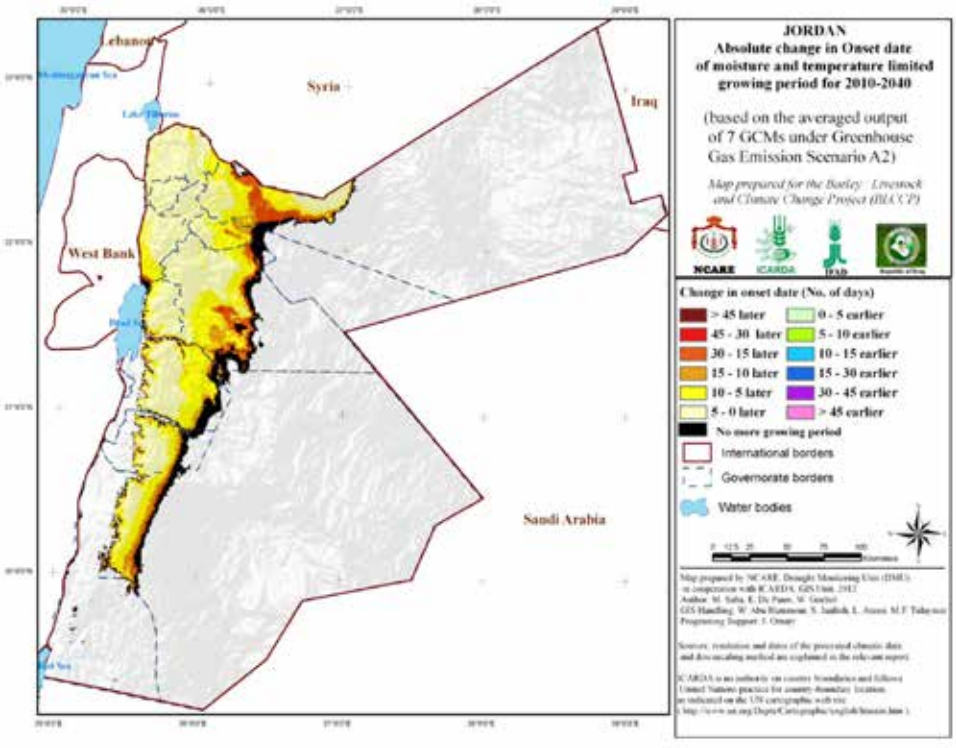
Lebanon
Syria
Iraq
West Bank
Saudi Arabia
JORDAN
Absolute change in Onset date of moisture and temperature limited growing period for 2010-2040
(based on the averaged output of 7 GCMs under Greenhouse Gas Emission Scenario A2)
Map prepared for the Barley : Livestock and Climate Change Project (BLCCP)
NCARE
ICARDA
IFAD
Change in onset date (No. of days)
> 45 later
45 - 30 later
30 - 15 later
15 - 10 later
10 - 5 later
5 - 0 later
0 - 5 earlier
5 - 10 earlier
10 - 15 earlier
15 - 30 earlier
30 - 45 earlier
> 45 earlier
No more growing period
International borders
Governorate borders
Water bodies

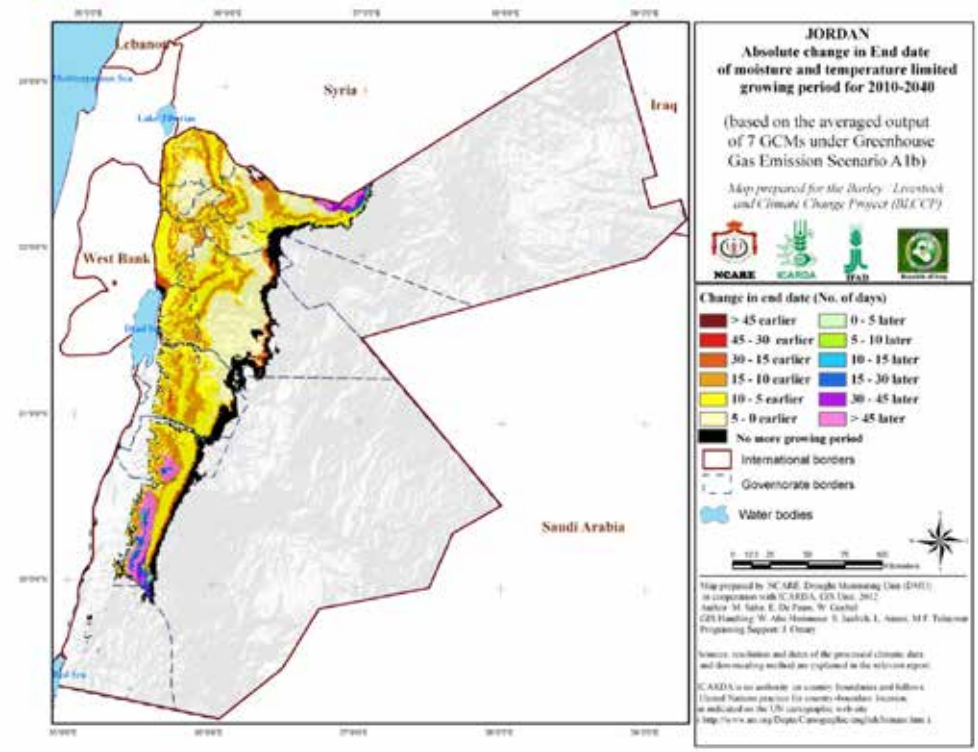
Lebanon
Syria
Iraq
West Bank
Saudi Arabia
JORDAN
Absolute change in End date
of moisture and temperature limited
growing period for 2010-2040
(based on the averaged output
of 7 GCMs under Greenhouse
Gas Emission Scenario A1b)
Map prepared for the Barley : Livestock
and Climate Change Project (BLCCP)
NCARE
ICARDA
IFAD
Change in end date (No. of days)
> 45 earlier
45 - 30 earlier
30 - 15 earlier
15 - 10 earlier
10 - 5 earlier
5 - 0 earlier
0 - 5 later
5 - 10 later
10 - 15 later
15 - 30 later
30 - 45 later
> 45 later
No more growing period
International borders
Governorate borders
Water bodies

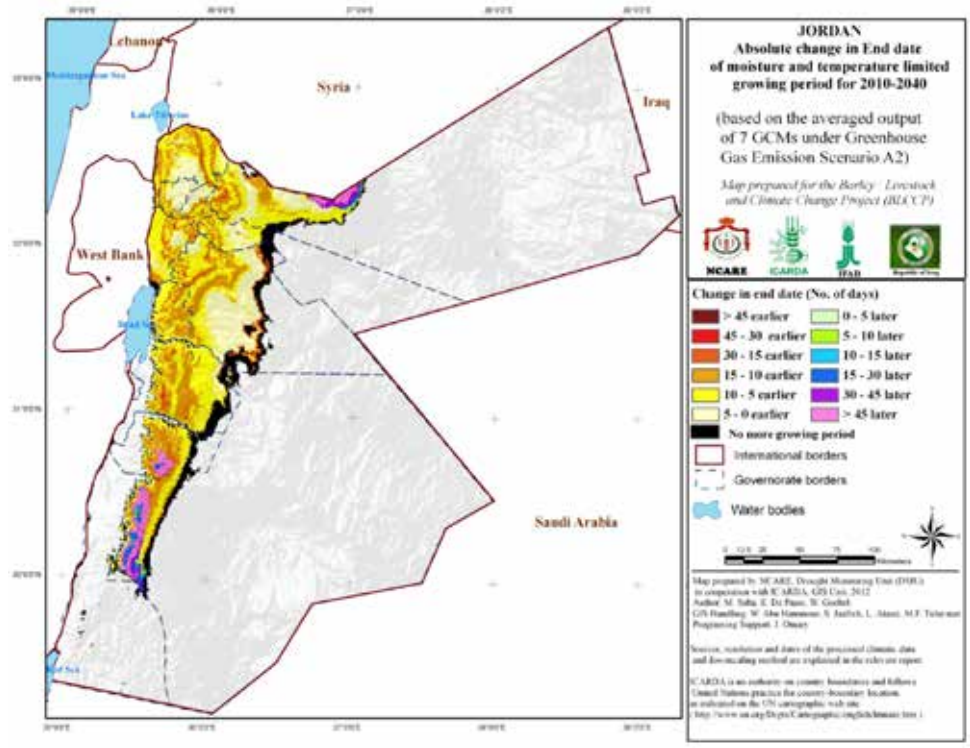
Lebanon
Syria
Iraq
West Bank
Saudi Arabia
JORDAN
Absolute change in End date
of moisture and temperature limited
growing period for 2010-2040
(based on the averaged output
of 7 GCMs under Greenhouse
Gas Emission Scenario A2)
Map prepared for the Barley : Livestock
and Climate Change Project (BLCCP)
NCARE
ICARDA
IFAD
Change in end date (No. of days)
> 45 earlier
45 - 30 earlier
30 - 15 earlier
15 - 10 earlier
10 - 5 earlier
5 - 0 earlier
0 - 5 later
5 - 10 later
10 - 15 later
15 - 30 later
30 - 45 later
> 45 later
No more growing period
International borders
Governorate borders
Water bodies

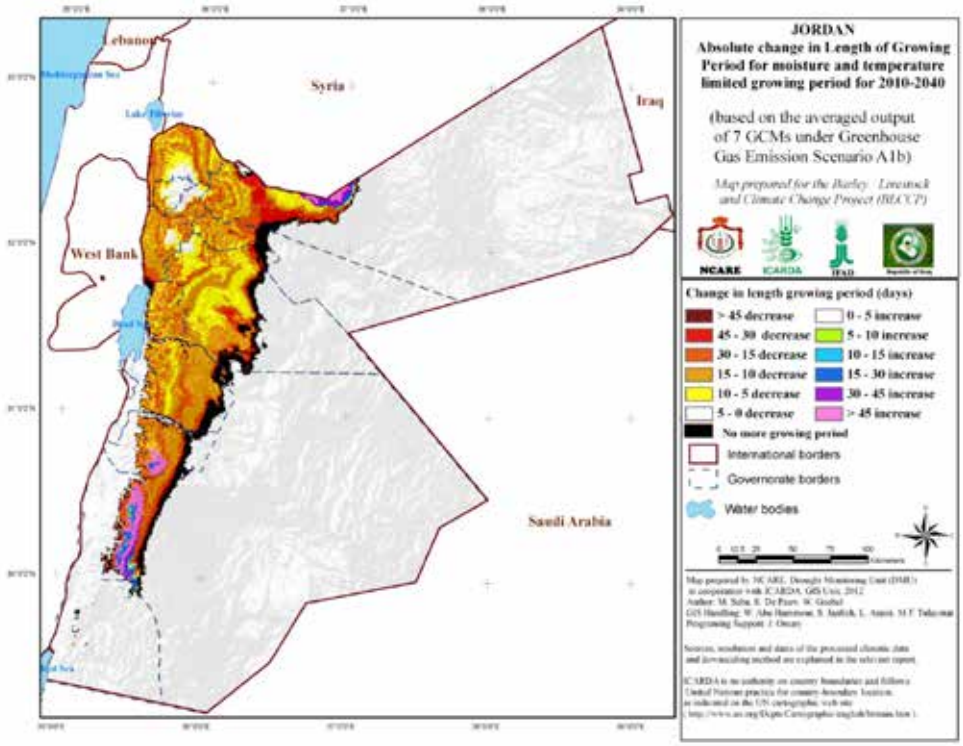
Lebanon
Syria
Iraq
West Bank
Saudi Arabia
JORDAN
Absolute change in Length of Growing Period for moisture and temperature limited growing period for 2010-2040
(based on the averaged output of 7 GCMs under Greenhouse Gas Emission Scenario A1b)
Map prepared for the Barley: Livestock and Climate Change Project (BLCCP)
NCARE
ICARDA
IFAD
Change in length growing period (days)
> 45 decrease
45 - 30 decrease
30 - 15 decrease
15 - 10 decrease
10 - 5 decrease
5 - 0 decrease
0 - 5 increase
5 - 10 increase
10 - 15 increase
15 - 30 increase
30 - 45 increase
> 45 increase
No more growing period
International borders
Governorate borders
Water bodies

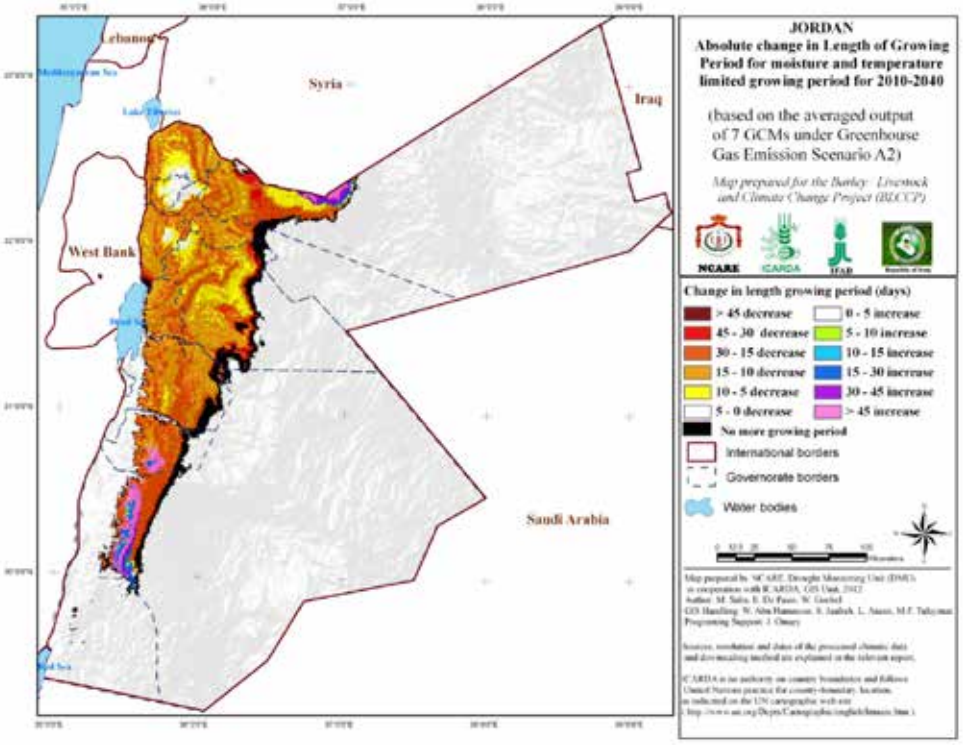
Lebanon
Syria
Iraq
West Bank
Saudi Arabia
JORDAN
Absolute change in Length of Growing Period for moisture and temperature limited growing period for 2010-2040
(based on the averaged output of 7 GCMs under Greenhouse Gas Emission Scenario A2)
Map prepared for the Barley: Livestock and Climate Change Project (BLCCP)
NCARE
ICARDA
IFAD
Change in length growing period (days)
> 45 decrease
45 - 30 decrease
30 - 15 decrease
15 - 10 decrease
10 - 5 decrease
5 - 0 decrease
0 - 5 increase
5 - 10 increase
10 - 15 increase
15 - 30 increase
30 - 45 increase
> 45 increase
No more growing period
International borders
Governorate borders
Water bodies

ANNEX 8

REPRESENTATIVE MAPS FROM THE CLIMATE CHANGE ATLAS OF IRAQ

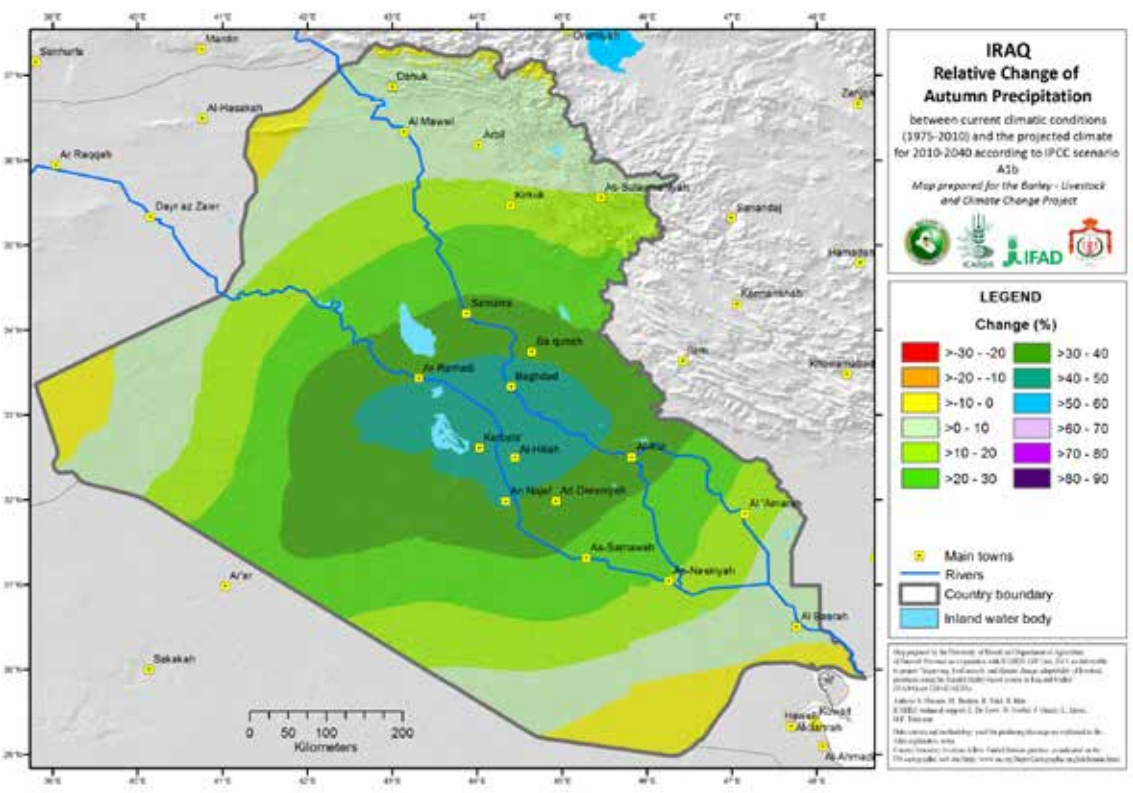

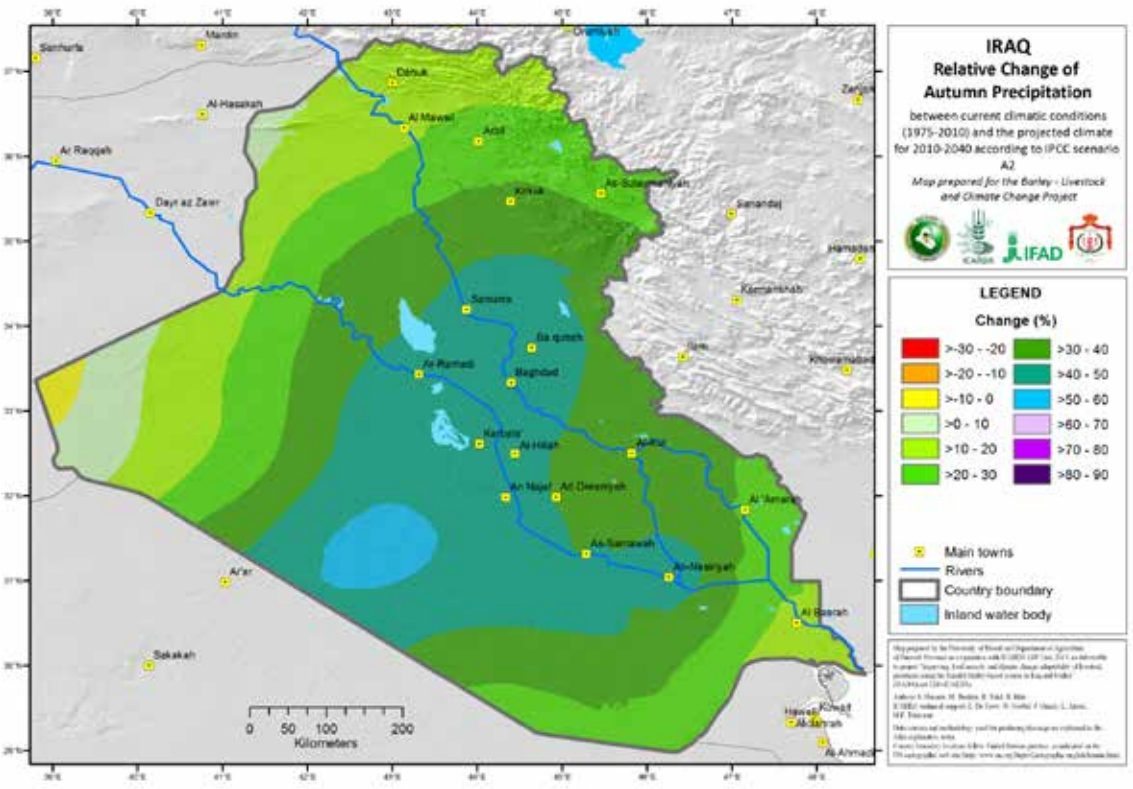

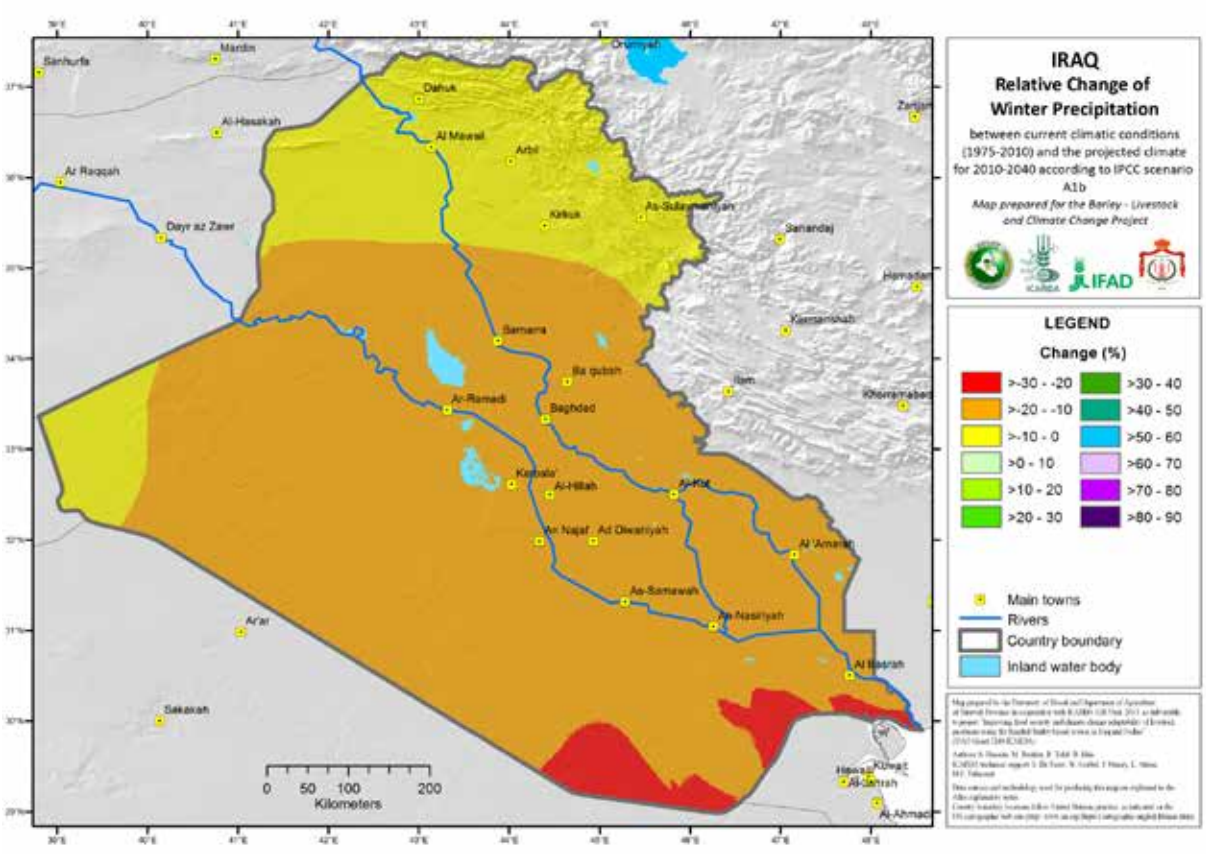
IRAQ
Relative Change of
Winter Precipitation
between current climatic conditions
(1975-2010) and the projected climate
for 2010-2040 according to IPCC scenario
A1b
Map prepared for the Barley - Livestock
and Climate Change Project
IFAD
LEGEND
Change (%)
>-30 - -20
>-20 - -10
>-10 - 0
>0 - 10
>10 - 20
>20 - 30
>30 - 40
>40 - 50
>50 - 60
>60 - 70
>70 - 80
>80 - 90
Main towns
Rivers
Country boundary
Inland water body
0 50 100 200
Kilometers
Sanhurfa
Mardin
Dahuk
Al-Hasakah
Al Mawsil
Arbil
Ar Raqqah
Kirkuk
Dayr az Zawr
Samarra
Ba qubah
Ar-Ramadi
Baghdad
Karbala'
Al-Hillah
An Najaf
Ad Diwaniyah
Al 'Amarah
As-Samawah
An Nasiriyah
Al Basrah
Ar'ar
Sakakah
Al-Ahmadi

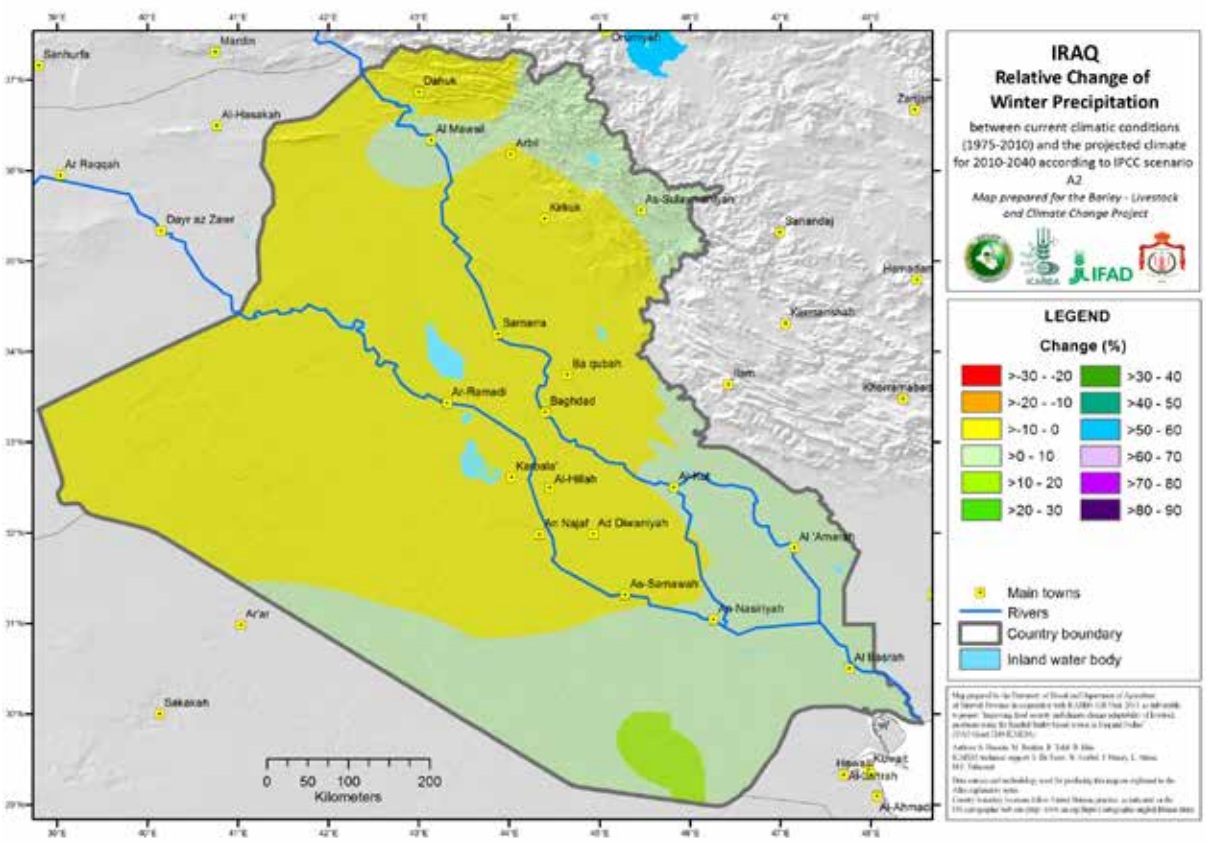
IRAQ
Relative Change of
Winter Precipitation
between current climatic conditions
(1975-2010) and the projected climate
for 2010-2040 according to IPCC scenario
A2
Map prepared for the Barley - Livestock
and Climate Change Project
IFAD
LEGEND
Change (%)
>-30 - -20
>-20 - -10
>-10 - 0
>0 - 10
>10 - 20
>20 - 30
>30 - 40
>40 - 50
>50 - 60
>60 - 70
>70 - 80
>80 - 90
Main towns
Rivers
Country boundary
Inland water body
0 50 100 200
Kilometers
Sanhurfa
Mardin
Dahuk
Al-Hasakah
Al Mawsil
Arbil
Ar Raqqah
Kirkuk
Dayr az Zawr
Samarra
Ba qubah
Ar-Ramadi
Baghdad
Karbala'
Al-Hillah
An Najaf
Ad Diwaniyah
Al 'Amarah
As-Samawah
An Nasiriyah
Al Basrah
Ar'ar
Sakakah
Al-Ahmadi

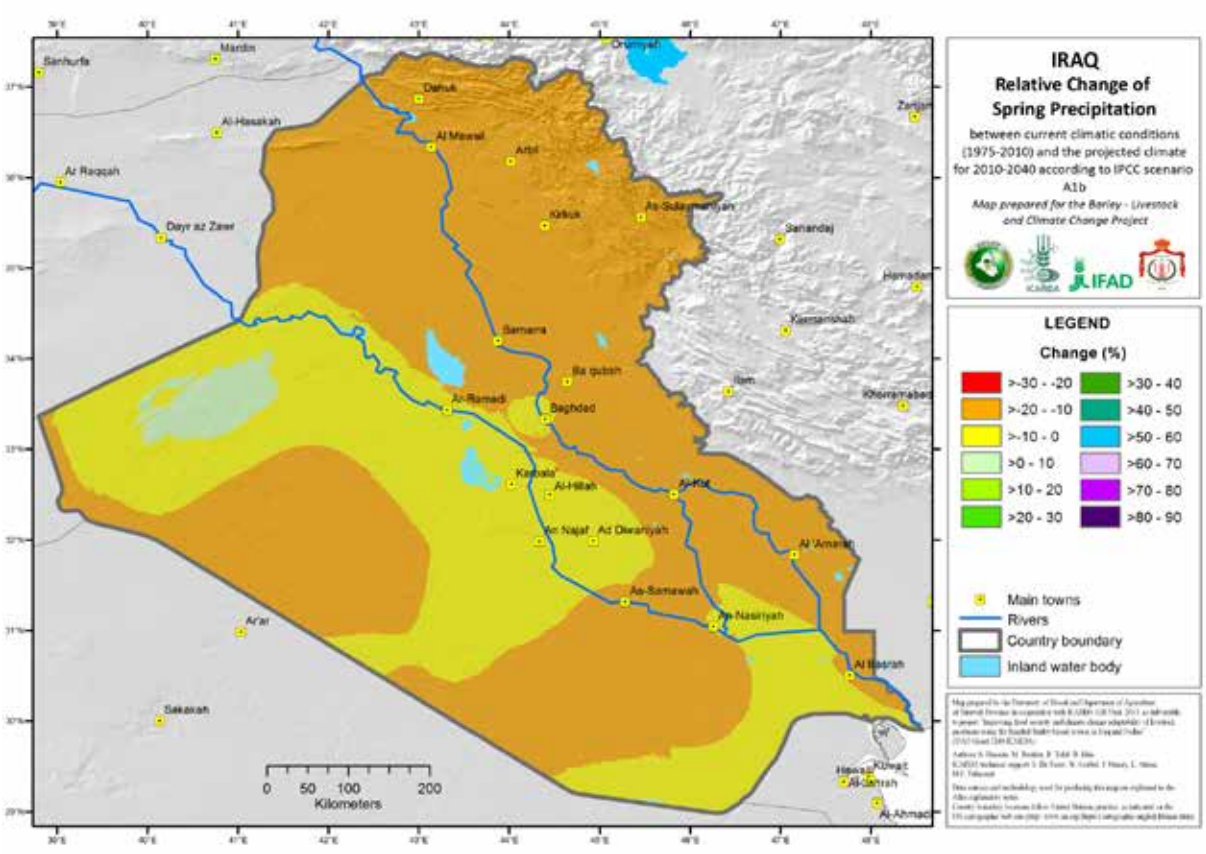
IRAQ
Relative Change of
Spring Precipitation
between current climatic conditions
(1975-2010) and the projected climate
for 2010-2040 according to IPCC scenario
A1b
Map prepared for the Barley - Livestock
and Climate Change Project
IFAD
LEGEND
Change (%)
>-30 - -20
>-20 - -10
>-10 - 0
>0 - 10
>10 - 20
>20 - 30
>30 - 40
>40 - 50
>50 - 60
>60 - 70
>70 - 80
>80 - 90
Main towns
Rivers
Country boundary
Inland water body
0 50 100 200
Kilometers
Sanhurfa
Mardin
Dahuk
Al-Hasakah
Ar Raqqah
Al Mawsil
Arbil
Kirkuk
As-Sulaymaniyah
Dayr az Zawr
Sanandaj
Hamadan
Kermanshah
Samarra
Ba qubah
Ilam
Khorramabad
Ar-Ramadi
Baghdad
Karbala'
Al-Hillah
Al-Kut
An Najaf
Ad Diwaniyah
Al 'Amarah
As-Samawah
An Nasiriyah
Ar'ar
Al Basrah
Sakakah
Hafar al-Batin
Al-Jahrah
Al-Ahmadi

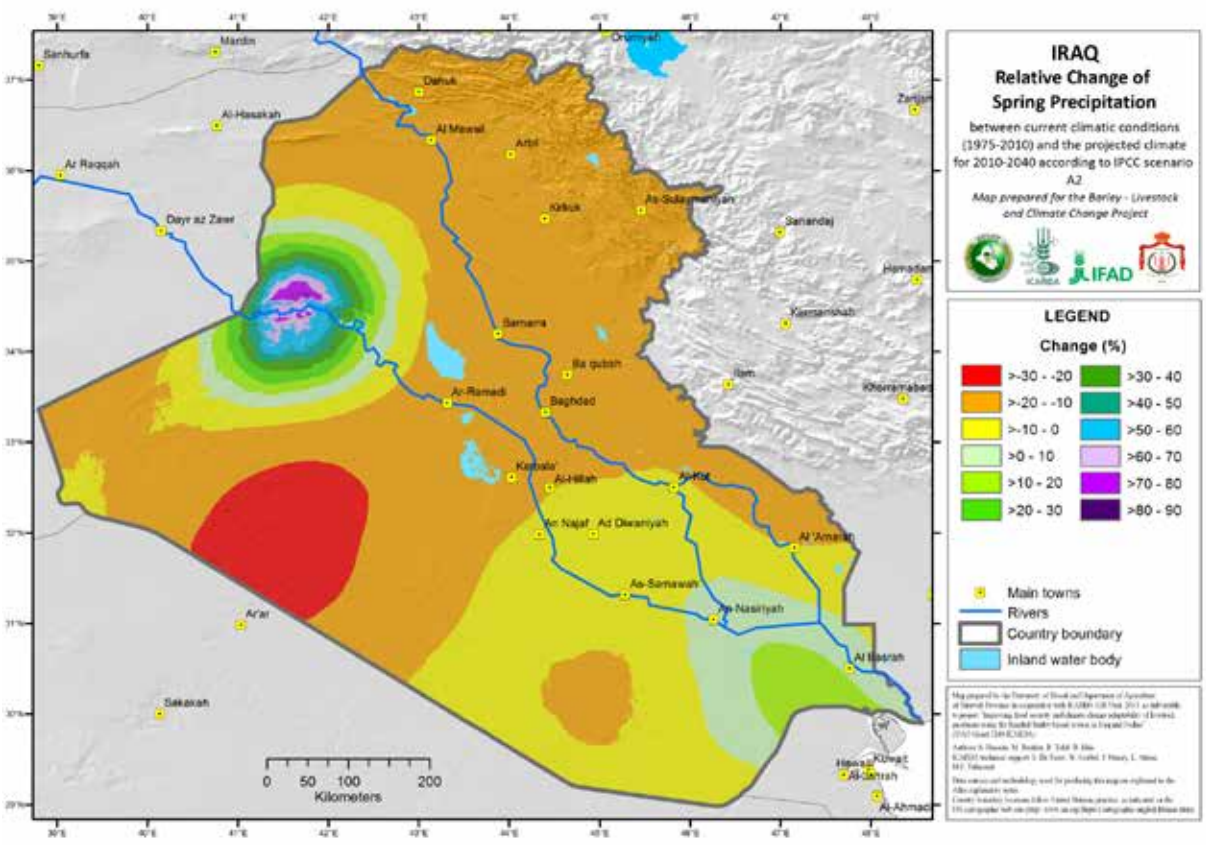
IRAQ
Relative Change of
Spring Precipitation
between current climatic conditions
(1975-2010) and the projected climate
for 2010-2040 according to IPCC scenario
A2
Map prepared for the Barley - Livestock
and Climate Change Project
IFAD
LEGEND
Change (%)
>-30 - -20
>-20 - -10
>-10 - 0
>0 - 10
>10 - 20
>20 - 30
>30 - 40
>40 - 50
>50 - 60
>60 - 70
>70 - 80
>80 - 90
Main towns
Rivers
Country boundary
Inland water body
0 50 100 200
Kilometers
Sanhurfa
Mardin
Dahuk
Al-Hasakah
Ar Raqqah
Al Mawsil
Arbil
Kirkuk
As-Sulaymaniyah
Dayr az Zawr
Sanandaj
Hamadan
Kermanshah
Samarra
Ba qubah
Ilam
Khorramabad
Ar-Ramadi
Baghdad
Karbala'
Al-Hillah
Al-Kut
An Najaf
Ad Diwaniyah
Al 'Amarah
As-Samawah
An Nasiriyah
Ar'ar
Al Basrah
Sakakah
Hafar al-Batin
Al-Jahrah
Al-Ahmadi

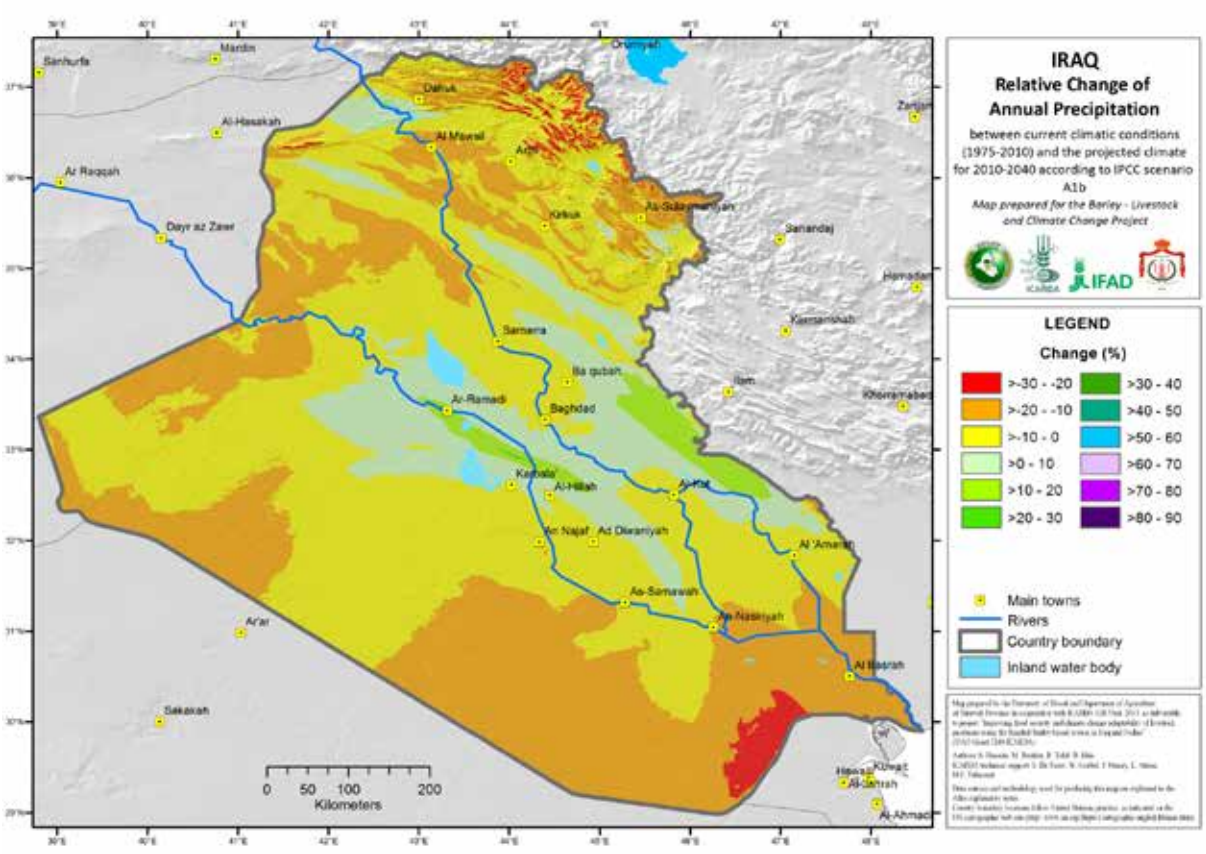
IRAQ
Relative Change of
Annual Precipitation
between current climatic conditions
(1975-2010) and the projected climate
for 2010-2040 according to IPCC scenario
A1b
Map prepared for the Barley - Livestock
and Climate Change Project
IFAD
LEGEND
Change (%)
>-30 - -20
>-20 - -10
>-10 - 0
>0 - 10
>10 - 20
>20 - 30
>30 - 40
>40 - 50
>50 - 60
>60 - 70
>70 - 80
>80 - 90
Main towns
Rivers
Country boundary
Inland water body
0 50 100 200
Kilometers
Sanhurfa
Mardin
Dahuk
Al-Hasakah
Al Mawsil
Arbil
Ar Raqqah
Kirkuk
As-Sulaymaniyah
Dayr az Zawr
Sanandaj
Hamadan
Kermanshah
Samarra
Ba`qubah
Ilam
Khorramabad
Ar-Ramadi
Baghdad
Karbala'
Al-Hillah
Al-Kut
An Najaf
Ad Diwaniyah
Al 'Amarah
As-Samawah
An Nasiriyah
Ar'ar
Al Basrah
Sakakah
Kuwait
Hafar al-Batin
Al-Ahmadi

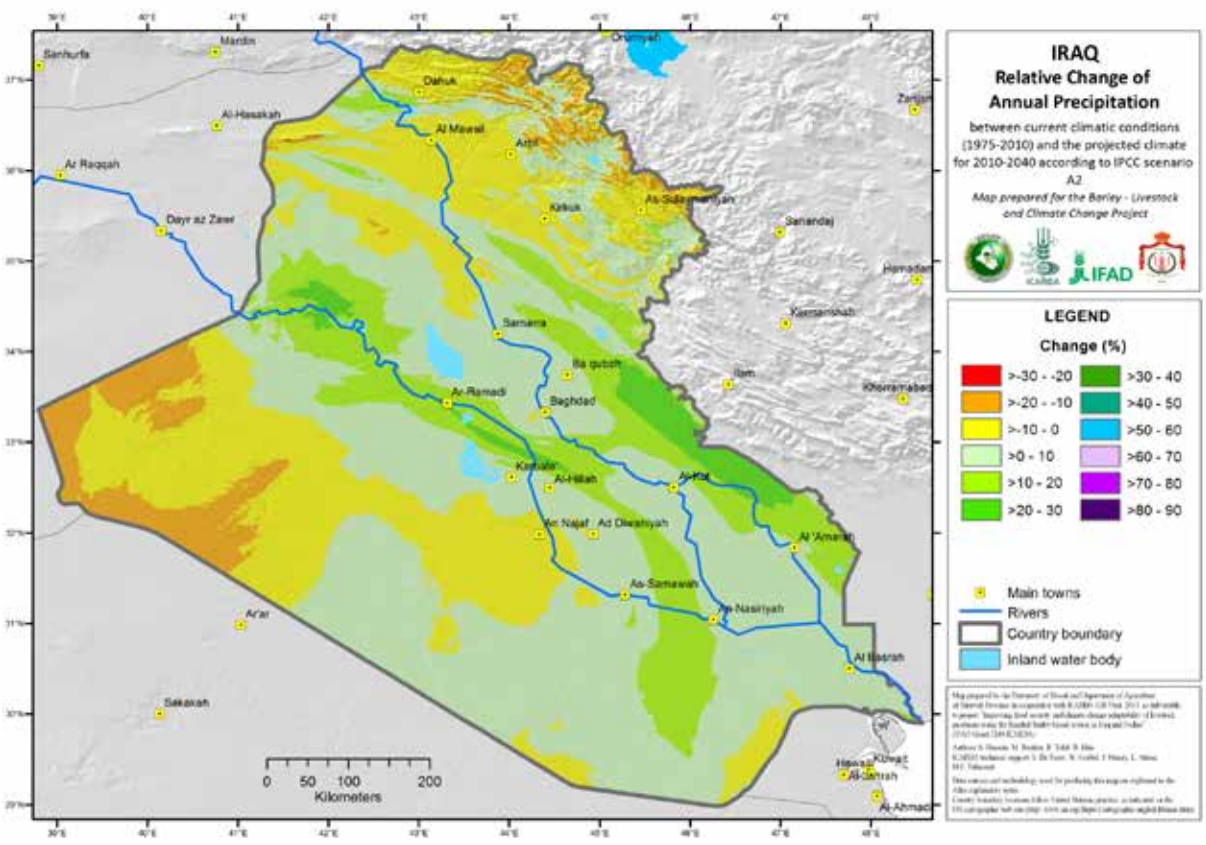
IRAQ
Relative Change of
Annual Precipitation
between current climatic conditions
(1975-2010) and the projected climate
for 2010-2040 according to IPCC scenario
A2
Map prepared for the Barley - Livestock
and Climate Change Project
IFAD
LEGEND
Change (%)
>-30 - -20
>-20 - -10
>-10 - 0
>0 - 10
>10 - 20
>20 - 30
>30 - 40
>40 - 50
>50 - 60
>60 - 70
>70 - 80
>80 - 90
Main towns
Rivers
Country boundary
Inland water body
0 50 100 200
Kilometers
Sanhurfa
Mardin
Dahuk
Al-Hasakah
Al Mawsil
Arbil
Ar Raqqah
Kirkuk
As-Sulaymaniyah
Dayr az Zawr
Sanandaj
Hamadan
Kermanshah
Samarra
Ba`qubah
Ilam
Khorramabad
Ar-Ramadi
Baghdad
Karbala'
Al-Hillah
Al-Kut
An Najaf
Ad Diwaniyah
Al 'Amarah
As-Samawah
An Nasiriyah
Ar'ar
Al Basrah
Sakakah
Kuwait
Hafar al-Batin
Al-Ahmadi

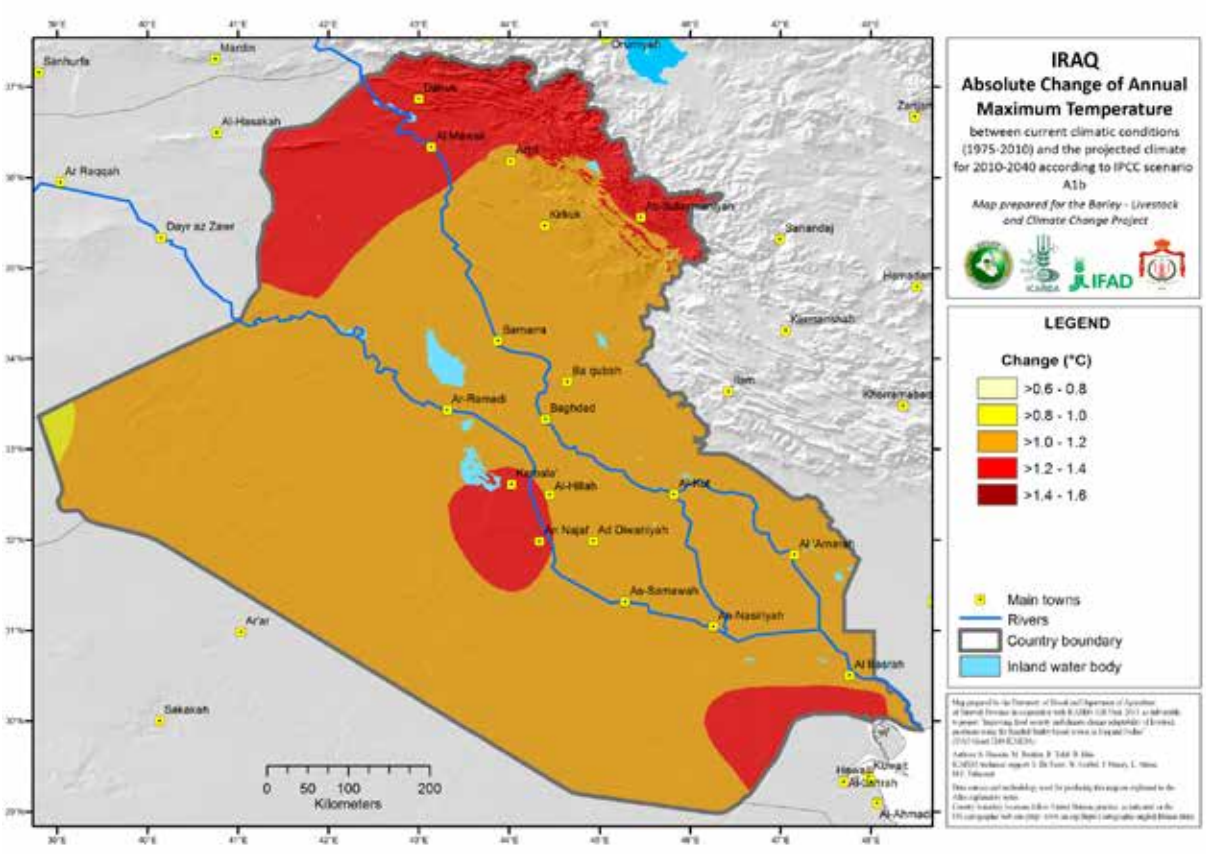
IRAQ
Absolute Change of Annual Maximum Temperature
between current climatic conditions (1975-2010) and the projected climate for 2010-2040 according to IPCC scenario A1b
Map prepared for the Barley - Livestock and Climate Change Project
IFAD
LEGEND
Change (°C)
>0.6 - 0.8
>0.8 - 1.0
>1.0 - 1.2
>1.2 - 1.4
>1.4 - 1.6
Main towns
Rivers
Country boundary
Inland water body
0 50 100 200
Kilometers
Sanhurfa
Mardin
Dahuk
Al-Hasakah
Al Mawsil
Arbil
Ar Raqqah
Kirkuk
Dayr az Zawr
Sanandaj
Hamadan
Kermanshah
Samarra
Ba qubah
Ilam
Khorramabad
Ar-Ramadi
Baghdad
Karbala'
Al-Hillah
Al-Kut
An Najaf
Ad Diwaniyah
Al 'Amarah
As-Samawah
An Nasiriyah
Ar'ar
Al Basrah
Sakakah
Hafar Al-batin
Kuwait
Al-Ahmadi

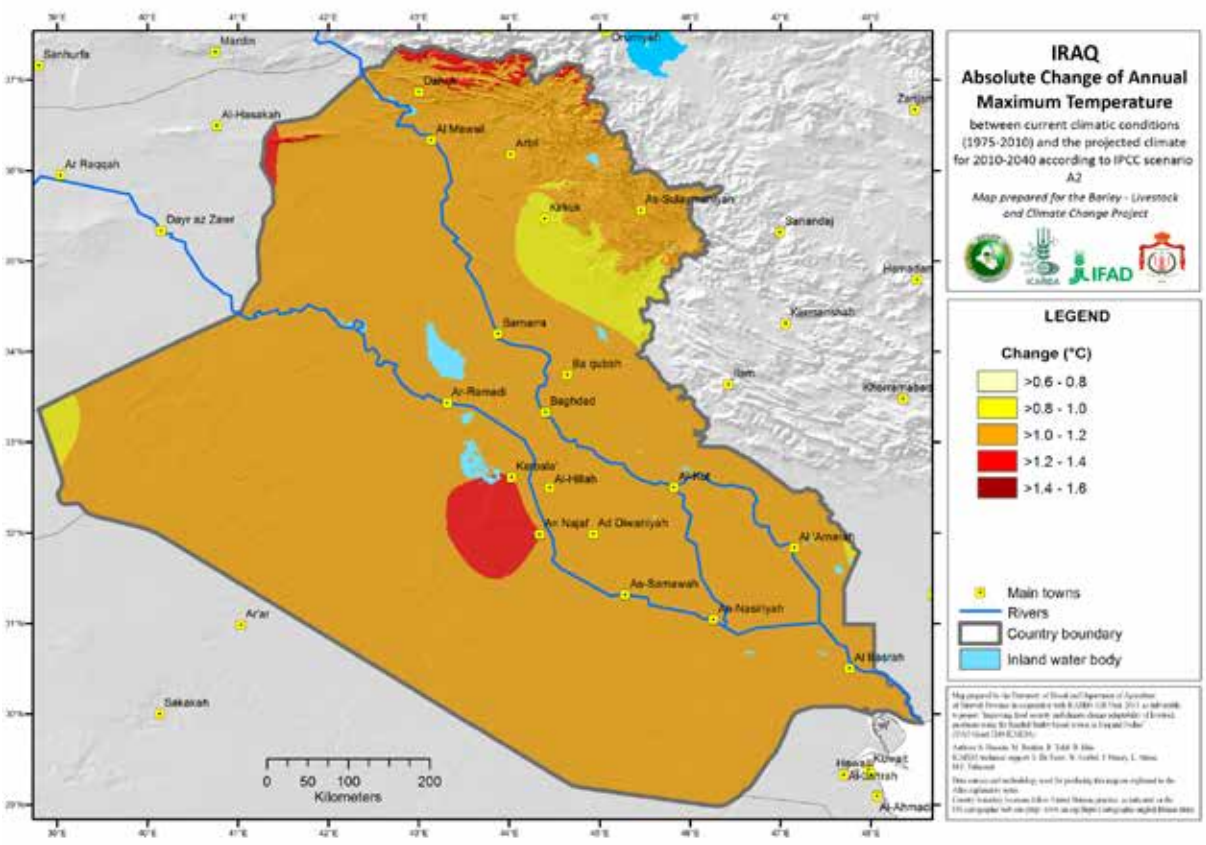
IRAQ
Absolute Change of Annual Maximum Temperature
between current climatic conditions (1975-2010) and the projected climate for 2010-2040 according to IPCC scenario A2
Map prepared for the Barley - Livestock and Climate Change Project
IFAD
LEGEND
Change (°C)
>0.6 - 0.8
>0.8 - 1.0
>1.0 - 1.2
>1.2 - 1.4
>1.4 - 1.6
Main towns
Rivers
Country boundary
Inland water body
0 50 100 200
Kilometers
Sanhurfa
Mardin
Dahuk
Al-Hasakah
Al Mawsil
Arbil
Ar Raqqah
Kirkuk
Dayr az Zawr
Sanandaj
Hamadan
Kermanshah
Samarra
Ba qubah
Ilam
Khorramabad
Ar-Ramadi
Baghdad
Karbala'
Al-Hillah
Al-Kut
An Najaf
Ad Diwaniyah
Al 'Amarah
As-Samawah
An Nasiriyah
Ar'ar
Al Basrah
Sakakah
Hafar Al-batin
Kuwait
Al-Ahmadi

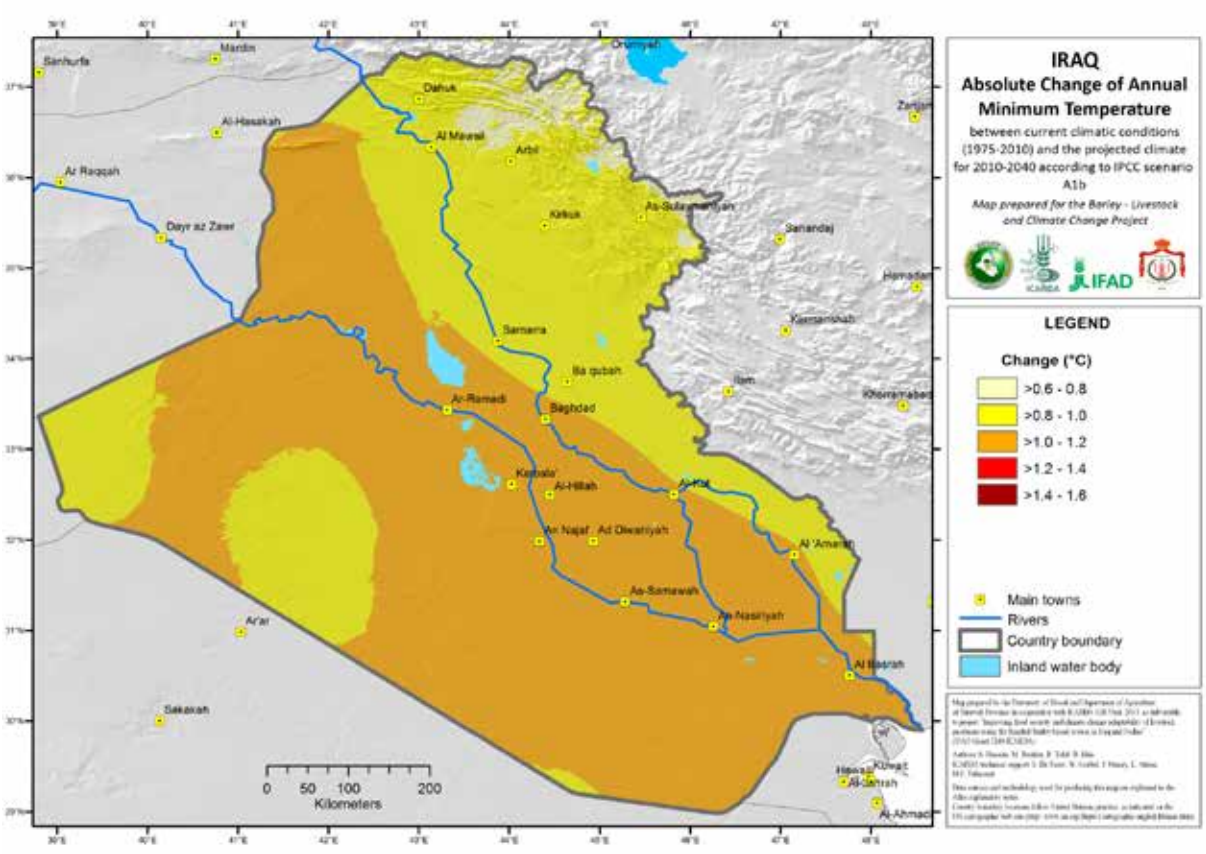
IRAQ
Absolute Change of Annual Minimum Temperature
between current climatic conditions (1975-2010) and the projected climate for 2010-2040 according to IPCC scenario A1b
Map prepared for the Barley - Livestock and Climate Change Project
IFAD
LEGEND
Change (°C)
>0.6 - 0.8
>0.8 - 1.0
>1.0 - 1.2
>1.2 - 1.4
>1.4 - 1.6
Main towns
Rivers
Country boundary
Inland water body
0 50 100 200
Kilometers
Sanhurfa
Mardin
Dahuk
Al-Hasakah
Al Mawsil
Arbil
Ar Raqqah
Kirkuk
Dayr az Zawr
Sanandaj
Hamadan
Kermanshah
Samarra
Ba qubah
Ilam
Khorramabad
Ar-Ramadi
Baghdad
Karbala'
Al-Hillah
Al-Kut
An Najaf
Ad Diwaniyah
Al 'Amarah
As-Samawah
An Nasiriyah
Ar'ar
Al Basrah
Sakakah
Al-Jahrah
Al-Ahmadi

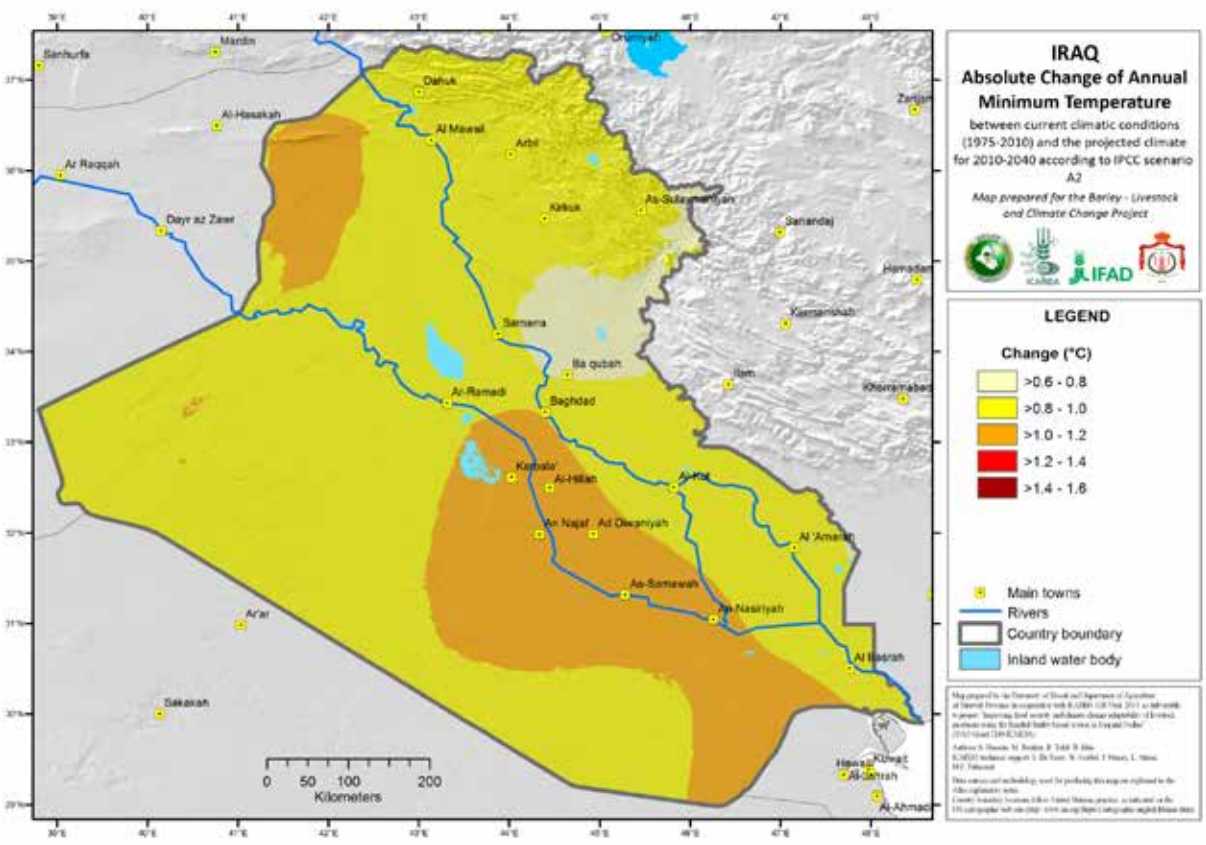
IRAQ
Absolute Change of Annual Minimum Temperature
between current climatic conditions (1975-2010) and the projected climate for 2010-2040 according to IPCC scenario A2
Map prepared for the Barley - Livestock and Climate Change Project
IFAD
LEGEND
Change (°C)
>0.6 - 0.8
>0.8 - 1.0
>1.0 - 1.2
>1.2 - 1.4
>1.4 - 1.6
Main towns
Rivers
Country boundary
Inland water body
0 50 100 200
Kilometers
Sanhurfa
Mardin
Dahuk
Al-Hasakah
Al Mawsil
Arbil
Ar Raqqah
Kirkuk
Dayr az Zawr
Sanandaj
Hamadan
Kermanshah
Samarra
Ba qubah
Ilam
Khorramabad
Ar-Ramadi
Baghdad
Karbala'
Al-Hillah
Al-Kut
An Najaf
Ad Diwaniyah
Al 'Amarah
As-Samawah
An Nasiriyah
Ar'ar
Al Basrah
Sakakah
Al-Jahrah
Al-Ahmadi

IRAQ

Absolute Change in Maximum Temperature between current climate (1975-2010) and the projected climate for 2010-2040

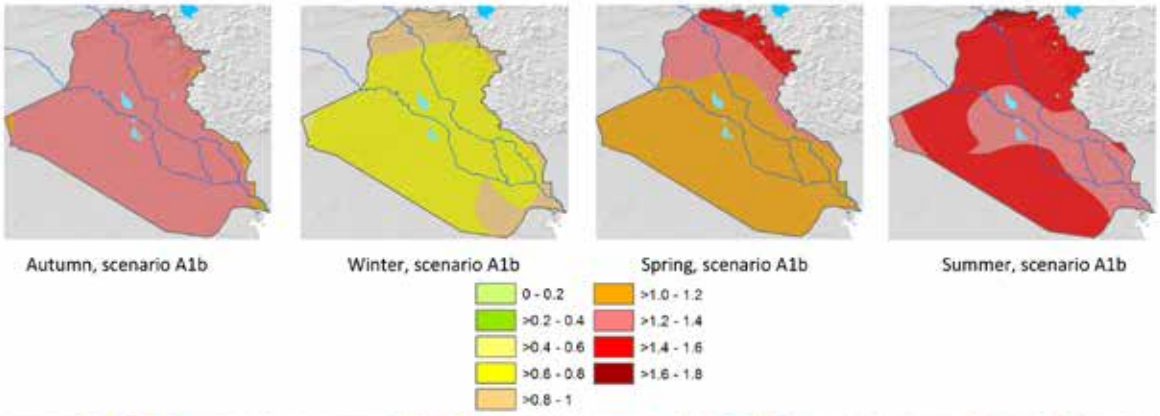

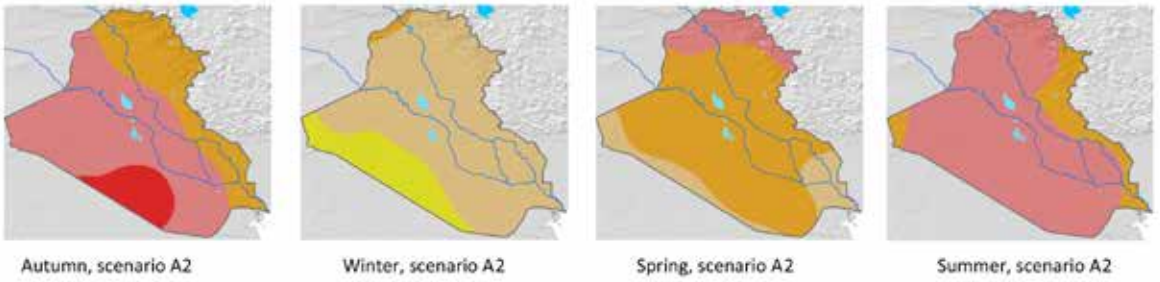

IRAQ

Absolute Change in Minimum Temperature between current climate (1975-2010) and the projected climate for 2010-2040

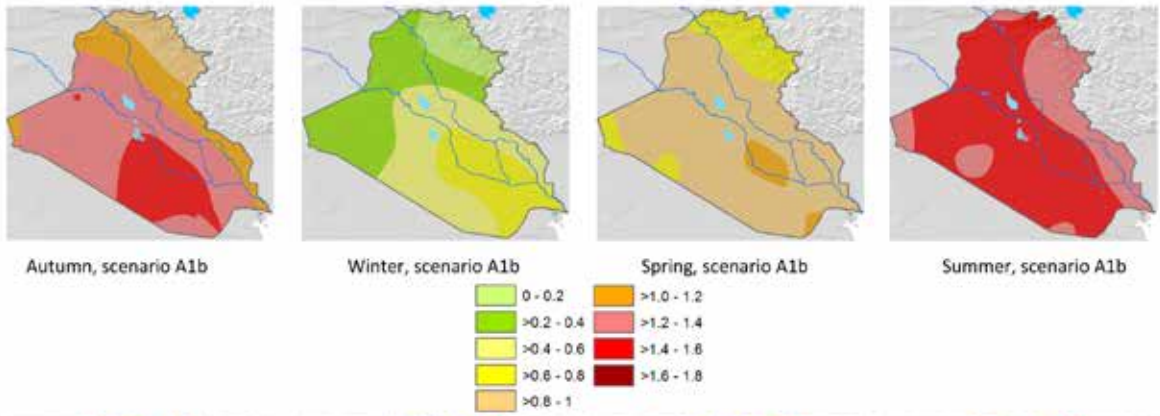

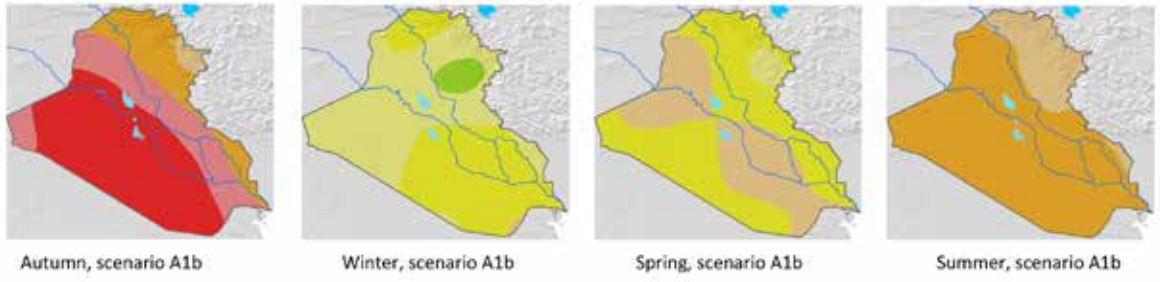

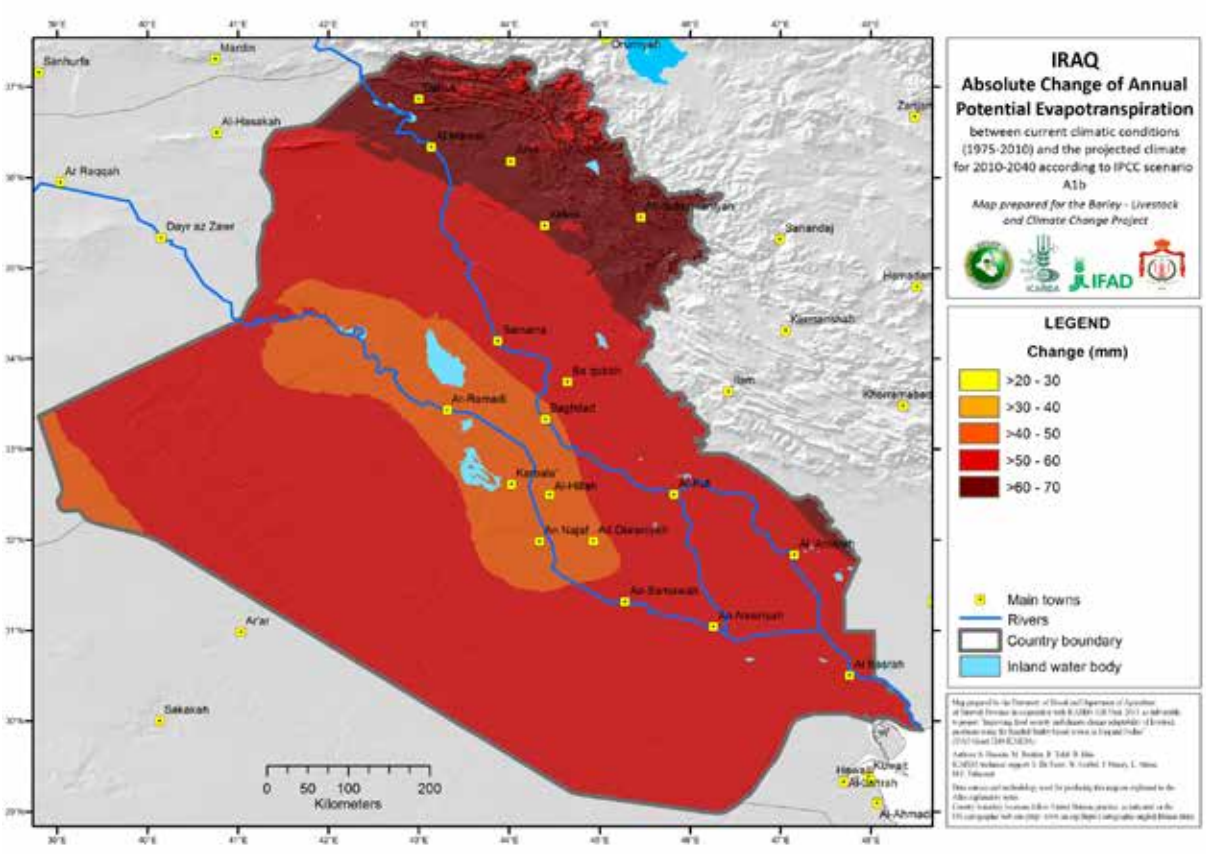
IRAQ
Absolute Change of Annual Potential Evapotranspiration
between current climatic conditions (1975-2010) and the projected climate for 2010-2040 according to IPCC scenario A1b
Map prepared for the Barley - Livestock and Climate Change Project
IFAD
LEGEND
Change (mm)
>20 - 30
>30 - 40
>40 - 50
>50 - 60
>60 - 70
Main towns
Rivers
Country boundary
Inland water body
0 50 100 200
Kilometers
Sanhurfa
Mardin
Al-Hasakah
Ar Raqqah
Deyr az Zawr
Sanandaj
Hamadan
Kermanshah
Ilam
Khorramabad
Samarra
Ba`qubah
Ar-Ramadi
Baghdad
Karbala
Al-Hillah
Al Kut
An Najaf
Ad Diwaniyah
Al Amarah
As Samawah
Al Basrah
Ar'ar
Sakakah
Kuwait
Al-Jahrah
Al Ahmadi

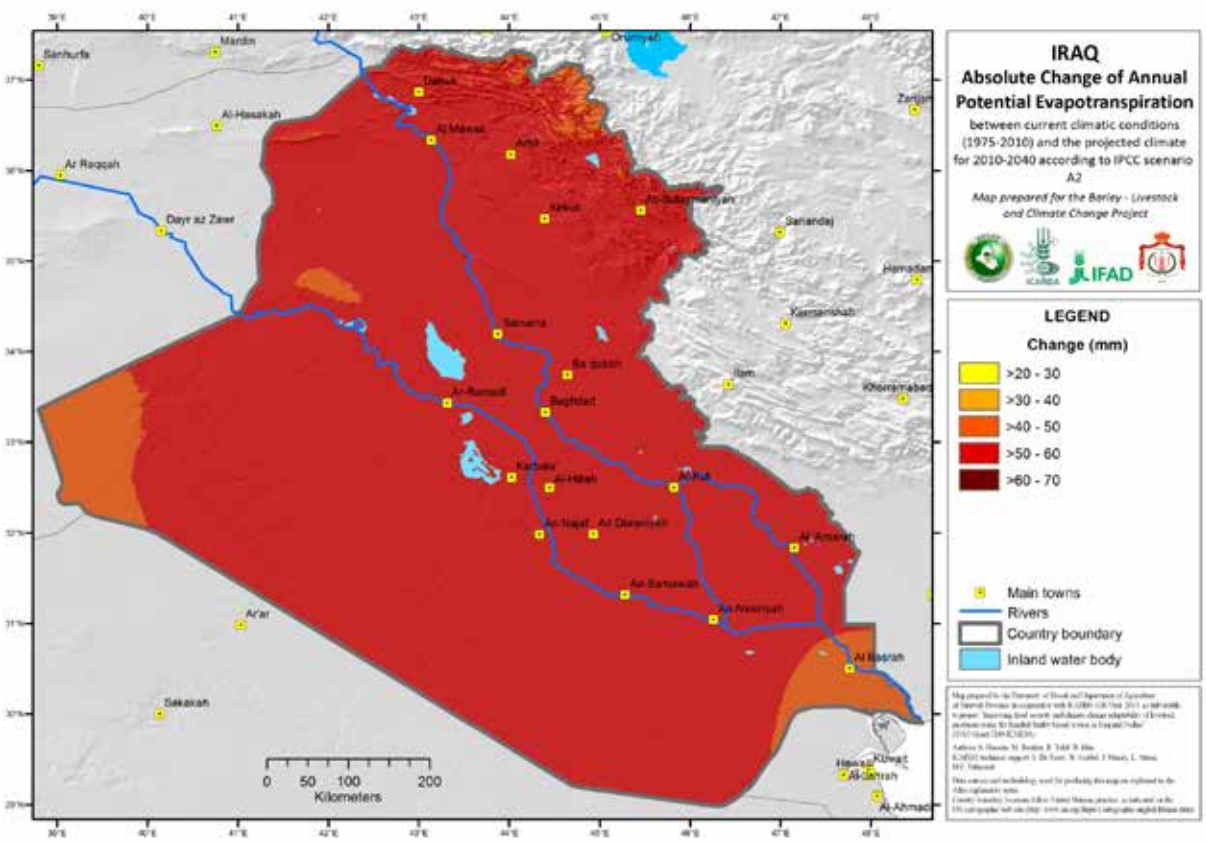
IRAQ
Absolute Change of Annual Potential Evapotranspiration
between current climatic conditions (1975-2010) and the projected climate for 2010-2040 according to IPCC scenario A2
Map prepared for the Barley - Livestock and Climate Change Project
IFAD
LEGEND
Change (mm)
>20 - 30
>30 - 40
>40 - 50
>50 - 60
>60 - 70
Main towns
Rivers
Country boundary
Inland water body
0 50 100 200
Kilometers
Sanhurfa
Mardin
Al-Hasakah
Ar Raqqah
Deyr az Zawr
Sanandaj
Hamadan
Kermanshah
Ilam
Khorramabad
Samarra
Ba`qubah
Ar-Ramadi
Baghdad
Karbala
Al-Hillah
Al Kut
An Najaf
Ad Diwaniyah
Al Amarah
As Samawah
Al Basrah
Ar'ar
Sakakah
Kuwait
Al-Jahrah
Al Ahmadi

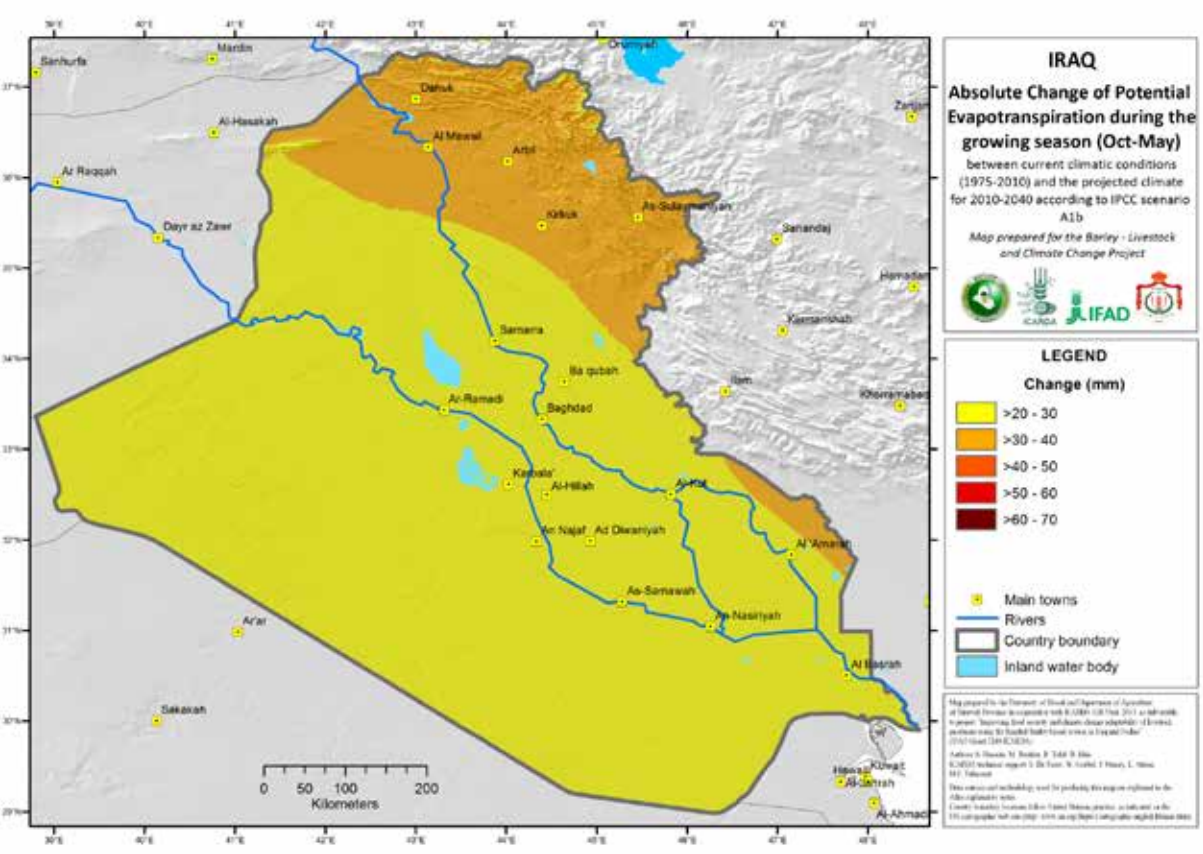
IRAQ
Absolute Change of Potential Evapotranspiration during the growing season (Oct-May)
between current climatic conditions (1975-2010) and the projected climate for 2010-2040 according to IPCC scenario A1b
Map prepared for the Barley - Livestock and Climate Change Project
ICARDA
IFAD
LEGEND
Change (mm)
>20 - 30
>30 - 40
>40 - 50
>50 - 60
>60 - 70
Main towns
Rivers
Country boundary
Inland water body
Sanliurfa
Mardin
Dahuk
Al-Hasakah
Ar Raqqah
Al Mawsil
Arbil
Kirkuk
As-Sulaymaniyah
Dayr az Zawr
Sanandaj
Hamadan
Kermanshah
Samarra
Ba qubah
Ilam
Khorramabad
Ar-Ramadi
Baghdad
Karbala'
Al-Hillah
Al-Kut
An Najaf
Ad Diwaniyah
Al 'Amarah
As-Samawah
An Nasiriyah
Ar'ar
Al Basrah
Sakakah
Hafar al-Batin
Kuwait
Al-Jahrah
Al-Ahmadi
0 50 100 200
Kilometers

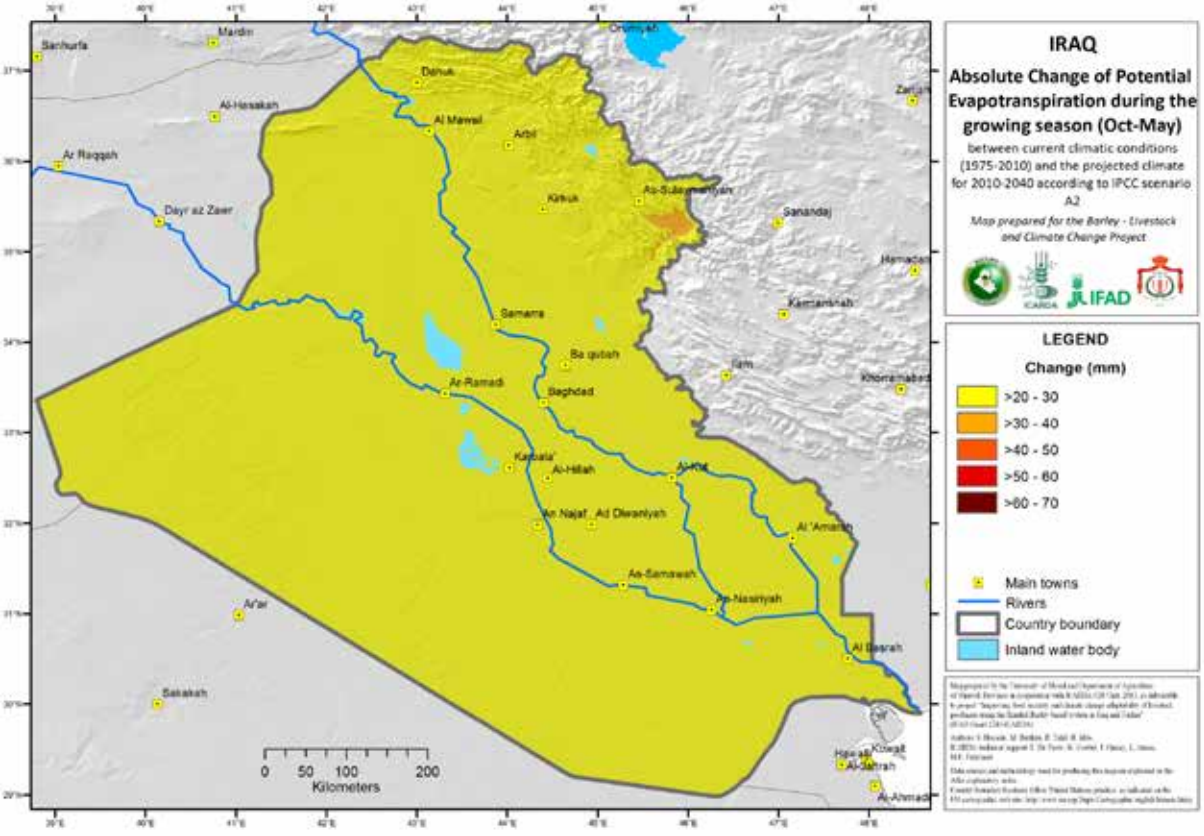
IRAQ
Absolute Change of Potential Evapotranspiration during the growing season (Oct-May)
between current climatic conditions (1975-2010) and the projected climate for 2010-2040 according to IPCC scenario A2
Map prepared for the Barley - Livestock and Climate Change Project
ICARDA
IFAD
LEGEND
Change (mm)
>20 - 30
>30 - 40
>40 - 50
>50 - 60
>60 - 70
Main towns
Rivers
Country boundary
Inland water body
Sanliurfa
Mardin
Dahuk
Al-Hasakah
Ar Raqqah
Al Mawsil
Arbil
Kirkuk
As-Sulaymaniyah
Dayr az Zawr
Sanandaj
Hamadan
Kermanshah
Samarra
Ba qubah
Ilam
Khorramabad
Ar-Ramadi
Baghdad
Karbala'
Al-Hillah
Al-Kut
An Najaf
Ad Diwaniyah
Al 'Amarah
As-Samawah
An Nasiriyah
Ar'ar
Al Basrah
Sakakah
Hafar al-Batin
Kuwait
Al-Jahrah
Al-Ahmadi
0 50 100 200
Kilometers

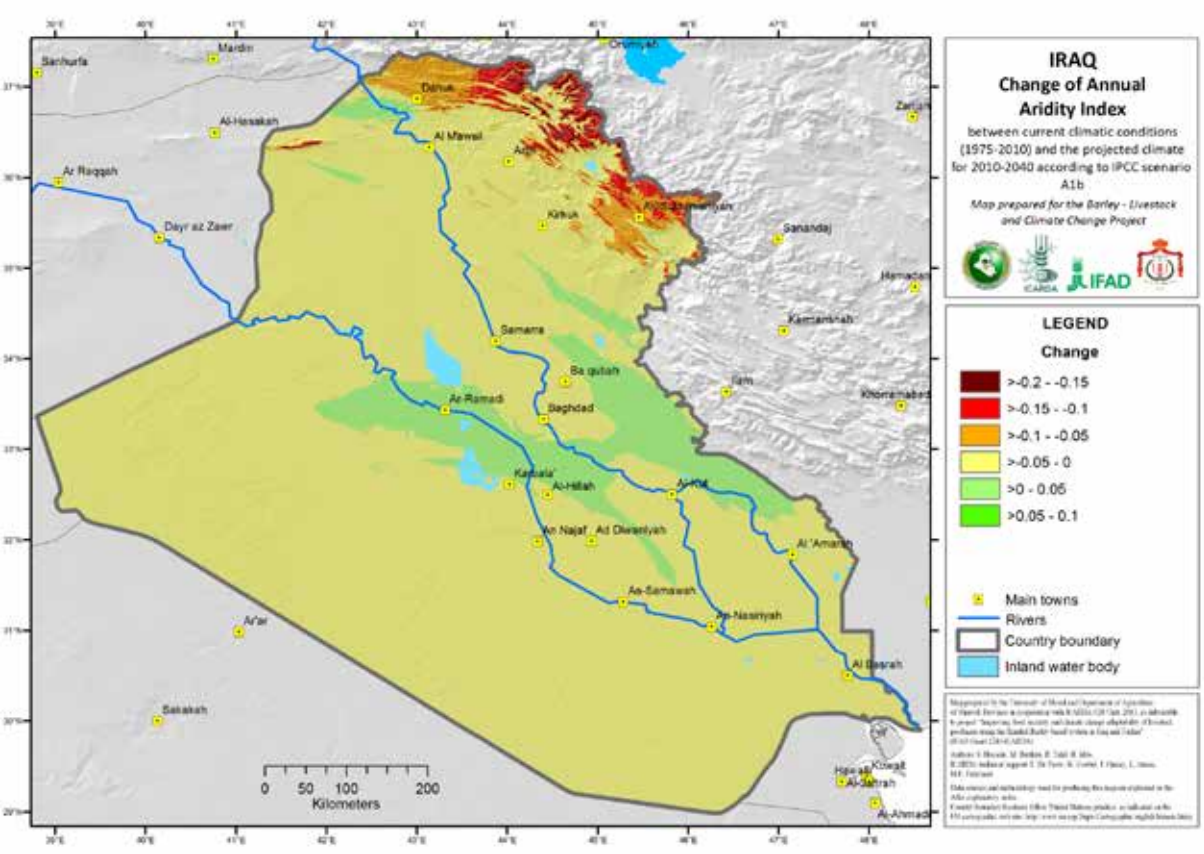
IRAQ
Change of Annual Aridity Index
between current climatic conditions (1975-2010) and the projected climate for 2010-2040 according to IPCC scenario A1b
Map prepared for the Barley - Livestock and Climate Change Project
LEGEND
Change
>-0.2 - -0.15
>-0.15 - -0.1
>-0.1 - -0.05
>-0.05 - 0
>0 - 0.05
>0.05 - 0.1
Main towns
Rivers
Country boundary
Inland water body
0 50 100 200
Kilometers
Sanliurfa
Mardin
Dohuk
Al-Hasakah
Ar Raqqah
Dayr az Zawr
Al Mawsil
Arbil
Kirkuk
Sulaymaniyah
Sanandaj
Hamadan
Kermanshah
Samarra
Ba qubah
Ilam
Khorramabad
Ar Ramadi
Baghdad
Karbala'
Al-Hillah
Al-Kut
An Najaf
Ad Diwaniyah
Al 'Amarah
As-Samawah
An-Nasiriyah
Al Basrah
Ar'ar
Sakakah
Hafar al-Batin
Al-Jahrah
Al-Ahmadi

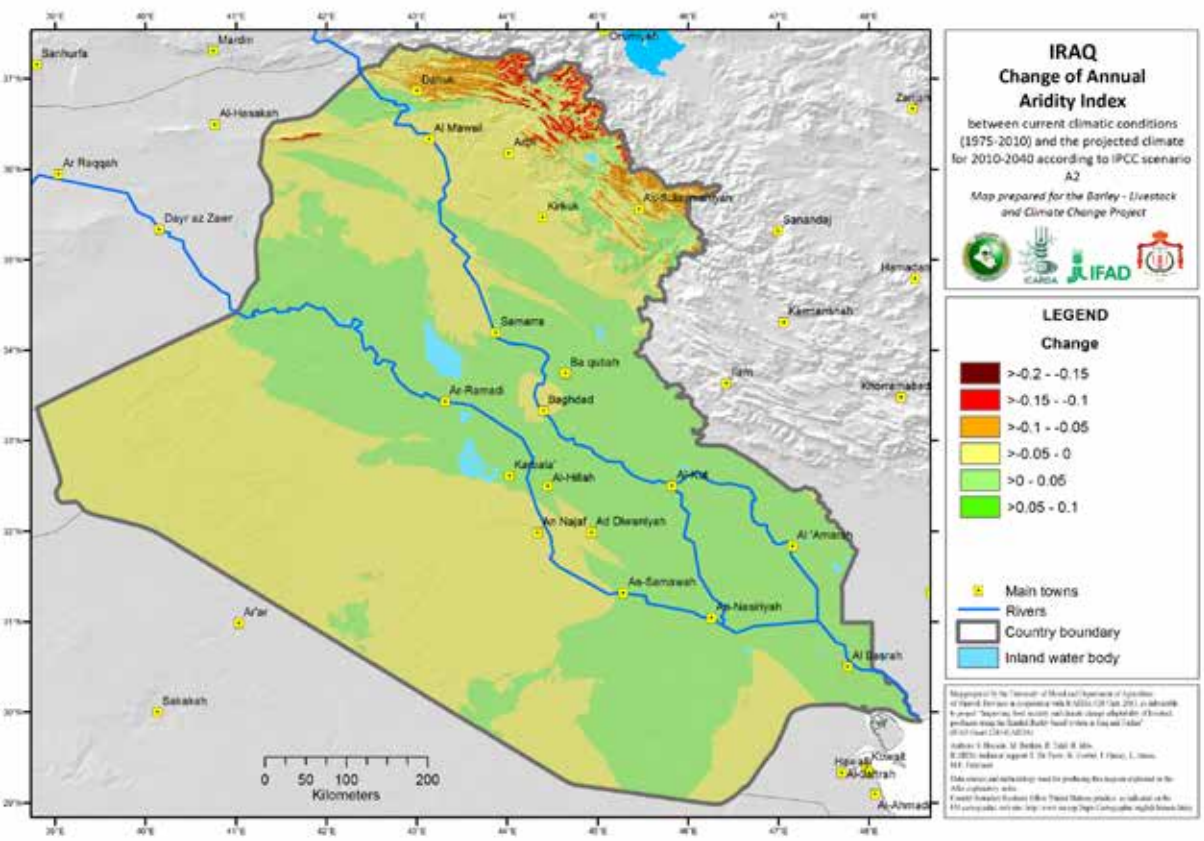
IRAQ
Change of Annual Aridity Index
between current climatic conditions (1975-2010) and the projected climate for 2010-2040 according to IPCC scenario A2
Map prepared for the Barley - Livestock and Climate Change Project
LEGEND
Change
>-0.2 - -0.15
>-0.15 - -0.1
>-0.1 - -0.05
>-0.05 - 0
>0 - 0.05
>0.05 - 0.1
Main towns
Rivers
Country boundary
Inland water body
0 50 100 200
Kilometers
Sanliurfa
Mardin
Dohuk
Al-Hasakah
Ar Raqqah
Dayr az Zawr
Al Mawsil
Arbil
Kirkuk
Sulaymaniyah
Sanandaj
Hamadan
Kermanshah
Samarra
Ba qubah
Ilam
Khorramabad
Ar Ramadi
Baghdad
Karbala'
Al-Hillah
Al-Kut
An Najaf
Ad Diwaniyah
Al 'Amarah
As-Samawah
An-Nasiriyah
Al Basrah
Ar'ar
Sakakah
Hafar al-Batin
Al-Jahrah
Al-Ahmadi

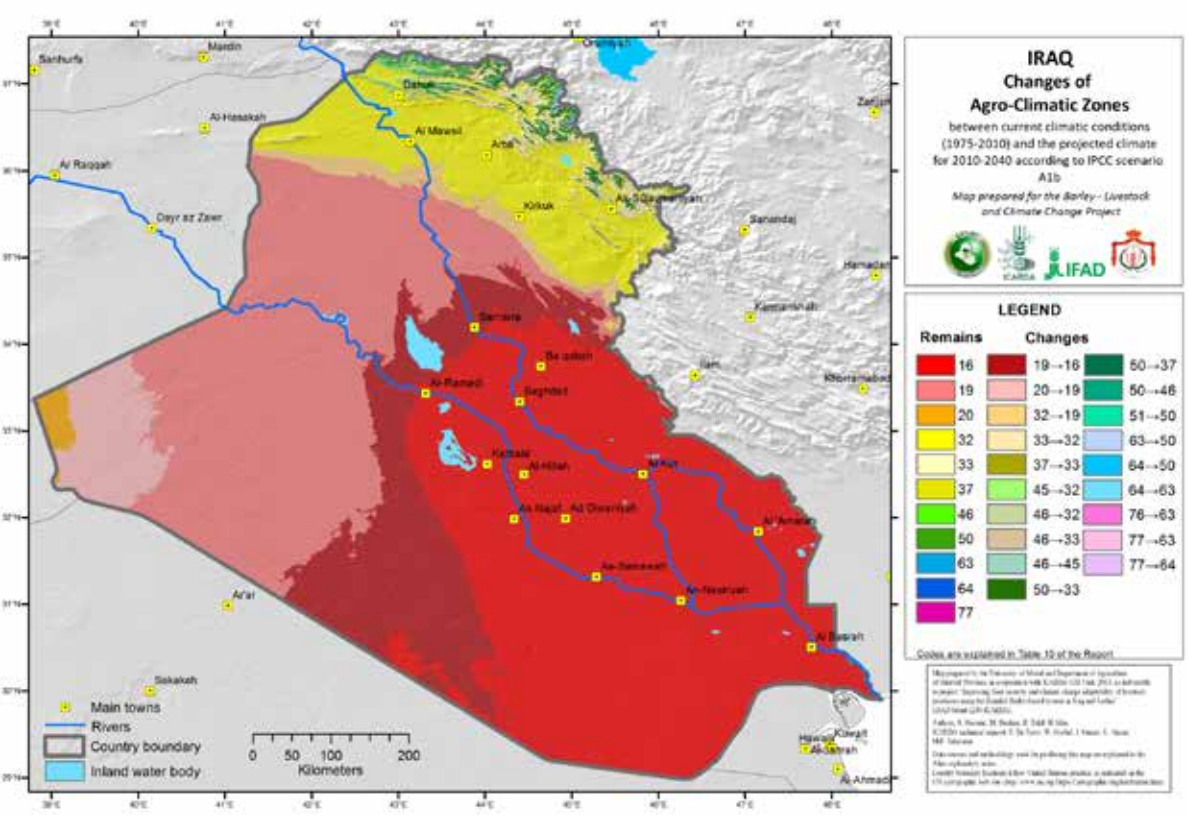
IRAQ
Changes of
Agro-Climatic Zones
between current climatic conditions
(1975-2010) and the projected climate
for 2010-2040 according to IPCC scenario
A1b
Map prepared for the Barley - Livestock
and Climate Change Project
LEGEND
Remains
Changes
16
19
20
32
33
37
46
50
63
64
77
19→16
20→19
32→19
33→32
37→33
45→32
46→32
46→33
46→45
50→33
50→37
50→46
51→50
63→50
64→50
64→63
76→63
77→63
77→64
Codes are explained in Table 10 of the Report
Main towns
Rivers
Country boundary
Inland water body
0 50 100 200
Kilometers

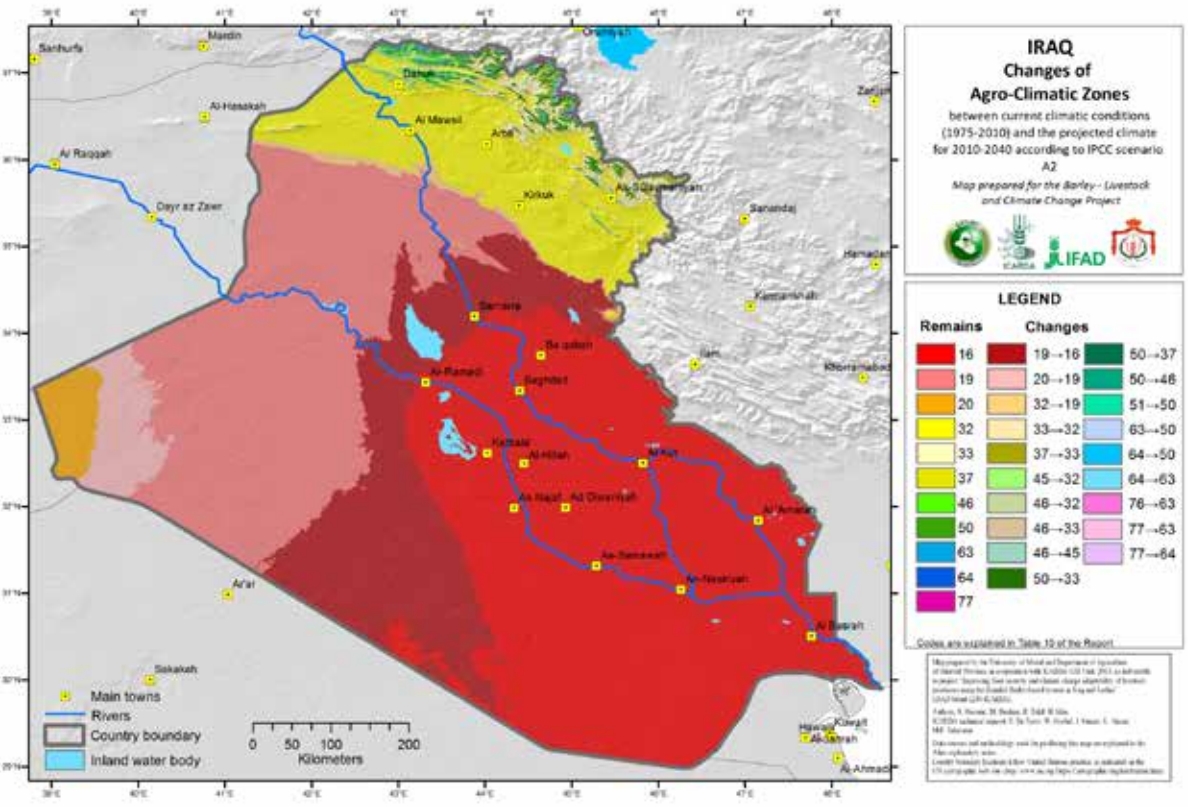
IRAQ
Changes of
Agro-Climatic Zones
between current climatic conditions
(1975-2010) and the projected climate
for 2010-2040 according to IPCC scenario
A2
Map prepared for the Barley - Livestock
and Climate Change Project
LEGEND
Remains
Changes
16
19
20
32
33
37
46
50
63
64
77
19→16
20→19
32→19
33→32
37→33
45→32
46→32
46→33
46→45
50→33
50→37
50→46
51→50
63→50
64→50
64→63
76→63
77→63
77→64
Codes are explained in Table 10 of the Report
Main towns
Rivers
Country boundary
Inland water body
0 50 100 200
Kilometers

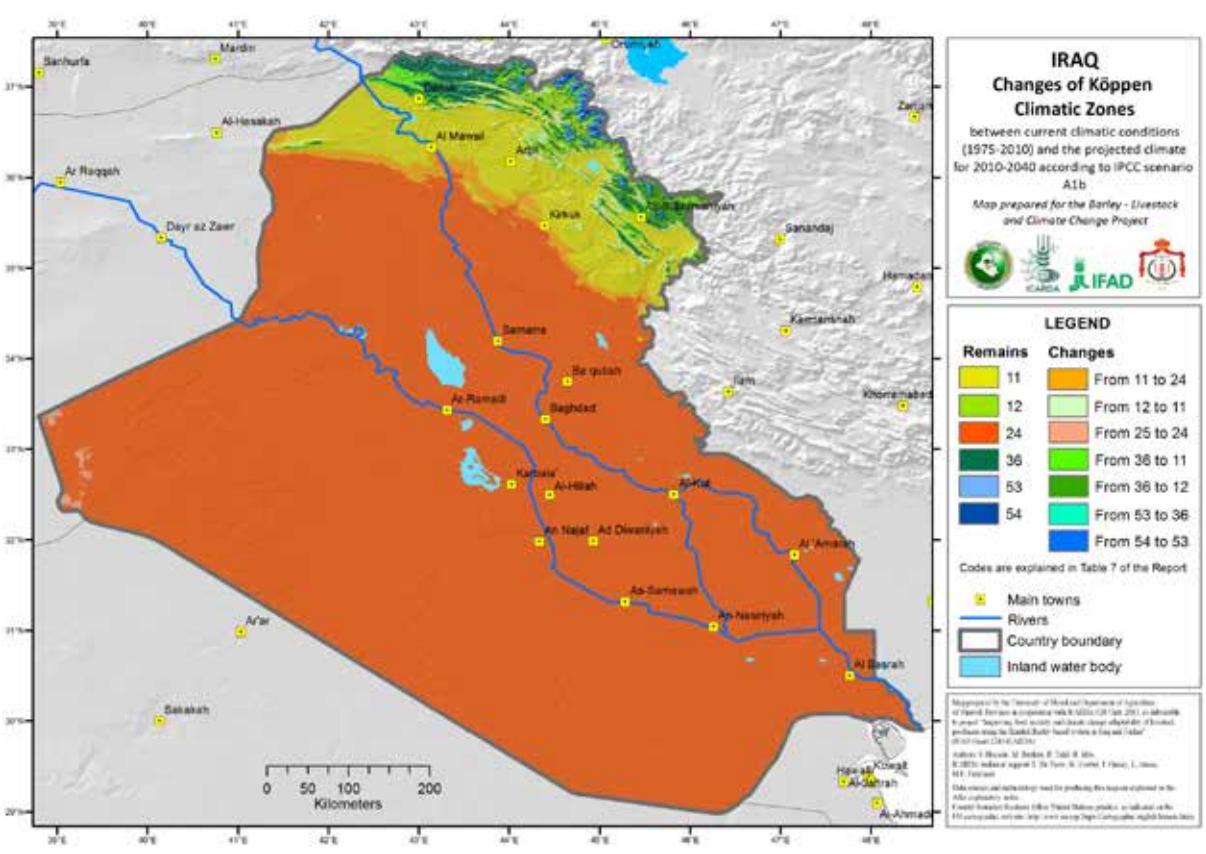
IRAQ
Changes of Köppen
Climatic Zones
between current climatic conditions
(1975-2010) and the projected climate
for 2010-2040 according to IPCC scenario
A1b
Map prepared for the Barley - Livestock
and Climate Change Project
LEGEND
Remains
11
12
24
36
53
54
Changes
From 11 to 24
From 12 to 11
From 25 to 24
From 36 to 11
From 36 to 12
From 53 to 36
From 54 to 53
Codes are explained in Table 7 of the Report
Main towns
Rivers
Country boundary
Inland water body
0 50 100 200
Kilometers

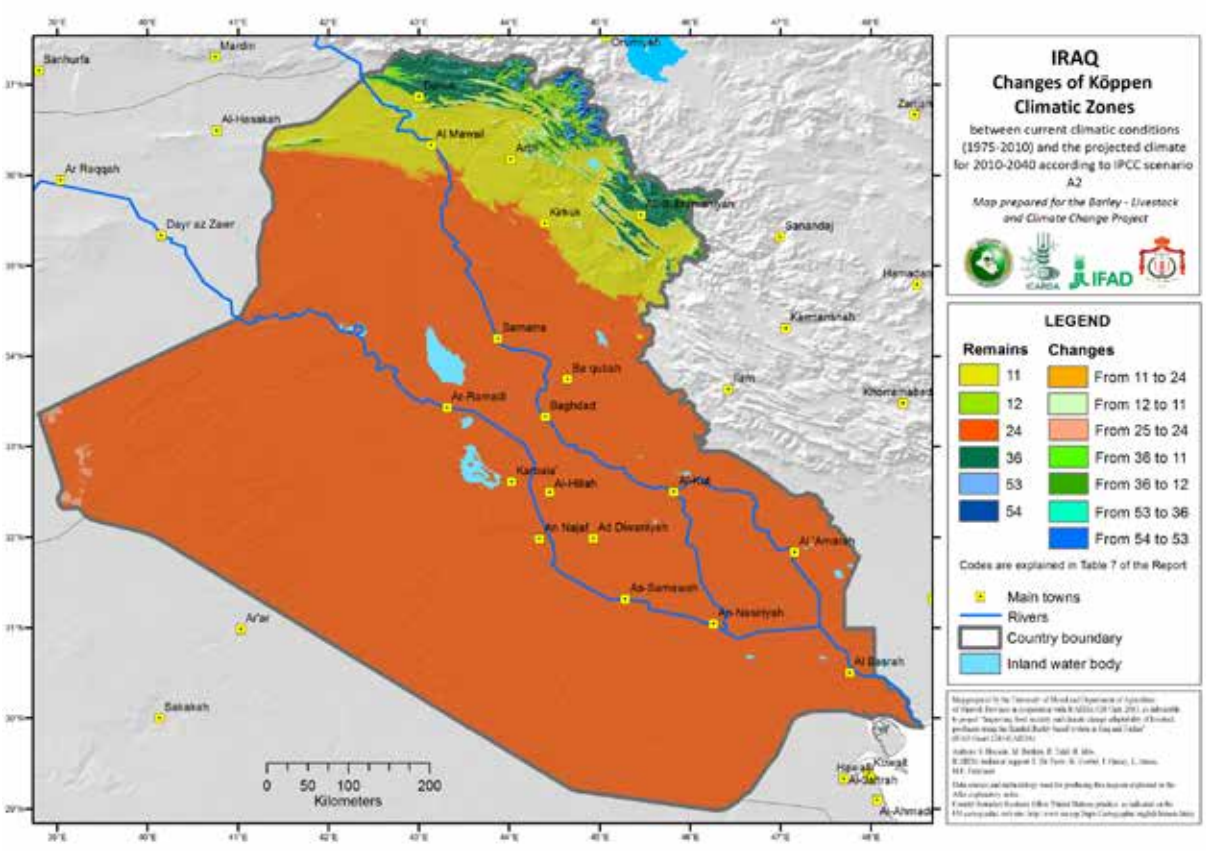
IRAQ
Changes of Köppen
Climatic Zones
between current climatic conditions
(1975-2010) and the projected climate
for 2010-2040 according to IPCC scenario
A2
Map prepared for the Barley - Livestock
and Climate Change Project
LEGEND
Remains
11
12
24
36
53
54
Changes
From 11 to 24
From 12 to 11
From 25 to 24
From 36 to 11
From 36 to 12
From 53 to 36
From 54 to 53
Codes are explained in Table 7 of the Report
Main towns
Rivers
Country boundary
Inland water body
0 50 100 200
Kilometers

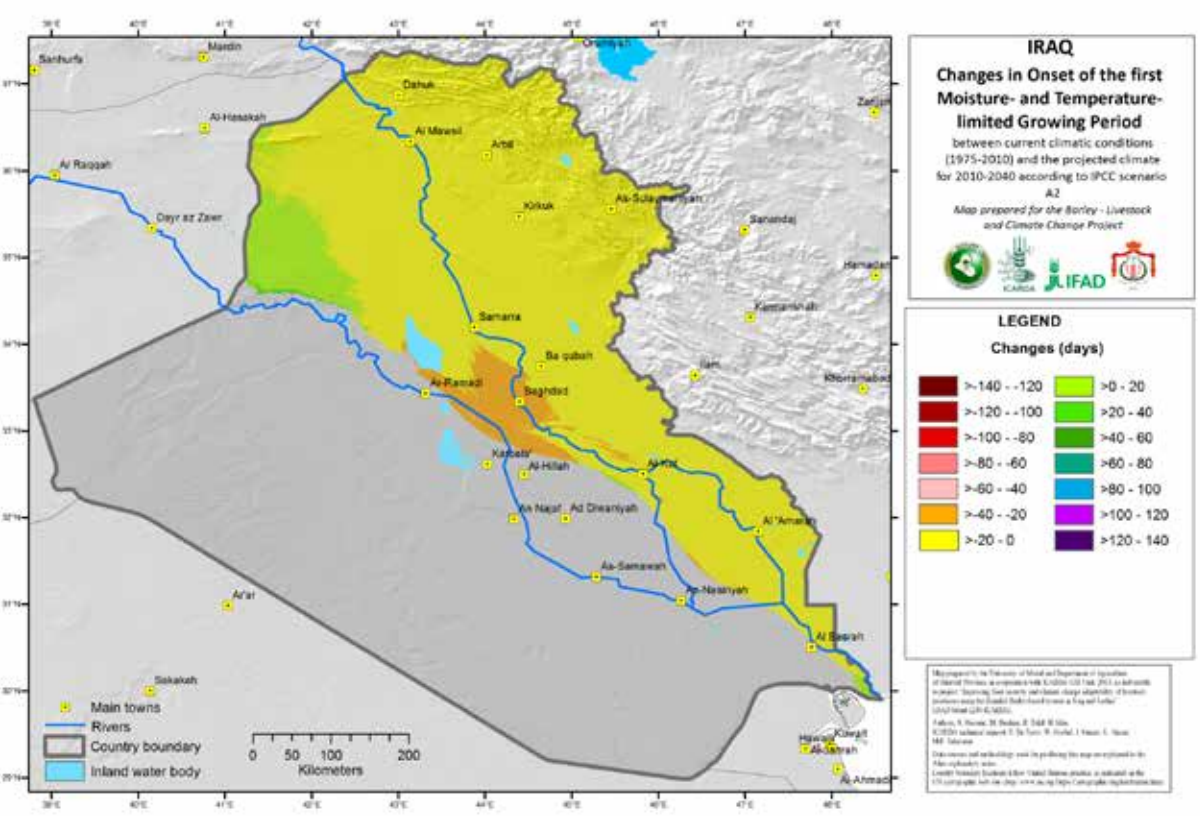
IRAQ
Changes in Onset of the first Moisture- and Temperature-limited Growing Period
between current climatic conditions (1975-2010) and the projected climate for 2010-2040 according to IPCC scenario A2
Map prepared for the Barley - Livestock and Climate Change Project
LEGEND
Changes (days)
>-140 - -120
>-120 - -100
>-100 - -80
>-80 - -60
>-60 - -40
>-40 - -20
>-20 - 0
>0 - 20
>20 - 40
>40 - 60
>60 - 80
>80 - 100
>100 - 120
>120 - 140
Main towns
Rivers
Country boundary
Inland water body
0 50 100 200
Kilometers
Sanhurfa
Mardin
Dahuk
Al-Hasakah
Al Mawsil
Arbil
Ar Raqqah
Dayr az Zawr
Kirkuk
As-Sulaymaniyah
Sanandaj
Hamadan
Kermanshah
Samarra
Ba`qubah
Ilam
Khorramabad
Ar-Ramadi
Baghdad
Karbala'
Al-Hillah
An Najaf
Ad Diwaniyah
Al 'Amarah
As-Samawah
An-Nasariyah
Al Basrah
Ar'ar
Sakakah
Hafar al Batin
Kuwait
Al-Jahrah
Al-Ahmadi

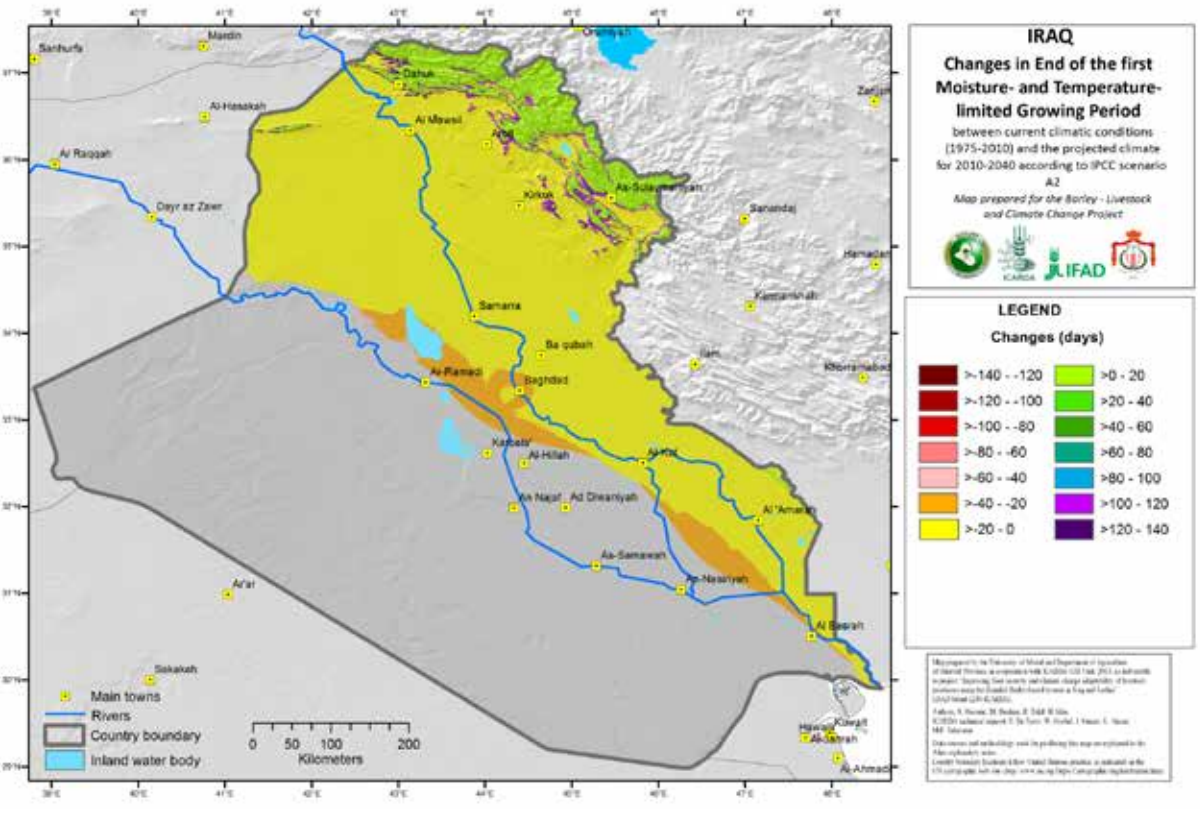
IRAQ
Changes in End of the first Moisture- and Temperature-limited Growing Period
between current climatic conditions (1975-2010) and the projected climate for 2010-2040 according to IPCC scenario A2
Map prepared for the Barley - Livestock and Climate Change Project
LEGEND
Changes (days)
>-140 - -120
>-120 - -100
>-100 - -80
>-80 - -60
>-60 - -40
>-40 - -20
>-20 - 0
>0 - 20
>20 - 40
>40 - 60
>60 - 80
>80 - 100
>100 - 120
>120 - 140
Main towns
Rivers
Country boundary
Inland water body
0 50 100 200
Kilometers
Sanhurfa
Mardin
Dahuk
Al-Hasakah
Al Mawsil
Arbil
Ar Raqqah
Dayr az Zawr
Kirkuk
As-Sulaymaniyah
Sanandaj
Hamadan
Kermanshah
Samarra
Ba`qubah
Ilam
Khorramabad
Ar-Ramadi
Baghdad
Karbala'
Al-Hillah
An Najaf
Ad Diwaniyah
Al 'Amarah
As-Samawah
An-Nasariyah
Al Basrah
Ar'ar
Sakakah
Hafar al Batin
Kuwait
Al-Jahrah
Al-Ahmadi

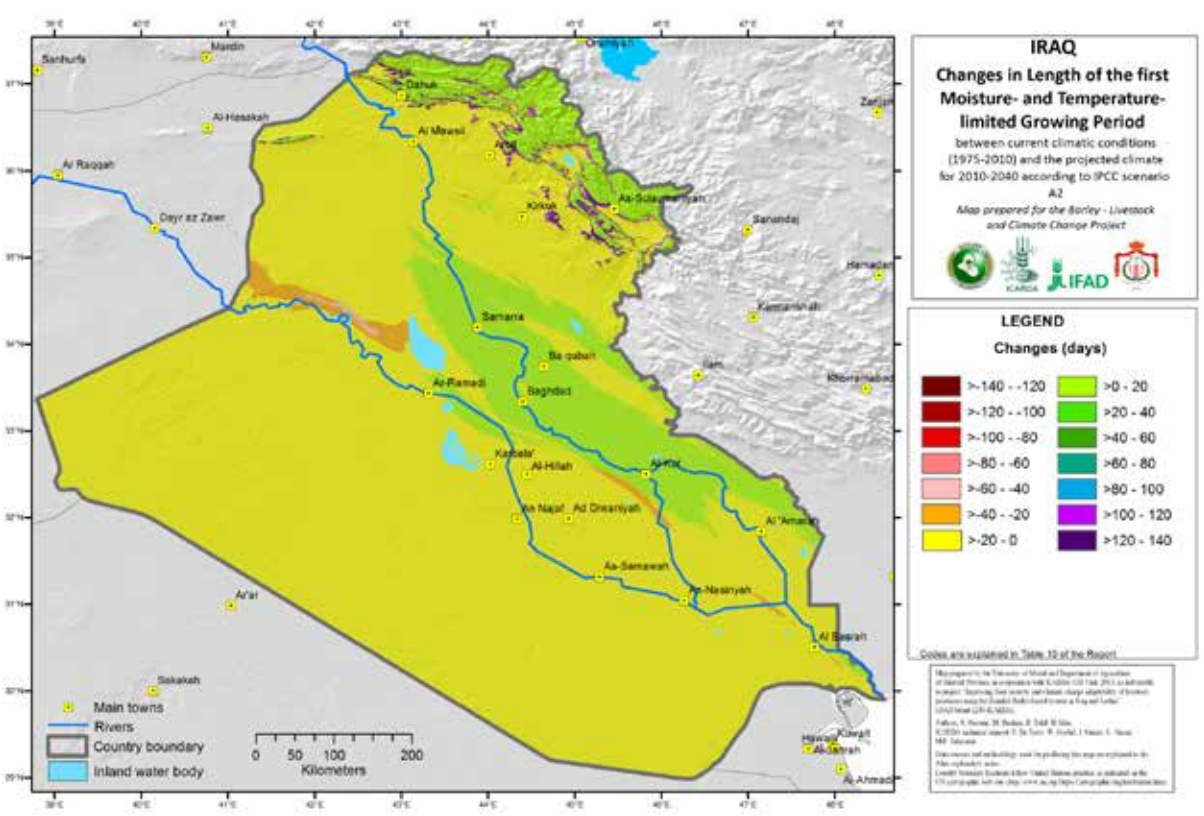
IRAQ
Changes in Length of the first Moisture- and Temperature-limited Growing Period
between current climatic conditions (1975-2010) and the projected climate for 2010-2040 according to IPCC scenario A2
Map prepared for the Barley - Livestock and Climate Change Project
LEGEND
Changes (days)
>-140 - -120
>-120 - -100
>-100 - -80
>-80 - -60
>-60 - -40
>-40 - -20
>-20 - 0
>0 - 20
>20 - 40
>40 - 60
>60 - 80
>80 - 100
>100 - 120
>120 - 140
Codes are explained in Table 10 of the Report
Main towns
Rivers
Country boundary
Inland water body
0 50 100 200
Kilometers

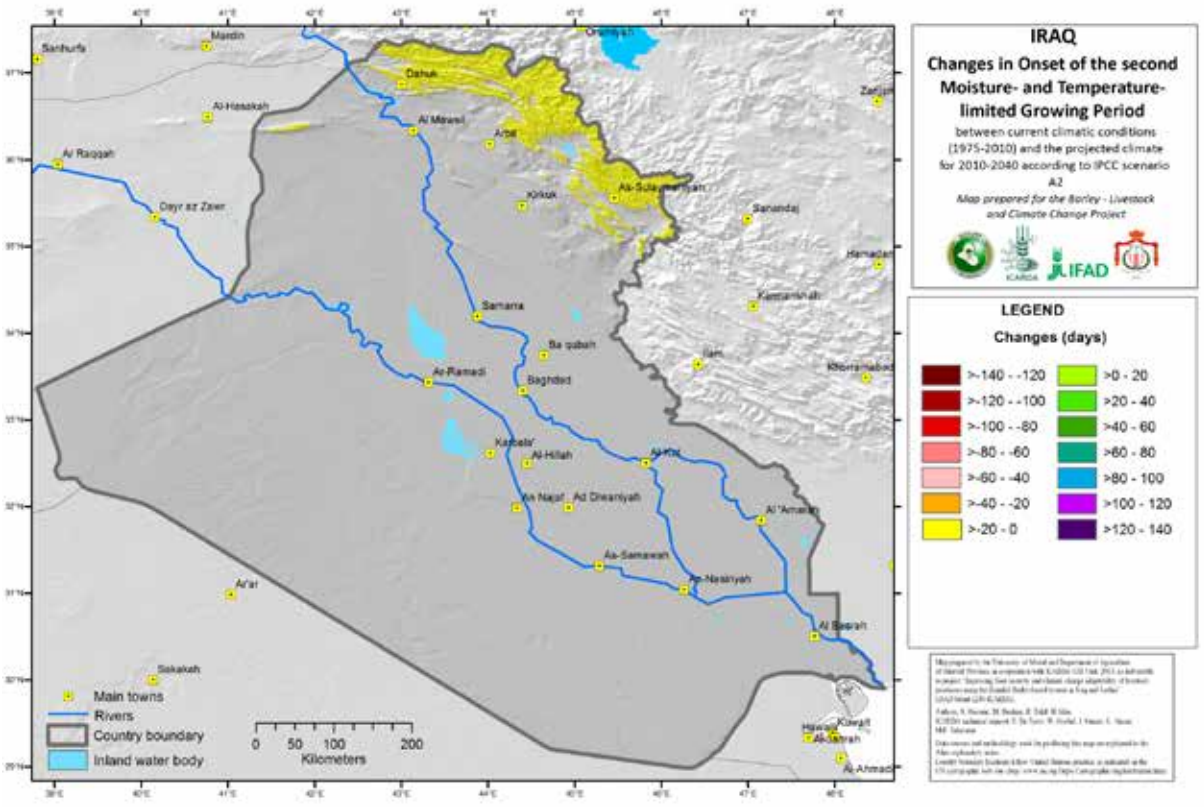
IRAQ
Changes in Onset of the second Moisture- and Temperature-limited Growing Period
between current climatic conditions (1975-2010) and the projected climate for 2010-2040 according to IPCC scenario A2
Map prepared for the Barley - Livestock and Climate Change Project
LEGEND
Changes (days)
>-140 - -120
>-120 - -100
>-100 - -80
>-80 - -60
>-60 - -40
>-40 - -20
>-20 - 0
>0 - 20
>20 - 40
>40 - 60
>60 - 80
>80 - 100
>100 - 120
>120 - 140
Main towns
Rivers
Country boundary
Inland water body
0 50 100 200
Kilometers

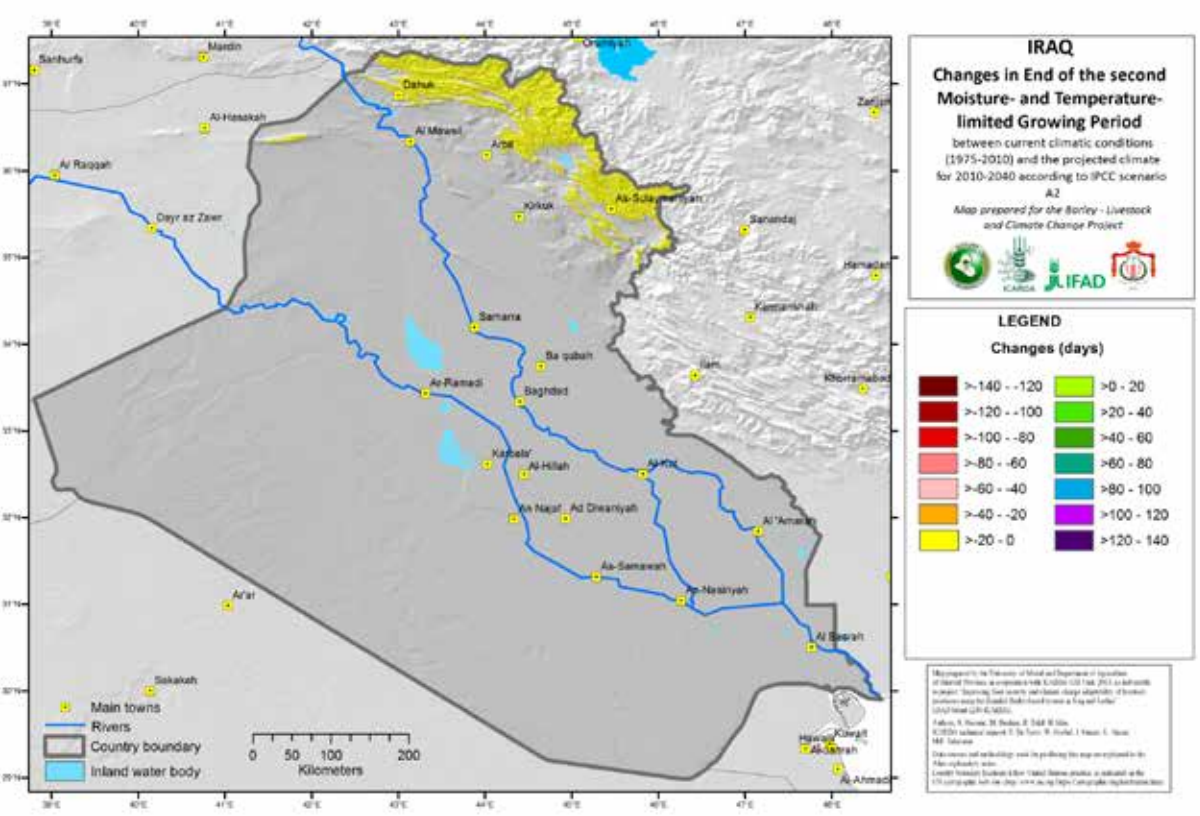
IRAQ
Changes in End of the second Moisture- and Temperature-limited Growing Period
between current climatic conditions (1975-2010) and the projected climate for 2010-2040 according to IPCC scenario A2
Map prepared for the Barley - Livestock and Climate Change Project
LEGEND
Changes (days)
>-140 - -120
>-120 - -100
>-100 - -80
>-80 - -60
>-60 - -40
>-40 - -20
>-20 - 0
>0 - 20
>20 - 40
>40 - 60
>60 - 80
>80 - 100
>100 - 120
>120 - 140
Main towns
Rivers
Country boundary
Inland water body
0 50 100 200
Kilometers

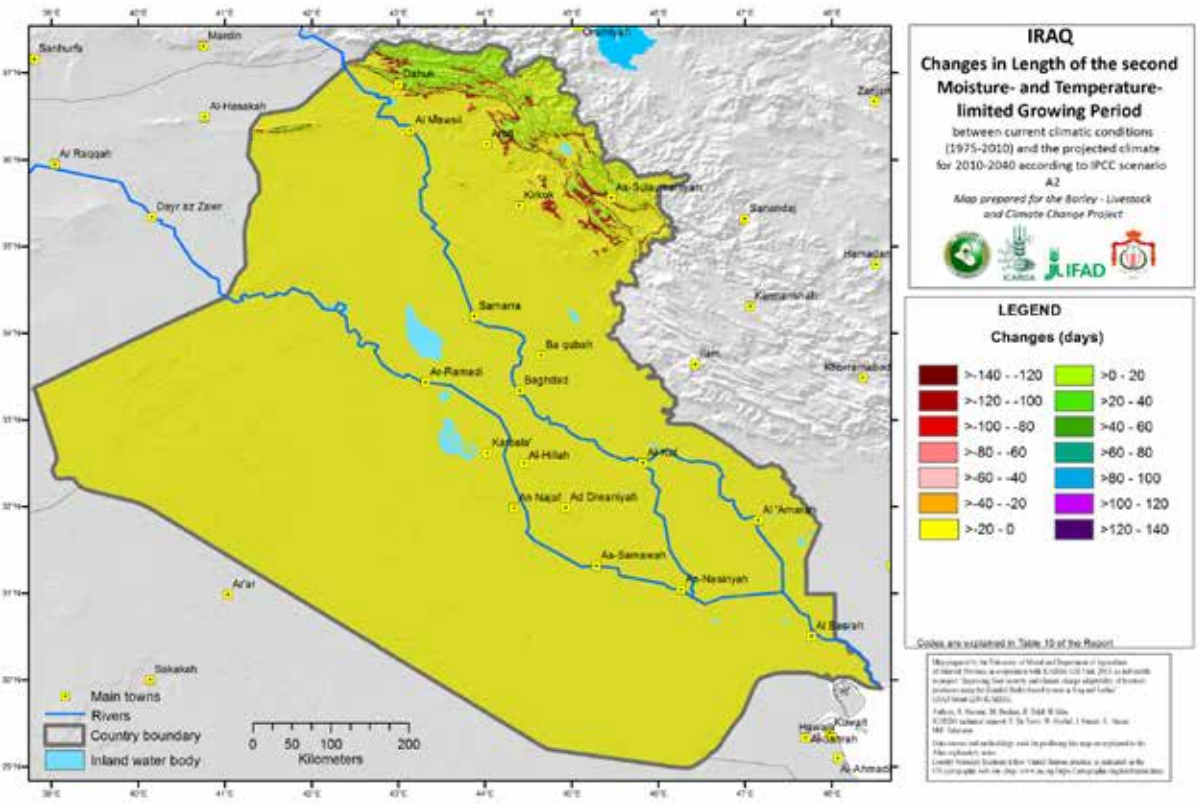
IRAQ
Changes in Length of the second Moisture- and Temperature-limited Growing Period
between current climatic conditions (1975-2010) and the projected climate for 2010-2040 according to IPCC scenario A2
Map prepared for the Barley - Livestock and Climate Change Project
LEGEND
Changes (days)
>-140 - -120
>-120 - -100
>-100 - -80
>-80 - -60
>-60 - -40
>-40 - -20
>-20 - 0
>0 - 20
>20 - 40
>40 - 60
>60 - 80
>80 - 100
>100 - 120
>120 - 140
Main towns
Rivers
Country boundary
Inland water body
0 50 100 200
Kilometers

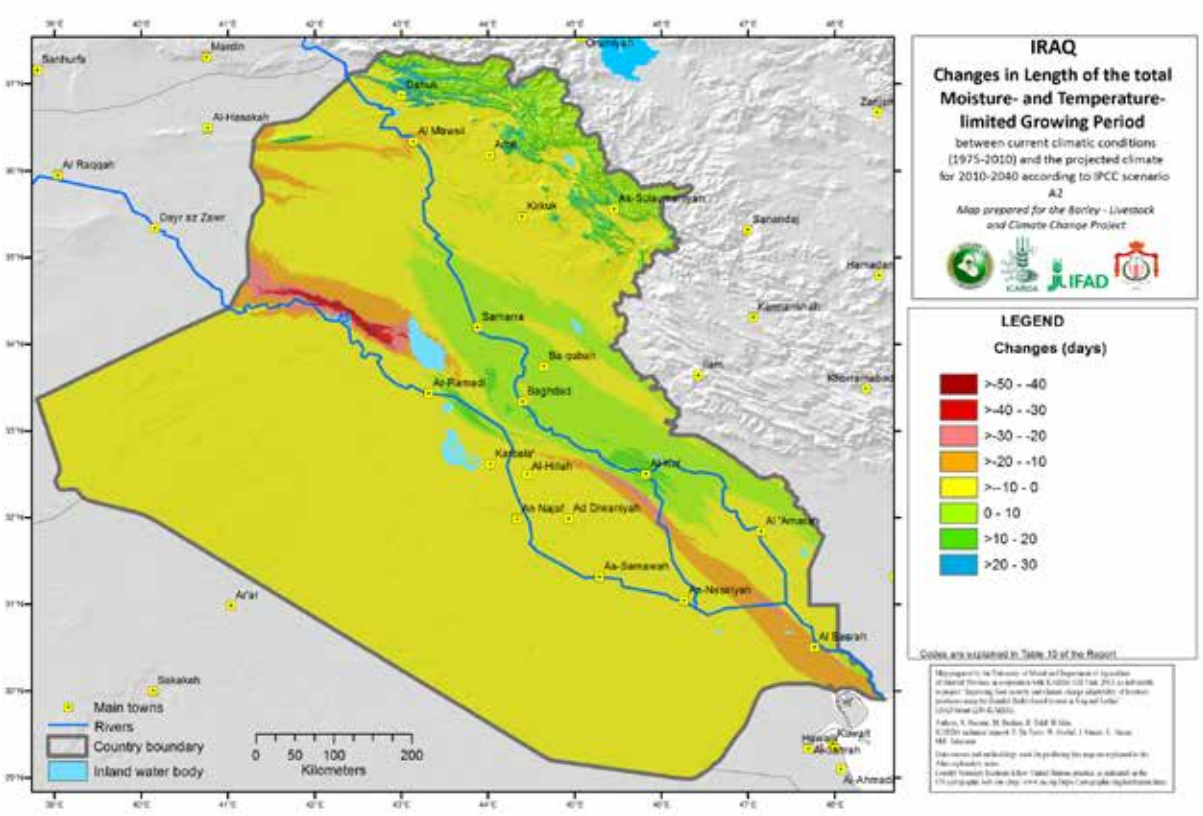
IRAQ
Changes in Length of the total Moisture- and Temperature-limited Growing Period
between current climatic conditions (1975-2010) and the projected climate for 2010-2040 according to IPCC scenario A2
Map prepared for the Barley - Livestock and Climate Change Project
LEGEND
Changes (days)
>-50 - -40
>-40 - -30
>-30 - -20
>-20 - -10
>--10 - 0
0 - 10
>10 - 20
>20 - 30
Codes are explained in Table 10 of the Report
Main towns
Rivers
Country boundary
Inland water body
0 50 100 200
Kilometers
Sanhurfa
Mardin
Dahuk
Al-Hasakah
Al Mawsil
Arbil
Ar Raqqah
Kirkuk
As-Sulaymaniyah
Dayr az Zawr
Sanandaj
Hamadan
Kermanshah
Samarra
Ba`qubah
Ilam
Khorramabad
Ar-Ramadi
Baghdad
Karbala'
Al-Hillah
Al-Kut
An Najaf
Ad Diwaniyah
Al 'Amarah
As-Samawah
An-Nasiriyah
Al Basrah
Ar'ar
Sakakah
Hafar al-Batin
Kuwait
Al-Jahrah
Al-Ahmadi

About ICARDA and the CGIAR

Established in 1977, ICARDA is one of the 15 centers supported by the CGIAR. ICARDA's mission is to improve the livelihoods of the resource- poor in dry areas through research and partnerships dedicated to achieving sustainable increases in agricultural productivity and income, while ensuring efficient and more equitable use and conservation of natural resources.

ICARDA has a global mandate for the improvement of barley, lentil and faba bean, and serves the non-tropical dry areas for the improvement of on- farm water use efficiency, rangeland and small ruminant production. In Central Asia, West Asia, South Asia, and North Africa regions, ICARDA contributes to the improvement of bread and durum wheats, kabuli chickpea, pasture and forage legumes, and associated farming systems. It also works on improved land management, diversification of production systems, and value-added crop and livestock products. Social, economic and policy research is an integral component of ICARDA's research to better target poverty and to enhance the uptake and maximize impact of research outputs.

CGIAR is a global agriculture research partnership dedicated to reducing rural poverty, increasing food security, improving human health and nutrition, and ensuring more sustainable management of natural resources. It is carried out by the 15 centers who are members of the CGIAR Consortium in close collaboration with hundreds of partner organizations and the private sector. www.cgiar.org